Relating Methanogen Community Structure and Function in Anaerobic Digesters

Benjamin T.W. Bocher
Marquette University

RELATING METHANOGEN COMMUNITY STRUCTURE AND FUNCTION IN ANAEROBIC DIGESTERS

by

Benjamin T.W. Bocher

A Dissertation submitted to the Faculty of the Graduate School,
Marquette University,
in Partial Fulfillment of the Requirements for
the Degree of Doctor of Philosophy

Milwaukee, Wisconsin

August 2012

ABSTRACT
RELATING METHANOGEN COMMUNITY STRUCTURE AND FUNCTION IN ANAEROBIC DIGESTERS

Benjamin T.W. Bocher

Marquette University, 2012

A deeper understanding of how microbial community structure relates to process function would help improve anaerobic digester design. This dissertation describes both qualitative and quantitative relationships between anaerobic digester function and microbial community structure. Community structure was characterized using banding pattern intensities from denaturing gradient gel electrophoresis (DGGE) for the *mcrA* gene of methanogenic *Archaea*.

The first project compared a single-stage continuously mixed stirred tank reactor (CSTR) and staging with an acidogenic CSTR followed by a methanogenic CSTR. After seeding with the same biomass, these unique process configurations exhibited different function and qualitatively different methanogen communities. Compared to a single-stage CSTR, staging increased the maximum rate of methane production by 41, 26, and 57% with propionate, acetate, and hydrogen, respectively. Additionally, the staged digester produced 10% more methane and achieved 10% greater volatile solids (VS) destruction.

The second project also provided a qualitative relationship: methanogen community structure impacted digester function upon bioaugmentation. Specific methanogenic activity (SMA) with propionate statistically increased (up to 57%) in six of nine bioaugmented anaerobic cultures. These increases correlated to methanogen community structure above the 98% level ($r_s = 0.770$) using Spearman's Rank Correlation Coefficient (two-tailed).

In the third project, a quantitative structure-activity relationship (QSAR) was established between methanogen community structure and two activities using multiple linear regression (MLR). Two different QSARs were predictive of SMA values with propionate ($q^2 = 0.52$) and with glucose ($q^2 = 0.56$), respectively. A MLR model may be applicable to other biological communities when trophic redundancy and a ubiquitous gene are present and when a linear model is appropriate.

Greater understanding of anaerobic digester microbial communities is possible using these QSARs. This research serves as a template that can be used to construct additional QSARs for other complex microbial communities in engineered systems.

ACKNOWLEDGEMENTS

Benjamin T.W. Bocher

I am indebted to Dr. Dan Zitomer not only for your insightful advising, but also for helping me deepen my understanding of all a Ph.D entails—being at home doing novel research as well as sleeping in a hammock in rural El Salvador. Mike Dollhopf, for conducting full-scale sample tests and contributing countless hours to ensure every piece of lab equipment functioned well, I thank you. My committee—Dr. Michael Switzenbaum, Dr. James Maki, and Dr. Sherry Seston—provided me with insight on topics that I was less well-versed in, especially the complex microbial ecology inside these "black boxes." I am indeed grateful for your generosity and for perspective on the kind of engineer I want to become. Dr. Lars Olson and Dr. Michael Johnson, I greatly appreciate your programming and statistical analysis help during the final stretch.

Anne Schauer-Gimenez, you welcomed me into the Water Quality center, taught me to extract DNA, and more. Vaibhav Tale, you modeled the determination needed to complete this endeavor (16 times before your first successful mcrA extraction!). Ujwal Bhattad, you smiled often, a poignant and simple reminder of Julian of Norwich's words: Indeed, all will be well. Navaneethan Navaratnam, you were my infinitely patient teacher, teaching me SMAs, BMPs, and ATAs. From day one on, my four seniors graciously answered my innumerable questions.

I thank, Rachel Morris, for teaching me not only how to perform DGGE, but also that I could be a great parent and Ph.D. student. Keerthi Cherukuri and Prince Mathai, thank you for performing all of the molecular work (PCR, qPCR, DGGE, etc.) presented in chapters 3 – 5.

Kaushik Venkiteshwaran, thanks for modeling working and playing hard, and for

giving me a new definition of multi-cultural. Matt Seib: I appreciate your directness. To both of you, I am grateful for your constant inquiring about what, why, and how—the core of great scientists!

Steve Graziano, your work made it possible for me to be present to my family my first year; your "woo hoo" text upon hearing of our first daughter's birth was a fantastic confirmation that a Ph.D. was the best way for me to use my gifts. When I began to wonder how to continue to do great work, different personalities and much needed skills arrived via John Ross, Caitlin Collins, and Kyle Hill—your abilities to be amazed, do exacting work, and analyze every aspect of the project. Sarah Walsh, long shifts, no food, no breaks! I could not have completed that volume of work without you. Kevin Glauber, you came as I was beginning to see the end and helped affirm my desire to teach. A willingness to do whatever, simply to gain lab experience came named as Mike Leipus, allowing the research to finish strong.

God provided via Seeds of Faith, Inc.: a Fellowship indicative of who I am and what I strive to be about. Bill and Sandy, I have no words, only profound gratitude. I am very humbled. Veolia Environnement and WE Energies, I thank in a special way for funding this research.

Of course, I thank my girls. My bride, Tammy, you took on the truly blessed and beautifully demanding role of a stay-at-home mom. My *Little Bear*, Nadia, you began life as I began this endeavor. As you put it, "my best friend in the whole world," you, indeed, give me Divine Hope. My *Little Wolf*, Norah, you have enamored your father so much that I cannot imagine the powerful Light that is yet to shine through you.

"We need an holistic approach, no monopolization of activities by 'top specialists and scientists', but participation of all people, so that they will get more time for spiritual and

intellectual development… and enjoyment. The best renewable resource is mankind." (Lettinga, G. 2005. *Water Science and Technology*, *52*(1-2), p11.) May we all "run with perseverance the race that is set before us" (Hebrews 12:1c) by living with ever greater sustainability, justice, and authenticity. Hallelujah. Amen.

TABLE OF CONTENTS

LIST OF TABLES

LIST OF FIGURES

1.0 GENERAL INTRODUCTION

Over 25 years ago in *Our Common Future*, the World Commission on Environment and Development (Brundtland Commission) formally introduced the term sustainable development, defined as "development which meets the needs of current generations without compromising the ability of future generations to meet their own needs". While it has had a controversial history in its tangible application and remains a highly politicized concept, it has much light to shed on recent desires in pop culture as well as scientific fields. May this work be ordered in the same direction as that document—to lead not only to a more sustainable world, but also a more just one for our children. Anaerobic biotechnologies have a vital role to play in that world. This work represents on small step in that direction. A.M.D.G.

1.1 Anaerobic Degradation Pathway

An overview of the series of interrelated steps that comprise the anaerobic degradation pathway helps illustrate the importance and complexity of the microbes involved in anaerobic digestion. A general understanding of this overall process, such as that described in Anaerobic Digestion Model 1 (ADM1), involves: (1) disintegration, (2) hydrolysis, (3) acidogenesis, (4) acetogenesis, and (5) methanogenesis (Batstone et al., 2002).

Disintegration, which is mainly non-biological, and hydrolysis, which is catalyzed by enzymes, are both extracellular. Disintegration is the breakdown of heterogeneous particulate substrates into inert materials, particulate carbohydrates, proteins, and lipids. It includes lysis, non-enzymatic decay, phase separation, and physical breakdown (e.g., shearing). It is crucial to note that the substrate (the portion of the COD that is degradable

and will, therefore, go through the biochemical processes described here) and the TCOD are different. A completely degradable influent is very rare. Therefore, some portion of the TCOD in the influent will remain as inert particulates. The hydrolysis step comes next. It is important to include as it models many substrates that are fed to anaerobic digesters (e.g., cellulose, starch, or protein). Hydrolysis is the enzymatic depolymerization of carbohydrates, proteins, and lipids into soluble monomers—monosaccharides, amino acids and long chain fatty acids (LCFA), respectively (Vavilin et al., 2008).

Monosaccharides and amino acids are then degraded into organic acids (e.g., valeric, butyric, and propionic acid) by acidogens (one for monosaccharides and another for amino acids). Hydrogen (H_2), which is used later on in the degradation pathway, and carbon dioxide (CO_2) are also produced during acidogenesis, which is a fermentation reaction without an additional electron acceptor or donor (Gujar and Zehnder, 1983). Three distinct groups of acetogenic bacteria then degrade the LCFA, valerate and butyrate (one group for the two), and propionate into acetate, H_2, and carbon dioxide through an anaerobic oxidation. LCFA degradation is complicated due to transport difficulties and different physico-chemical characteristics of these large molecules compared to valerate and shorter volatile fatty acids (VFAs). Note that, parallel pathways are present in hydrolysis, acidogenesis, and acetogenesis (Batstone et al., 2002).

The final step of anaerobic degradation is the conversion of either: (1) acetate into methane (CH_4) and CO_2 (acetoclastic methanogenesis) or (2) H_2 and CO_2 into CH_4 and water (hydrogenotrophic methanogenesis). While H_2 may be consumed in other areas, such as sulfate reduction, these have not been included in the ADM1 model (Batstone et al., 2002).

Within the anaerobic degradation pathway there are a few key steps that demand special attention. For example, the conversion rate of CH_4 to wastes with high levels of particulate organic matter, especially cellulosic material, may be limited by hydrolysis (Ferrara et al., 1984; Climent et al., 2007; Myint et al., 2007; Zhuang et al., 2009). It is worthy of mention that there are other waste-specific issues that may pertain to hydrolysis or other steps, such as the degradation of other recalcitrant compounds. Often, however, the bottleneck is degradation of propionate.

1.2 REFERENCES

Batstone, D. J., Keller, J., Angelidaki, I., Kalyuzhnyi, S. V., Pavlostathis, S. G., Rozzi, A, Sanders, W. T. M., et al. (2002). Anaerobic Digestion Model No. 1 (ADM1). *IWA Task Group for Mathematical Modeling of Anaerobic Digestion Processes*. IWA Publishing.

Climent, M., Ferrer, I., Baeza, M. D. M., Artola, A., Vázquez, F., & Font, X. (2007). Effects of thermal and mechanical pretreatments of secondary sludge on biogas production under thermophilic conditions. *Chemical Engineering Journal*, *133*(1-3), 335-342. doi:10.1016/j.cej.2007.02.020

Ferrara, R. Barberis, R., Jodice, R. and Vicenzino, E. (1984). Influence of kinetics of hydrolysis, acidogenesis and methanogenesis on enhancement of the production of biogas from animal excreta. *Agricultural Wastes* 11, 79-90.

Gujer, W., Zender, A.J.B. (1983). Conversion processes in anaerobic digestion. *Water Science and Technology*. 15, 127-167.

Myint, M., Nirmalakhandan, N., & Speece, R. E. (2007). Anaerobic fermentation of cattle manure: modeling of hydrolysis and acidogenesis. *Water Research*, *41*(2), 323-332. Elsevier. Retrieved from http://www.ncbi.nlm.nih.gov/pubmed/17141822

Vavilin, V. A, Fernandez, B., Palatsi, J., & Flotats, X. (2008). Hydrolysis kinetics in anaerobic degradation of particulate organic material: an overview. *Waste Management*, *28*(6), 939-51. doi:10.1016/j.wasman.2007.03.028

Zhuang, X., Yuan, Z., Ma, L., Wu, C., Xu, M., Xu, J., Zhu, S., et al. (2009). Kinetic study of hydrolysis of xylan and agricultural wastes with hot liquid water. *Biotechnology Advances*, *27*(5), 578-82. Elsevier Inc. doi:10.1016/j.biotechadv.2009.04.019

2.0 ANAEROBIC DIGESTER STAGING ALTERS METHANOGEN COMMUNITY STRUCTURE AND PROCESS FUNCTION

2.1 Introduction

Anaerobic digestion is a practical technology for renewable energy production and sludge stabilization. Improved process design has the potential to simultaneously increase biogas generation and volatile solids (VS) destruction while reducing the build-up of intermediates like propionate, which can be detrimental to digester performance (McCarty and Smith, 1986; Smith, 1990; Kida et al., 1993; McInerney et al., 2009; Wong et al., 2009). However, a lack of understanding regarding the relationship between process configuration and digester function is a challenge to process improvement. For too long, practitioners have relied on a complete mix stirred tank reactor (CSTR) configuration and regarded methanogenic cultures as "black boxes" that are difficult to characterize (Rivière et al., 2009). The typical approach is to pump waste into a CSTR and rely on whatever culture predominates. The questions sometimes left unasked include the following: what process configurations other than a single CSTR can improve performance and how does the process configuration affect the microbial community structure and digester function, such as methane (CH_4) production, VS destruction, and propionate metabolism?

2.1.1 Staging Anaerobic Digesters

Anaerobic digestion is a series of biochemical reactions. Though dependent upon the substrate, these steps are generally termed hydrolysis, acidogenesis, acetogenesis, and methanogenesis (Batstone et al., 2002). The four steps are catalyzed by different trophic groups of microorganisms (Chouari et al., 2005) that can have different growth kinetics,

responses to toxicants and environmental stresses, as well as nutrient and pH requirements (Demirer and Chen, 2005). Hence, it is reasonable to consider optimizing environmental conditions in a series of different vessels for different biological steps in an effort to improve operation.

Staging is a process wherein two or more tanks in series perform digestion, rather than just one traditional tank and biomass recycle between the final and initial tanks occurs. Staged digestion with biomass recycle has been described as providing both greater stability and higher efficiency, in part, because, compared to a CSTR, it more closely approaches plug flow (Lettinga, 1995), which has been shown to produce more CH_4 and remove more VS and volatile fatty acid (VFA) because of the presence of variations in substrate and VFA concentrations, pH, and other environmental conditions conducive to the growth of different trophic groups of anaerobic microorganisms throughout the tank (Liu, 1998). Many terms have been used in literature to refer to staging, including two-step (Weiland, 1993; Elmitwalli et al., 2001), two-phase (Pohland, 1971; Cavinato et al., 2010) and two-stage (Smith, 1996; Young et al., 2000; Azbar and Speece, 2001; Andersson and Björnsson, 2002; Blumensaat and Keller, 2005). Other processes have used two tanks to provide a solubilization phase (Wang et al., 2010) or a thermal pre-treatment phase (Kade, 2004).

2.1.1.1 Staging as a Means of Process Improvement

Significant process improvement achieved via staged anaerobic digestion can be utilized for a variety of treatment objectives. For example, Azbar and Speece (2001) compared staged and traditional anaerobic digesters fed glucose. In all cases, the staged systems out-performed the traditional one-tank system, with staged configurations achieving higher CH_4 production compared to a single CSTR. Staged digestion generated more CH_4

and removed more COD than single stage operation (Cohen et al., 1979; Cohen et al., 1980; Anderson et al., 1994; Siegrist, 2002; Yang et al., 2003). Others have described the significant improvement due to temperature staging for pathogen inactivation (e.g., Vandenburgh and Ellis, 2002) and acid-gas phasing for increased VS destruction (e.g., Wilson and Dichtl, 2000). A two-stage, thermophilic system that had spatial separation of propionate degradation improved treatment efficiency by 10 to 13% (Wiegant et al., 1986).

2.1.2 Improvement by Beneficial Organisms

Anaerobic digestion may also improve if beneficial organisms are present or if microbial community diversity is increased. At the least, an adequate methanogenic consortium will predominate in a digester if the retention time, temperature, nutrients, and substrates are correctly controlled and if there is no toxicity (Speece, 1988). However, even if all these parameters are properly controlled, the identity of individual genera and species in anaerobic digester microbial communities as well as the overall microbial diversity within digesters still varies greatly (Leclerc et al., 2004; Werner et al., 2011). This is contrary to typical assumptions of many designers and operators who do not consider microbial community structure as a process variable (Curtis et al., 2003). In addition, it has been shown that maximum specific CH_4 production rates vary greatly from digester to digester, ostensibly due to microbial community differences (Tale, 2011).

Digester function has been linked to the microbes present (Briones and Raskin, 2003). For example, researchers have suggested that digesters containing flexible microbial community structures that change rapidly can produce CH_4 at a more consistent rate during process upset. When two different digesters containing different groups of microbes were upset, the one in which the community changed the most produced more CH_4 than the

other; this occurred even though the physical digester conditions were identical (Fernandez et al., 2000). It was suggested that microbial communities with trophic redundancy (i.e., cultures that contain many different organisms that can perform the same metabolic function, such as convert acetate to CH_4) are more stable and produce CH_4 more consistently during and after transient organic overload compared to cultures with less trophic redundancy (Hashsham et al., 2000).

Process configuration may influence the microbial community diversity in a digester, and this may influence digester function. In order to more fully understand the benefits of process configuration and provide a basis for improved municipal anaerobic digester design, changes in the microbial community structure due to staging must be understood. Shin et al. (2010) compared co-digestion (95% municipal wastewater and 5% food-waste, v/v) in two staged digesters operated at hydraulic retention times (HRT) ranging from 25 to 4 days, and concluded that overall process performance remained relatively stable even though the structures of the bacterial and archaeal communities changed. Yet, a comparison of the effects of staged and unstaged digesters treating the same waste sludge on microbial community structure and digester function has not been published to the author's knowledge.

2.1.3 Research Objectives

The hypothesis of this research was that staged digestion causes a shift in methanogen community structure, leading to an increase in microbial activity. Therefore, community structures and biomass activities in staged and unstaged digesters treating synthetic municipal wastewater primary sludge were compared.

2.2 Methods and Materials

2.2.1 Digester Configuration, Set-up, and Operation

In this study, staging referred to two tanks in series with a portion of the second stage biomass recycled to the first stage. Three anaerobic digesters (2-L working volume; 15-day solids retention time (SRT)) were operated in parallel at 35 ±1°C for over 300 days (Table 2-1, Figure 2-1). They are referred to as CSTR (unstaged CSTR serving as the control), A/M staged (staged digester with an acidogenic first stage and a methanogenic second stage), and M/M staged (staged digester with methanogenic first and second stages). All stages were continuously mixed using magnetic stir bars. Each first and second stage was connected to a polyvinyl fluoride (PVF) gas-sampling bag (Lab Pure® Laboratory Products, Saint-Gobain Performance Plastics, Poestenkill, NY) to collect biogas. All digesters were seeded with a mix of biomass from three full-scale anaerobic digesters in an attempt to increase microbial diversity of seed biomass. Digesters were fed daily with 133 mL of synthetic primary sludge (Nature's Choice Large Breed Adult Dog Food at 3% TS; VS/TS ratio of 84%), a basal nutrient medium described elsewhere (Schauer-Gimenez et al., 2010), and 5 g/L $NaHCO_3$. From the control, 133 mL was removed daily. For the staged digesters, 133 mL of digested sludge was removed daily from the second stage vessel and replaced with 133 mL of first stage effluent. In addition to this second stage effluent, a recycle of 25% of the first stage working volume (40 and 167 mL in the A/M and M/M digesters, respectively) was removed from the second stage and added into the first stage each day along with the feed.

Table 2-1. Digester Configurations

	Control (CSTR*)	A/M** Staged	M/M*** Staged
Staged	No	Yes	Yes
Total System SRT (days)	15	15	15
First Stage SRT (days)	0	1.2	5
Second Stage SRT (days)	15	13.8	10
pH at quasi steady state (first stage)	7.31 ±0.10	5.16 ±0.29	7.31 ±0.11
pH at quasi steady state (second stage)	-	7.46 ±0.10	7.48 ±0.09

*CSTR = complete mix stirred tank reactor
**A/M = acidogenic/methanogenic digesters with a short-SRT, first-stage acidic reactor followed by a second-stage methanogenic reactor.
***M/M = methanogenic/methanogenic digesters with a longer-SRT, first-stage methanogenic reactor followed by a second-stage methanogenic reactor.

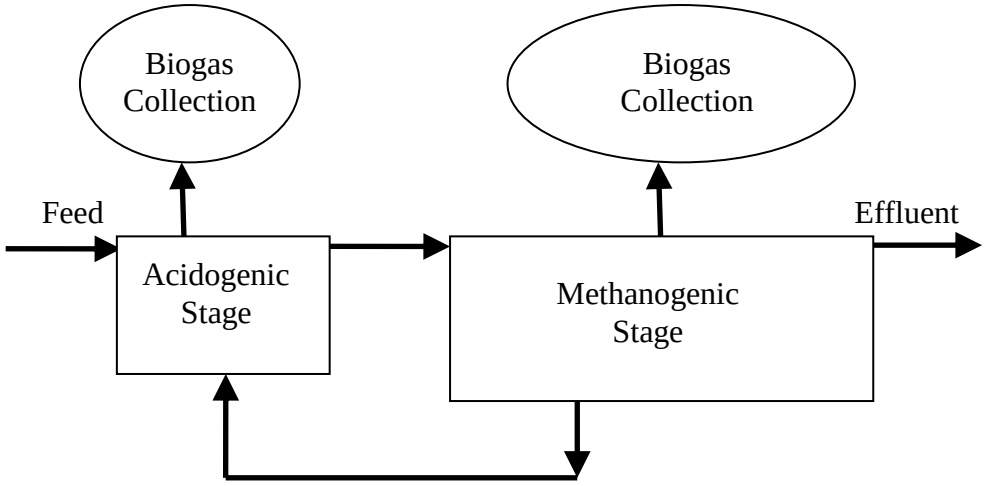

Figure 2-1. Schematic of acidogenic-methanogenic (A/M) staged digester.
Methanogenic-methanogenic (M/M) staged digester was a similar set-up, but with two methanogenic stages.

2.2.2 Transient Organic Overloading

On day 181 (after 12 SRTs), the solids loading rate to all digesters was increased from 1.7 to 5.9 g VS/L-d for 12 days to simulate a transient overload; then the initial, lower loading rate was resumed. At quasi steady state both before and after overloading (6 and 18 SRTs, respectively), specific methanogenic activity (SMA) tests were performed. Digester operating data were collected, and digester recovery was observed and compared.

2.2.3 Methanogen Community Analysis

DNA Extraction. DNA was extracted from all digesters throughout operation during both non-steady and quasi steady state periods as well as both before and after overloading. Each 50-mL biomass sample was thickened in a centrifuge (IEC Centra-4B, International Equipment Company, Needham Heights, MA) for 10 min at 2500 x g. Then 0.75-mL of thickened biomass was used with a DNA isolation kit (PowerSoil™ DNA Isolation Sample Kit, MoBio Laboratories, Carlsbad, CA) according to the manufacturer's instructions using the alternative lysis method, which states: "If cells are difficult to lyse, a 10 minute incubation at 70°C, after adding Solution C1, can be performed" (PowerSoil Protocol, 2009). This method replaced the horizontal vortexing of the PowerBead™ Tubes and was meant to reduce shearing of DNA. The presence of extracted DNA was confirmed with gel electrophoresis (1% agarose in 1X Tris-Acetate-EDTA, TAE) using ethidium bromide (0.8 μL/mL) (Sambrook and Russell, 2001). A mixture of 3 μL of 6X blue-orange loading dye and 10 μL of DNA sample was injected into the wells (Hartwell et al., 2004). A λϕ (HindIII, HaeIII) ladder was placed into the first well as a marker. This marker had 40 ng/μL Lambda (λ) DNA, HindIII cut and 30 ng/μL phi (ϕ) X174 DNA, HaeIII cut. A 100-hundred millivolt (mV) potential was maintained across the gel for 60 to 90 minutes. This potential caused migration of the DNA molecules, which were illuminated and photographed under ultraviolet light using a bioimaging system (GDS-8000 Bioimaging System, UVP Inc., Upland, CA). After confirming via agarose gel, DNA samples were stored at -80°C until further analysis. All extractions were carried out in duplicate.

DNA Amplification Using Polymerase Chain Reaction (PCR). DNA was amplified using polymerase chain reaction (PCR) with primers for the methyl coenzyme M

reductase (*mcrA*) gene of methanogenic *Archaea* (Luton et al., 2002). These are: mcrA1f: 5'-GGTGGTGTMGGATCACACARTAYGCWACAGC -3', (mcrF); GCmcrA1f: 5'- *GC-clamp-GGTGGTGTMGGA TTCACACARTAYGCWACAGC -3', (mcrA1f), where GC-clamp = 5' – CGCCCGCCGCGCCCCGCGCCCGTGCCGCCGCCCCCGCCCG – 3', (GC-clamp); mcrA500r: 5' – TTCATTGCRTAGTTWGGRTAGTT – 3', (mcrR). The *mcrA* gene was used because numerous studies have exploited its ubiquity and specificity in all known methanogens to find them in various locations ranging from marine environments (Bidle et al., 1999; Wilms et al., 2007) to termite guts (Ohkuma et al., 1995), rice paddies (Lueders et al., 2001) to anaerobic digesters (Rastogi, 2008; Tale, 2010), oligotrophic fen (Galand et al., 2002), and more. PCR utilized prepared master mix, which included Taq polymerase (EconoTaq® PLUS 2X Master Mix, Lucigen Corporation, Middleton, WI). Forward and reverse primers were added to the PCR tube with nuclease-free H_2O to make a 100-µL reaction.

Nested PCR was performed on the extracted DNA by first amplifying using mcrA1f and mcrA500r primers in the following program: 95°C for 5 min; then six cycles of 95°C for 1 min, 49°C for 1 min, 72°C for 3 min; next 30 cycles of 95°C for 1 min, 49°C for 1 min, 72°C for 3 min; then 95°C for 1 min, 49°C for 1 min, 72°C for 10 min; stop and stay at 4°C. The second cycle re-amplified with GCmcrA1f (GC clamp) and mcrA500r primers in the following program: 95°C for 5 min; then six cycles of 95°C for 1 min, 58°C for 1 min, 72°C for 3 min; next 36 cycles of 95°C for 1 min, 58°C for 1 min, 72°C for 3 min; then 95°C for 1 min, 58°C for 1 min, 72°C for 10 min; stop and stay at 4°C. This ideally yielded a gene product that was 470 nucleotides long (Luton et al., 2002). PCR was done on a thermalcycler

(PTC-200 DNA Engine Cycler, Bio-Rad, Hercules, CA; or T-Personal thermocycler, Biometra, Goettingen, Germany).

2.2.3.1 Denaturing Gradient Gel Electrophoresis (DGGE)

Amplified genes were separated with denaturing gradient gel electrophoresis (DGGE). DGGE results were used to provide a fingerprint to distinguish the microbial communities of the unstaged and staged digesters. The denaturant concentration varied linearly over 75 mm, from 40% at the top of the gel to 70% at the bottom of the gel (expressed as v/v of the total gel volume) using a vertically poured gel (Universal DCode Mutation Detection System, BioRad, Hercules, CA). DGGE was performed on 1-mm-thick 8% polyacrylamide gel following the manufacturer's protocol. Approximately, 600 ng of DNA product was added to each lane of the polyacrylamide gel with 2X blue loading dye. A sample from the CSTR was run on both gels as a reference ladder that allowed comparison between gels. An electric potential of 100 V was maintained across the gel for 12 hours. A 1% SYBR® gold dye solution (Invitrogen, Carlsbad, CA) was used to stain the gel. After immersing the gel in the staining solution and rotating it for 30 minutes on a shaker table at a speed sufficient to mix the dye solution, it was viewed under ultraviolet light using a bioimaging system (GDS-8000 Bioimaging System, UVP Inc. Upland, CA).

2.2.3.2 Analysis of Molecular Data

Principal component analysis (PCA) was performed using MATLAB (v. R2010bSP1, MathWorks®, Natick, MA). Optical densities of the DGGE bands, obtained from Labworks™ software (v. 4.6.00.0, Lablogics, Inc., Mission Viejo, CA), provided dimensional values for community structure. All available samples (days 142, 181, 284, and 326) were

used for PCA analysis. Previous work has suggested a correlation between *mcrA* densitometric data and SMA values, with samples having similar SMA values clustering together (Tale, 2011; Navaratnam, 2012).

Pearson's correlation coefficient was used to develop similarities between the banding patterns (i.e., 0 signified uncorrelated, +1 was a perfect positive correlation, and -1 was a perfect negative correlation) since it accounted for band intensities (i.e., brightness), unlike coefficients like Jaccard that merely account for the presence or absence of bands. This was done in MATLAB (v. R2010bSP1) using the "pdist" function and a predefined command entitled "correlation" that calculated one minus the Pearson's correlation coefficient to develop dissimilarities between banding patterns. These dissimilarity values were compiled into a distance matrix using the "squareform" function in MATLAB because the output of "pdist" is a vector variable. This matrix was then uploaded into Plain Text Editor (v. 5.1), formatted to be readable by the Phylogency Inference Package (PHYLIP, v. 3.69, Joe Felsenstein, University of Washington, Seattle, Washington) and the unweighted pair group method with arithmetic mean (UPGMA), Fitch-Margolish and Neighbor-joining algorithms were used for clustering (Shin et al., 2010). Phylogenetic trees were viewed and formatted for publication in FigTree (v. 1.3.1, University of Edinburgh, Edinburgh, United Kingdom).

2.2.3.3 Range Weighted Richness (R_r) and Functional Organization (F_o)

While fingerprinting techniques have often been limited to determining similarity or difference, some parameters have been developed in an attempt to extract more information from DGGE banding patterns for the 16S rRNA gene. Range weighted richness (Rr) and functional organization (Fo), as defined by Marzorati et al. (2008), were used in this research.

Range weighted richness quantifies microbial community diversity (Equation 2-1).

Equation 2-1. Range Weighted Richness

$$Rr = \left(N^2 \times Dg\right)$$

wherein N is the total number of bands in the gel (or portion being analyzed) and Dg is the denaturing gradient (v/v fraction) difference from the first through the last bands in a particular lane (Marzorati et al., 2008).

Functional organization, Fo, describes how well a community is organized such that, upon perturbation, it can adapt and remain functionally stable (Marzorati et al., 2008). Functional and structural stability of a microbial community do not always coincide. In fact, structural flexibility (i.e., instability) may be necessary for functional stability under stressed conditions (Fernandez et al., 2000), and community evenness may be an indicator of the structural flexibility of microbial community structure (Wittebolle et al., 2009). Therefore, quantification of evenness may help provide a better understanding of microbial community response to perturbations. To do this, Pareto-Lorenz (PL) evenness curves were constructed from DGGE banding patterns to graphically represent the methanogenic diversity according to the procedure found in Mertens et al. (2005) and Wittebolle et al. (2008). High Fo values were synonymous with low evenness and vice versa. Thus, a perfectly even community would be graphed as a 45° line through the origin, whereas an increasingly uneven community would have an initial slope much greater than 45° and then a gradually decreasing slope that asymptotically approaches a slope of zero.

2.2.4 Specific Methanogenic Activity (SMA) Testing

Microbial community activity was quantified using SMA tests of biomass samples from the final effluent (i.e., second stage biomass from the A/M and M/M) in each digester

with propionate (SMA_{Pr}), acetate (SMA_{Ac}), and H_2 (SMA_{H2}) as substrates according to procedures described by Angelidaki et al. (2007) and Coates et al. (1996). Digester effluent was placed into 160-mL serum bottles, sparged with oxygen-free gas (7:3 v/v N_2:CO_2), and sealed with solid black, butyl rubber stoppers. A biomass concentration of 5 to 6 g/L was used for SMA_{Ac} and SMA_{Pr} tests, whereas 300 to 500 mg/L was used for SMA_{H2} tests, all with a total volume of 25 mL. After four days (to consume residual substrate and determine the endogenous biogas production.), the bottles were fed with 15 g/L calcium acetate ($Ca(CH_3COO)_2$), 5 g/L calcium propionate ($Ca(CH_3CH_2COO)_2$), or 100 mL of a CO_2 and H_2 gas mixture (added at a ratio of 1:4, v/v). For the SMA_{Ac} and SMA_{pr}, the biogas volume produced was measured at ambient pressure and 35°C every day using a glass syringe with a wetted glass barrel (Perfektum® Popper & Sons, Inc., New Hyde Park, NY). The SMA_{H2} tests were done similarly, except the decrease in the previously added biogas volume was measured and converted into equivalent CH_4 volume using a stoichiometric ratio (1:4, v/v, CH_4:biogas based on: $4H_2 + CO_2 = CH_4 + 2H_2O$). SMA tests were performed in triplicate at 35°C and 150 rpm using an incubator shaker (model C25KC, New Brunswick Scientific, Edison, NJ).

2.2.5 Physical and Chemical Analysis

Temperature and pH were measured daily using a glass electrode and meter (Orion 4 Star pH-DO Benchtop electrode - 9206BN, Thermo Scientific, Marietta, OH). Feed sludge, effluent, and biogas were sampled two times per week to determine the following parameters (specific method used given in parentheses): total solids (TS) (2540 B), VS (2540 E), soluble chemical oxygen demand (SCOD) (5220 D), and CH_4 composition of the biogas (2720 C) according to standard methods (APHA et al., 1998). VS destruction was calculated for all

digesters at quasi steady state both before and after overload. For SCOD analysis, the samples were thickened at 13,000 rpm for 10 minutes in a centrifuge (Clinical 200 VWR International LLC Radnor, Pennsylvania) and prepared by filtering the supernatant through a 0.45 μm filter (Whatman International Ltd., Maidstone, England). The filtrate COD was then measured using the aforementioned method. The biogas volume produced was collected in PVF bags and measured daily at ambient pressure before feeding using a gas meter (Wet Test Meter, Precision Scientific Petroleum Instruments, San Antonio, TX). Biogas CH_4 content as well as the influent and effluent VFA concentrations were determined by gas chromatography (GC) (Series 7890A GC system, Agilent Technologies, Santa Clara, CA) with a thermal conductivity detector (TCD) and flame ionization detector (FID), respectively. For CH_4 content the carrier gas was helium at a flow of 4.5 mL/min. Temperatures of the injector and detector were 150°C and 250°C, respectively, and the temperature of the oven was 40°C. Individual VFA concentrations (acetic, propionic, butyric, iso-butyric, valeric, and iso-valeric acids) (5560 B) were determined by acidifying samples using 1% phosphoric acid and analyzed as descried in Standard Method 5560D (APHA et al., 2005). For VFA analysis, the carrier gas was helium at a flow of 18 mL/min. Temperatures of the injector and detector were 150°C and 300°C, respectively, and the temperature of the column was 40°C (detector airflow at 400 mL/min, H_2 flow at 30 mL/min).

2.3 Results

2.3.1 Process Configuration Impact on Steady State Digester Function

CH_4 Production and VS Destruction Before Overload. At quasi steady state prior to overload (days 46 to 180), the A/M digester yielded greater VS destruction than both the unstaged control ($p = 1.2 \times 10^{-6}$) and the M/M staged digester ($p = 0.00013$); CH_4 production during this time was also greater in the A/M digester than in the control ($p = 0.0052$) and the M/M digester ($p = 0.020$) (Table 2-2). In the A/M system, nearly all CH_4 production occurred in the second stage, whereas the M/M digester contained two CH_4-producing stages (Table 2-2). Thus, the high loading rate (over 21 g VS/L-d) for the 1.2-day SRT, first stage of the A/M digester led to an acidic environment that fostered the initial steps in the anaerobic degradation pathway (i.e., hydrolysis and acidogenesis), while acetogenesis and methanogenesis were promoted in the second stage of the A/M due to the neutral pH. The low CH_4 content in the first stage and higher CH_4 content in the second stage of the A/M digester biogas affirmed these findings (Table 2-2). The CH_4 content of the second stage of the A/M digester was greater than the control ($p = 8.5 \times 10^{-6}$) as well as the first ($p = 1.3 \times 10^{-5}$) and second ($p = 0.00026$) stages of the M/M digester. While the control biogas had higher CH_4 content than the first ($p = 0.14$) or second ($p = 0.0013$) stages of the M/M digester, the M/M digester demonstrated greater VS destruction ($p = 0.00043$) and CH_4 production ($p = 0.045$) than the unstaged control. Both stages of the M/M digester had pH values that allowed methanogenesis. The pH of the control was different from the second stage pH values of the A/M ($p = 1.0 \times 10^{-67}$) and M/M staged digesters ($p = 9.0 \times 10^{-82}$), but was similar to the first stage of the M/M digester ($p = 0.99$). The pH values of the second stages of the A/M and M/M were statistically different ($p = 0.024$).

Table 2-2. Digester Operating Parameters at Quasi Steady State Prior to Organic Overload (Days 46 to 180)

Digester*	Biogas CH_4 (%)	CH_4 (L/d)	Increase CH_4**	$VS_{destruction}$ (%)***	Increase** $VS_{destruction}$	pH
Control	60 ±1.4	1.35 ±0.03	N/A	67 ±1.5	N/A	7.31 ±0.10
A/M Stage 1	3.1 ±2.6	1.48 ±0.02	10.3%	74 ±1.5	10%	5.16 ±0.29
A/M Stage 2	67 ±2.0					7.46 ±0.10
M/M Stage 1	58 ±2.6	1.42 ±0.01	5.8%	71 ±0.3	5.8%	7.31 ±0.11
M/M Stage 2	38 ±11					7.48 ±0.09

*Single values for both stages indicate totals for both stages of the A/M and M/M staged digesters.
**Percent increase compared to control (CSTR).
***Percentages were based on final (i.e., second stage for the A/M and M/M digesters) effluent concentrations.

Specific Methanogenic Activity (SMA). Compared to the unstaged control, the A/M staged digester SMA values increased by 41, 26, and 57% for SMA_{Pr}, SMA_{Ac}, and SMA_{H2}, respectively (Figure 2-2). Compared to the control, the M/M staged digester SMA values decreased by 34, 2.0, and 18% for SMA_{Pr}, SMA_{Ac}, and SMA_{H2}, respectively; SMA values were 114%, 28%, 91% higher in the A/M digester compared to the M/M staged digester (Figure 2-2).

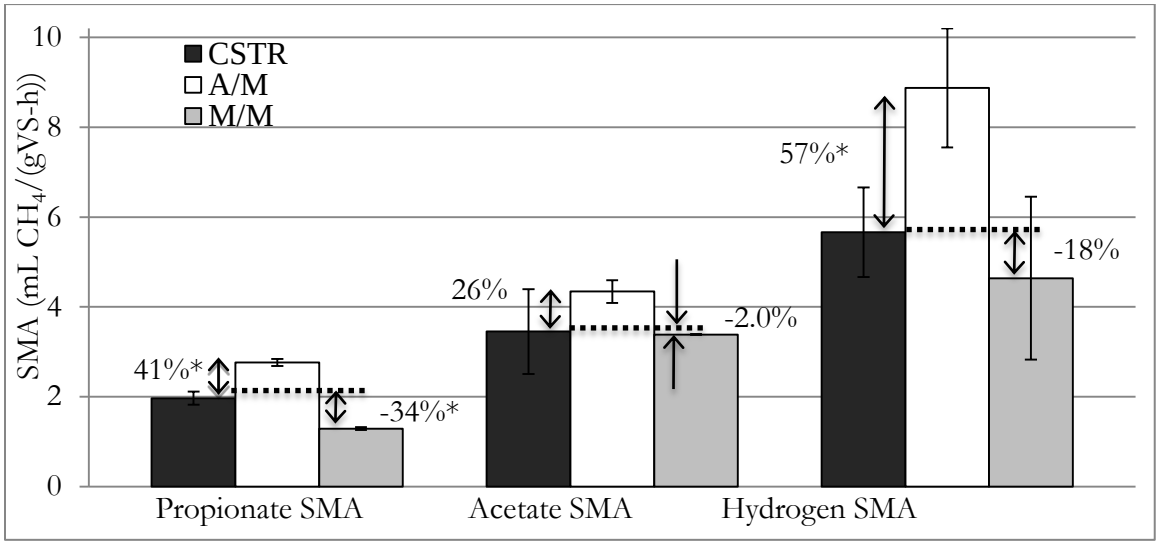

Figure 2-2. Specific Methanogenic Activity (SMA) results with propionate, acetate, and H_2. A/M and M/M activity tests used second stage biomass. Percent change from A/M shown as indicated by arrows and adjacent percentages. Black: CSTR; White: A/M digester; Gray: M/M digester. *Indicates statistical difference from CSTR.

2.3.2 Process Configuration Impacted Resistance to Solids Overload

Maximum Propionate Concentrations and VS Destruction at Quasi Steady State After Overload. Different digester configurations functioned differently during overload. At steady state prior to overloading, total VFA concentration in each digester varied from 300 to 400 mg/L as acetic acid (only acetic and propionic acid were above the 20-mg/L detection limit) (Figure 2-3c). Upon overload, the SCOD values in all reactors increased to slightly above 5 g SCOD/L (Figure 2-3b) and increases in propionate (Figures 2-3c) and acetate concentrations were observed. However, the A/M staged digester exhibited enhanced stability in its resistance to propionate build up, reaching a maximum of 760 mg/L propionate, whereas the unstaged control and M/M staged digester propionate concentrations peaked at 1300 and 2300 mg/L propionate, respectively (Figure 2-3c; Table 2-3). The increase in solids loading rate (SLR) coincided with the propionate spike (Figures 2-3a and 2-3c). The A/M and M/M staged systems returned to pre-overload quasi steady state VS destruction values 24 and 63% faster than the control, respectively, and all digester systems recovered to greater quasi steady state VS destruction values after overload compared to beforehand ($p = 0.0017$, 0.021, and 0.20 in the CSTR, A/M, and M/M digesters, respectively) (Table 2-3).

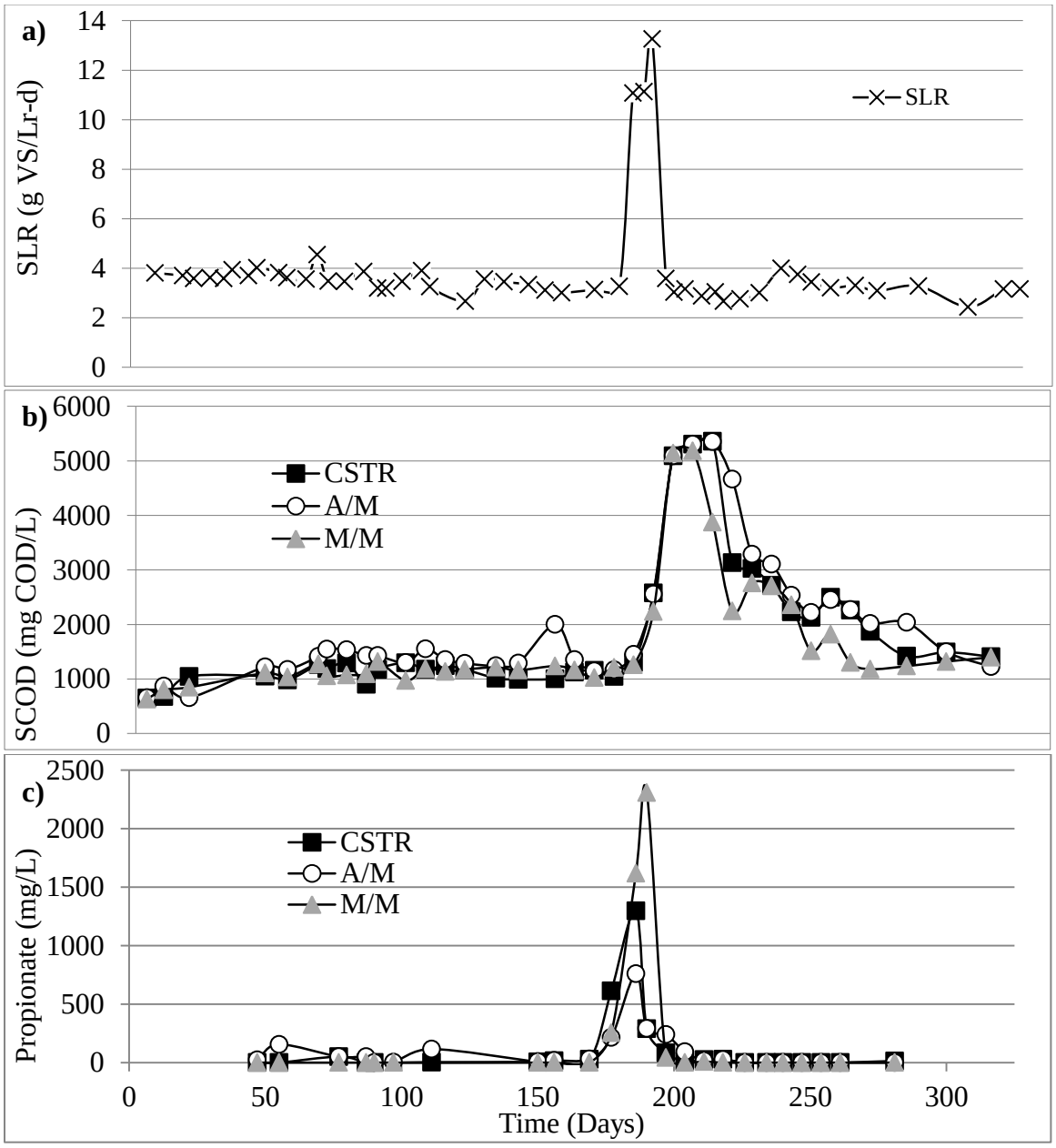

Figure 2-3. Digester performance in response to organic overload: solids loading rate (SLR) (a) effluent SCOD (b), and propionate concentration (c).

Table 2-3. Post-Overload Quasi Steady State VS and Propionate Data

Parameter	Control	A/M	M/M
$VS_{destruction}$ (%)	70±0.00	77±0.03	72±0.01
Difference (%)*	-	10.4%	3.0%
Days to reach QSS**	75	57	28
Difference (%)*	-	24.0%	62.7%
Propionate (mg/L)***	1300	760	2300
Difference (%)*	-	41.5%	(76.9)

*Percent increase or decrease compared to the control (CSTR)
**QSS is quasi steady state after overloading, determined when $VS_{destruction}$ reached pre-overload levels.
***Maximum propionate concentration during organic overload.

Specific methanogenic activities upon overloading. All digesters also had greater quasi steady state SMA_{Ac} and SMA_{Pr} values after solids overload (at 18 SRTs from day 0) than prior to overloading (at six SRTs from day 0); however, the quasi steady state SMA_{H2} values in all digesters after overloading were less than the SMA_{H2} values prior to overloading (Figure 2-4; Appendix A). This suggests a shift in the microbial community to less hydrogenotrophic methanogens and more acetoclastic methanogens.

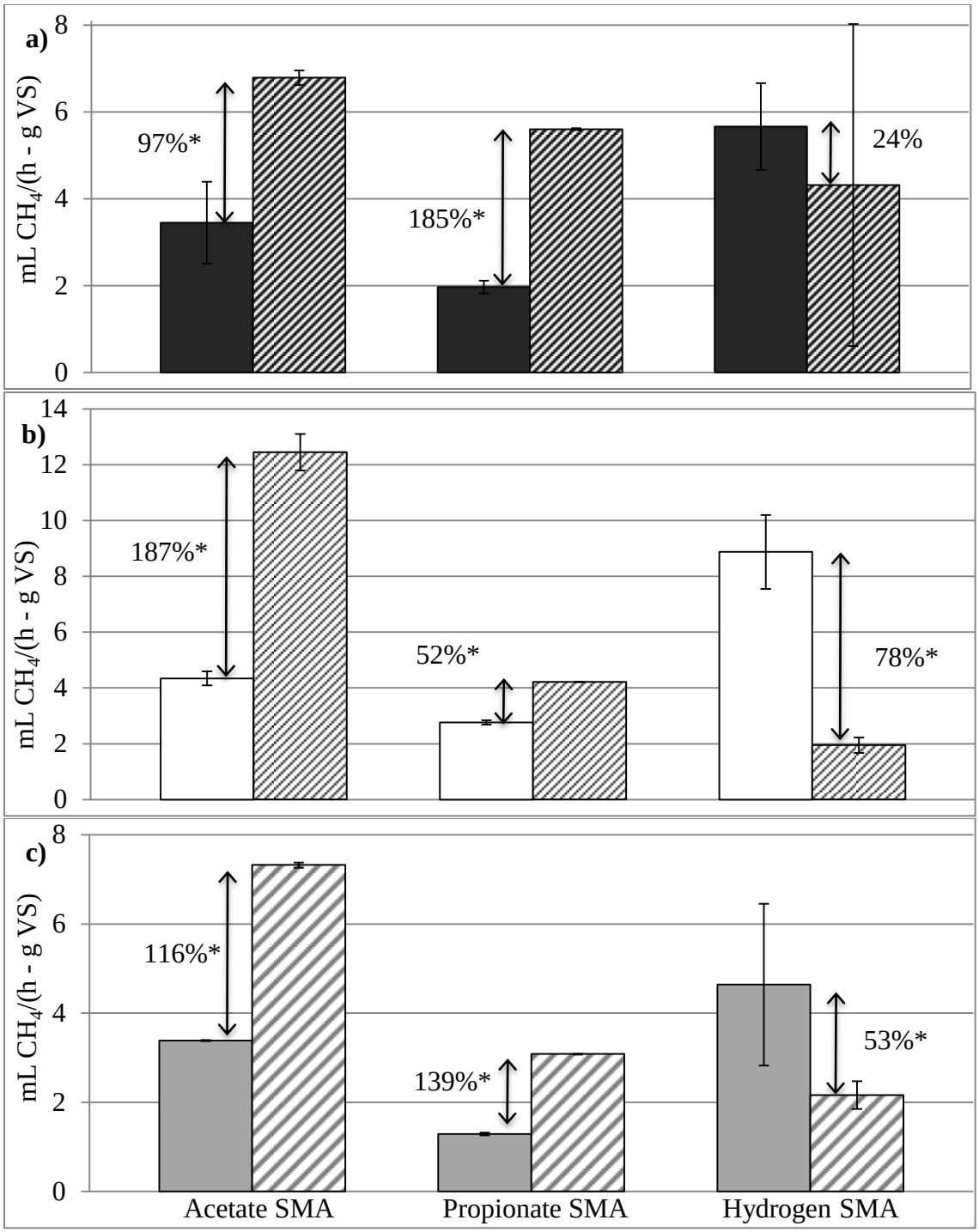

Figure 2-4. SMA values at quasi steady state before (left solid-colored column of each pair) and after (right, hatched column) overload in the CSTR (control) (a), A/M Digester (b), and M/M digester (c). *Indicates statistical difference in SMA values between before and after overload.

2.3.3 Process Configuration Impacted Methanogen Community Structure

The different methanogen communities of unstaged and staged digesters at quasi steady state both before and after overload were distinguished by differences in DGGE fingerprints (Figure 2-5). PCA using band intensities graphically displayed differentiable microbial communities in all three process configurations (Figure 2-6). Relative magnitudes of SMA values were graphically depicted in the size and shape for each symbol on the PCA plot. Progressively higher SMA values were found in those samples with both a greater proportion of the microorganism(s) found in band 2 and less of those found in band 5; thus, band 2 organisms may have played a key role in enhanced CH_4 production and band 5 organisms may be less advantageous to rapid CH_4 production (Figure 2-6).

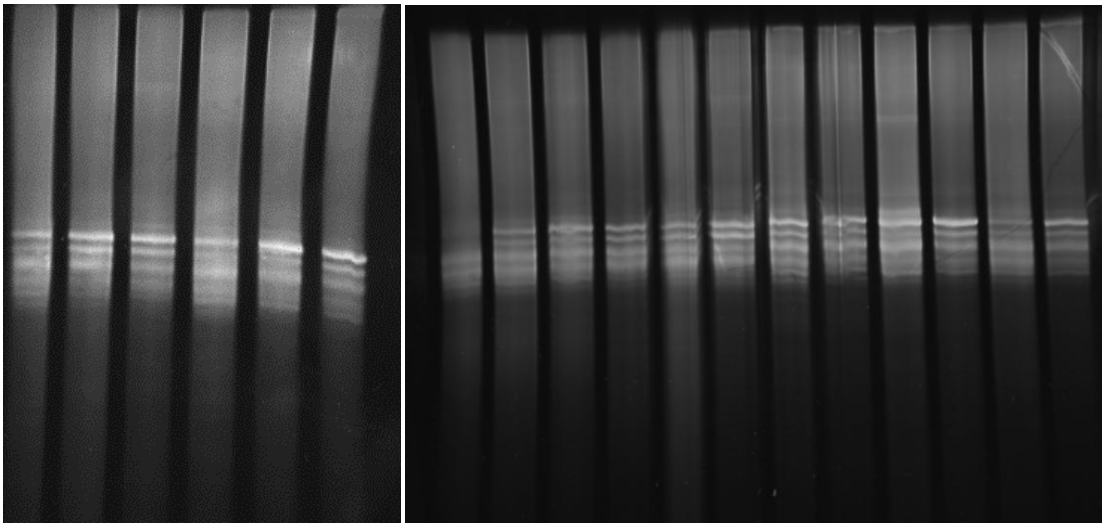

(a) **(b)**

Figure 2-5. DGGE gel for (left to right) (a) CSTR on days 109, 142, 181; A/M staged digester on days 109, 142, 181 and (b) M/M staged digester on days 109, 142, 181; CSTR on days 109 (ladder), 284, 324, and 326; A/M staged digester on days 284, 324, and 326; M/M staged digester on days 284, 324, and 326.
Days 109, 142, and 181 are at quasi steady state prior to overloading. Days 284, 324, and 326 are at quasi steady state after overloading.

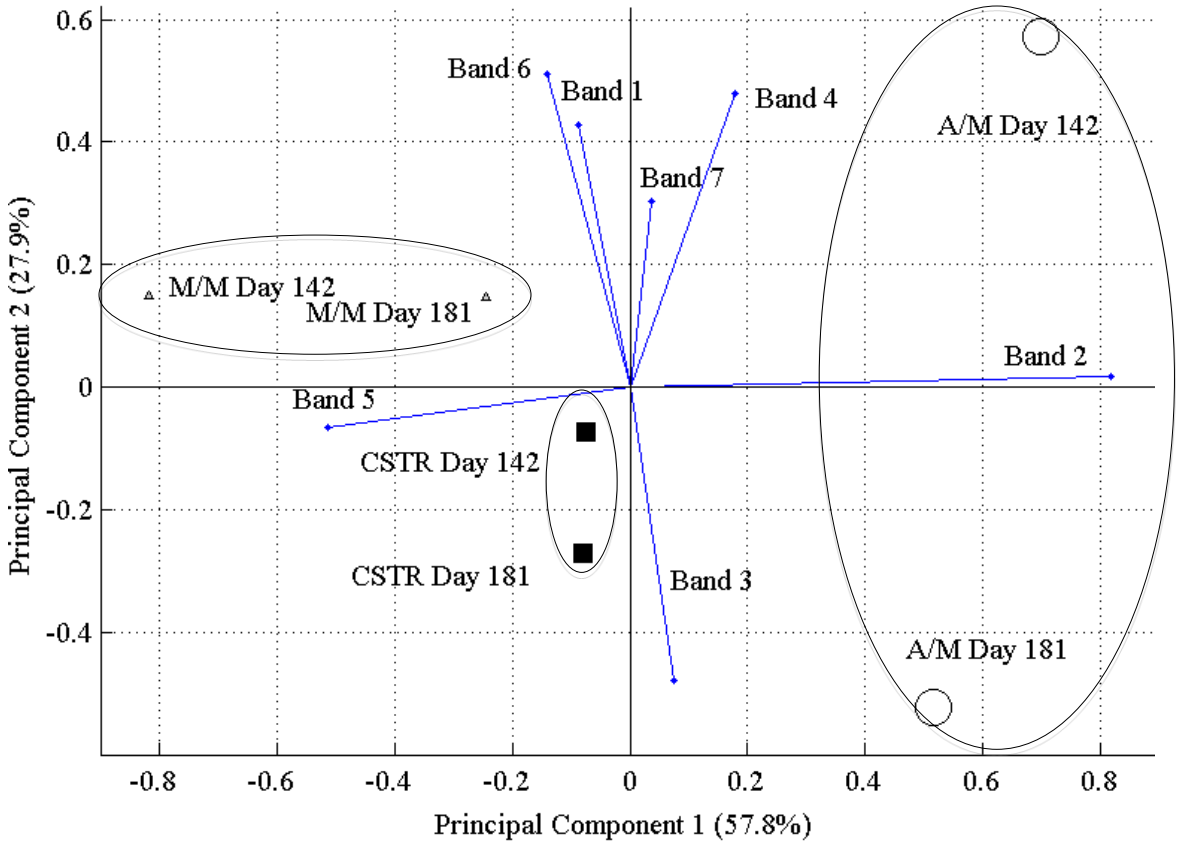

Figure 2-6. Principal Component Analysis (PCA) at steady state before overloading. Points are labeled with the digester description (See Table 2-1) and day the DNA was extracted. The sizes of the squares, circles, and triangles for each of the three digesters (M/M staged, CSTR, and A/M staged, respectively) correspond to the relative sizes of their average SMA values. Ovals represent the grouping of each duplicate sample for the reactors. Where: X_m is the demeaned optical band intensity of m^{th} band for a particular digester. First Principal Component = - 0.0876 (X_1) + 0.4274 (X_2) + 0.2462 (X_3) - 0.1329 (X_4) - 0.1872 (X_5) + 0.7225 (X_6) - 0.4176 (X_7). Second Principal Component = 0.8180 (X_1) + 0.0177 (X_2) + 0.3460 (X_3) - 0.3376 (X_4) + 0.2588 (X_5) + 0.0678 (X_6) + 0.1591 (X_7). Days 109, 142, and 181 are at quasi steady state prior to overloading. Days 284, 324, and 326 are at quasi steady state after overloading.

There was an average of 50 and 70% higher Band 2 intensity in the A/M digester results than the CSTR and M/M digester, respectively (optical density not shown). Furthermore, Band 2 averaged over 30% of the entire lane intensity in the A/M digester, whereas it was only 20% in the CSTR and M/M digester. Thus, it is likely that the difference in activity was a product of greater numbers of phylotypes represented by Band 2. Schauer-Gimenez et al. (2010) and Bhattad (2012) showed *Methanospirillum* species were common (comprising up to 80% or more of a methanogenic community), especially in those

communities that had shorter recovery time following environmental stressors. It is possible Band 2 phylotypes are most similar to *Methanospirillum*.

Evenness among the digesters was different. Since typically 20% of the bands correspond to 40% or more of the total intensity, Wittebolle et al. (2008) suggest measuring evenness at 20% of the phylotypes (x = 0.2), which represented 30 to 40% of the total intensity in this research (Figure 2-7). At 20% of all phylotypes, the A/M digester before overload had the highest Fo (approximately 0.40-0.42 compared to 0.32 to 0.37 in the A/M digester after overload; 0.31 to 0.33 in the M/M digester; and 0.33 before overload and 0.26 to 0.30 after overload in the CSTR) of all samples measured either before or after overload (Figures 2-7a and b). Because Rr values revealed low diversity (6<Rr<9) (Appendix D; Table 2D-1), the unique evenness suggested that all digesters contained the same methanogenic species, yet had different proportions of these species. Rather than similar amounts of each species, the greater SMA values in the A/M digester compared to the CSTR and M/M digester were likely due to a greater presence of dominant species(s), which corresponds to the low evenness in the A/M digester.

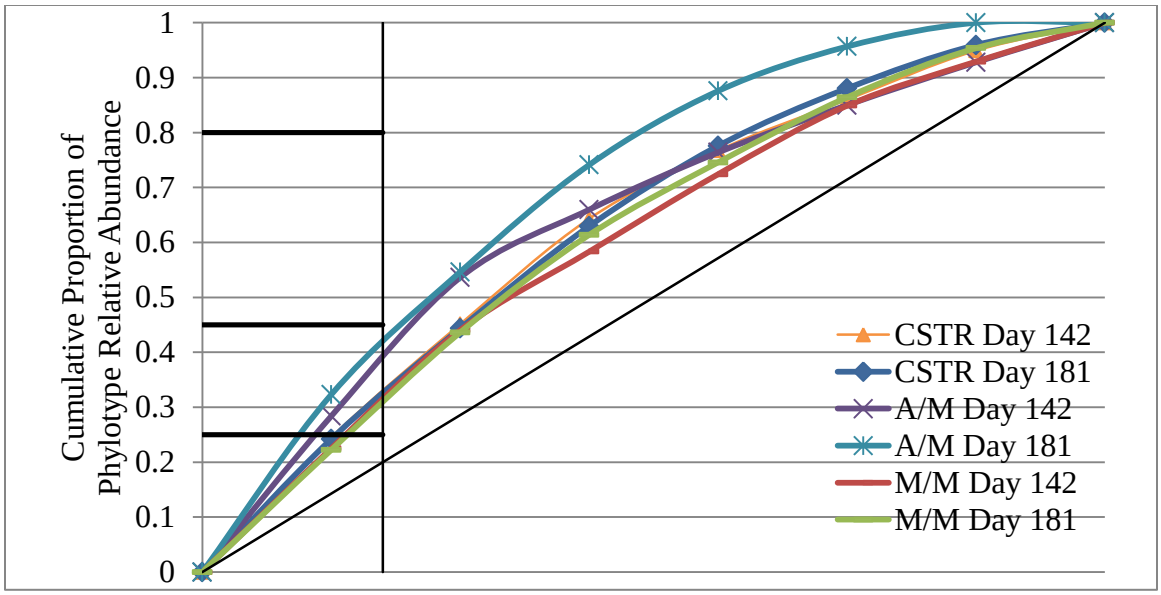

Figure 2-7. Pareto-Lorenz evenness curves depicting Functional organization, Fo, at quasi steady state before overloading. The 45° line represents a perfectly even community (low functional organization).

2.3.3.1 Organic Overload Impacted Methanogen Community Structure Uniquely in Different Process Configurations

In addition to the different effects in digester function (e.g., CH_4 production, VS destruction, resistance and resilience to perturbation, and SMA values) upon overload, different process configurations also exhibited different effects from overload in terms of methanogen community structure. Separate PCA for samples from each of the three digesters helped clarify the effects of overloading in each process configuration. Individual graphs avoided the influence of other digesters on principal components, thereby measuring overload effects for each digester configuration (Figures 2-8, 2-9, and 2-10). In the PCA, the duplicate control (CSTR) and A/M digester samples taken before overloading were separated from the duplicates taken afterward, indicating a distinction in methanogen community structure with respect to before and after overload (Figures 2-8, and 2-9). For example, CSTR samples before overload were more influenced by the presence of Bands 2 and 3, whereas after overload Band 1, 5, 6, and 7 were more influential (Figure 2-8).

Likewise, the A/M digester samples before overload were more influence by the presence of Bands 2, 7, 4, and 3, while those after overload were more influenced by Bands 5, 1, 6, and 3.

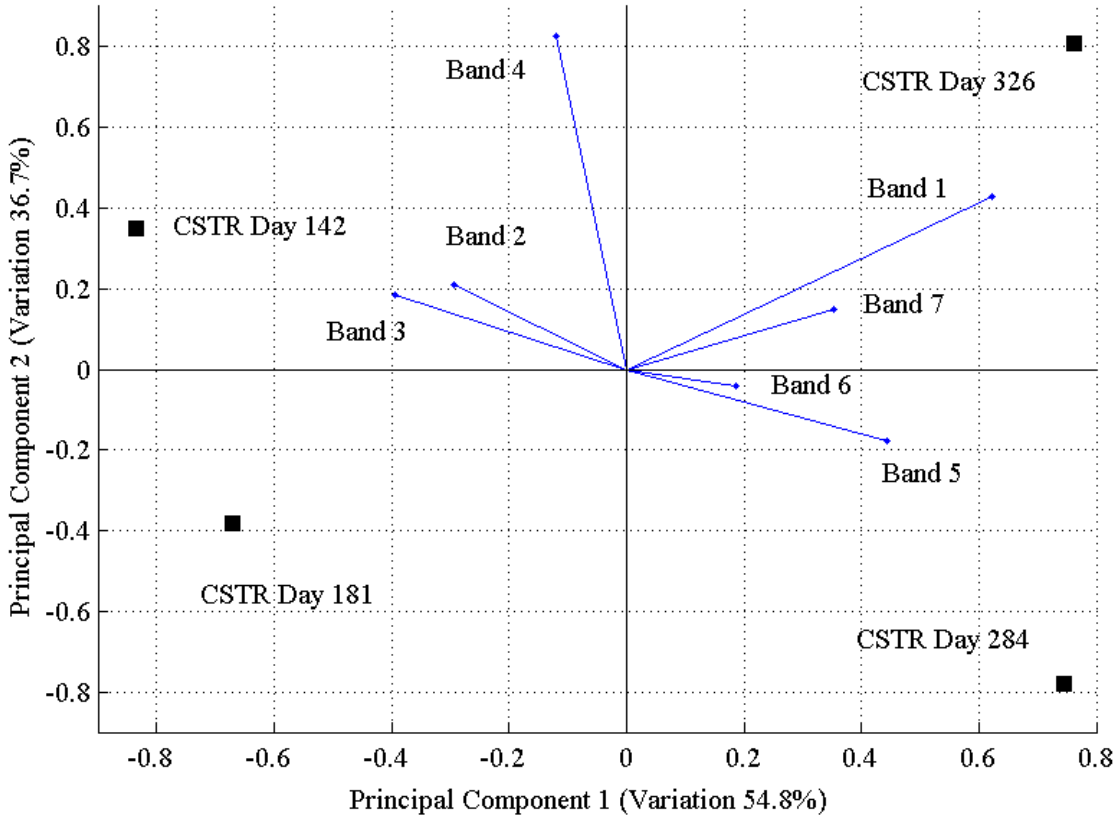

Figure 2-8. PCA for CSTR samples taken before (days 142 and 181) and after (days 284, and 326) overloading.

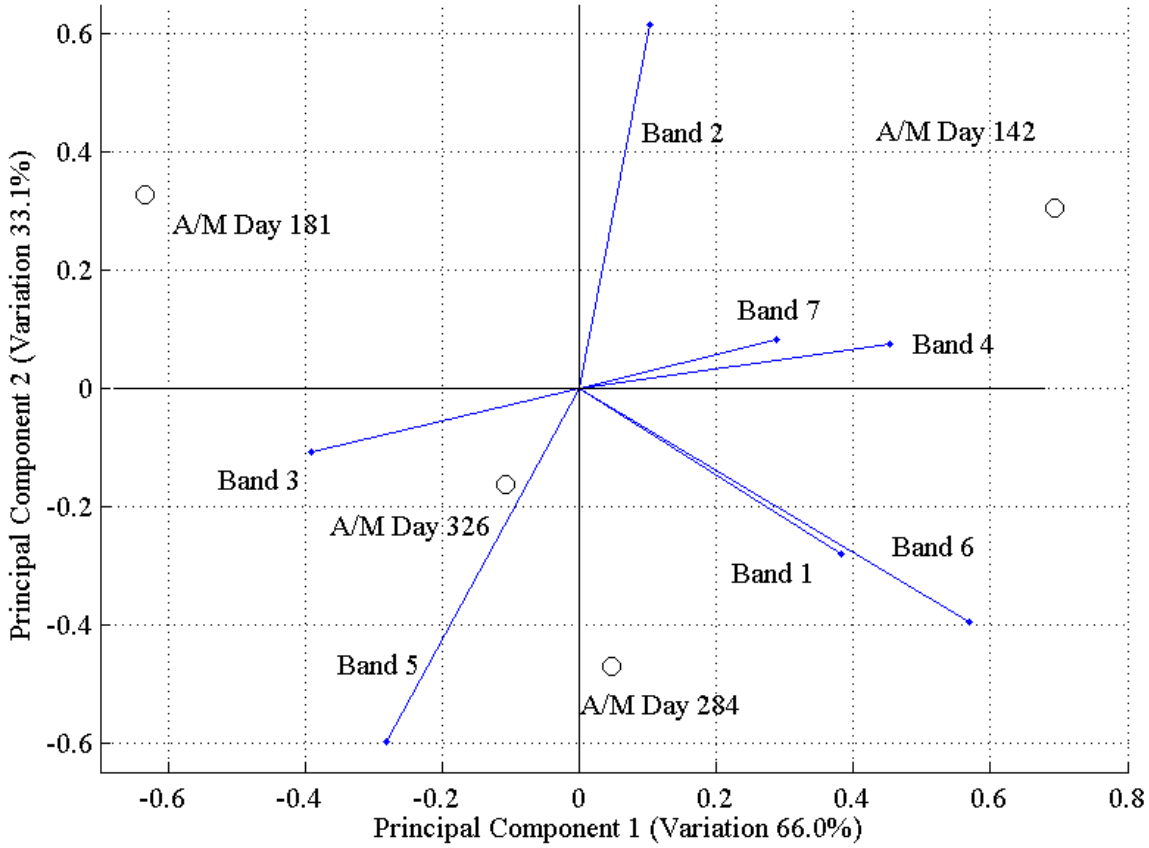

Figure 2-9. PCA for A/M staged digester samples taken before (days 142 and 181) and after (days 284, and 326) overloading.

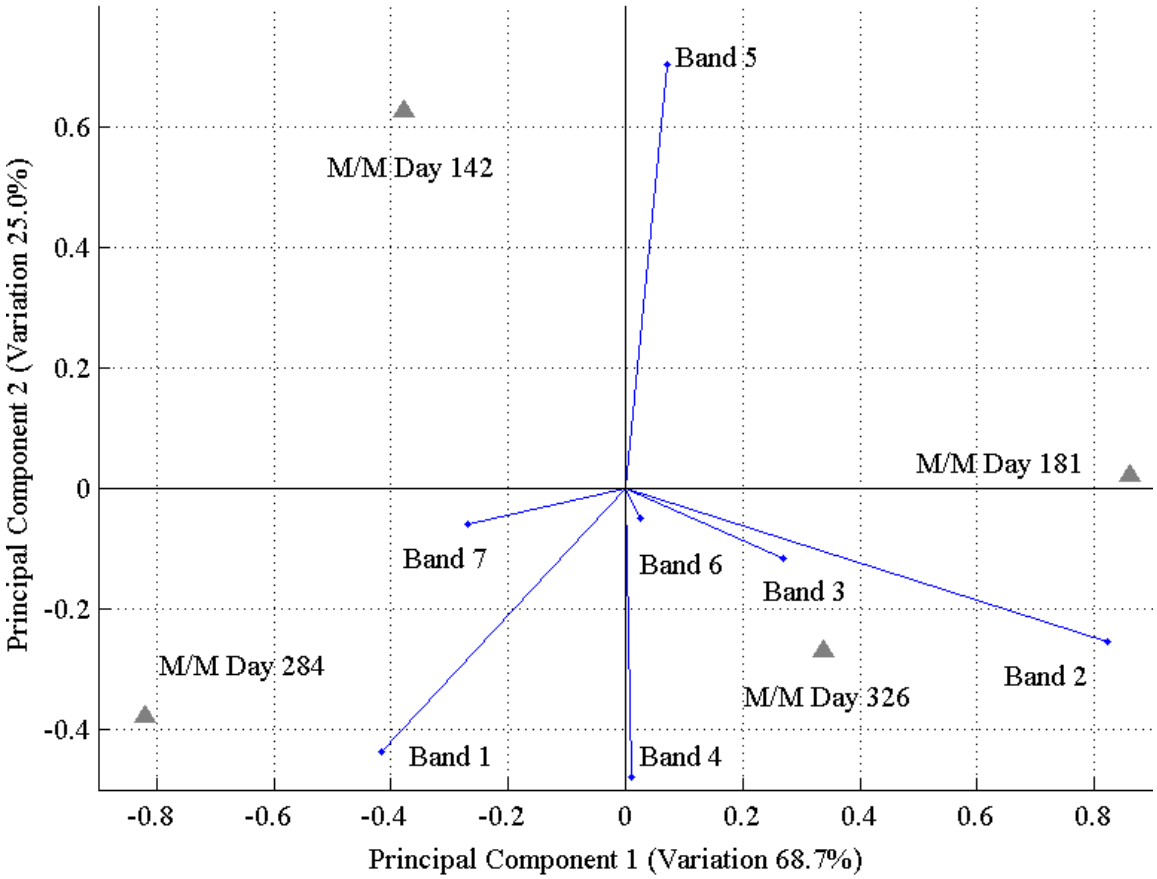

Figure 2-10. PCA for M/M staged digester samples taken before (days 142 and 181) and after (days 284, and 326) overloading.

However, clustering did not depict clear differences in methanogen community before and after overload (Figures 2-11, 12, and 13). Rather, the structures of the pre- and post-overload samples that had the most time to reach steady state (i.e., Day 181 and 326) more closely resembled one another than those communities that had less time to reach steady state (Days 142 and 284), suggesting a slow, gradual convergence of the microbial communities (i.e., the more time the community had to reach steady state, the more the pre- and post-overload communities resembled one another). This convergence was seen in all three digester configurations. The CSTR, A/M staged, and M/M staged samples taken at day 181 clustered closer to the samples taken at day 326 in the same digester (Figures 2-11, 12, 13). UPGMA clustering is shown for all samples on the same plot in Appendix B.

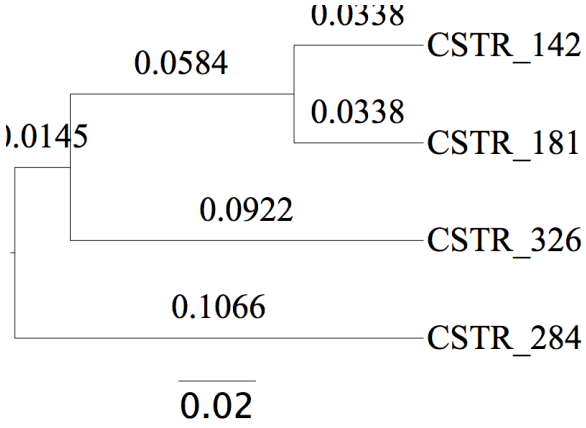

Figure 2-11. Clustering for duplicate control (CSTR) samples taken at quasi steady state before (days 142 and 181) and after (days 284 and 326) overloading using the UPGMA algorithm.

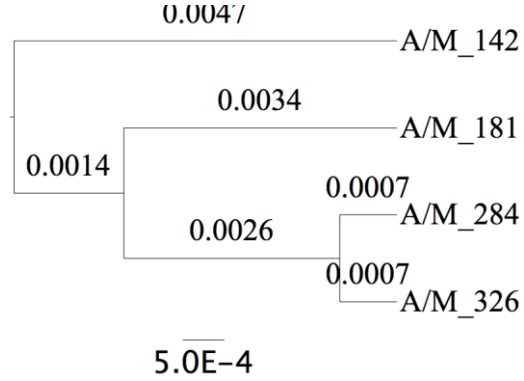

Figure 2-12. Clustering for duplicate A/M digester samples taken at quasi steady state before (days 142 and 181) and after (days 284 and 326) overloading using the UPGMA algorithm.

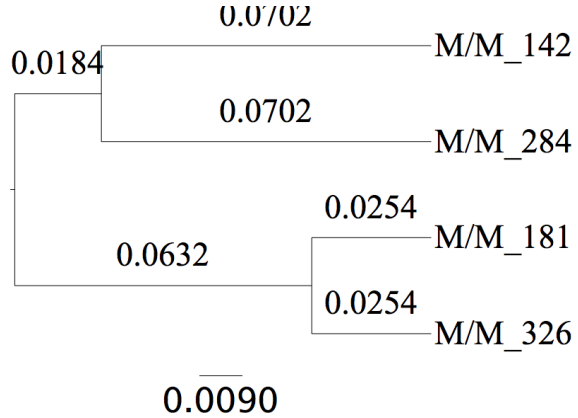

Figure 2-13. Clustering for duplicate M/M digester samples taken at quasi steady state before (days 142 and 181) and after (days 284 and 326) overloading using the UPGMA algorithm.

Similarity distances of samples from days 181 and 326) in the CSTR, M/M, and A/M systems were 0.1844, 0.0508, and 0.0068, respectively, which indicated that the methanogen community of the A/M staged digester changed less than those of the other digester systems. This indicated greater stability in the community structure of the A/M staged digester.

In all three systems, the two samples that had the most time to reach steady state (days 181 and 326) clustered closer together than those two samples that had less time, either from seeding or from overload, to reach steady state (days 142 and 284) (Figures 2-11, 12, and 13). In particular, M/M digester samples from days 181 and 326 clustered more closely than any other M/M samples. This may suggest a convergent methanogen community over a sufficiently long period of time of similar operation.

Rr values indicated similar diversity among all samples before and after overload (Table 2-4). The common seed culture used in all digesters may have a greater effect on the observed methanogen community diversity than organic overload.

Table 2-4. Range Weighted Richness, Rr, at Quasi Steady State Before Overloading

Sample	CSTR Day 142	CSTR Day 181	CSTR Day 284	CSTR Day 326	A/M Day 142	A/M Day 181	A/M Day 284	A/M Day 326	M/M Day 142	M/M Day 181	M/M Day 284	M/M Day 326
Rr	8	8	8	8	8	6	8	8	9	9	9	9
Classification*	L	L	L	L	L	L	L	L	L	L	L	L

*L = low Rr (Rr < 10); M = medium Rr (10 < Rr < 30); H = high Rr (Rr > 30)

Although overloading did not significantly impact the evenness of the M/M digester (Figure 2-14c), the post-overload community evenness was greater in the CSTR (Figure 2-14a) and A/M digester (Figure 2-14b) than in their pre-overload communities (see also Appendix C). The M/M digester had the greatest accumulation of propionate, yet, as seen in

the cluster analysis, the evenness changed less than other digesters (Figure 2-14c). As with both samples from the A/M digester prior to overloading, the steady state A/M digester culture after overloading was the least even of the three configurations (Figure 2-15).

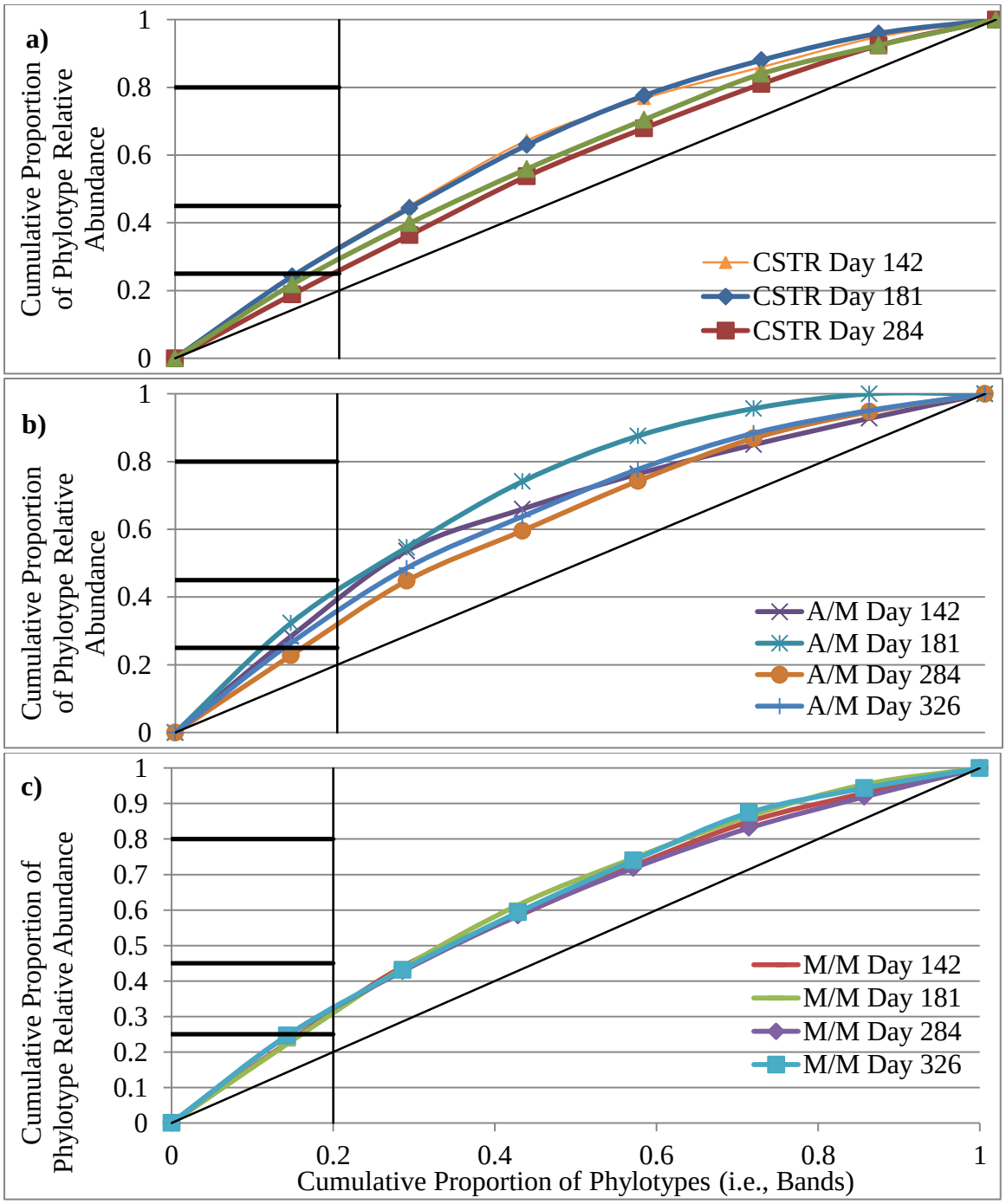

Figure 2-14. Pareto-Lorenz Distribution Curves depicting Functional Organization, Fo, for (a) CSTR, (b) A/M staged, and (c) M/M staged systems before (Days 142 and 181) and after (Days 284 and 326) overload. The 45° line indicates a completely even community (i.e., low Fo). Measurements were taken at 20% of the total phylotypes.

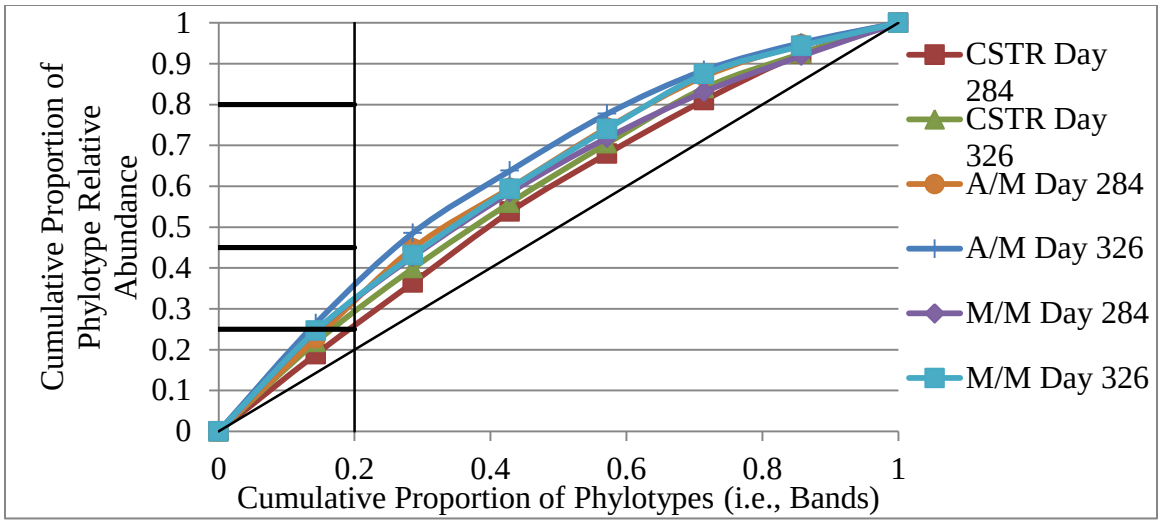

Figure 2-15. Pareto-Lorenz Distribution Curve depicting Functional Organization, Fo, for CSTR, A/M staged, and M/M staged systems at two time points after overload. The 45° line indicates a completely even community (i.e., low Fo). Measurements were taken at 20% of the total phylotypes

2.4 Discussion

Identical overall system solids loading rates and hydraulic retention times in all three systems provided for comparison of an unstaged CSTR with acidogenic-methanogenic staging and two methanogenic tanks in series, both with recycle.

Process Configuration: Methanogen Community Structure. Although all systems were seeded with the same microbial community, different methanogen community structures were observed over time in the unstaged control, A/M staged digester, and M/M staged digester (Figure 2-6). Furthermore, the A/M digester culture was less even (higher Fo) than the CSTR and M/M digester cultures. Therefore, staging altered the methanogen community structure.

Methanogen community is important since H_2 utilization by methanogens is often the rate-limiting step in anaerobic digestion (McInerney et al., 2009). This H_2 is a byproduct from the energetically unfavorable degradation of propionate (McCarty and Smith, 1986),

which has a greater tendency to persist in a digester (Smith and McCarty, 1990). Without H_2 utilization by methanogens, VFA concentrations increase, pH can drop, and CH_4 production may cease, leading to process upset and even digester failure (Dogan et al., 2005).

Process Configuration: Function. A link between process configuration and biomass activity was also determined. A/M staging resulted in more CH_4 and more VS destruction than M/M staging, which outperformed the unstaged control (Table 2-2). The different community structures that were present in different digester configurations resulted in different SMA values (Appendix A). For example, A/M staging had the highest SMA_{Ac}, SMA_{Pr}, and SMA_{H2} values before overloading (Figure 2-2), demonstrating that acidogenic-methanogenic separation in two distinct tanks shifted the methanogen community to a higher-activity biomass compared to unstaged digestion or two methanogenic tanks in series. Significant CH_4 production in the first stage of the M/M digester resulted in low organic loading in the second stage, which may have led to the low activity measured for the M/M digester biomass. Collectively, these operational parameters and activity results revealed that process configuration affected digester function.

The connection between configuration, structure, and function is in agreement with Hawkes et al. (2002) who concluded that changes in process configuration shifted metabolic pathways, which, in turn, altered product yields. Likewise, in this research, staging altered the methanogen community, and thus, process metabolism and the corresponding performance parameters.

Process Configuration: Resistance and Resilience. Process configuration also impacted functional resistance (stability against product build-up) and resilience (ability to rebound after perturbation). For the aforementioned reasons and because it has been used successfully elsewhere as an indicator of process instability (Ma et al., 2009), propionate was

used in this study to monitor response to process overloading. Higher propionate effluent concentrations indicated lower functional resistance of the digester system. Maximum propionate accumulations indicated that the A/M staged digester was 71 and 200% more resistant to perturbation than the control and M/M digester, respectively (Figure 2-3d; Table 2-3). Greater resilience in the methanogen community structure was demonstrated through the shorter clustering distances in the A/M digester from before (day 181) to after (day 326) overload compared to the CSTR and M/M digester (Figures 2-11, 12, and 13).

Organic overload can result in increased VFA concentrations because fermentation occurs more rapidly than methanogenesis. Due to differences in pH and consistency of all other operating parameters (e.g., organic loading rate, feed type), it is most likely that before overload the influent to the second stage of the A/M digester had higher VFAs (fermented in the acidogenic first stage) compared to the influent to the second stage of the M/M digester. Therefore, the microbial community in the A/M second stage was acclimated to higher VFA concentrations that occurred during overload. Thus, the A/M more readily degraded propionate, resisting propionate build up (Table 2-3). However, prior to overloading, the unstaged control was not acclimated to high-VFA concentrations, nor was the second stage of the M/M digester. This lack of acclimation to high-VFA influent concentrations may also explain why the M/M digester had the lowest pre-overload SMA values from its low-organically-loaded second stage biomass (Figure 2-2).

Since propionate is a key intermediate for about 30% of all CH_4 produced in anaerobic processes (Speece, 2008), the greater SMA_{Pr} and resistance to propionate accumulation during overload in the A/M digester was beneficial and related to previous findings that staged digester configuration increases propionate metabolism rate (Azbar et al., 2001).

2.5 Conclusions

Process configuration altered the methanogen community as well as the activity and operational parameters in staged and unstaged digester systems. A/M staging improved digester function (i.e., 10% increase in VS destruction and CH_4 production). The SMA values in the A/M staged digester increased by 41%, 26%, and 57% with propionate, acetate, and H_2, respectively, compared to the single-stage CSTR and by 114%, 28%, 91% compared to the M/M staged digester. The A/M staged digester was 70% more resistant to increased propionate levels when subjected to organic overloading than the CSTR. The diversity (measured as richness, Rr) of the methanogenic community remained the same in all process configurations before and after overloading; yet, the A/M community was less even than other digesters. Organic overloading caused a shift in the methanogenic community, as seen in PCA results as well as functionally in a decline in hydrogenotrophic methanogenesis and an increase in acetoclastic methanogenesis from before to after overloading. Further work is needed to elucidate the organisms responsible for the altered function as well as to optimize the SRT and SLR.

2.6 Supplementary Material

2.6.1 Appendix A: Specific Methanogenic Activity (SMA) Data

Numerical data for all SMA values are presented in Table 2A-1. Differences are shown in the percent increase or decrease, including percent change from before to after overloading.

Table 2A-1. Quasi Steady State SMA Values Before and After Overloading as well as Percent Increase or Decrease From Before to After Overloading

	SMA_{Ac} mL CH_4/ (h-gVS)	StDev	SMA_{Pr} mL CH_4/ (h-gVS)	StDev	SMA_{H2} mL CH_4/ (h-gVS)	StDev
Quasi Steady State Before Overloading						
$CSTR_0$	3.45	0.94	1.97	0.15	5.66	1.00
A/M_0	4.34	0.25	2.77	0.08	8.88	1.32
M/M_0	3.39	0.01	1.29	0.03	4.64	1.81
Quasi Steady State After Overloading						
$CSTR_f$	6.79	0.17	5.60	0.02	4.32	3.71
A/M_f	12.45	0.66	4.21	0.01	1.95	0.27
M/M_f	7.32	0.06	3.08	0.01	2.16	0.31
Percent Increase (+) or Decrease (-) from before to after overloading						
CSTR	97%		185%		-24%	
A/M	187%		52%		-78%	
M/M	116%		139%		-53%	

2.6.2 Appendix B: Cluster Analysis for All Digester Samples

UPGMA cluster analysis was performed on all three digesters before and after overloading (Figure 2B-1).

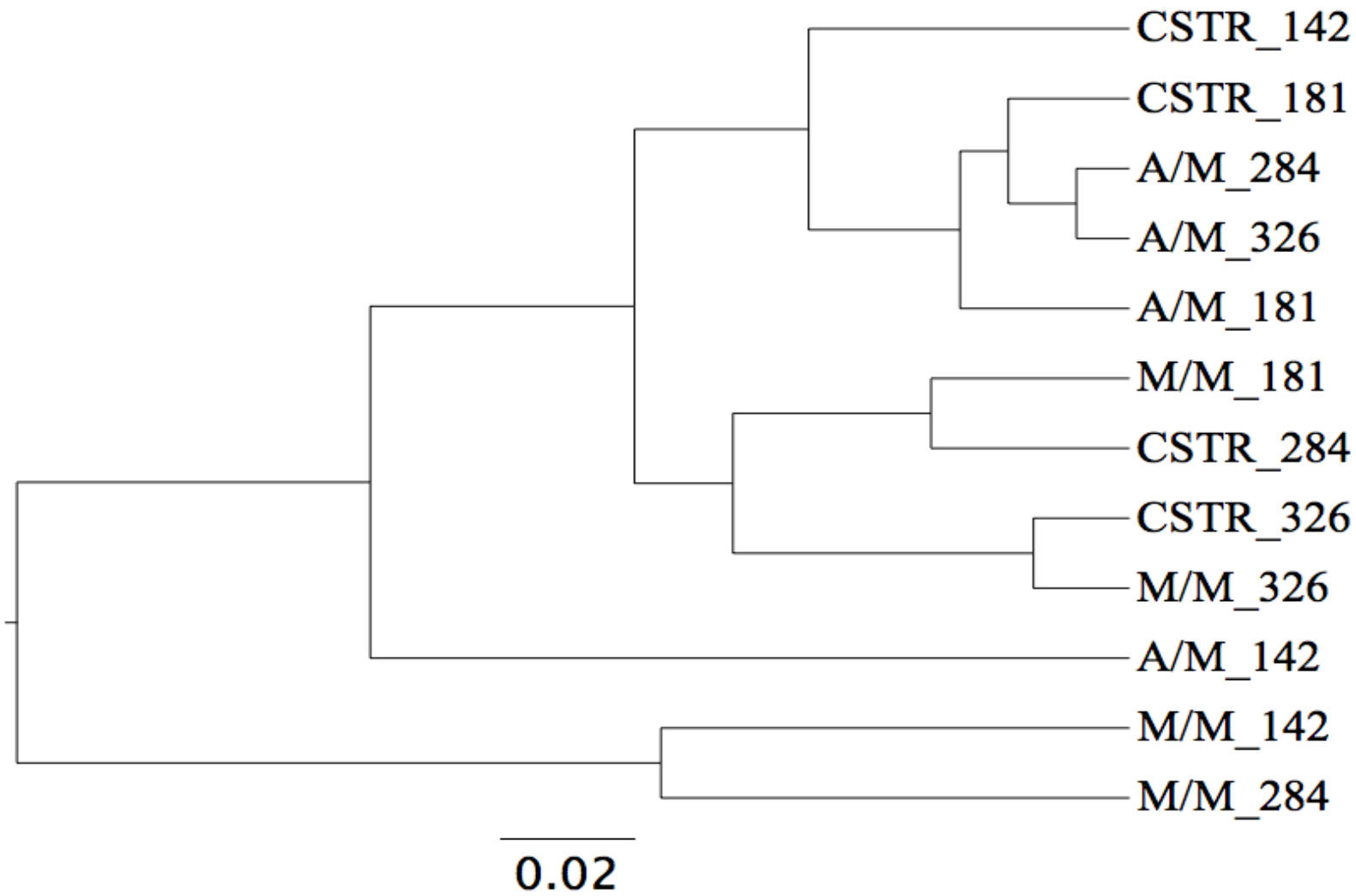

Figure 2B-16. UPGMA cluster analysis for CSTR, A/M digester, and M/M digester samples before (days 142 and 181) and after (days 284 and 326) overload.

2.6.3 Appendix C: Overloading Impacts Richness and Evenness

Pareto Lorenz evenness curves are depicted for all three digesters at two time samples each before and after overload (Figure 2C-1).

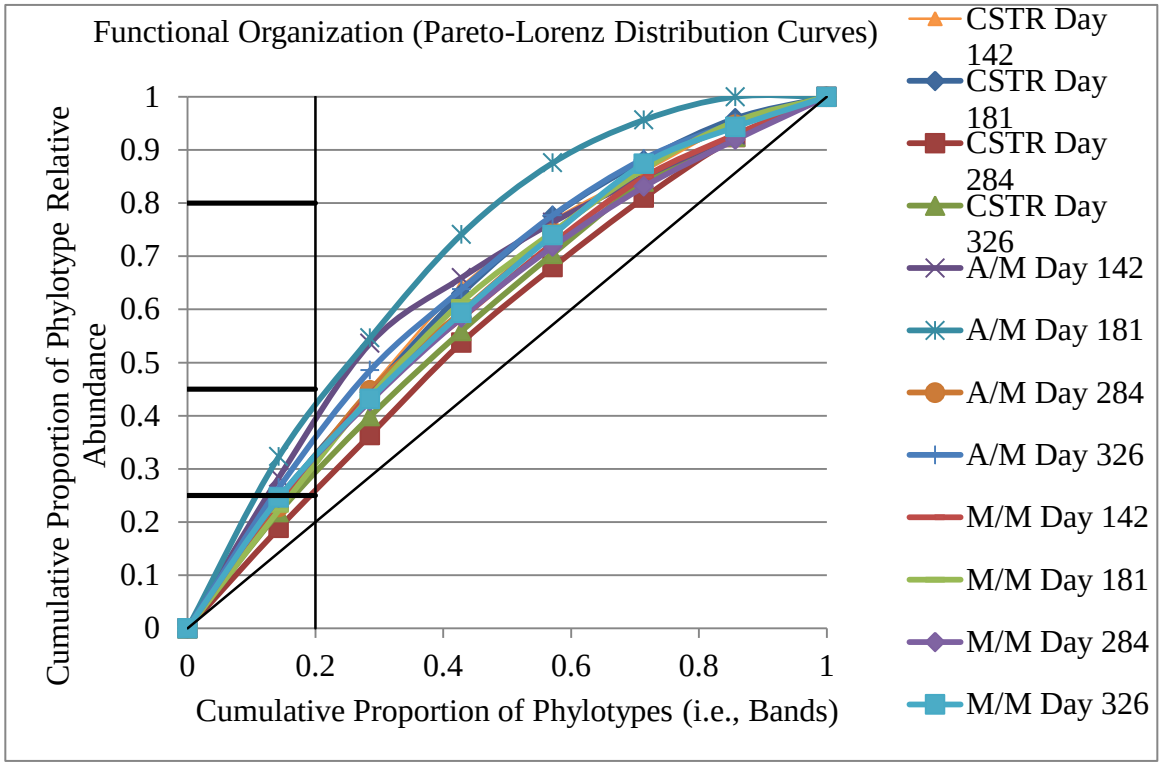

Figure 2C-1. Pareto-Lorenz Distribution Curve depicting Functional Organization, Fo, for CSTR, A/M staged, and M/M staged systems at two time points before (Days 142 and 181) and after (Days 284 and 326) overload. The 45° line indicates a completely even community (i.e., low Fo). Measurements were taken at 20% of the total phylotypes

2.6.4 Appendix D: Staging Related to Microbial Community Richness and Evenness

It is quite possible that the selection of stage-specific microorganisms during digester operation led to organisms that were more well-adapted to perform specific steps in the anaerobic degradation pathway. The Rr values pointed out that there was similar diversity among all samples (Table 2D-1). Evenness among the digesters was different. The A/M

digester samples were less even (Fo approximately 0.40-0.42) than either the control or the M/M digester (Fo approximately 0.31-0.33) (Figure 2D-1). Since typically 20% of the bands correspond to 40% or more of the total intensity, Wittebolle et al. (2008) suggest measuring evenness at 20% of the phylotypes (x = 0.2 in Figure B-1). Though 20% ranged from 30 to 40% of the total intensity, evenness was measured at x = 0.2 because the difference between A/M and other samples remained the same for $0.2 < x < 0.4$. This combination of similar Rr and unique evenness suggested that all digesters contained the same methanogenic species, yet had different proportions of these species. Rather than similar amounts of each species, the greater SMA values in the A/M digester compared to the CSTR and M/M digester were likely due to a greater presence of dominant organisms.

Table 2D-1. Quasi Steady State Range Weighted Richness, Rr, Before Overloading

Sample	CSTR Day 142	CSTR Day 181	CSTR Day 284	CSTR Day 326	A/M Day 142	A/M Day 181	A/M Day 284	A/M Day 326	M/M Day 142	M/M Day 181	M/M Day 284	M/M Day 326
Rr	8	8	8	8	8	6	8	8	9	9	9	9
Classification*	L	L	L	L	L	L	L	L	L	L	L	L

*L = low Rr (Rr < 10); M = medium Rr (10 < Rr < 30); H = high Rr (Rr > 30)

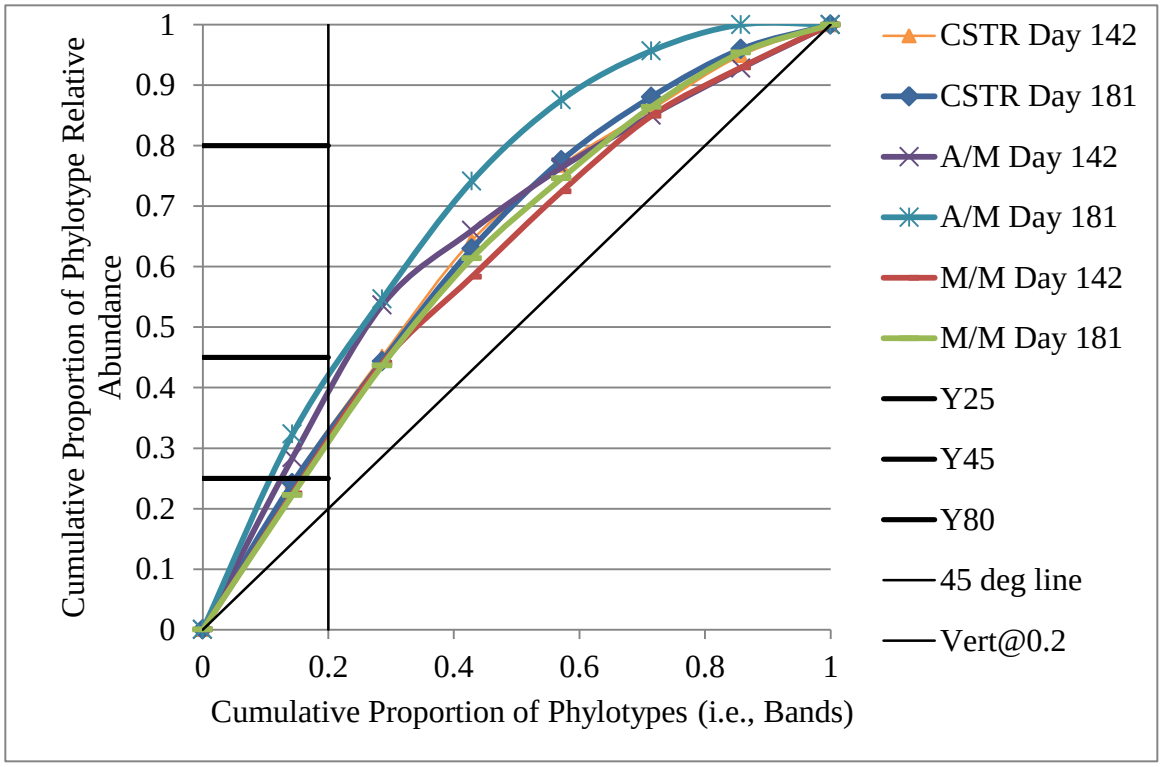

Figure 2D-1. Pareto-Lorenz evenness curves depicting Functional organization, Fo, at quasi steady state before overloading. The 45° line represents a perfectly even community (low functional organization).

2.7 REFERENCES

Anderson, G. K., Kasapgil, B., & Ince, O. (1994). Microbiological study of two stage anaerobic digestion start-up. *Water Research*, *28*, 2383-2392. Retrieved from http://www.ncbi.nlm.nih.gov/pubmed/12146643

Andersson, J., & Björnsson, L. (2002). Evaluation of straw as a biofilm carrier in the methanogenic stage of two-stage anaerobic digestion of crop residues. *Bioresource Technology*, *85*(1), 51-6. Retrieved from http://www.ncbi.nlm.nih.gov/pubmed/12146643

Angelidaki, I., Alves, M., Bolzonella, D., Borzacconi, L., Campos, L., Guwy, A., Jeníicek, P., et al. (2006). *Anaerobic Biodegradation, Activity and Inhibition (ABAI): Task Group Meeting Report. October* (pp. 1-29).

APHA: Standard Methods for the Examination of Water and Wastewater (1998). 20th ed., American Public Health Association/American Water Works Association/Water Environment Federation, Washington D.C., USA.

APHA: Standard Methods for the Examination of Water and Wastewater (2005). 21st ed., American Public Health Association/American Water Works Association/Water Environment Federation, Washington D.C., USA.

Azbar, N., Ursillo, P., & Speece, R. E. (2001). Effect of process configuration and substrate complexity on the performance of anaerobic processes. *Water Research*, *35*(3), 817-829. Retrieved from http://www.ncbi.nlm.nih.gov/pubmed/11228981

Azbar, N., & Speece, R. E. (2001). Two-phase, two-stage, and single-stage anaerobic process comparison. *Journal of Environmental Engineering-ASCE*, *127*(3), 240-248.

Batstone, D. J., Keller, J., Angelidaki, I., Kalyuzhnyi, S. V., Pavlostathis, S. G., Rozzi, A., Sanders, W. T. M., et al. (2002). The IWA Anaerobic Digestion Model No. 1 (ADM1). *Water Science and Technology*, *45*(10), 65-73. Retrieved from http://www.ncbi.nlm.nih.gov/pubmed/12188579

Bhattad, U. H. (2012). *Preservation of methanogenic cultures to enhance anaerobic digestion*. Ph.D. Thesis, Civil, Construction, and Environmental Engineering, Marquette University, Milwaukee, WI, USA.

Bidle, K. A, Kastner, M., & Bartlett, D. H. (1999). A phylogenetic analysis of microbial communities associated with methane hydrate containing marine fluids and sediments in the Cascadia margin (ODP site 892B). *FEMS Microbiology Letters*, *177*(1), 101-8. Retrieved from http://www.ncbi.nlm.nih.gov/pubmed/10436927

Blumensaat, F., & Keller, J. (2005). Modelling of two-stage anaerobic digestion using the IWA Anaerobic Digestion Model No. 1 (ADM1). *Water Research*, *39*(1), 171-83. doi:10.1016/j.watres.2004.07.024

Bocher, B. T., Agler, M. T., Garcia, M. L., Beers, A. R., & Angenent, L. T. (2008). Anaerobic digestion of secondary residuals from an anaerobic bioreactor at a brewery to enhance bioenergy generation. *Journal of Industrial Microbiology & Biotechnology*, *35*(5), 321-9. doi:10.1007/s10295-007-0295-4

Briones, a. (2003). Diversity and dynamics of microbial communities in engineered environments and their implications for process stability. *Current Opinion in Biotechnology*, *14*(3), 270-276. doi:10.1016/S0958-1669(03)00065-X

Cavinato C., D. Bolzonella, F. Fatone, F. Cecchi, P. Pavan, Two-phase thermophilic anaerobic digestion process for biohythane production treating biowaste, in *International Water Association Specialty Group on Anaerobic Digestion: 12th World Congress on Anaerobic Digestion*. 2010: Guadalajara, Mexico 2010, IWA Publishing: Guadalajara, Mexico.

Chouari, R., Le Paslier, D., Daegelen, P., Ginestet, P., Weissenbach, J., & Sghir, A. (2005). Novel predominant archaeal and bacterial groups revealed by molecular analysis of an anaerobic sludge digester. *Environmental Microbiology*, *7*(8), 1104-15. doi:10.1111/j.1462-2920.2005.00795.x

Coates J.D., Coughlan M.F. and Colleran E. (1996). Simple method for the measurement of the hydrogenotrophic methanogenic activity of anaerobic sludges. *Journal of Microbiology Methods*. 26(3), 237-246.

Cohen A., Zoctemeyer R. J., Van Deursen A. & Van Andel J. G. (1979) Anaerobic digestion of glucose with separated acid production and methane formation. *Water Research* 13, 571-580.

Cohen, A., Breure, A. M., van Andel, J. G., & van Deursen, A. (1980). Influence of Phase-Separation on the Anaerobic-Digestion of Glucose--I Maximum COD Turnover Rate during Continuous Operation. *Water Research*, *4*(10), 1439-1448.

Curtis, T. P., Head, I. M., & Graham, D. W. (2003). Theoretical Ecology for Engineering Biology. *Environmental Science and Technology*, *37*(3), 64A-70A. doi:10.1021/es0323493

Demirer, G. N., & Chen, S. (2005). Two-phase anaerobic digestion of unscreened dairy manure. *Process Biochemistry*, *40*(11), 3542-3549. doi:10.1016/j.procbio.2005.03.062

Dogan, T., Ince, O., Oz, N., & Ince, B. (2005). Inhibition of Volatile Fatty Acid Production in Granular Sludge from a UASB Reactor. *Journal of Environmental Science and Health, Part A: Toxic/Hazardous Substances & Environmental Engineering*, *40*(3), 633-644. doi:10.1081/ESE-200046616

Elmitwalli, T. A., Soellner, J., Keizer, A. D. E., Zeeman, G., & Lettinga, G. (2001). Biodegrabability and Change of Physical Characteristics of Particles During Anaerobic Digestion of Sewage. *Water Research*, *35*(5), 1311-1317.

Fernandez, A. S., Hashsham, S. A., Dollhopf, S. L., Raskin, L., Glagoleva, O., Dazzo, F. B., Hickey, R. F., et al. (2000). Flexible Community Structure Correlates with Stable

Community Function in Methanogenic Bioreactor Communities Perturbed by Glucose. *Applied and Environmental Microbiology*, *66*(9), 4058-4067. doi:10.1128/AEM.66.9.4058-4067.2000.Updated

Foresti, E., Zaiat, M., & Vallero, M. (2006). Anaerobic Processes as the Core Technology for Sustainable Domestic Wastewater Treatment: Consolidated Applications, New Trends, Perspectives, and Challenges. *Reviews in Environmental Science and Bio/Technology*, *5*(1), 3-19. doi:10.1007/s11157-005-4630-9

Galand, P. E., Saarnio, S., Fritze, H., & Yrjälä, K. (2002). Depth related diversity of methanogen *Archaea* in Finnish oligotrophic fen. *FEMS Microbiology Ecology*, *42*(3), 441-9. doi:10.1111/j.1574-6941.2002.tb01033.x

Gebrezgabher, S. A., Meuwissen, M. P. M., Prins, B. a. M., & Lansink, A. G. J. M. O. (2010). Economic analysis of anaerobic digestion—A case of Green power biogas plant in The Netherlands. *NJAS - Wageningen Journal of Life Sciences*, *57*(2), 109-115. Royal Netherlands Society for Agriculture Sciences. doi:10.1016/j.njas.2009.07.006

Hartmann, P., Ibáñez, V. A., & Sainz, F. J. F. (2005). Green branding effects on attitude: functional versus emotional positioning strategies. *Marketing Intelligence and Planning*, *23*(1), 9-29. doi:10.1108/02634500510577447

Hartwell, L.H., Hood L., Goldberg, M.L., Reynolds, A.E., Silver, L.M., and Veres, R.C. (2004) *Genetics: From Genes to Genomes*. 2nd ed. McGraw-Hill Companies, Inc. New York, NY.

Hashsham, S. A., Fernandez, A. S., Dollhopf, S. L., Dazzo, F. B., Hickey, R. F., Tiedje, J. M., & Criddle, C. S. (2000). Parallel processing of substrate correlates with greater functional stability in methanogenic bioreactor communities perturbed by glucose. *Applied and Environmental Microbiology*, *66*(9), 4050-7. Retrieved from http://www.pubmedcentral.nih.gov/articlerender.fcgi?artid=92258&tool=pmcentrez&rendertype=abstract

Hawkes, F. R., Dinsdale, R., Hawkes, D. L., & Hussy, I. (2002). Sustainable fermentative hydrogen production: challenges for process optimisation. *International Journal of Hydrogen Energy*, *27*, 1339-1347.

Holm-Nielsen, J. B., Al Seadi, T., & Oleskowicz-Popiel, P. (2009). The future of anaerobic digestion and biogas utilization. *Bioresource technology*, *100*(22), 5478-84. Elsevier Ltd. doi:10.1016/j.biortech.2008.12.046

Kade, F. (2004) *Enhancing Solids Destruction from Anaerobic Municipal Digesters*, in *Civil and Environmental Engineering*. Master's Thesis. Marquette University Milwaukee, WI, USA.

Kida, K., Morimura, S., & Sonoda, Y. (1993). Accumulation of Propionic Acid during Anaerobic Treatment of Distillery Wastewater from Barley-Shochu Making. *Journal of Fermentation and Bioengineering*, *75*(3), 213-216.

Leclerc, M., Delgenes, J.P., and Godon, J.J. (2004). Diversity of the archaeal community in 44 anaerobic digesters as determined by single strand conformation polymorphism analysis and 16S rDNA sequencing. *Environmental Microbiology*. 6(8), 809-819.

Lettinga, G. (1995). Anaerobic digestion and wastewater treatment systems. *Antonie van Leeuwenhoek*, *67*, 3-28.

Lettinga, G. (2005). The anaerobic treatment approach towards a more sustainable and robust environmental protection. *Water Science and Technology*, *52*(1-2), 1-11. Retrieved from http://www.ncbi.nlm.nih.gov/pubmed/16180404

Liu, T. (1998). Anaerobic Digestion of Substrates in an Innovative Two-Phase Plug-Flow Reactor (TPPFR) and a Conventional Single-Phase Continuously stirred-tank reactor 1998 Liu.pdf. *Water Science and Technology*, *38*(8-9), 453-461.

Lueders, T., Chin, K.-J., Conrad, R., & Friedrich, M. (2001). Molecular analyses of methyl-coenzyme M reductase alpha-subunit (mcrA) genes in rice field soil and enrichment cultures reveal the methanogenic phenotype of a novel archaeal lineage. *Environmental Microbiology*, *3*(3), 194-204.

Luton, P. E., Wayne, J. M., Sharp, R. J., & Riley, P. W. (2002). The *mcrA* gene as an alternative to 16S rRNA in the phylogenetic analysis of methanogen populations in landfill. *Microbiology*, *148*, 3521-30. Retrieved from http://www.ncbi.nlm.nih.gov/pubmed/12427943

Ma, J., Carballa, M., Van De Caveye, P., & Verstraete, W. (2009). Enhanced propionic acid degradation (EPAD) system: proof of principle and feasibility. *Water Research*, *43*(13), 3239-48. Elsevier Ltd. doi:10.1016/j.watres.2009.04.046

Marzorati, M., Wittebolle, L., Boon, N., Daffonchio, D., & Verstraete, W. (2008). How to get more out of molecular fingerprints: practical tools for microbial ecology. *Environmental Microbiology*, *10*(6), 1571-1581. Elsevier B.V. Retrieved from http://www.ncbi.nlm.nih.gov/pubmed/18331337

McCarty, P., and Smith, D. (1986). Anaerobic wastewater treatment. *Environmental Science and Technology*, *20*(12), 1200-1206.

McCarty, P. L., Bae, J., & Kim, J. (2011). Domestic wastewater treatment as a net energy producer--can this be achieved? *Environmental Science and Technology*, *45*(17), 7100-6. doi:10.1021/es2014264

McInerney, M. J., Sieber, J. R., & Gunsalus, R. P. (2009). Syntrophy in anaerobic global carbon cycles. *Current Opinion in Biotechnology*, *20*(6), 623-32. doi:10.1016/j.copbio.2009.10.001

Mertens, B., Boon, N., & Verstraete, W. (2005). Stereospecific effect of hexachlorocyclohexane on activity and structure of soil methanotrophic communities. *Environmental Microbiology*, *7*(5), 660-669. doi:10.1111/j.1462-2920.2004.00735.x

Navaratnam, N. (2012). *Anaerobic co-digestion for enhanced renewable energy and green house gas emission reduction*, Ph.D. Thesis, Civil, Construction, and Environmental Engineering. Marquette University, Milwaukee, USA.

Ohkuma, M., Noda, S., Horikoshi, K., & Kudo, T. (1995). Phylogeny of symbiotic methanogens in the gut of the termite Reticulitermes speratus. *FEMS Microbiology Letters*, *134*(1), 45-50. Retrieved from http://www.ncbi.nlm.nih.gov/pubmed/8593954

Pohland, F. G. (1971). Development in anaerobic stabilization of organic waste: the two phase concept. *Environmental Letters*, *1*(4), 255-266.

Rastogi, G., Ranade, D. R., Yeole, T. Y., Patole, M. S., & Shouche, Y. S. (2008). Investigation of methanogen population structure in biogas reactor by molecular characterization of methyl-coenzyme M reductase A (mcrA) genes. *Bioresource Technology*, *99*(13), 5317-26. doi:10.1016/j.biortech.2007.11.024

Rivière, D., Desvignes, V., Pelletier, E., Chaussonnerie, S., Guermazi, S., Weissenbach, J., Li, T., et al. (2009). Towards the definition of a core of microorganisms involved in anaerobic digestion of sludge. *The ISME Journal*, *3*(6), 700-14. doi:10.1038/ismej.2009.2

Sambrook, J. and Russell, D.W., 2001. Molecular Cloning: A Laboratory Manual, 3rd Ed., Cold Spring Harbor Laboratory Press, Cold Springs, NY.

Schauer, A. (2008) *Bioaugmentation for Recovery of Anaerobic Digesters Subjected to a Toxicant*. Ph.D. Dissertation. Anaerobic Biotechnology Group, Marquette University, Milwaukee, WI, U.S.A.

Schauer-Gimenez, A. E., Zitomer, D. H., Maki, J. S., & Struble, C. a. (2010). Bioaugmentation for improved recovery of anaerobic digesters after toxicant exposure. *Water research*, *44*(12), 3555-64. Elsevier Ltd. doi:10.1016/j.watres.2010.03.037

Shin, S. G., Han, G., Lim, J., Lee, C., & Hwang, S. (2010). A comprehensive microbial insight into two-stage anaerobic digestion of food waste-recycling wastewater. *Water Research*, *44*(17), 4838-49. doi:10.1016/j.watres.2010.07.019

Siegrist, H., Vogt, D., Garcia-Heras, J. L., & Gujer, W. (2002). Mathematical model for meso- and thermophilic anaerobic sewage sludge digestion. *Environmental Science and Technology*, *36*(5), 1113-23. Retrieved from http://www.ncbi.nlm.nih.gov/pubmed/11917999

Smith, L.H. (1996) *Performance of a Two-Stage Process for Cometabolic Treatment of Trichloroethylene-Contaminated Water by Methane-OxidizingMixed Cultures*, in *Department of Civil Engineering*. Thesis. Stanford University: Stanford, CA.

Smith, D. P., & Mccarty, P. L. (1990). Factors governing shock following methane loading fluctuations of digesters. *Water Pollution Control*, *62*(1), 58-64.

Speece, R.E. (1988) A Survey of Municipal Anaerobic Sludge Digesters and Diagnostic Activity Assays. *Water Research*, 22(3), 365-372.

Speece, R.E. (2008) *Anaerobic Biotechnology and Odor/Corrosion Control for Municipalities and Industries*; Archae Press: Nashville Tennessee.

Tale, V. P., Maki, J. S., Struble, C. A., & Zitomer, D. H. (2011). Methanogen community structure-activity relationship and bioaugmentation of overloaded anaerobic digesters. *Water Research*, *45*(16), 5249-5256. Elsevier Ltd. doi:10.1016/j.watres.2011.07.035

Tale, V. (2010). *Bioaugmentation for Recovery of Anaerobic Digesters Subjected to Organic Overload*, in Ph.D. Thesis. Civil and Environmental Engineering. Marquette University: Milwaukee, WI, USA.

Vandenburgh, S. R., & Ellis, T. G. (2002). Effect of Varying Solids Concentration and Organic Loading on the Performance of Temperature Phased Anaerobic Digestion Process. *Water Environment Research*, *74*(2), 142-148.

Wang, F., T Oishi, T Hidaka, S Osumi, J Tsubota, H Tsuno, *DIgradation characteristics of polylactide in thermophilic anaerobic digestion with hyperthermophilic solubilization phase*, in *International Water Association: 12th World Congress on Anaerobic Digestion*. 2010, IWA Publishing: Guadalajara, Mexico.

Werner, J. J., Knights, D., Garcia, M. L., Scalfone, N. B., Smith, S., Yarasheski, K., Cummings, T. A., et al. (2011). Bacterial community structures are unique and resilient in full-scale bioenergy systems. *Proceedings of the National Academy of Sciences of the United States of America*, *108*(10), 4158-63. doi:10.1073/pnas.1015676108

Weiland, P. (1993). One-Step and 2-Step Anaerobic-Digestion of Solid Agroindustrial Residues. *Water Research*, *27*(2), 145-151.

Wiegant, W. M., Hennink, M., & Lettinga, G. (1986). Separation of the Propionate Degradation to Improve the Efficiency of Thermophilic Anaerobic Treatment of Acidified Wastewaters. *Water Research*, *20*(4), 517-524. http://www.sciencedirect.com/science/article/pii/0043135486902022

Wilms, R., Sass, H., Köpke, B., Cypionka, H., & Engelen, B. (2007). Methane and sulfate profiles within the subsurface of a tidal flat are reflected by the distribution of sulfate-reducing bacteria and methanogenic archaea. *FEMS Microbiology Ecology*, *59*(3), 611-21. doi:10.1111/j.1574-6941.2006.00225.x

Wilson, T. E. and Dichtl, N. A. (2000). Two-phase anaerobic digestion: an update on the AG process, *Proceedings of WEFTEC 2000*, Water Environment Federation, Alexandria, VA.

Wittebolle, L., Marzorati, M., Clement, L., Balloi, A., Daffonchio, D., Heylen, K., De Vos, P., et al. (2009). Initial community evenness favours functionality under selective stress. *Nature*, *458*(7238), 623-6. doi:10.1038/nature07840

Wong, B.-T., Show, K. Y., Lee, D. J., & Lai, J. Y. (2009). Carbon balance of anaerobic granulation process: carbon credit. *Bioresource Technology*, *100*(5), 1734-9. Elsevier Ltd. doi:10.1016/j.biortech.2008.09.045

Yang, K., Yu, Y., & Hwang, S. (2003). Selective optimization in thermophilic acidogenesis of cheese-whey wastewater to acetic and butyric acids: partial acidification and methanation. *Water Research*, *37*(10), 2467-77. doi:10.1016/S0043-1354(03)00006-X

Young, J. C., Kim, I. S., Page, I. C., Wilson, D. R., Brown, G. J., & Cocci, A. A. (2000). Two-stage anaerobic treatment of purified terephthalic acid production wastewaters. *Water Science and Technology*, *42*(5-6), 277-282.

Zhang, R., El-Mashad, H. M., Hartman, K., Wang, F., Liu, G., Choate, C., & Gamble, P. (2007). Characterization of food waste as feedstock for anaerobic digestion. *Bioresource Technology*, *98*(4), 929-35. doi:10.1016/j.biortech.2006.02.039

3.0 THE EFFECTS OF OXYGEN ON METHANOGEN COMMUNITY STRUCTURE DURING PROPIOANTE DEGRADATION

3.1 Introduction

Anaerobic digestion is a practical technology to treat wastewater and generate renewable energy from biomass. In the process, select microorganisms convert wastes and other feedstocks into biogas that contains CH_4, which can be used to generate heat and electricity. In a comprehensive review of issues encountered in anaerobic digesters, several methods for improvement have been suggested, including co-digesting other wastes, removing or counteracting toxicants (e.g., ammonia, metals, and sulfide) prior to anaerobic digestion, acclamation to inhibitory substances (Chen et al., 2008), and the addition of trace metal nutrients (Speece, 2008). However, the failure to acknowledge the possible improvement in performance due to improvement of microbial community design may not be justified since current molecular biology methods can now be used to characterize microbial communities. Furthermore, digester designers could possibly utilize microbial community structure data to improve digester design and operation. It is now possible to extract deoxyribonucleic acids (DNA) and theoretically determine the probable identities of organisms present, the numbers of each, and the microbial community structure within biomass (Madigan and Martinko, 2009). The microbial community could then be designed along with the physical structure of the digester to optimize biological treatment. One way to improve the community is to select for certain microbes by varying environmental parameters.

3.1.1 Anaerobic Degradation of Propionate

Within the overall anaerobic degradation pathway, propionate degradation is often

the rate-limiting step, controlling the rate of CH_4 production (Kida et al., 1993; McInerney et al., 2009; Wong et al., 2009). Hereafter, propionate will be used to refer to both propionate and propionic acid since the former is the dominate species at pH greater than 4.87. Propionate is a key intermediate in the production of CH_4 from complex feedstocks since nearly one third of all complex carbon that is transformed into CH_4 passes through propionate (Speece, 2008). Part of the challenge with propionate degradation is overcoming its energetically unfavorable conversion into acetate, H_2, and CO_2, shown in equation (a) in Table 3-1. However, the overall reaction (equation (d) in Table 3-1) becomes favorable via the concomitant degradation of H_2/CO_2 as well as acetate (equations (b) and (c) in Table 3-1) (McCarty and Smith, 1986). Additionally, propionate at elevated concentrations can be toxic to microorganisms. Thus, it is only due to the balance of syntrophic relationships that anaerobic degradation of propionate can occur (Hatamoto et al., 2007; McInerney et al., 2009).

Table 3-1 Conversion of Propionate into CH_4 (McCarty and Smith, 1986).

	Stoichiometric Reaction	$\Delta G^{o'}$ kJ/mole propionate
(a)	$CH_3CH_2COO^- + 2H_2O = CH_3COO^- + 3H_2 + CO_2$	+71.67
(b)	$3H_2 + (3/4)\ CO_2 = (3/4)\ CH_4 + (3/2)\ H_2O$	-98.06
(c)	$CH_3COO^- + H^+ = CH_4 + CO_2$	-35.83
(d)	$CH_3CH_2COO^- + H^+ + (1/2)\ H_2O = (7/4)\ CH_4 + (5/4)\ CO_2$	-62.22

If taken a step further in the anaerobic degradation pathway, this interrelationality is also evident in that the H_2 partial pressure must fall between 10^{-4} and 10^{-6} atm for these syntrophic reactions to occur (McCarty and Smith, 1986). When the H_2 concentration is greater than 10^{-4} atm (i.e., build-up of product, H_2), propionate degradation becomes thermodynamically unfavorable, and propionate along with n-propanol and C-4 to C-7 n-carboxylic acids (commonly called volatile fatty acids, VFAs) accumulate (Smith and

McCarty, 1990). Therefore, propionate can only be degraded as fast as H_2 can be consumed to maintain this range of H_2 partial pressure. Ultimately, then, it is the H_2 utilization by hydrogenotropic methanogens that often leads to the accumulation of propionate and other reduced products, which, in turns, can lead to detrimental pH drops and, subsequently, to cessation of methanogenesis, process upset, and even digester failure (Hanaki et al., 1981; Koster and Cramer, 1987; Lalman and Bagley, 2001). Because acetate oxidation (acetate conversion into H_2 and CO_2) can occur (especially when *Methanosaetaceae* are not present), acetoclastic methanogenesis also plays a role in the propionate degradation rate (Karakashev et al., 2006). Therefore, methanogenesis and methanogenic organisms are indicative of both propionate conversion and, indirectly, anaerobic degradation in general.

The difficulty of propionate degradation was shown in a complete mix stirred tank reactor (CSTR) fed 0.10 M ethanol and 0.10 M propionate at a residence time of 9.1 days until achieving steady state (Smith and McCarty, 1990). Then the ethanol and propionate concentrations were increased by 0.30 M and 0.01 M, respectively. The ethanol was degraded within four days (less than 0.5 residence times); yet, the propionate persisted for 19 days (more than 2 residence times) (Figure 3-1).

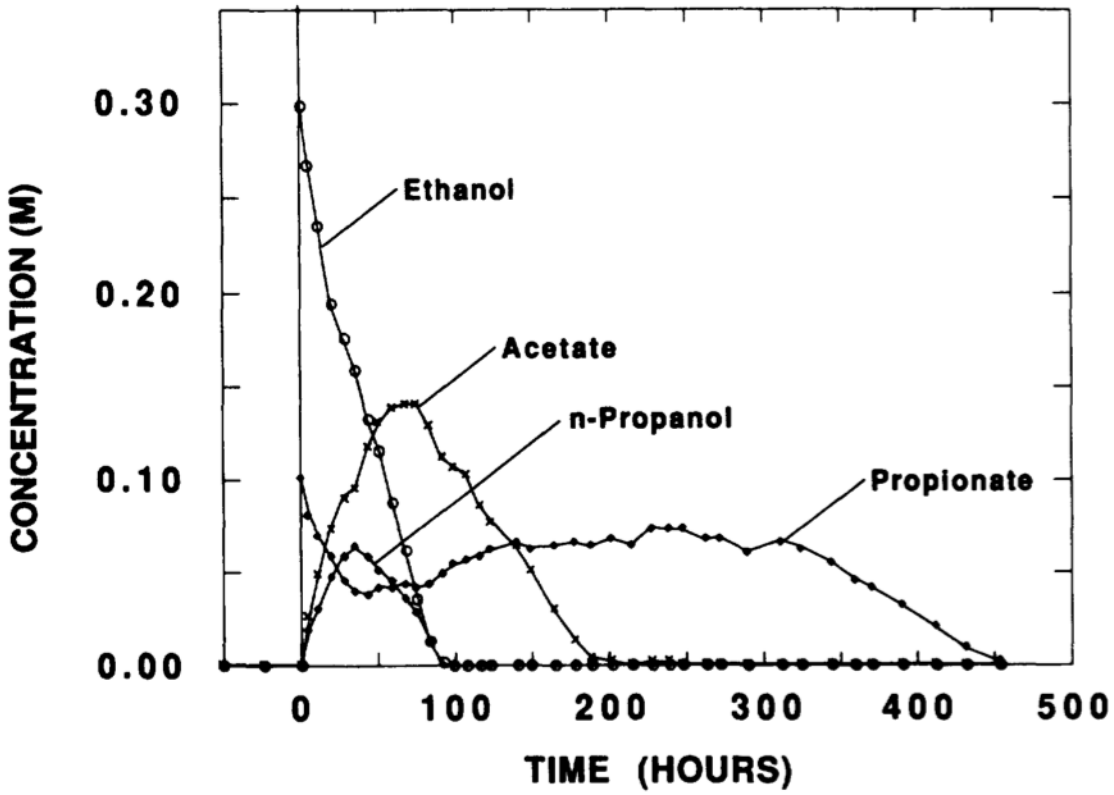

Figure 3-1. Concentrations of some of the intermediates in the anaerobic degradation pathway upon transient overload. Adopted from Smith and McCarty, 1990.

In addition, propionate inhibition was found to be toxic at far lower concentrations than typically assumed. Maximum CH_4 production was 389, 432, and 162 mL/g VS-d at 3000 mg/L acetate, 5000 mg/L butyrate, and 1000 mg/L propionate (Dogan et al., 2005), respectively. Furthermore, at a pH between 5.5 and 6.0, CH_4 production was 50% inhibited at 13,000 mg/L acetate, 15,000 mg/L butyrate, and only 3500 mg/L propionate, respectively; likewise, 100% inhibition occurred at 25,000 mg/L acetate, 25,000 mg/L butyrate, and only 5000 mg/L propionate (Dogan et al., 2005). Collectively, these factors that contribute to the difficulty of degrading propionate point to the need for more efficient propionate treatment methods.

3.1.2 Effects of Oxygen (O_2) on Methanogens

Because Earth's atmosphere is approximately 20% oxygen (O_2), it is not uncommon

that O_2 will contact wastewater during conveyance (Kato et al., 1997). This may seem problematic given that methanogenic Archaea have been physiologically categorized as obligate anaerobes (Kato et al., 1993; Shen and Guiot, 1996; Chu, 2005; Madigan and Martinko, 2009). Yet, numerous studies have also described at least some tolerance of methanogens to O_2 (Zitomer, 1998; Zitomer and Shrout, 1998; Johansen and Bakke, 2006; Hao et al., 2009; Jagadabhi et al., 2009). Four general means by which anaerobic microorganisms survive in the presence of O_2 have been outlined. First, some methanogens have a limited intrinsic tolerance to O_2 since they produce superoxide dismutase enzymes that neutralize toxic free radicals (e.g., O_2^{2-}, O^{2-}, and OH^-) (Kato et al., 1997). Second, O_2 may be consumed in the chemical breakdown of the added substrate (i.e., aerobic oxidation) (Hungate and Macy, 1973; Scott et al., 1983; Kato et al., 1997). Third, sulfides (and other abiotic sinks) may account for O_2 consumption when little or no organic substrate is used (Zee et al., 2007). Lastly, in some studies, an incomplete diffusion of the O_2 throughout the microbial culture may allow O_2-free zones (e.g., inside granules) wherein the methanogens survive and generate CH_4 (Kurosawa and Tanaka, 1990; Kato et al., 1997).

Although high concentrations of O_2 are toxic to methanogenic microorganisms, low O_2 doses (1 to 0.1 g O_2/L-day) have been shown to increase methanogenic activity of mixed methanogenic cultures by up to 20% under some conditions and even decrease the time for overloaded digesters to return to a neutral pH whereat methanogenesis can occur (Zitomer and Shrout, 1998; Tale, 2010). Similarly, Gerritse et al. (1990) found a 20% "stimulation of CH_4 production…at low oxygen fluxes" in mixed cultures of aerobic, fermentative bacteria and methanogens fed formate. In another study, limited aeration, defined as the simultaneous occurrence of aerobic and anaerobic biological functions in the same reactor, improved hydrolysis by 50% in batch reactors (Johansen and Bakke, 2006); yet, the reactors

produced 50% less CH_4, presumably, because this carbon was lost as CO_2 via oxidation of hydrolyzed products, as is consistent with other studies (Botheju et al., 2010). Further review of the effects of O_2 on methanogenesis can be found in Botheju and Bakke (2011). While shown to reduce the hydrolysis hurdle in the anaerobic degradation pathway, the influences of various O_2 doses on propionate degradation, CH_4 production rate, and, subsequently, on methanogenic community structure remain under-studied.

3.1.3 Digester Function and Microbial Community Structure

Though often assumed to be similar in all full-scale anaerobic digesters, microbial community structures actually vary greatly (Luton et al., 2002; Leclerc et al., 2004; Werner *et al.*, 2011), and the diversity within the various trophic groups involved in anaerobic degradation may be linked to functional stability (Briones and Raskin, 2003). The rates at which biomass samples from different full-sale digesters produce CH_4 vary greatly (e.g., from <0.1 to >10 mL CH_4/gVS-hr), and the methanogen community structure in some biomass samples has correlated to the rate of CH_4 production (Tale, 2010). Dissolved O_2 concentration, N or P deficiency, pH, VFA, organic loading rate, food:mass (F:M) ratio, and H_2S can all impact the presence of different microbes and, therefore, how stable a digester will function (Hashshem, 2000; Fernandez, 2000; Madigan and Martinko, 2009; Switzenbaum, 2010; Schauer-Gimenez, 2010; Tale, 2010).

3.1.4 Goals of Research

Given: (1) the need to better understand anaerobic degradation, especially as it pertains to propionate, (2) the potential importance of O_2 contact in biological treatment processes intended to be anaerobic, and (3), the potential impact of microbial community

structure on digester function, the function and microbial community structure of propionate enrichment cultures subjected to various doses of O_2 were investigated.

It was hypothesized that propionate enrichments given different O_2 doses would have significantly different specific methane activities (SMA) with propionate as the substrate, have different organic overload response, and exhibit different methanogen community structures as characterized by denaturing gradient gel electrophoresis (DGGE).

3.2 Methods and Materials

There were three fundamental tasks included in this research: (1) develop and maintain four propionate enrichment cultures in triplicate, (2) measure methanogenic activity and response to organic overloading, and (3) relate biomass function to microbial community structure.

Another key reason to use propionate as the substrate was to avoid hydrolysis, the other common rate-limiting step. Since propionate is only two steps away from complete conversion in the anaerobic degradation pathway, it is seldom avoided, whereas the challenges associated with hydrolysis only pertain to complex feedstocks. Also, propionate degradation rate can be readily measured and controlled by feeding calcium propionate.

3.2.1 Enrichment Cultures

Twelve propionate enrichment cultures with a working volume of 1 L were maintained for 317 days in 2-L, polyethylene terephthalate (PETE) plastic, anaerobic reactors that were continuously shaken on a shaker table housed in a temperature-controlled (35 ± 1°C) incubator (Model 4350, Thermo Scientific, Marietta, OH) (Figure 3-2). Each propionate enrichment was fed a different O_2 dose, calculated to satisfy a portion of the

added total chemical oxygen demand (TCOD) (Table 3-2). Thus, enrichments that received 0, 1.3, 6.7, and 12.5% of the total chemical oxygen demand (TCOD) added as O_2 were referred to as 0%, 1.3%, 6.7%, and 12.5%, respectively, throughout this chapter. Up to 75 mL of O_2 (aviator's breathing grade; 99.9% purity; approximately 1 atm and 22°C) per L of liquid was added by injecting it directly into the bottle headspace with a wetted-barrel, glass syringe immediately after being fed.[1] Propionate enrichment cultures 1 through 3, which received no O_2, served as controls.

Figure 3-2. Propionate enrichment cultures.

Table 3-2. Propionate O_2 Additions

Propionate Enrichment Numbers	1, 2, 3	4, 5, 6	7, 8, 9	10, 11, 12
Liquid O_2 Dose (mL O_2/L-d)	0	8	40	75
Headspace O_2 Dose (mg O_2/L-d)*	0	11	53	99
Percent of COD_{total}	0.0%	1.3%	6.7%	12.5%

*O_2 concentration in headspace, based on dose at 22°C and 1 atm.

[1] Pure O_2, rather than air, was used in this study. The volume of O_2 in air (assuming 21%) needed to satisfy 12.5% of the influent TCOD (~280 mL) and resulting pressure would have been too great to perform daily lab procedures. Also, use of pure O_2 avoided the disadvantage of diluting biogas with N_2. Some studies have yielded different results between air and pure O_2. For example, Stephenson, et al. (1999) added air without a significant change in methane production rate in a UASB reactor, whereas pure O_2 reduced methane production.

Since seed cultures with diverse microbial communities have been shown to be functionally beneficial (Wittebolle, 2009), all propionate enrichment cultures were seeded with a blend of biomass from two municipal, two brewery, one agricultural, one beverage industry, one food industry, and one pilot scale anaerobic digester (see Table 5-2).

Calcium propionate and a limited O_2 dose were then added to each enrichment culture. Liquid effluent (100 mL) was removed once per day to maintain a solids residence time (SRT) and hydraulic retention time (HRT) of ten days. Effluent was replaced with 100 mL of aerated (to remove residual chlorine) tap water containing calcium propionate (0.77 ±0.03 g COD/L-day), 5 g/L $NaHCO_3$, and the basal nutrient medium described in Table 3-3. This feed led to a theoretical maximum of 1.5 g Ca^{+2}/L in the propionate enrichments, which is well below the 4.8 g Ca^{+2}/L that can cause a 50% reduction in CH_4 production (Switzenbaum, 2010).

Table 3-3. Basal Nutrient Medium Added Daily to Propionate Enrichment Cultures

Constituent	Concentration* (mg/L)
NH_4Cl	400
$MgSO_4$	250
KCl	400
$CaCl_2$	120
$(NH_4)_2HPO_4$	80
$FeCl_3.6H_2O$	55
$CoCl2.6H_2O$	10
KI	10
Metals**	0.5
Alkalinity ($NaHCO_3$)	5000

*Concentrations given as those present in the propionate enrichments.
**The following metals were added together in solution (each at 0.5mg/L): $MnCl_2.4H_2O$, NH_4VO_3, $CuCl_2.2H_2O$, $Zn(C_2H_3O_2)_2.2H_2O$, $AlCl_3.6H_2O$, $NaMoO_4.2H_2O$, H_3BO_3, $NiCl_2.6H_2O$, $NaWO_4.2H_2O$ and Na_2SeO_3.

A COD mass balance was performed on the 12 propionate enrichments using the influent and effluent TCOD, CH_4 produced, as well as the O_2 added and the effluent headspace O_2 concentration. Sample calculations are provided in Appendix A.

3.2.2 Quantification of Microbial Community Activity

Microbial community activity was quantified using the specific methanogenic activity (SMA) test with propionate and an organic overload perturbation activity (OOPA) test using glucose.

3.2.2.1 Specific Methanogenic Activity (SMA) Tests

Specific methanogenic activity tests were conducted to determine the maximum rate that a microbial culture generates CH_4 when fed propionate. A modified approach to a standard SMA protocol outlined by Andelicki et al. (2007) was implemented. On days 243 to 247, biomass samples were collected and composited. The composite sample was then thickened at 6000 rpm for five minutes in a centrifuge (Clinical 200, VWR International, Radnor, Pennsylvania). Next, thickened biomass samples were resuspended in de-ionized (DI) water that included basal nutrient medium described in Table 3-3 to achieve a standard active biomass concentration based on the intracellular adenosine-5'-triphosphate (iATP) concentration (0.74 mg iATP/L). A 25-mL sample of standard active biomass concentration was placed in a 160-mL serum bottle, sparged with O_2-free gas (3:7 v/v mix of CO_2 and N_2), and allowed to produce biogas for three days to determine endogenous biogas production. Excess biogas was removed on day three to depressurize the headspace, and the sample was then given a non-limiting dose (3 g/L) of calcium propionate ($Ca(C_2H_5COO)_2$). SMA analyses of all enrichments were run in triplicate alongside one additional bottle serving as the blank that contained no exogenous substrate to account for endogenous CH_4 production. This substrate concentration has been used elsewhere (Speece, 2008; Zitomer, 2008), is non-toxic to anaerobic microorganisms, and is well above the Monod half-saturation constant values. SMA assays were incubated at 35 ±1°C in a gyratory shaker-

incubator rotating at 150 rpm (C25KC Incubator Shaker Classic Series, New Brunswick Scientific, Edison, NJ).

Biogas production was measured for 20 days using a glass syringe displacement method. Methane content was measured after 20 days by gas chromatography (GC). Graphs of cumulative biogas production versus time were plotted and the SMA values (mL CH_4/mg iATP-h) were calculated using linear regression on the portion of the curve within the first 60 hours of biogas production with the steepest slope. This initial maximum slope was used because the biomass samples used for molecular analyses were taken on the day the assays were set-up. Thus, the use of initial slopes ensured that the SMA values measured were as representative as possible of the microbial community structure that was analyzed and not the community that developed in the SMA bottle after feeding. The average and standard deviation of SMA values were calculated for each enrichment culture.

3.2.2.2 Organic Overload Perturbation Assays (OOPA)

Stressed conditions such as organic overload are not uncommon in anaerobic digesters. Thus, the OOPA test was developed to provide a simple laboratory test that provided information about biomass response to organic overload.

After propionate enrichments were maintained for 23 retention times (230 days), biomass was removed and diluted to a standard active biomass concentration (0.74 mg iATP/L) using DI water that included 5 g/L $NaHCO_3$ and the basal nutrient medium described in Table 3-3. A 25-mL sample of standard active biomass was placed in a 160-mL serum bottle and sparged with O_2-free gas (3:7 v/v mix of CO_2 and N_2). OOPA tests were incubated at 35 ±1°C in a gyratory shaker-incubator rotating at 150 rpm (C25KC Incubator Shaker Classic Series, New Brunswick Scientific, Edison, NJ). The biogas volume was

measured until it ceased after three days to determine endogenous biogas production. Excess biogas was removed on day three to depressurize the headspace, and the sample was then given a one-time dose of 5.2 g glucose/L (5.6 g COD/L) using DI water. This glucose dose was chosen because, during preliminary testing (Appendix B), it was found to be high enough to perturb the system, but not so high that CH_4 production stopped for an extended period. Triplicates were run for all OOPA analyses.

Glucose overload conditions were monitored over three key periods. The first two periods were distinguished by different slopes of the cumulative biogas production versus time graph and corresponded to acidogenesis and methanogenesis, respectively (Figure 3-3). Methane production at the end of the first period was negligible as indicated by CH_4 concentration measurements. A third period, distinguished by a slope of essentially zero followed, depicting the consumption of all substrate occurred within 20 days in all testing. Cumulative biogas production was measured for 20 days and plotted with respect to time. Biogas composition was determined on day 20. The quotient of the initial acidogenesis and secondary methanogenesis slopes was defined as the methanogenesis-to-fermentation (M/F) ratio.

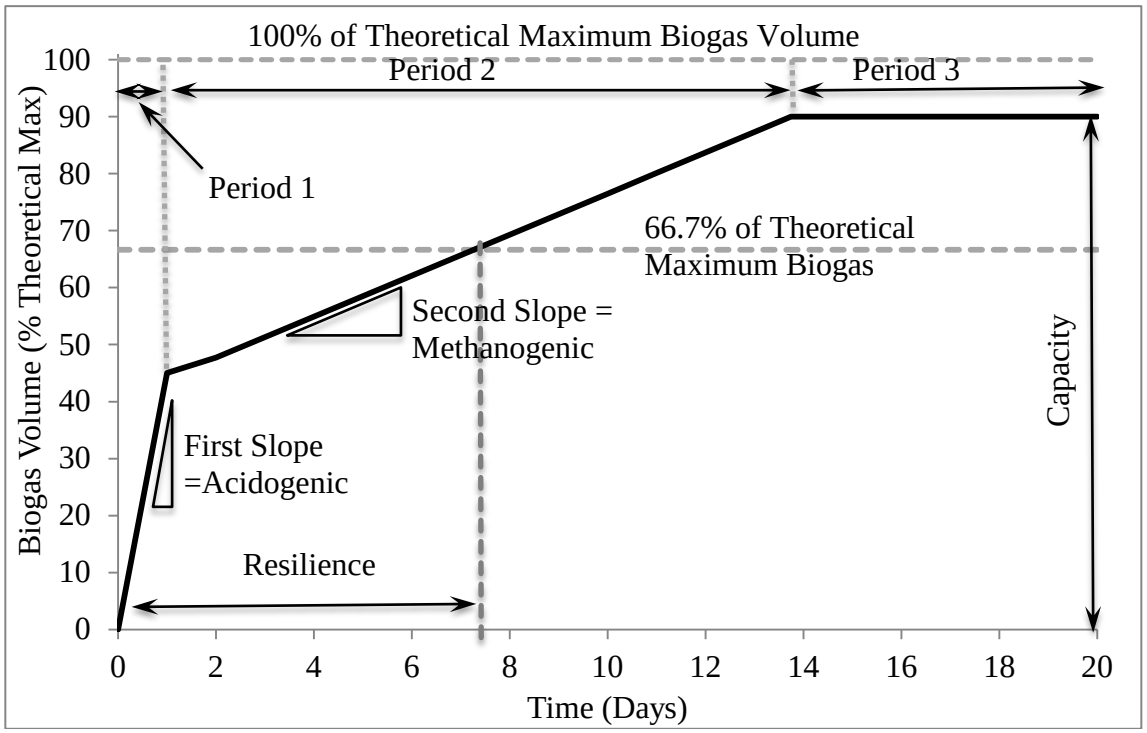

Figure 3-3. Theoretical OOPA graph shown to depict the parameters obtained via overload testing, including resilience, capacity, methanogenesis to fermentation (M/F) ratio, and perturbed biogas yield (maximum biogas volume divided by theoretical maximum biogas volume).

Capacity was defined as the cumulative amount of biogas production after 20 days. This metric quantified both resistance and resilience by identifying the cumulative amount of biogas production after 20 days. For example, a biomass that is less able to handle organic overload would consume less of the total substrate added due to greater inhibition, thereby, producing proportionally less of the theoretical maximum biogas. If too much substrate was added, then the glucose would not be consumed; thus, significantly less than the theoretical maximum would be produced at the end of 20 days. A resilience coefficient was calculated as the inverse of the time (hours) it took for biogas production to reach two-thirds (66.7%) of the theoretical yield, multiplied by 100.

The cumulative biogas volume produced after 20 days was divided by the total theoretical biogas production volume expected based on the glucose added. This quotient was the 20-day perturbed biogas yield (PBY), the value of which quantified functional

stability. Higher PBY values represented a greater ability to achieve the theoretical biogas production and indicated greater functional stability.

3.2.3 Microbial Community Analysis

3.2.3.1 DNA Extraction

DNA was extracted from all enrichments using biomass collected when SMA and OOPA testing was performed. DNA was extracted using the DNA Elution Accessory kit with the RNA Powersoil™ Total RNA Isolation Kit (MoBio Laboratories, Carlsbad, CA) according to the manufacturer's instructions. Gel containing 1% agarose was prepared by mixing agarose with 100 mL of 1X Tris-Acetate-EDTA (TAE). The resulting mixture was heated in a microwave until all the solid agarose was dissolved in the TAE solution. Then 80 μL of ethidium bromide was added to the gel mixture for staining purposes. Prepared gel solution was poured into a gel box and was allowed to solidify. A mixture of 3 μL of 6X blue-orange loading dye and 10 μL of DNA sample was injected into the wells (Hartwell et al., 2004). A λϕ (HindIII, HaeIII) ladder was placed into one of the wells as a marker. This marker had 40 ng/μL Lambda (λ) DNA, HindIII cut and 30 ng/μL phi (ϕ) DNA, HaeIII. A 100 millivolt (mV) potential was maintained across the gel for approximately 60 minutes. This potential caused the DNA to migrate across the gel, which was then illuminated and photographed under ultraviolet light using an imaging system (GDS-8000 Bioimaging System, UVP Inc., Upland, CA) to confirm the presence of extracted DNA. DNA samples were stored at -80°C until further analysis.

3.2.3.2 Polymerase Chain Reaction (PCR)

Extracted DNA was amplified using polymerase chain reaction (PCR) with primers

for the methyl coenzyme M reductase (*mcrA*) gene of methanogenic *Archaea* designed by Luton et al. (2002). These are as follows: mcrA1f: 5'-GGTGGTGTMGGATCACACARTAYGCWACAGC -3', (mcrF); GCmcrA1f: 5'- *GC-clamp-GGTGGTGTMGGA TTCACACARTAYGCWACAGC -3', (mcrA1f), where GC-clamp = 5' – CGCCCGCCGCGCCCCGCGCCCGTGCCGCCGCCCCCGCCCG – 3', (GC-clamp); mcrA500r: 5' – TTCATTGCRTAGTTWGGRTAGTT – 3', (mcrR). Since it is a functional gene that is specific to and ubiquitous in methanogens (Thauer, 1998), the *mcrA* gene has been used to compare methanogen community structure and identify the taxonomically distinct methanogens present. Furthermore, numerous studies have exploited the ubiquity of the *mcrA* gene in all known methanogens to find them in various locations, including marine environments (Bidle, 1999; Wilms, 2007), termite guts (Ohkuma, 1995), rice paddies (Lueders, 2001), oligotrophic fen (Galand et al., 2002), and anaerobic digesters (Rastogi, 2008; Tale, 2011).

The primer product was an approximately 460 -bp long segment of *mcrA*, which codes for the α subunit of methyl coenzyme M reductase (Luton, 2002). PCR was performed on the DNA sample using EconoTaq® PLUS 2X Master Mix, which includes the Taq polymerase (Lucigen Corporation, Middleton, WI). Forward and reverse primers were added to the PCR tube with nuclease-free H_2O to make a 100-µL reaction. Nested PCR was performed on the extracted DNA by first amplifying for mcrA1f and mcrA500r primers in the following program: 95°C for 5 min; then six cycles of 95°C for 1 min, 49°C for 1 min, 72°C for 3 min; next 30 cycles of 95°C for 1 min, 49°C for 1 min, 72°C for 3 min; then 95°C for 1 min, 49°C for 1 min, 72°C for 10 min; and stop and stay at 4°C. The second cycle was employed to re-amplify with GCmcrA1f (GC clamp) and mcrA500r primers in the

following program: 95°C for 5 min; then six cycles of 95°C for 1 min, 58°C for 1 min, 72°C for 3 min; next 36 cycles of 95°C for 1 min, 58°C for 1 min, 72°C for 3 min; then 95°C for 1 min, 58°C for 1 min, 72°C for 10 min; and stop and stay at 4°C. PCR was done on a thermocycler (PTC-200 DNA Engine Cycler, Bio-Rad, Foster City, CA).

3.2.3.3 Denaturing Gradient Gel Electrophoresis (DGGE)

Each microbial community was fingerprinted using denaturing gradient gel electrophoresis (DGGE), which separated amplified genes into bands on a polyacrylamide gel. DGGE has been used with *mcrA* as a target gene (e.g., Galand, 2002; Wilms et al., 2007; Morris, 2011; Tale et al., 2011). The denaturant concentration used for DGGE varied linearly over 75 mm and ranged from 40% at the top of the gel to 70% at the bottom of the gel (expressed as v/v of the total gel volume). A detection system (Universal DCode Mutation Detection System, BioRad, Hercules, CA) was used to run the DGGE gels. DGGE was performed on 1-mm-thick 8% polyacrylamide gel following the manufacturer's protocol. Approximately 300 ng of DNA product was added to each lane of the gel with 2X blue loading dye. An electric potential of 100 V was maintained across the gel for 12 hours. A 1% SYBR® gold dye solution (Invitrogen, CA) was used to stain the gel. After immersing the gel in the staining solution and rotating it for 30 minutes on a shaker table at a speed sufficient to mix the dye solution, it was viewed under ultraviolet light using an imaging system (GDS-8000 Bioimaging System, UVP Inc., Upland, CA). Densitometric data were obtained using gel viewing software (Lab Works v. 4.6.00.0 Lablogics, Inc., Mission Viejo, CA) with a minimum band height of 0.050, allowed error of ±5%, ten largest bands retained, and the following options activated: dark bands and bright background, rows of equal molecular weight, maximum OD level for the image, and center peak.

3.2.3.4 Quantitative Polymerase Chain Reaction (qPCR)

The *mcrA* gene was also used in quantitative PCR (qPCR) according to the procedures outlined by Smith et al. (2006) and Smith and Osborn (2009), but the standard curve and guidelines for environmental samples were followed as specified in the Minimum Information for Publication of Quantitative Real-Time PCR Experiments (MIQE) (Bustin et al., 2009). The aforementioned primers for *mcrA* (Luton et al., 2002) were used to perform qPCR and have been used previously for qPCR (Vianna et al., 2006; Goffredi et al., 2008; Freitag and Prosser, 2009; Freitag et al., 2010; Morris, 2011). The final qPCR mix per 25 μL reaction was as follows: 1X iQ™SYBR® Green Supermix reaction buffer containing dNTPS , iTaq DNA polymerase, and 3 mM MgCl (Biorad, Hercules, CA); 750 nM mcrF and mcrR; and template DNA (0.3-1 ng) or cDNA. Samples were 1 μl of reverse transcriptase (RT)-PCR reaction; if RT input was less than 1400 ng, then the volume of RT reaction added to qPCR mix was increased to ensure 1400 ng was used. As described elsewhere (Morris, 2011), no-template controls and no-RT controls from the RT reactions were used in each qPCR run. Samples were kept on ice during run set up. All qPCR reactions were performed with the Biorad MyIQ™ Single-Color Real-Time PCR Detection System with the following program: initial denaturation at 95°C (10 min), 45 cycles of 95°C (30 sec) and 58.5°C (1 min), and a final extension of 7 minutes at 72°C. After the amplification program, a denaturation curve program was run (80 cycles 10 sec in length starting at 55°C and increasing in 0.5°C increments) to check for product specificity. Products from initial runs were also examined for specificity using 1.5% agarose gels. Starting quantities and threshold cycle values were calculated using MyiQ™ optical system software (v. 1.0). Standards for all runs were developed from *mcrA* DNA clones from anaerobic biomass samples as outlined by Morris (2011). Spectrophotometry (Nanodrop ND-1000, Thermo-Scientific, Waltham,

MA) was used to estimate concentrations of purified (QIAquick® PCR Purification Kit, Qiagen) *mcrA* clones. Then 50 ng of each purified clone sample was added to the standard mix. Mix concentration was confirmed and diluted to 0.1ng/ µl. Diluted mixes (in 5 µl aliquots) were stored at -80 °C. Freshly thawed aliquots were used for each qPCR run.

3.2.3.5 Principal Component Analysis (PCA)

Principal component analysis (PCA) was done using MATLAB (v. R2010bSP1, MathWorks®, Natick, MA). Optical densities of DGGE bands (obtained from Lab Works v. 4.6.00.0) were used as dimensional values for community structure. In previous work, PCA was used to relate DGGE banding patterns both to CH_4 production rates (i.e., SMA values) of 14 anaerobic, microbial communities from full-scale digesters (Tale, 2011) and of six anaerobic, microbial communities in bench-scale digesters (Navaratnam, 2012). Therefore, it was expected that samples with similar SMA values would cluster based on DGGE banding pattern.

3.2.3.6 Cluster Analysis

Similarity coefficients (e.g., Dice, Jaccard), simple mismatch coefficients, the squared Euclidean distance (Kosman and Leonard, 2005), the Shannon Index (Boon et al., 2002), as well as Pearson correlation coefficients (Dalirsefat, 2009) have been used in molecular ecology to analyze phylogenetic similarity. While other methods were also tested, the Pearson correlation coefficient was deemed most suitable since band intensities (i.e., brightness) were accounted for, whereas coefficients like Jaccard only account for the presence or absence of bands and avoids incorporating evenness into the value as in the Shannon Index. Thus, Pearson's correlation coefficient was used to develop similarities

between the banding patterns (i.e., a 0 signified uncorrelated, a +1 was a perfect positive correlation and -1 was a perfect negative correlation).

The distance between two samples in a cluster was calculated as one minus the Pearson's correlation coefficient between the optical density data from two propionate enrichments (Appendix C). This was done using MATLAB (v. R2010bSP1) and the "pdist" function as well as a predefined command entitled "correlation" that calculated one minus the Pearson's correlation coefficient to develop dissimilarities between the banding patterns.

These dissimilarity values were compiled into a distance matrix using the "squareform" function in MATLAB. This matrix was then uploaded into Plain Text Editor v. 5.1, formatted to be readable by the Phylogency Inference Package (PHYLIP, v. 3.69), and the unweighted pair group method with arithmetic mean (UPGMA) algorithm was used for clustering. FigTree v. 1.3.1 was then used to view phylogenetic trees.

Additional statistical analysis was performed. The 12 SMA values were ranked 1 to 12, highest to lowest. One minus Pearson's correlation coefficient was used to determine if the dissimilarity distance (i.e., difference) between samples correlated with SMA rank. First, the differences between the densitometric data (i.e., DGGE banding pattern intensities) from the samples were calculated using one minus Pearson's Correlation Coefficient. These data were then used to list the propionate enrichments in ascending order of their pair-wise distances from the sample with the greatest SMA. Then the rank based on SMA values was correlated with the densitometric ranking using Spearman's rank correlation coefficient (Appendix C), which measured the correlation between ranks of samples (Spearman, 1904; Zar, 1972).

3.2.4 Physical and Chemical Analysis

Intracellular adenosine-5'-triphosphate (iATP) concentration was measured using a luciferase-based test kit (QuenchGone21^{TM} Wastewater Test Kit, LuminUltra, Fredericton, New Brunswick, Canada). Briefly, this protocol included measuring each biomass sample both for extracellular ATP using a proprietary stabilizing agent and for total ATP using a proprietary NaOH-based lysing agent. The difference between total ATP and extracellular ATP was iATP. Biomass samples were resuspended in DI water that included basal nutrient medium (Table 3-3) to achieve a standard active biomass concentration (0.74 mg iATP/L).

The temperature and pH of the propionate enrichments were measured daily using a glass electrode and meter (Orion 4 Star pH-DO Benchtop electrode - 9206BN, Thermo Scientific, Marietta, OH). Two samples of feed and effluent per week were used to determine the following parameters (specific method used given in parentheses): total solids (TS) (2540 B), volatile solids (VS) (2540 E), volatile suspended solids (VSS) (filtered as in 2540 D, volatized as in 2540 E), soluble chemical oxygen demand (SCOD) (5220 D), and individual volatile fatty acid (VFA) concentrations (acetic, propionic, butyric, iso-butyric, valeric, and iso-valeric acids) (5560 B) according to standard methods (APHA et al., 1998). From the beginning of the study until day 280, effluent SCOD was measured and from day 280 until the end of the study effluent TCOD was monitored. For SCOD analysis, the samples were thickened at 13,000 rpm for 10 minutes in a centrifuge (Clinical 200, VWR International, Radnor, PA) and the supernatant filtered through a 0.45 μm filter (Whatman International, Maidstone, England). The filtrate was then tested for COD. The biogas volume produced was measured daily at ambient pressure before feeding using a water displacement method (Wet Test Meter, Precision Scientific Petroleum Instruments, San Antonio, TX), and biogas CH_4 content (2720 C) was measured by standard methods (APHA

et al., 1998). Methane content in the biogas as well as the influent and effluent VFA concentrations were determined by gas chromatography (GC) (Series 7890A, Agilent Technologies, Santa Clara, CA) with a thermal conductivity detector (TCD) and flame ionization detector (FID), respectively. For CH_4 content the carrier gas was helium at a flow of 4.5 mL/min. Temperatures of the injector and detector were 150°C and 250°C, respectively; the temperature of the oven was 40°C. VFA samples were acidified using 1% phosphoric acid and analyzed as described in Standard Method 5560D (APHA et al., 2005). For VFA analysis, the carrier gas was helium at a flow of 18 mL/min. Temperatures of the injector and detector were 150°C and 300°C, respectively, and the temperature of the column was 40°C (detector airflow at 400 mL/min, H_2 flow at 30 mL/min).

3.3 Results and Discussion

3.3.1 Enrichments Function and Mass Balance

3.3.1.1 Biogas and Methane Production

Significant CH_4 production was observed at all four O_2 doses. A consistent temperature (35 ±1°C) and pH (7.1 ±0.3) were maintained in all 12 enrichments. Oxygen addition was not only tolerable since all enrichments produced CH_4 throughout the study (Figure 3-4a), but also advantageous under some conditions. The advantage was shown during the first 100 days when greater CH_4 production (Figure 3-4a) and CH_4 content in the biogas (Figure 3-4b) were observed in the enrichment cultures that received higher O_2 doses (Table 3-4). During the first 100 days of operation, the propionate enrichments receiving 0% and 1.3% O_2 produced the least amount of CH_4, and, as the O_2 dose increased, the CH_4 production progressively increased (Table 3-4; Figure 3-4a). Compared to 0%, these are 111,

245, and 210% increases in 1.3, 6.7, and 12.5% enrichments, respectively. Evidence of biomass acclimation was observed between days 100 and 200 since by the end of the study the CH_4 production trends were reversed; those receiving the lowest O_2 dose produced the most CH_4 (Table 3-4). This translated into average decreases of 2.4, 7.8, and 12.4% in enrichments 1.3, 6.7, and 12.5%, respectively. This was expected; the anaerobic cultures yielded a greater volume of CH_4, as all of the substrate was available for anaerobic degradation in those not receiving O_2, whereas up to 12.5% of the substrate was consumed via aerobic oxidation in those fed the highest O_2 dose. Other researchers have observed less CH_4 production in anaerobic digesters that received more O_2 (Kato et al., 1997; Zitomer and Shrout, 1998). Ultimately, however, adding O_2 decreased CH_4 production at quasi steady state after 100 days.

Table 3-4. Methane and Biogas Data for Propionate Enrichments. T-Test results are (1 – p-value)

Propionate Enrichment O_2 Dose	**0%**	**1.3%**	**6.7%**	**12.5%**
Average CH_4 Production Before Day 100 (mL/d)	58.8	124.1	202.6	182.2
Standard Deviation (mL/d)	35.5	91.9	10.6	15.3
T-Test compared with 0%	-	0.02	6.6E-11	7.5E-10
Average CH_4 Production After Day 274 (mL/d)	243.0	235.7	219.5	205.6
Standard Deviation (mL/d)	4.4	8.4	4.3	2.6
T-Test compared with 0%	-	0.28	0.02	7.1E-04
CH_4 Content Before Day 100 (%)	63.6	67.1	72.2	69.3
Standard Deviation (%)	5.5	6.1	1.9	2.4
T-Test compared with 0%	-	0.05	1.3E-07	7.8E-05
CH_4 Content After Day 150 (%)	79.9	78.6	74.2	72.1
Standard Deviation (%)	3.3	2.8	3.8	2.3
T-Test compared with 0%	-	0.18	1.9E-06	1.0E-10
Average Biogas production (mL/d)	301.9	297.7	300.9	283.8
Standard Deviation (mL/d)	2.5	9.5	1.4	6.5
T-Test compared with 0%	-	0.41	0.82	1.4E-04

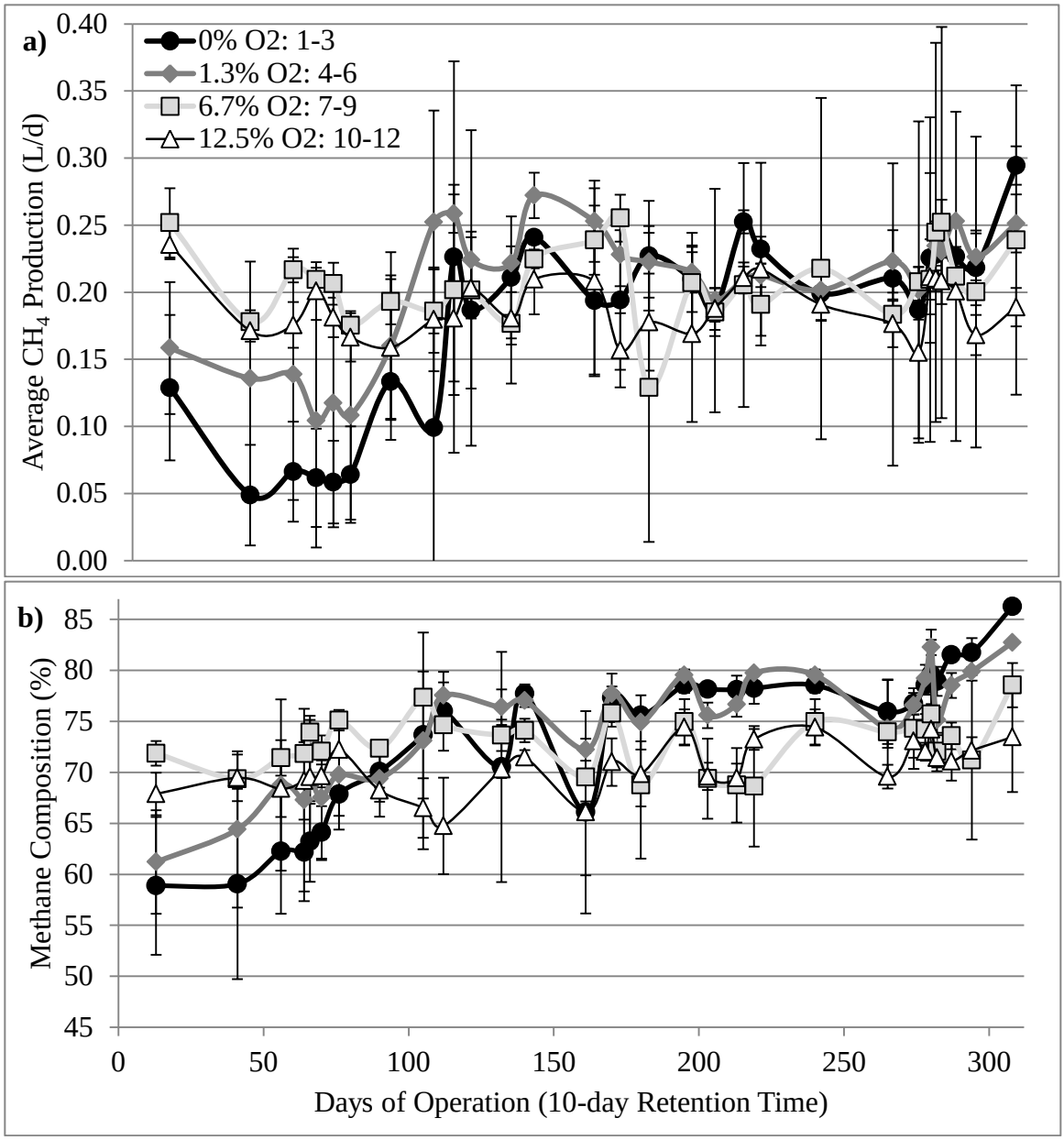

Figure 3-4. Methane production (a) and methane composition in propionate enrichments (b). Each point is an average of three physical replicates.

A similar pattern was evident in the CH_4 composition. Initially the higher biogas CH_4 contents were found in the propionate enrichments receiving higher O_2 doses, and this was reversed at after day 150 (Table 3-4; Figure 3-4b). After day 150, however, greater O_2 loading led to decreased CH_4 content; 0% and 1.3% biogas had higher CH_4 content than 6.7 and 12.5% (Table 3-4; Figure 3-4b). Again, this suggests aerobic oxidation was responsible for

the degradation of some of the propionate, which would cause an elevated concentration of CO_2, ultimately decreasing the percent of CH_4 in the biogas.

Average quasi steady state biogas production results (Table 3-4) were similar to results found by Botheju et al. (2010a) wherein the ratio of CH_4 to CO_2 decreased as the O_2 loading increased, even if the CH_4 yield improved, because the CO_2 generation increased even more.

Enrichments 0 and 1.3% were verging on being "stuck," as propionate accumulated (Figure 3-5a) and CH_4 production decreased (Figure 3-4a). Yet, after three retention times, a shift was observed in the onset of acetate accumulation (Figure 3-5b) and the increase of not only CH_4 generation, but also CH_4 content in the biogas. Given the diverse seed cultures (many of which were used to treat complex substrates that would necessitate hydrolysis and acidogenesis), this shift in function may be due to a corresponding shift in the microbial community away from a diverse community comprised of microorganisms from all guilds in the anaerobic pathway to a more specialized community composed primarily of the syntrophic and methanogenic organisms needed to degrade propionate.

3.3.1.2 Effluent Volatile Fatty Acid (VFA) Concentrations

Lower propionate (Figure3-5a) and acetate (Figure 3-5b) concentrations also evidenced the advantage of the higher O_2 doses. The effluent concentrations of acetate and propionate before day 100 were inversely proportional to O_2 dosing; the initial VFA concentrations were progressively lower with each increased step in the O_2 dose. The effluent propionate concentrations of all enrichments began at elevated values, whereas the acetate concentrations were initially low and gradually increased to a maximum at approximately day 60 (Figure 3-11). Butyric acid, iso-butyric acid, valeric acid, and iso-valeric acid concentrations were consistently below the 20-mg/L detection limit.

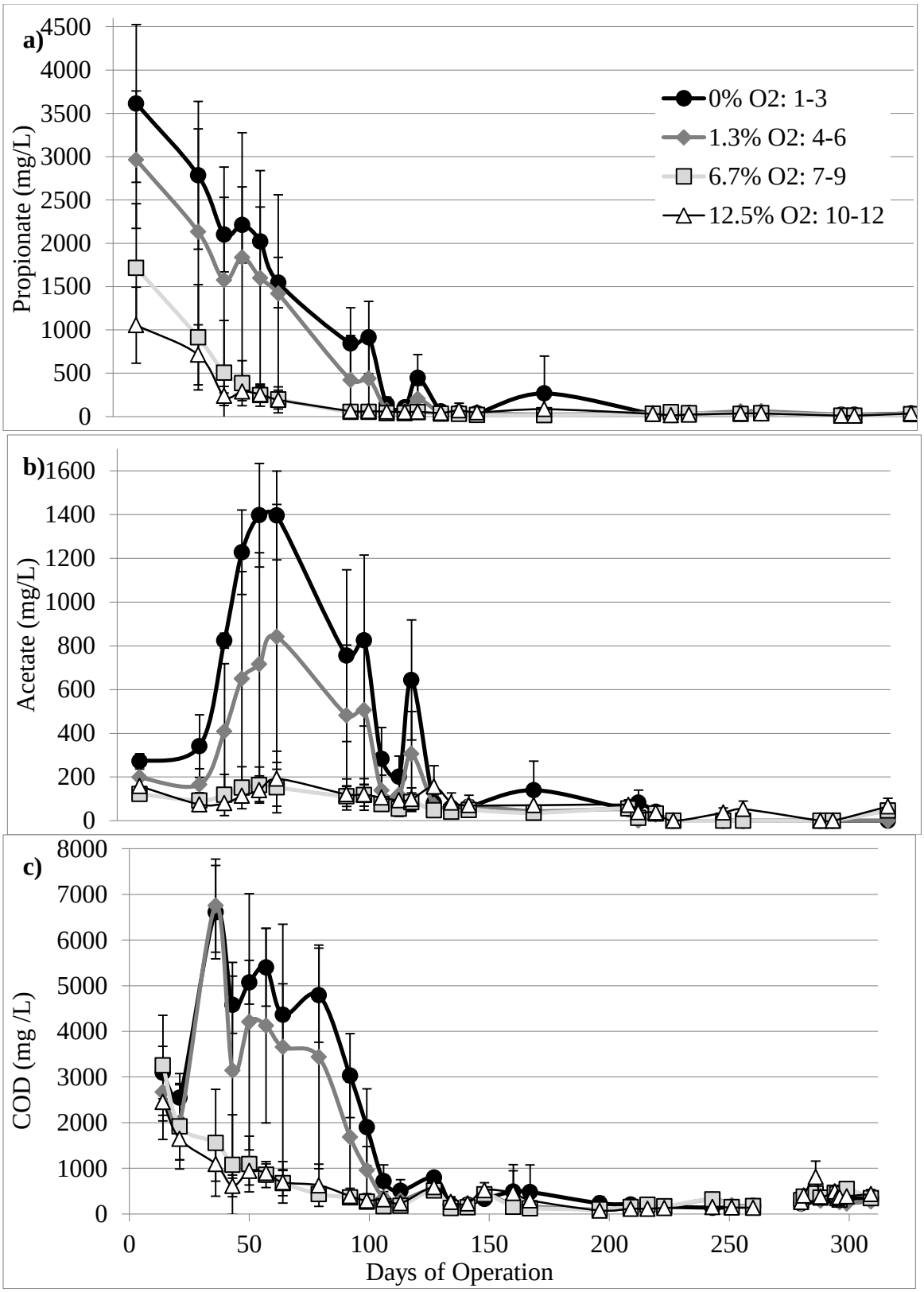

Figure 3-5. Average effluent concentrations of propionate (a), acetate (b), and COD (c), for three physical replicates of each enrichment culture. COD points before day 280 (break in graph) are SCOD and after day 280 are TCOD.

During the first six retention times, the propionate enrichments with low O_2 doses (0% and 1.3%) accumulated acetate and those that received higher O_2 doses (6.7% and 12.5%) did not accumulate acetate. This enhanced functional stability in the enrichments that received more O_2 is ostensibly due to the aerobic oxidation of intermediates (propionate, acetate, and H_2)—the added O_2 was used to convert a portion of the COD (propionate) into CO_2 and H_2O, as well as allowed pH values (6.98 ±0.16 and 6.96 ±0.15 in 6.7% and 12.5%, respectively) to remain in the normal range for anaerobic microorganisms. This is similar to previous work that found significantly lower VFA concentrations at higher O_2 doses (Hasegawa et al., 2000). Previously, the aerobic consumption of acetate and propionate occurred when O_2 supply was increased in anaerobic and aerobic cultures (Gerritse et al., 1990). In another study of anaerobic cultures, low O_2 loading rates (2.5% of the COD added as O_2) were linked to lower accumulation of VFAs (Botheju et al., 2010b). An upflow anaerobic sludge blanket (UASB) reactor with limited aeration also produced lower VFA concentrations (Zhou et al., 2007).

Another possible reason for the acetate accumulation may be that the initially diverse seed culture may have shifted over time away from organisms involved in the degradation of more complex substrates to organisms that effectively degraded propionate and acetate. That is, the very low VFA concentrations found after 12 retention times collectively suggest a gradual acclimation of the biomass to propionate, and, ostensibly, to those microbial guilds that degrade less complex substrates. This is important because propionate breakdown is often the rate-limiting step in the overall anaerobic degradation process, especially during start-up (Salminen, 2000; Wiegant, 1986; Kobayashi, 2009).

The decreasing acetate concentrations after day 70 may be linked to propionate concentrations. In enrichments with elevated concentrations of propionate, acetate

concentrations increased until propionate concentrations decreased to less than 1500 mg/L. All replicates receiving no O_2 and two of the three that received 1.3% of the TCOD as O_2 displayed this clear shift and did so at the same time (after six retention times). In previous research of anaerobic cultures (no added O_2), elevated propionate concentrations had similar detrimental effects. Ethanol, acetic acid, and butyric acid at 2400, 2400 and 1800 mg/L, respectively, did not cause a decrease in methanogen populations, whereas increasing propionic acid to 900 mg/L led to a nearly ten-fold reduction in methanogen numbers and the methanogenic activity dropped and remained low (Wang et al., 2009). Furthermore, a maximum CH_4 yield and maximum methanogen cell numbers occurred when the acetic acid was 1600 mg/L (Wang et al., 2009), which is similar to the 1400 mg/L to which the oxygenless cultures rose in this research. Thus, there may be a relationship between acetate utilization rate and propionate concentration.

A potential option to increase organic loading rate, especially during start-up, may be to add a limited amount of O_2, thereby degrading a portion of the COD via aerobic oxidation, which is in agreement with other research results (Zitomer and Shrout, 1998; Chu et al., 2005). A successive reduction in the increase of acetate concentration as O_2 dose increased points to an optimal O_2 dose. For example, for this substrate, the acetate concentration remained below 1000 mg/L when 1.3% of the TCOD was added as O_2. Therefore, an operator could conduct similar tests with a specific substrate and various O_2 doses to determine the dose that will maintain the propionate (or other VFA) level below a desired concentration.

Additionally, acclimation of the microbial consortium may allow the O_2 loading rate to be decreased to zero over time and the desired reduction in VFA still to be achieved through anaerobic biological degradation alone. This would simplify operation and avoid

costs of continued O_2 addition. Further investigation is needed to correlate different substrates, specific O_2 doses, and individual VFA concentrations.

3.3.1.3 Chemical Oxygen Demand (COD) Concentrations

SCOD concentrations depicted the advantage of the higher O_2 doses since the general trend of higher effluent SCOD in those enrichments receiving less O_2 during the first six retention times (Figure 3-5c) coincided with elevated effluent VFA concentrations (Figure 3-5a,b). Nevertheless, all 12 enrichments exhibited statistically similar TCOD effluent concentration at quasi steady state (days 280 through 308). Specifically, nine TCOD measurements on days 280 through 308 yielded the following for propionate enrichments 0, 1.3, 6.7, and 12.5% [mg TCOD/L] (percent COD removal given in parentheses): 340 ±62 (96.1 ±0.72%), 320 ±100 (96.3 ±1.2%), 400 ±90 (95.4 ±1.1%), 400 ±110 (95.0 ±2.2%), respectively. Thus, biomass acclimation was evident in that the COD removals in enrichments receiving 0 and 12.5% of the TCOD added as O_2 were statistically similar.

3.3.1.4 Volatile Suspended Solids (VSS) Concentrations

Biomass yields (0.090 ±0.02, 0.094 ±0.019, 0.097 ±0.027, 0.098 ±0.018 g VSS/g $COD_{removed}$ for propionate enrichments 0, 1.3, 6.7, and 12.5%, respectively) were statistically the same for all propionate enrichments according to VSS concentrations, with quasi steady state biomass concentration [g VSS/L] as follows: 0.66 ±0.21, 0.70 ±0.23, 0.71 ±0.23, and 0.72 ±0.22 in 0, 1.3, 6.7, and 12.5% enrichments, respectively. However, biomass yields (17 ±0.14, 24 ±0.34, 35 ±0.45, 53 ±1.5 ng iATP/mg $COD_{removed}$) positively correlated to O_2 dose according to ATP concentrations, with quasi steady state iATP concentrations [ng iATP/mL] as follows: 126 ±16.1, 177 ±92.0, 252 ±40.2, and 383 ±53.6 in 0, 1.3, 6.7, and

12.5% enrichments, respectively (compared to 0%, p >0.6, >0.98, >0.99 for 0, 1.3, 6.7, and 12.5% enrichments, respectively). This was expected, given the greater Gibbs' Free Energy available for biomass growth with O_2 as the electron acceptor ($\Delta G^{0'}$ = -78.72 kJ/eq) than with CO_2 as the electron acceptor ($\Delta G^{0'}$ = 23.52 kJ/eq) (Sawyer et al., 2003). Thus, relative to other enrichments, the ATP results were more in agreement with theoretical expectations than the VSS data. Low VSS concentrations were expected since propionate degradation provides little free energy (compared to more complex substrates) for biomass growth in anaerobic systems. Calcium was deposited (from calcium propionate substrate) on the filter during analysis; thus, the results of the total suspended solids (TSS) tests were unreliable. As such, these data were not presented.

3.3.2 Mass Balance of Propionate Enrichment Cultures

Biogas composition as well as influent and effluent COD concentrations allowed COD mass balances to be prepared for all 12 cultures (see Appendix D for example calculation). The averages of all four operational conditions balanced within 10%, and two lowest oxygen doses balanced within 5% (Table 3-5). The greatest error (percent closure) was present in those propionate enrichments that received the greatest O_2 dose (Table 3-5).

Table 3-5. COD Mass Balance Average Data of the Four Operating Conditions

O_2 Dose ($\%\ O_2$)	**COD_{in}** (gCOD/d)	**$O_{2,in}$** (g/d)	**$CH_{4(g)}$** (gCOD/d)	**TCOD** (gCOD/d)	**$O_{2,out}$** (g/d)	**COD_{out}** (g/d)	**Closure** (%)
0% O_2: 1-3	0.76	0.00	0.615±0.011	0.034±0.001	0.0000±0.001	0.655±0.011	86.4±1.3
1.3% O_2: 4-6	0.76	0.01	0.597±0.021	0.032±0.001	0.009±0.100	0.637±0.0202	83.9±2.4
6.7% O_2: 7-8	0.76	0.05	0.556±0.011	0.039±0.001	0.0177±0.006	0.637±0.0165	83.9±2.0
12.5% O_2: 10-12	0.76	0.10	0.521±0.006	0.043±0.001	0.0145±0.004	0.655±0.0036	86.3±0.4

Soluble CH_4 = 0.0068 g COD/d

Because less O_2 mass was measured after 24 h than immediately after adding O_2 (Table 3-10), some was consumed. One possible means is via aerobic oxidation of substrate. Although it cannot be defined using the data gathered, another mechanism for the consumption of O_2 (and for the decrease in CH_4 production rate at the highest O_2 doses) may be explained by methanotrophes: aerobic organisms that oxidize CH_4, forming CO_2 and water. Oxygen can foster their growth, thereby decreasing the measured overall CH_4 production of anaerobic reactors (Deublein and Steinhauser, 2008).

3.3.3 Effects of O_2 on Microbial Community Activity

Digester operating data, SMA and OOPA data, and community analysis show differences in the function and methanogen community of each enrichment.

3.3.3.1 Specific Methanogenic Activity (SMA) Testing

SMA values standardized using iATP were lower at 6.7% and 12.5% than SMA values at 0 and 1.3% ($p = 0.012$) (Figure 3-6a). Contrarily, the lowest SMA was observed for 0% and the highest SMA was demonstrated by 12.5% when SMA values were standardized using VSS mass ($p = 0.002$) (Figure 3-6b). Additionally, the standard deviations in the VSS-based SMA data were disproportionately greater than the iATP-based SMA standard deviations, which yielded statistically similar SMA values for 0%, 1.3%, and 6.7% as well as between 1.3% and 12.5%. Though more work investigating the relationship between VSS and iATP is needed, it appeared that inactive VSS may have distorted the data. Quasi steady state CH_4 production rates followed a pattern similar to the iATP SMA results in that 0% and 1.3% were statistically greater than 6.7% and 12.5% (Figure 3-6c).

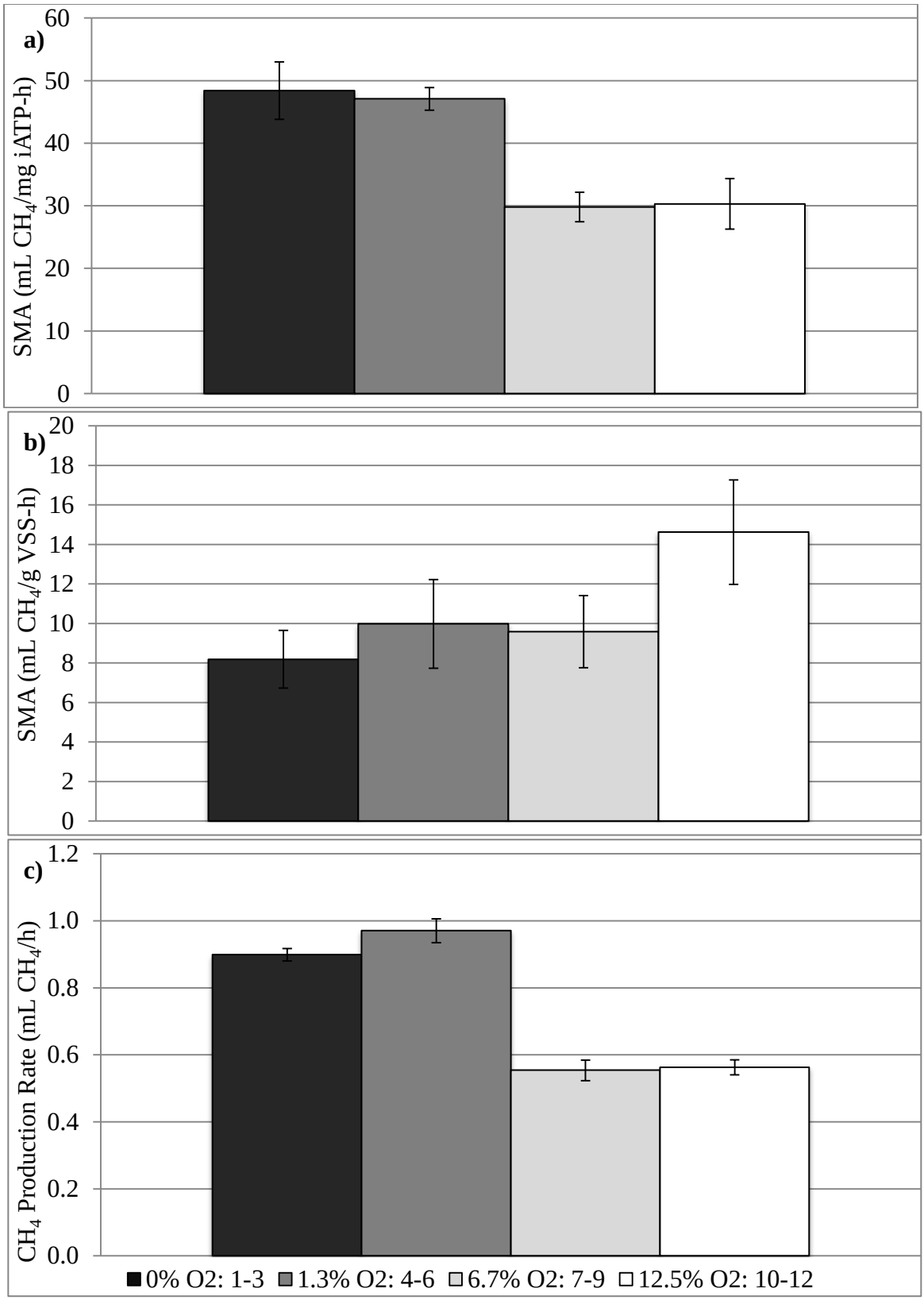

Figure 3-6. Relationship between SMA and O_2 dose. Data given: biomass in mg intracellular ATP (a), biomass in g VSS (b), and CH_4 production rate (c). Black, dark gray, light gray, and white columns represent enrichments with 0, 1.3, 6.7, and 12.5% of the TCOD added as O_2, respectively.

Anaerobic metabolism occurred in the partially aerated, completely mixed environments. A small mass of oxygen had no statistical effect on the CH_4 production rate. Propionate enrichments 1-3 (0% of the COD added as O_2) and 4-6 (1.3%) had statistically similar SMA values. Others have also found that methanogenic activities with propionate were not affected by low oxygen addition rates (Shen and Guiot, 1996). Additionally, there was a 60% greater SMA based on iATP in 1.3% enrichments compared to 6.7% enrichments.

One previous explanation for a similar SMA in 0% and 1.3% is that aeration oxidizes some available substrate, thereby removing some of the CH_4 potential, but enhanced hydrolysis can compensate for this reduction in hydrolysis-limited anaerobic digestion (Johansen and Bakke, 2006). However, with propionate as the substrate, this explanation did not apply to these enrichments. Therefore, it was posited that the consumption of some substrate may reduce the total amount of CH_4 produced, but would not reduce the rate of CH_4 production since a non-limiting propionate dose (3 g/L) was added in SMA tests.

3.3.3.2 Organic Overload Perturbation Activity (OOPA)

OOPA test results helped categorize the ability of each propionate enrichment culture to sustain a one-time organic overload of a readily fermentable sugar, glucose. The OOPA assay provided four fundamental parameters to quantify response to organic overload: capacity, M/F ratio, resilience coefficient, and PBY (Table 3-6).

Table 3-6. Average OOPA Parameters Obtained From Triplicates of Each Propionate Enrichment

Propionate Enrichment Cultures	**Resilience Coefficient** (h^{-1})	RC Std. Dev.	**M/F Ratio**	M/F Std. Dev.
0% O_2: 1-3	1.96	0.19	0.212	0.028
1.3% O_2: 4-6	2.11	0.63	0.226	0.048
6.7% O_2: 7-9	1.54	0.12	0.202	0.034
12.5% O_2: 10-12	1.20	0.15	0.160	0.052

	First Slope (mL biogas/h)	1^{st} Sl. Std. Dev.	**Secondary Slope** (mL biogas/h)	2^{nd} Sl. Std. Dev.
0% O_2: 1-3	4.38	0.21	0.92	0.10
1.3% O_2: 4-6	4.42	0.47	1.00	0.24
6.7% O_2: 7-9	4.10	0.43	0.81	0.08
12.5% O_2: 10-12	3.81	0.76	0.58	0.09

	Capacity (mL)	**Cap. Std. Dev.**	**Perturbed Biogas Yield** (% Theoretical max)	PBY Std. Dev.
0% O_2: 1-3	97.0	1.4	0.819	0.017
1.3% O_2: 4-6	98.0	2.2	0.827	0.019
6.7% O_2: 7-9	97.2	0.2	0.821	0.011
12.5% O_2: 10-12	97.8	1.1	0.826	0.013

*Inverse of time from feeding to 66.7% theoretical maximum biogas production x 100.
**Cumulative biogas production after 20 days divided by the theoretical maximum biogas production.

The propionate enrichments that received less O_2 (0 and 1.3% of the TCOD added as O_2) had statistically higher resilience coefficients and higher M/F ratios than the two that received more O_2 (6.7 and 12.5% of the TCOD added as O_2). This enhanced recovery without O_2 was different from the findings of Zitomer and Shrout (1998) who showed that digesters fed sucrose and given 1 and 0.1 g/L-d of O_2 returned to the initial pH after 34 and 28 days, respectively, whereas the completely anaerobic digesters did not recover in 52 days. While their smallest O_2 dose was comparable to the largest dose here, the authors noted that "oxygen transfer rates were significantly lower than the addition rates since some oxygen

escaped in off-gas" (Zitomer and Shrout, 1998). The difference may be attributable to lack of $NaHCO_3$ in the Zitomer and Shrout study. The buffer in the research described herein may have enabled methanogenesis to occur uninhibited.

Resilience coefficients and M/F ratios were higher in samples receiving lower O_2 doses. The resilience coefficients were greatest in 0% and 1.3%, which had statistically similar resilience coefficients (Figure 3-5). M/F ratios were highest in 0%, 1.3%, and 6.7%, which all had statistically similar values. Enrichment 1.3% had the highest average resilience coefficient and M/F ratio. The average capacity of the four physical conditions was statistically the same. Because the glucose dose was intentionally below a dose that would inhibit methanogenesis all together, the community was able to degrade substrate until essentially all was consumed. The capacity results confirmed that the test systems were not too severely overloaded. The PBY was found to be statistically the same in all enrichments, confirming that the biomass consumed all glucose to complete OOPA testing.

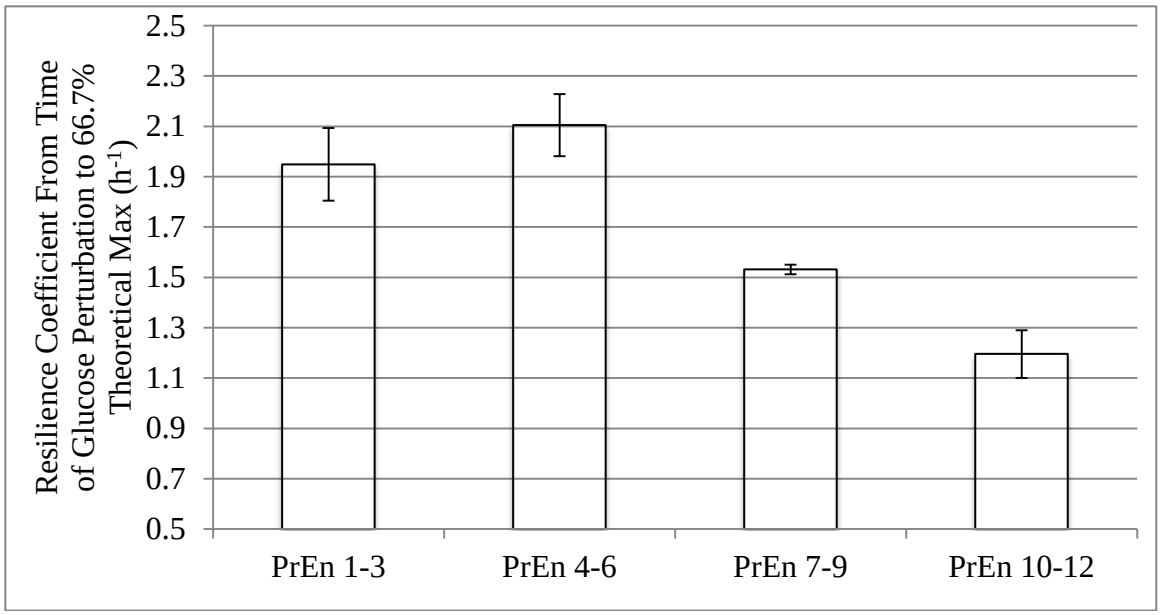

Figure 3-7. OOPA resilience coefficients (RC). Each column represents triplicates of each of the three physical replicates (nine per column). RC was defined as 100 times the inverse of the time from glucose perturbation until 66.7% of the theoretical maximum biogas production.

3.3.4 Effects of O_2 on Microbial Community Structure

Each of the DGGE banding patterns from the 12 propionate enrichments provided a unique fingerprint of one microbial culture (Figure 3-8). The optical densities of the nine bands found were measured and used in subsequent analysis.

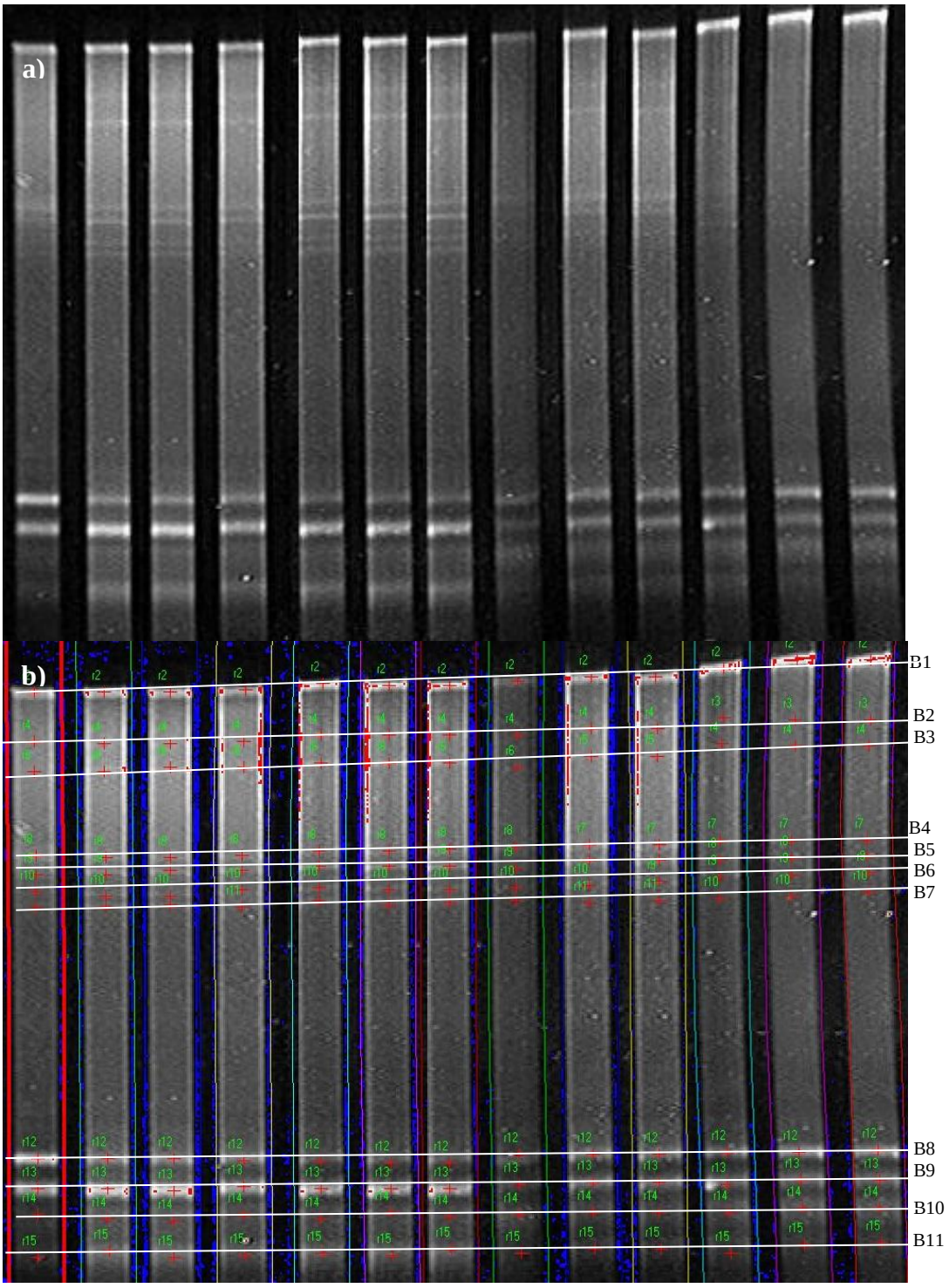

Figure 3-8. DGGE banding patterns: optical densities (a) and 11 bands for which optical densities were quantified in Lab Works v. 4.6.00.0 (b). Among these, the bottom nine rows were used in PCA because they had the greatest impact on principal components. Lanes are from left to right: ladder, propionate enrichment 12, propionate enrichment 11, …, propionate enrichment 1. B1, B2, …, B11 are band numbers, as used in subsequent analysis. Numbers seen on (b) are generated by Lab Works and, thus, different from those in analysis.

3.3.4.1 Clustering and Principal Component Analysis (PCA)

Optical density data from DGGE bands were plotted using PCA to depict 74.7% of the total variation for the optical density data: 48.6% and 26.1% of the variation on the first and second principal components, respectively (Figure 3-9). Each circle symbol represented one of the 12 enrichment cultures. The position of the circle was a function of the methanogenic community structure as defined by DGGE banding pattern. Bands 1 and 2 in the DGGE gel (Figure 3-8) were omitted in the PCA since they were nearly in line with the well and difficult to precisely measure. The nine remaining bands having the highest contribution to the principal components were included in the PCA (Figure 3-9). SMA values based on iATP were depicted the diameter of the data symbol (larger symbols correspond to higher SMA values). Lastly, the clustering results from the UPGMA algorithm were delineated with lines around clustered symbols.

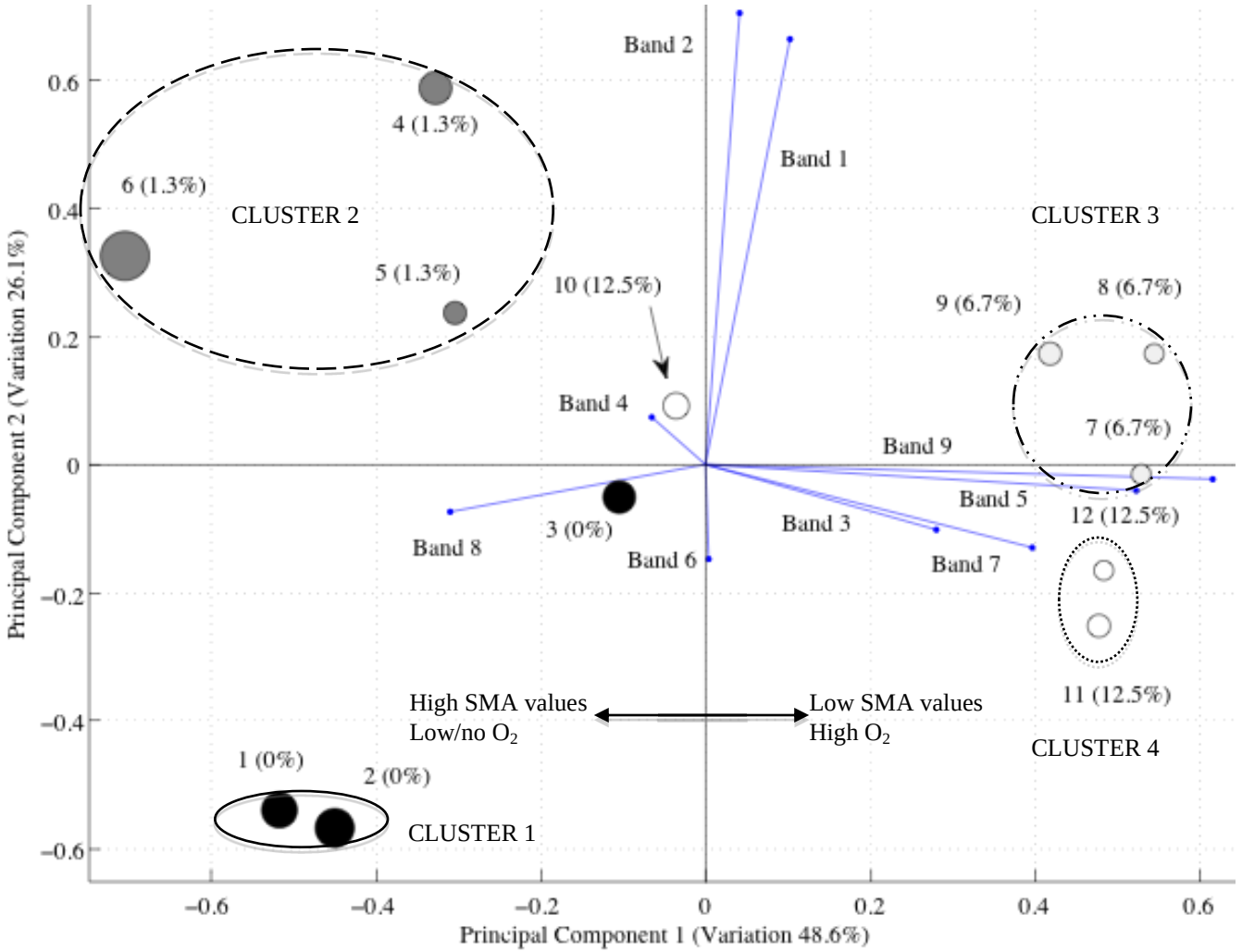

Figure 3-9. Principal Component Analysis (PCA) results for composite samples (taken on days 243-247) of 12 propionate enrichments (labeled according the numbers found in Table 3-4 and percent of TCOD added as O_2. Each vector represents one DGGE band and the diameter of each data point corresponds to the SMA magnitude. Four differently patterned circles indicate four clusters determined using the UPGMA algorithm.

First principal component = $0.1013(X_1) + 0.6650(X_2) - 0.2190(X_3) + 0.5431(X_4) – 0.2586(X_5) – 0.3625(X_6) + 0.0206 (X_7) – 0.0761(X_8) + 0.0058(X_9)$
Second principal component = $0.0402(X_1) + 0.7045(X_2) + 0.1844(X_3) – 0.3829(X_4) + 0.3229(X_5) + 0.4244(X_6) + 0.1202(X_7) – 0.1340 (X_8) + 0.0677(X_9)$
Where, X_1, X_2, X_3……X_9 are the normalized optical densities for bands B1, B2, B3……B9 of the DGGE banding pattern.

The PCA correlated microbial community structure with O_2 dose in that the DGGE banding patterns from triplicate enrichments that received the same O_2 dose typically clustered together (Figure 3-9). A clockwise progression on the PCA plot was revealed, as significant methanogenic population changes were observed with increasing O_2 dose. For example, Band 8 most significantly contributed positively to the banding pattern of 0% enrichments (1-3) and 1.3% enrichments (4-6), but had less impact on the other methanogenic communities.

The two outliers were enrichments 10 and 3. If enrichment 10 was excluded, then the four different O_2 doses corresponded to the four different quadrants in the PCA plot. Propionate enrichment 10, the most significant outlier, had a methanogenic community distinct from the other 12.5% replicates, which were most positively impacted by bands 3 and 7. At the time biomass samples used in DGGE analysis were taken, enrichment 10 had an acetate concentration that was 230% or more above the concentration in any other enrichment. This elevated concentration may have been caused by a smaller acetoclastic methanogen population.

The six greatest SMA values were on the left side of the PCA plot. Thus, bands 4 and 8 positively contributed to high SMA cultures. It is hypothesized that bands 4 and 8 may represent organisms that play a key metabolic role in the overall community, resulting in higher SMA values.

A phylogenetic tree constructed with the UPGMA algorithm applied to the optical density data from the DGGE banding patterns divided the enrichments into two higher-

level clusters, which further grouped into five sub- clusters (Figure 3-10). If the outlier (enrichment #10) was omitted from clustering, then all those receiving 0 and 1.3% of the TCOD added as O_2 clustered together and all those receiving 6.7 and 12.5% of the TCOD added as O_2 clustered together. Furthermore, the greatest four SMA values were found in one of the two main clusters (Cluster 1) and the smallest four on the other main cluster (Cluster 2) (Figure 3-10). Thus, the PCA and cluster analysis point to a link between methanogen community structure and SMA value.

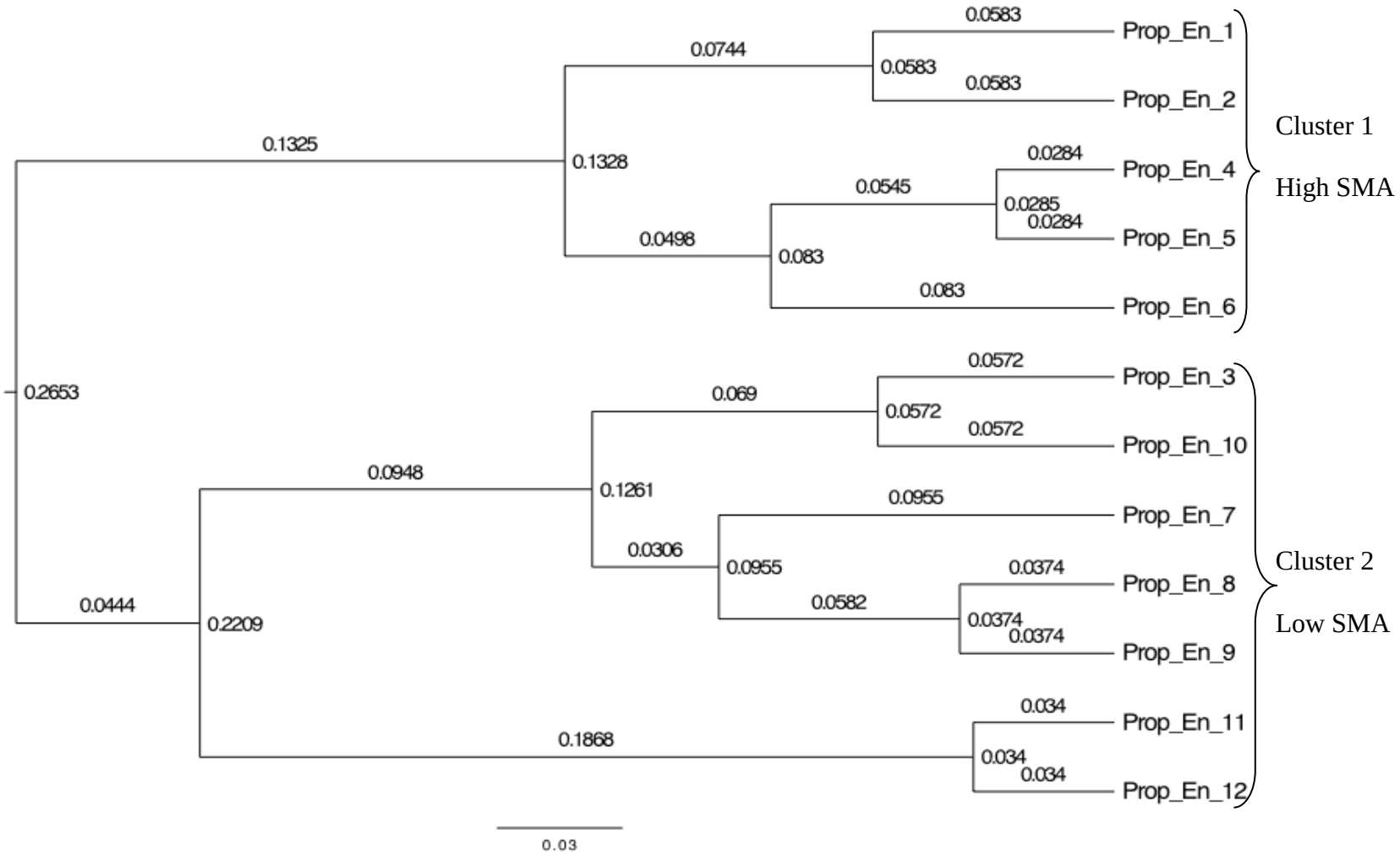

Figure 3-10. UPGMA Cluster analysis using one minus Pearson's Correlation Coefficient between the densitometric Datad of the two samples. Results are for microbial community biomass samples based on DGGE band densitometric data from 12 propionate enrichment cultures. Cultures defined with respect to oxygen dosing: #1-3 – 0% of TCOD added as O_2; #4-6 – 1.3% of TCOD added as O_2; #7-9 – 6.7% of TCOD added as O_2; #10-12 – 12.5% of TCOD added as O_2.

3.3.4.2 Relating SMA and Methanogen Community

Spearman's Correlation Coefficient was used to relate structure and function by using densitometric data (i.e., DGGE band intensities) and SMA values. A strong correlation between the SMA values and the densitometric data would lead to a strong correlation between the rankings of the two lists. With 12 samples, correlation scores above 0.671 and 0.727 were required to achieve 98 and 99% confidence (two-tailed) (Zar, 1972). The calculated Spearman's Rank Correlation Coefficient (r_s) of 0.699 indicated a statistically significant correlation above 98% between the rankings of the SMA and densitometric data (two-tailed) (Table 3-7). That is, microbial community structure correlated with SMA values at above the 98% correlation. This correlation between the SMA rank and the densitometric rank based on distance from the highest-SMA culture yielded a R^2 of 0.50 with linear regression (Figure 3-11).

Table 3-7. Spearman's Rank Correlation Coefficient Between SMA Values and Densitometric Data

Propionate Enrichment Number	SMA Data (mL CH_4/ mg iATP-h)	Rank (a)	Distance From PrEn6	Densitometric Data Rank (b)	d_i	d_i^2
1.3% O2 - 6	66.2	1	0.000	1	0	0
0% O2 - 2	51.7	2	0.393	7	-5	25
0% O2 - 1	50.3	3	0.292	5	-2	4
1.3% O2 - 4	44.0	4	0.195	3	1	1
0% O2 - 3	43.2	5	0.333	6	-1	1
12.5% O2 - 10	34.5	6	0.250	4	2	4
6.7% O2 - 9	32.4	7	0.398	8	-1	1
1.3% O2 - 5	31.1	8	0.187	2	6	36
12.5% O2 - 11	29.9	9	0.891	12	-3	9
6.7% O2 - 7	29.3	10	0.750	10	0	0
6.7% O2 - 8	27.7	11	0.529	9	2	4
12.5% O2 - 12	26.5	12	0.781	11	1	1

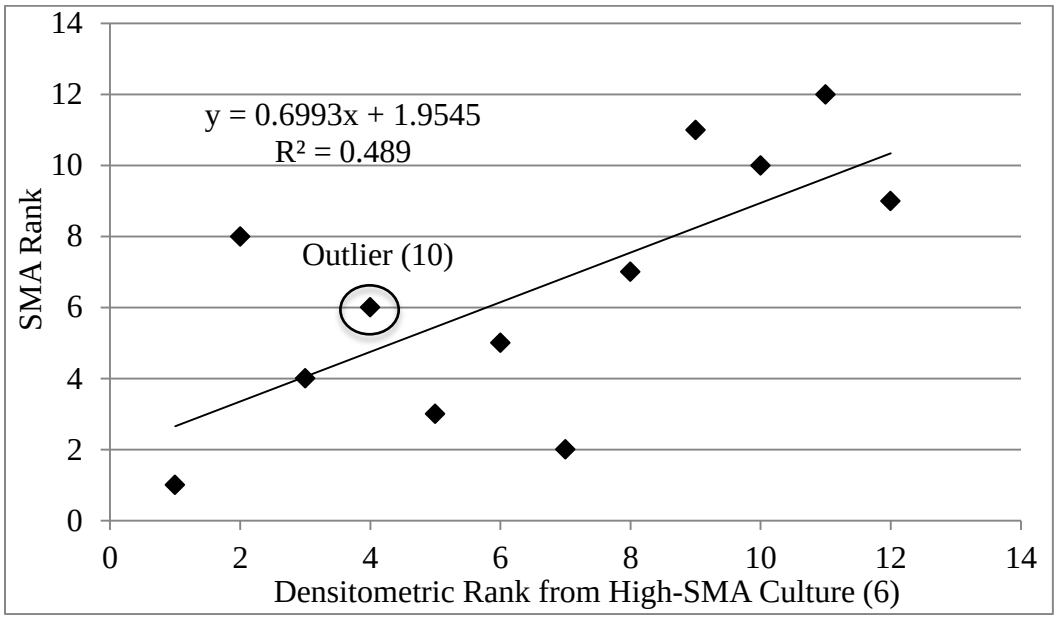

Figure 3-11. SMA Rank versus densitometric rank of enrichment culture with the highest SMA (greater SMA values indicated by lower numbers).

Tang et al. (2007) found that even the same substrate at different concentrations induced shifts in the bacterial community, as analyzed using DGGE. Though not the substrate, only the O_2 mass added varied among systems in this research, and that was sufficient to foster different microbial communities among the four conditions.

3.3.4.3 Quantitative Polymerase Chain Reaction (qPCR)

Two runs of qPCR, each in triplicate, were performed on the same biomass samples (from day 240) used for SMA and OOPA testing (Appendix F). The following *mcrA* gene copy numbers were measured in extracted DNA for enrichments receiving 0, 1.3, 6.7, and 12.5% of the TCOD added as O_2, respectively: $1.9x10^7 \pm 2.1x10^6$, $7.2x10^7 \pm 4.5x10^6$, $4.2x10^7 \pm 7.1x10^6$, and $5.8x10^7 \pm 9.1x10^6$ *mcrA* gene copies per mL extracted DNA. RNA transcripts were present in the following concentrations: $9.7x10^6 \pm 2.4x10^6$, $2.5x10^7 \pm 5.4x10^6$, $8.4x10^6 \pm 2.1x10^6$, and $2.3x10^6 \pm 2.5x10^5$ *mcrA* gene copies per mL extracted RNA. Results based on DNA showed statistically higher concentrations of *mcrA* gene copies in samples with no O_2

added compared to those that received 12.5% of the TCOD added as O_2. Furthermore, the results based on RNA showed statistically fewer *mcrA* gene copies were actually transcribed in progressively higher doses of O_2. In general, these results indicated that, especially for transcription, O_2 was detrimental to both the transcription of *mcrA* genes and to the specific rate of methanogenesis. Neither Spearman's correlation coefficient (r_s =-0.077) nor a scatter plot (R^2 = 0.036) comparing SMA versus qPCR data showed a correlation between the concentration of *mcrA* gene copies and SMA values.

3.4 Conclusions

Methane production occurred in the presence of up to 12.5% of the TCOD added as O_2. Limited O_2 addition (less than or equal to 6.7% of the TCOD added as O_2) reduced propionate accumulation during start up and may be a valuable tool to use at start up or in periods of increased loading. Along with digester operating data, SMA tests as well as a novel assay depicting response to overload were implemented to quantify microbial community function. Microbial community structure data were then analyzed. Function data correlated with community structure data in propionate enrichments given doses of O_2 that satisfied 0 to 12.5% of the TCOD. Hence, microbial community structure was correlated to the function of CH_4-producing bioprocesses. Further investigation is needed to understand the structure-function relationship with more complex substrates as well as to understand the advantages of specific oxygen doses on reducing VFA concentrations during start up.

3.5 Supplementary Material

3.5.1 Appendix A: Mass Balance Calculations

The following explains how the mass balance data were calculated. Propionate enrichment 4 (1.3% of the TCOD added as O_2) was used throughout this example. This was repeated in Excel for all 12 enrichments. COD is based upon aerobic oxidation and is the theoretical amount of O_2 needed to completely degrade a substrate (e.g., propionate). Thus, the theoretical half reactions were used to develop the overall reaction (Equation 3A-1).

Equation 3A-1. Propionate degradation with O_2 as the electron acceptor (Sawyer, et al., 2003)

$$2CH_3CH_2COO^- + 7O_{2(g)} \Leftrightarrow 4CO_2 + 2HCO_3^- + 4H_2O$$

The molar ratio of propionate to oxygen (2:7) was used to determine the theoretical mass of COD per day from the propionate added to the enrichments (Equation 3A-2). Feed was prepared daily using 1.4 L of aerated tap water, the basal nutrient media described in Table 3-3, and 9 g $Ca(CH_3CH_2COO)_2$ (98% purity). Therefore, 0.76 g COD/d was fed to each propionate enrichment.

Equation 3A-2. COD loading rate to propionate enrichments; Pr is propionate ($CH_3CH_2COO^-$)

$$\left(\frac{9gCa\,\mathrm{Pr}_2}{1.4L_{feed}}\right)\left(\frac{146g\,\mathrm{Pr}}{186gCa\,\mathrm{Pr}_2}\right)\left(\frac{mol\,\mathrm{Pr}}{73g\,\mathrm{Pr}}\right)\left(\frac{7molO_2}{2mol\,\mathrm{Pr}}\right)0.98 = 0.24\,{molO_2}/{L_{feed}}$$

$$\left(\frac{0.24molO_2}{L_{feed}}\right)\left(\frac{32gO_2}{molO_2}\right)\left(\frac{0.1L_{feed}}{1L_{reactor}\cdot d}\right)\left(\frac{gCOD}{gO_2}\right) = 0.76\,{gCOD}/{d}$$

The mass balance equation describes the individual components that contribute to COD in (COD_{in}, g COD/d) and out (COD_{out}, g COD/d) of the system per day. Effluent COD included the following: the COD in the CH_4 gas ($COD_{CH4(g)}$, g COD/d), COD of the soluble CH_4 ($COD_{CH4(s)}$, g COD/d), the TCOD in the liquid effluent ($TCOD_{Effluent}$, g COD/d), and the difference between the oxygen that was added to the enrichments (this

was based upon the O_2 dose) ($O_{2,in}$, g/d) minus the O_2 that was in the biogas ($O_{2,out}$, g/d) (Equation 3A-3).

Equation 3A-3. Overall mass balance on the COD of the propionate enrichments (units of g COD/d)

$$COD_{out} = COD_{in}$$

$$COD_{out} = COD_{CH_4,(g)} + \left(O_{2,in} - O_{2,out}\right) + TCOD_{effluent} + COD_{CH_4,(s)}$$

$$TCOD_{effluent} = COD_{biomass} + SCOD_{effluent} \quad (TCOD\ was\ exprimentally\ measured)$$

The ideal gas law was used along with experimental data on the average volume of CH_4 produced per day (which was 0.24 L/d for propionate enrichment 4 and was measured at 1 atm) and the biogas volume produced per day (which was 0.30 L/d of biogas and measured at 1 atm; this created 0.30 atm of partial pressure for a total of 1.3 atm in the 1-L headspace) to yield the average number of moles of CH_4 produced daily (Equation 3A-4).

Equation 3A-4. Experimental number of moles of CH_4 produced in propionate enrichments

$$n = \frac{PV}{RT}$$

$$n_{CH4(g)} = \frac{1\,atm\left(0.24^{LCH_4}\!/_{d}\right)}{\left(0.0821\frac{L\cdot atm}{mol\cdot K}\right)(273+35)K} = 0.0095^{molCH_4}\!/_{d}$$

In order to convert the moles of CH_4 per day into grams of COD, Equation 3A-5 was used.

Equation 3A-5. Reaction for O_2 and CH_4 (Sawyer, et al., 2003)

$$CH_{4(g)} + 2O_{2(g)} \Leftrightarrow CO_{2(g)} + 2H_2O$$

The ratio of moles of oxygen to moles of CH_4 (2:1) from Equation 3A-5 was then used to convert moles of CH_4 to grams of COD (Equation 3A-6).

Equation 3A-6. Mass of COD removed as CH_4 in biogas

$$COD_{CH4(g)} = 0.0095^{molCH_4}\!/_{d}\left(\frac{2molO_2}{molCH_4}\right)\left(\frac{32gO_2}{molO_2}\right)\left(\frac{gCOD}{gO_2}\right) = 0.61^{gCOD}\!/_{d}$$

The theoretical oxygen addition for each propionate enrichment was calculated using the daily volume of pure oxygen added (8, 40, and 75 mL, which corresponded to $3.3x10^{-4}$,

$1.7x10^{-3}$, $3.1x10^{-3}$ mol O_2/d in enrichments 4-6, 7-9, and 10-12) to determine the total mass of COD added as pure oxygen (Equation 3A-7).

Equation 3A-7. Theoretical daily oxygen addition into propionate enrichments 4 - 6 (1.3% of COD)

$$n = \frac{PV}{RT}$$

$$n_{O2(g),in} = \frac{1\,atm\left(0.008\,{LO_2}/{d}\right)}{\left(0.0821\frac{L\cdot atm}{mol\cdot K}\right)(273+22)K} = 0.00033\,{molO_2}/{d}$$

$$COD_{O2(g),in} = 0.00033\,{molO_2}/{d}\left(\frac{32gO_2}{mol\,O_2}\right)\left(\frac{gCOD}{g\,O_2}\right) = 0.0106\,{gCOD}/{d}$$

The O_2 mass out of the system per day was determined using the measured O_2 content and biogas volume produced at 35°C (Equation 3A-8).

Equation 3A-8. COD from oxygen in the effluent

$$n = \frac{PV}{RT}$$

$$n_{O2(g),in} = \frac{1\,atm\left(\frac{0.025L\,O_2}{L\,biogas}\right)0.3L\,biogas}{\left(0.0821\frac{L\cdot atm}{mol\cdot K}\right)(273+35)K} = 0.00030\,{molO_2}/{d}$$

$$COD_{O2(g),in} = 0.00030\,{molO_2}/{d}\left(\frac{32gO_2}{mol\,O_2}\right)\left(\frac{gCOD}{g\,O_2}\right) = 0.0095\,{gCOD}/{d}$$

Then the mass of TCOD in the effluent (measured as explained above) was converted into g COD/d (Equation 3A-9).

Equation 3A-9. TCOD in the effluent (measured)

$$TCOD_{effluent} = TCOD_{measured}$$

$$TCOD_{effluent} = 323\,{mgCOD}/{L}\left(\frac{g}{1000mg}\right)\frac{0.1L}{d} = 0.032\,{g\ COD}/{d}$$

The mass of COD present as soluble CH_4 in the effluent was accounted for using Engineering Toolbox solubility at 35°C (http://www.engineeringtoolbox.com/gases-

solubility-water-d_1148.html) to provide a mass of COD present in the 1-L liquid volume in all propionate enrichments (Equation 3A-10).

Equation 3A-10. COD from soluble CH_4 in the effluent (35°C)

$$COD_{CH_{4(s)}} = 0.017 \frac{gCH_4}{kg\ water}\left(\frac{molCH_4}{16\ gCH_4}\right)\left(\frac{2\ mol\ O_2}{molCH_4}\right)\left(\frac{32\ gO_2}{mol\ O_2}\right)\left(\frac{1kg}{1000g}\right)\left(\frac{1g\ H_2O}{mL\ H_2O}\right) = 0.000068\, {gO_2}/{mL}$$

$$COD_{CH_{4(s)}} = 0.000068\, {g\ O_2}/{mL}\left(\frac{100mL_{feed}}{d}\right)\left(\frac{1g\ H_2O}{mL\ H_2O}\right)\left(\frac{g\ COD}{g\ O_2}\right) = 0.0068\, {gCOD}/{d}$$

The total mass of COD out of the system was calculated, and the percent error between the measured COD into the system (0.76 g COD/d) and calculated mass out of the system was determined as follows (Equation 3A-11).

Table 3A-9. Total mass of COD out and error between theoretical and measured COD

$$COD_{out} = COD_{in}$$

$$COD_{out} = COD_{CH_4,(g)} + \left(O_{2,in} - O_{2,out}\right) + TCOD_{effluent} + COD_{CH_4,(s)}$$

$$COD_{in} = 0.76\, {gCOD}/{d}$$

$$COD_{out} = \left(0.61 + \left(0.0106 - 0.0095\right) + 0.032 + 0.0068\right) {gCOD}/{d} = 0.65\, {gCOD}/{d}$$

$$Percent\ Closure = \frac{0.65}{0.76} \times 100 = 86\%$$

$$Error = 1 - \frac{COD_{out}}{COD_{in}} = 1 - \frac{0.65}{0.76} = 14\%$$

3.5.2 Appendix B: Preliminary OOPA Testing

Preliminary testing to determine standard, active biomass concentration yielded three general trends in biogas production. Those with F:M ratios from 0.2 to 1 g COD/g VSS produced biogas and quickly leveled, indicating all substrate was consumed. When the F:M ratio was between approximately 3 and 10 g COD/g VSS, the biogas quickly increased to half of the final biogas volume and then gradually increased to a final biogas volume whereat the curve leveled. Final volumes were slightly less than the theoretical maximum in all samples. Lastly, F:M ratios from 12 to 33 g COD/g VSS quickly rose to slightly less than

half of the theoretical final biogas volume and remained there for the duration of the testing (more than two weeks), indicating a more severely overloaded condition. Because a clear distinction was evident between the initial and secondary slopes, the optimal overload concentration for OOPA analysis was in the middle range (3 and 10 g COD/g VSS). In particular, the greatest contrast between initial and secondary slopes was found at F:M ratios of 4.4 and 7.0 g COD/g VSS, which had initial average slopes of 1.51 ±0.05 and 3.62 ±0.12 as well as secondary slopes of 0.13 ±0.004 and 0.18 ±0.05, respectively (e.g., Figure 3B-1). Repeated results from this middle range of F:M ratios showed the same pattern—an initial spike to half of the 20-day maximum biogas level achieved followed by a less steep linear incline until reaching a maximum that was slightly below the theoretical maximum. Therefore, an F:M ratio of 5 was chosen as optimal for the OOPA test.

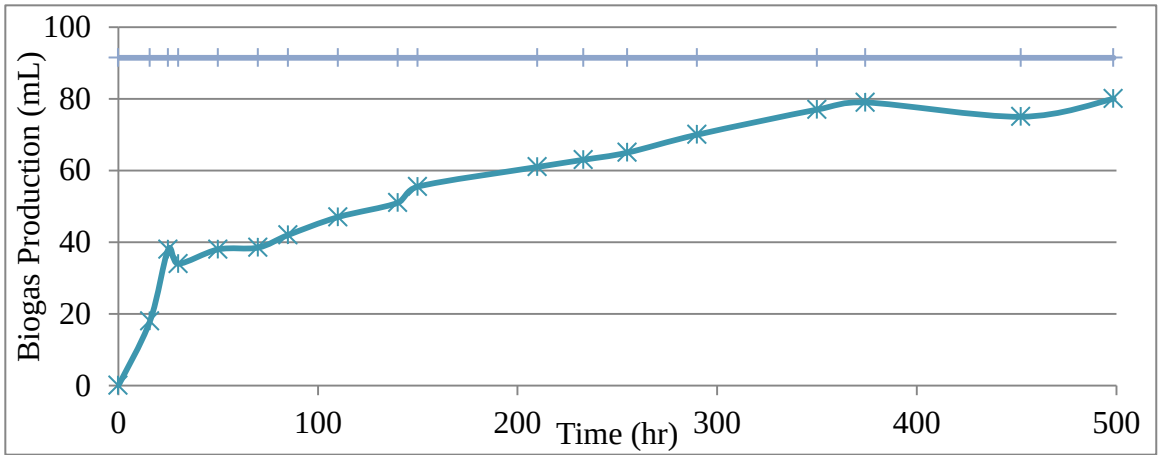

Figure 3B-12. OOPA: optimization of F/M ratio at 4.4 g COD/g VSS (3 g Glucose/L and 0.7g VSS/L) distinguished fermentation slopes ([mL biogas per h] of 1.548, 1.530, and 1.449) from methanogenesis slopes ([mL biogas per h] of 0.180, 0.177, and 0.141). Horizontal line at 92 mL represented 100% of the theoretical biogas production.

3.5.3 Appendix C: Correlation Coefficients

The correlation command, as quoted in MATLAB, determined: "one minus the sample correlation between points (treated as sequences of values)," thereby calculating the

distance matrix that was used to build phylogenetic trees and used Pearson's correlation coefficient (Equation 3C-1), r, which, for a set of n terms, is:

Equation 3C-1. Pearson's Correlation Coefficient

$$r = \frac{\sum_{i-1}^{n}\left(\left(x_i - \bar{x}\right)^2\left(y_i - \bar{y}\right)^2\right)}{\sqrt{\sum_{i-1}^{n}\left(x_i - \bar{x}\right)^2 \sum_{i-1}^{n}\left(y_i - \bar{y}\right)^2}}$$

Where x_i and y_i are the individual data points, x_{bar} and y_{bar} are the averages of the x and y data, respectively. Pearson's correlation coefficient is also known simply as the correlation coefficient or less simply as Pearson's Product Moment Correlation Coefficient.

Spearman's Correlation Coefficient (Equation 3C-2), r_s, was used to compare rankings of two data sets (e.g., SMA and densitometric data).

Equation 3C-2. Spearman's Correlation Coefficient (Zar, 1972)

$$r_s = 1 - 6\left(\frac{\sum_{i=1}^{n} d_i^{\,2}}{\left(n^3 - n\right)}\right)$$

where n is the number of samples (e.g., 12) and $d_i = \text{rank}(a_i) - \text{rank}(b_i)$, with a_i and b_i as individual data points for the same sample from the two data sets being compared.

3.5.4 Appendix D: Mass Balance Data

Tabulated data for each of the 12 propionate enrichments is presented below (Table 3D-1).

Table 3D-1. Mass Balance Using Theoretical COD_{in}, O_2 dose added, CH_4 production, and O_2 in effluent biogas.

Culture	COD_{in}	$O_{2,in}$	$CH_{4(g)}$	TCOD	O_2 Out		$CH_{4(s)}$	COD_{out}	Closure	Error
(% O_2)	(gCOD/d)	(g/d)	(gCOD/d)	(gCOD/d)	(%)	(g/d)	(gCOD/d)	(g/d)	(%)	(%)
0% O_2: 1-3	0.76	0.000	0.615	0.034	0.0	0.0000	0.0068	0.655	86.4%	13.6%
1.3% O_2: 4-6	0.76	0.011	0.597	0.032	2.4	0.0090	0.0068	0.637	83.9%	16.1%
6.7% O_2: 7-8	0.76	0.053	0.556	0.039	4.7	0.0177	0.0068	0.637	83.9%	16.1%
12.5% O_2: 10-12	0.76	0.099	0.521	0.043	4.0	0.0145	0.0068	0.655	86.3%	13.7%
0% O_2 - 1	0.76	0.000	0.603	0.035	0.05	0.0002	0.0068	0.645	85.0%	15.0%
0% O_2 - 2	0.76	0.000	0.618	0.033	0.00	0.0000	0.0068	0.659	86.9%	13.1%
0% O_2 - 3	0.76	0.000	0.624	0.032	0.17	0.0007	0.0068	0.663	87.3%	12.7%
1.3% O_2 - 4	0.76	0.011	0.608	0.032	2.48	0.0095	0.0068	0.648	85.5%	14.5%
1.3% O_2 - 5	0.76	0.011	0.610	0.032	2.44	0.0094	0.0068	0.649	85.6%	14.4%
1.3% O_2 - 6	0.76	0.011	0.572	0.032	2.27	0.0083	0.0068	0.613	80.8%	19.2%
6.7% O_2 - 7	0.76	0.053	0.563	0.039	3.84	0.0147	0.0068	0.647	85.3%	14.7%
6.7% O_2 - 8	0.76	0.053	0.548	0.040	5.49	0.0208	0.0068	0.626	82.5%	17.5%
*6.7% O_2 - 9**	*0.76*	*0.053*	*0.030*	*0.041*	*0.08*	*0.0000*	*0.0068*	*0.131*	*17.3%*	*82.7%*
12.5% O_2 - 10	0.76	0.099	0.517	0.043	4.04	0.0146	0.0068	0.652	85.9%	14.1%
12.5% O_2 - 11	0.76	0.099	0.528	0.043	4.72	0.0173	0.0068	0.659	86.9%	13.1%
12.5% O_2 - 12	0.76	0.099	0.516	0.044	3.34	0.0117	0.0068	0.654	86.3%	13.7%

*Methane production was not accurately measured in propionate enrichment 9 due to limitations in the apparatus.

3.5.5 Appendix E: Range Weighted Richness (R_r) and Functional Organization (F_o)

While fingerprinting techniques have often been limited to determining similarity or difference, some parameters have been developed to extract more information from DGGE banding patterns for the 16S rRNA gene. These parameters include microbial community dynamics (Dy), range weighted richness (Rr), and functional organization (Fo) (Marzorati et al., 2008). Briefly, Dy is essentially the ability to change. If fingerprints are taken at two or more time intervals (t_o, t_1,…, t_n), the higher change in the number of different organisms at t_n per unit of time, related to the number of organisms previously detected at t_o, the more dynamic the community. Because DGGE was only performed once at the onset of SMA and OOPA testing, Dy was not calculated in this study.

Range weighted richness is defined as follows:

Equation 3-11. Range Weighted Richness

$$Rr = \left(N^2 \times Dg\right)$$

wherein N is the total number of bands in the gel (or portion thereof that is being analyzed) and Dg is the denaturing gradient (v/v fraction) difference from the first through the last bands in a lane. Rr is a modified measure of alpha diversity. The originator of this variable suggested that: low Rr (less than ten) indicated an adverse environment that was restricted to colonization, high Rr (more than 30) indicated a favorable environment that encouraged colonization, and medium Rr ($10<Rr<30$) fell in between (Mertens et al., 2005; Marzorati et al., 2008). In this research, gel pictures were divided into sections along the gel height representing 5% of the denaturant concentration. Then the number of bands and sections of gel that contained all the bands were obtained, and, Rr was calculated.

Functional organization, Fo, describes how well a community is organized such that, upon perturbation, it can adapt and remain functionally stable (Marzorati et al., 2008). Functional and structural stability of a microbial community do not always coincide; in fact, structural flexibility (i.e., instability) may be necessary for functional stability in some situations, and structural flexibility may be linked to the evenness of a community (Fernandez et al., 2000). Therefore, quantification of evenness helps provide a better understanding of microbial community response to perturbations. To do this, Pareto-Lorenz (PL) evenness curves were constructed to graphically represent the DGGE banding patterns (Mertens et al., 2005; Wittebolle et al., 2008). All bands were ranked from high to low abundance (i.e., 1 to n) using band intensities (i.e., optical densities); this rank was divided by the total number of bands to give a normalized X (i.e., the cumulative number of bands, which was the x-coordinate). The intensity of each band was then normalized by dividing it by the total intensity of all bands in the lane, giving the proportion or relative abundance of each phylotype/band (y-coordinate). High Fo is synonymous with low evenness and vice versa. Thus, a perfectly even community would be graphed as a 45° line through the origin, whereas an increasingly uneven community approaches an L-shape (Figure 3E-1).

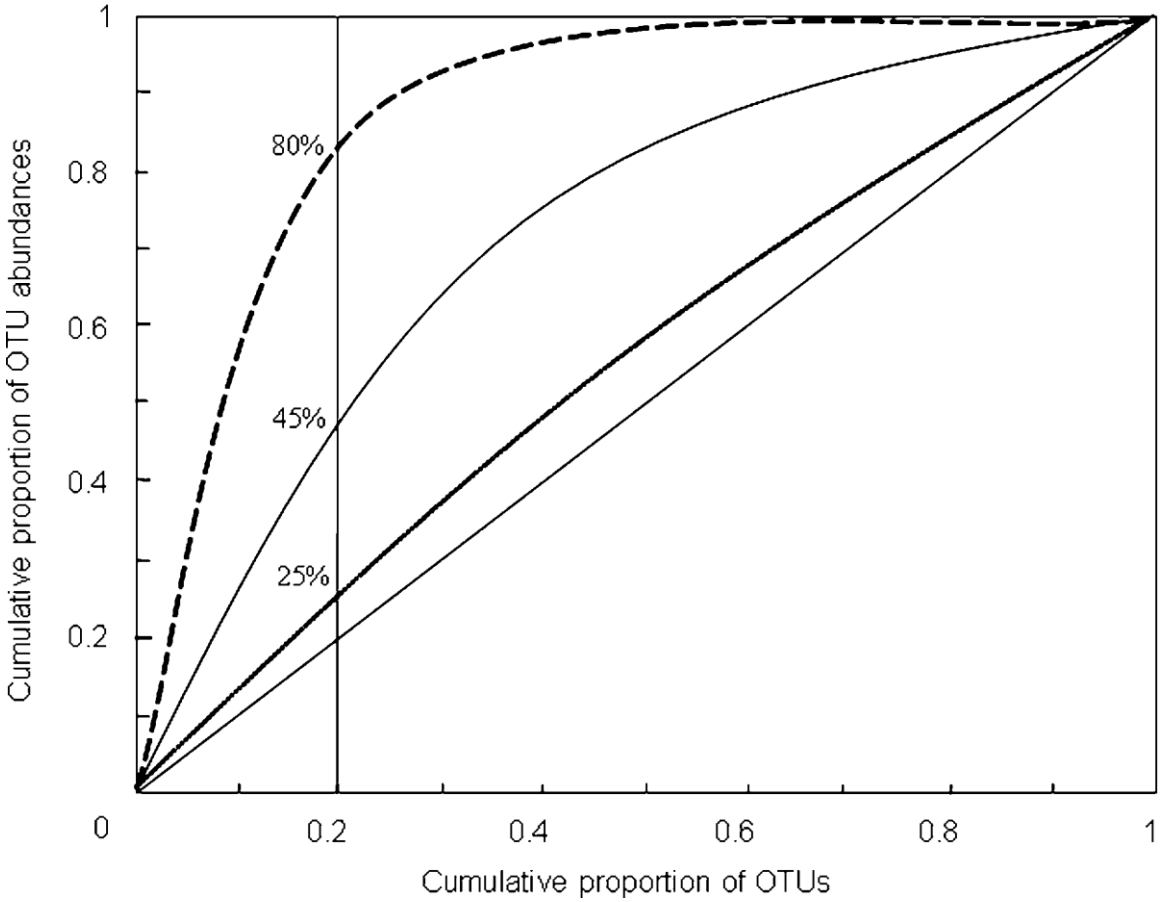

Figure 3E-1. Pareto-Lorenz curves of hypothetical DGGE banding patterns. A low, medium, and high functional organization are shown in the 25%, 45%, and 80% lines, respectively. The 45° diagonal line is a perfectly even community. Courtesy of Marzorati et al., 2008.

3.5.5.1 Range Weighted Richness (R_r) Results

Beta diversity was measured via range weighted richness (Rr) (Table 3E-1). The number of bands, N, varied from 4 in propionate enrichments receiving 0% of the TCOD added as O_2 to 10 in propionate enrichments receiving 12.5% of the TCOD added as O_2. The denaturant gradient, Dg, varied from less than 0.2 in propionate enrichments receiving 0% of the TCOD added as O_2 to 0.8 in propionate enrichments receiving 12.5% of the TCOD added as O_2. Lanes were classified as low, medium, or high Rr, according to the criteria specified elsewhere (Mazorati et al., 2008).

Table 3E-1. Range Weighted Richness (Rr) of Propionate Enrichments

Sample: Based on visual Detection of Bands	0% O_2-1	0% O_2-2	PrEn3	PrEn4	PrEn5	PrEn6	PrEn7	PrEn8	PrEn9	PrEn10	PrEn11	PrEn12
Rr	3	3	3	47	47	27	80	80	80	80	80	80
Classification*	L	H	H	H	H	H	H	H	H	H	H	H

*H = high Rr (Rr > 30); M = medium Rr (10 < Rr < 30); L = low Rr (Rr < 10).

3.5.5.2 Functional Organization (F_o) Results

The Pareto-Lorenz curves were plotted to describe the functional organization (Fo) of each of the 12 propionate enrichment communities (Figure 3-14). The developers of the Fo methodology used herein suggest focusing on the relative abundance (y-axis) at 20% of the cumulative number of bands (x-axis) because typically 20% of the bands correspond to 40% or more of the total intensity (Wittebolle et al., 2008). In this work, 20% ranged from 30 to 40% of the total intensity; thus, the dominant organisms were identified in just two bands. Additionally, a later study proposed to consider three general classifications for functional organization, as indicated by three horizontal lines in Figure 3-24 (Marzorati et al., 2008). At 25% cumulative phylotype abundance (y-axis) for 20% cumulative population (x-axis), the community was said to have high evenness and low Fo. This may have resulted from a lack of selective pressure; thus, many species survived—none as dominant. Around 45%, the community had medium Fo and was fairly balanced, and near 80%, the community was specialized with only a few dominant species and a high level of functional organization (Marzorati et al., 2008). Stresses to a high Fo community may require extensive recovery periods due to a lack of parallel metabolic pathways. This lack, which decreased the likelihood that the same function was performed by an unharmed organism, has been linked to decreased ability to handle perturbations (Hashsham, 2000).

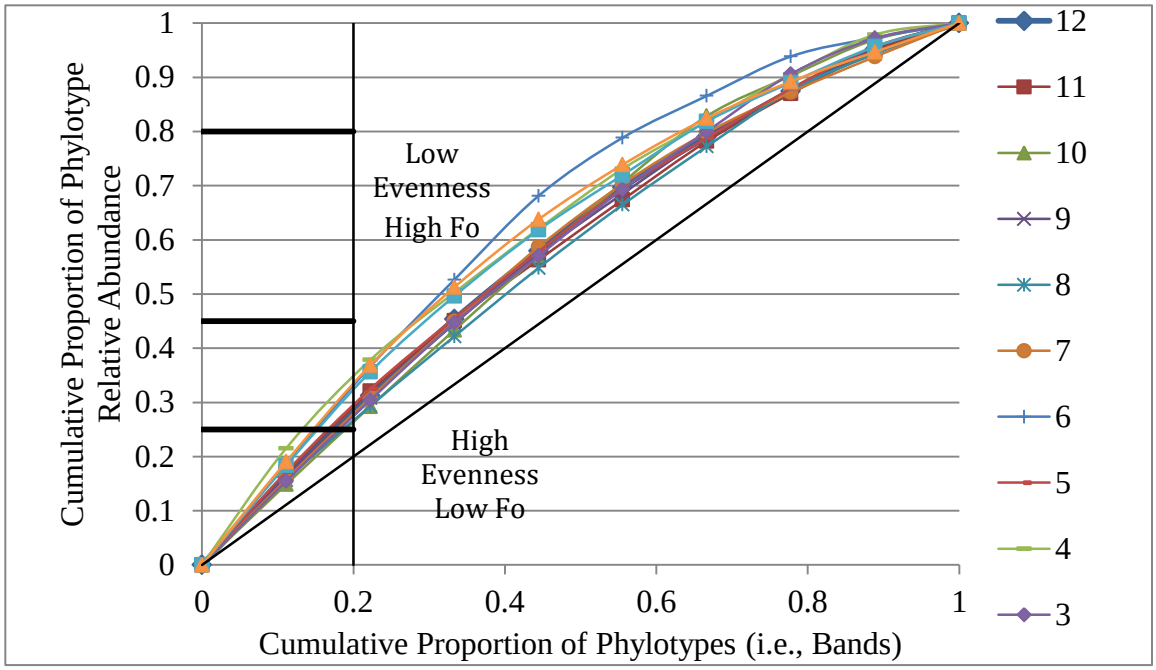

Figure 3E-2. Pareto Lorenz Evenness Curve describing functional organization (Fo). Propionate enrichment 6 had the greatest SMA and lowest evenness.

In spite of the low variability of evenness (i.e., small range of Fo) among the 12 propionate enrichments, there was still a clear relationship: those communities with greater Fo had higher SMA values. Propionate enrichment 6 (1.3% of TCOD added as O_2) had the highest Fo, followed by enrichments 2 (0%), 1 (0%), and then 4 (1.3%). Likewise, propionate enrichment 6, followed by enrichments 2, 1, and then 4 had the highest SMA values. This builds on the findings of Werner et al. (2011), who also correlated evenness and SMA. A deeper key here is that nearly all, if not all, of the propionate enrichments displayed a low Fo (high evenness). Werner concluded that the resilience observed might be due to the specialized metabolic functions of syntrophs; thus, syntroph populations are less susceptible to competition from functionally redundant organisms. Likewise, in these propionate-fed enrichments, selectivity may have occurred in the methanogenic populations measured. Since the cumulative abundance at 20% of the total population only ranged from 25% to 35%,

more investigation is needed to examine a broader range of Fo (e.g., above 80% to below 25%) to see if there is an optimal (Marzorati et al. (2008) hypothesized optimal was 45%).

The tight Fo values may be more indicative of the lack of diversity in measuring a functional gene that is less than 400 bp compared to 16S RNA, to which Rr and Fo were originally applied. Since syntrophs and methanogens have highly specific substrates, this similarity in Rr and Fo for methanogenic populations can be putatively compared with Werner et al. (2011) who found greater uniformity among syntrophic organisms in different anaerobic digesters than other guilds.

3.5.6 Appendix F: qPCR Data

Data for qPCR for all propionate enrichments are presented below.

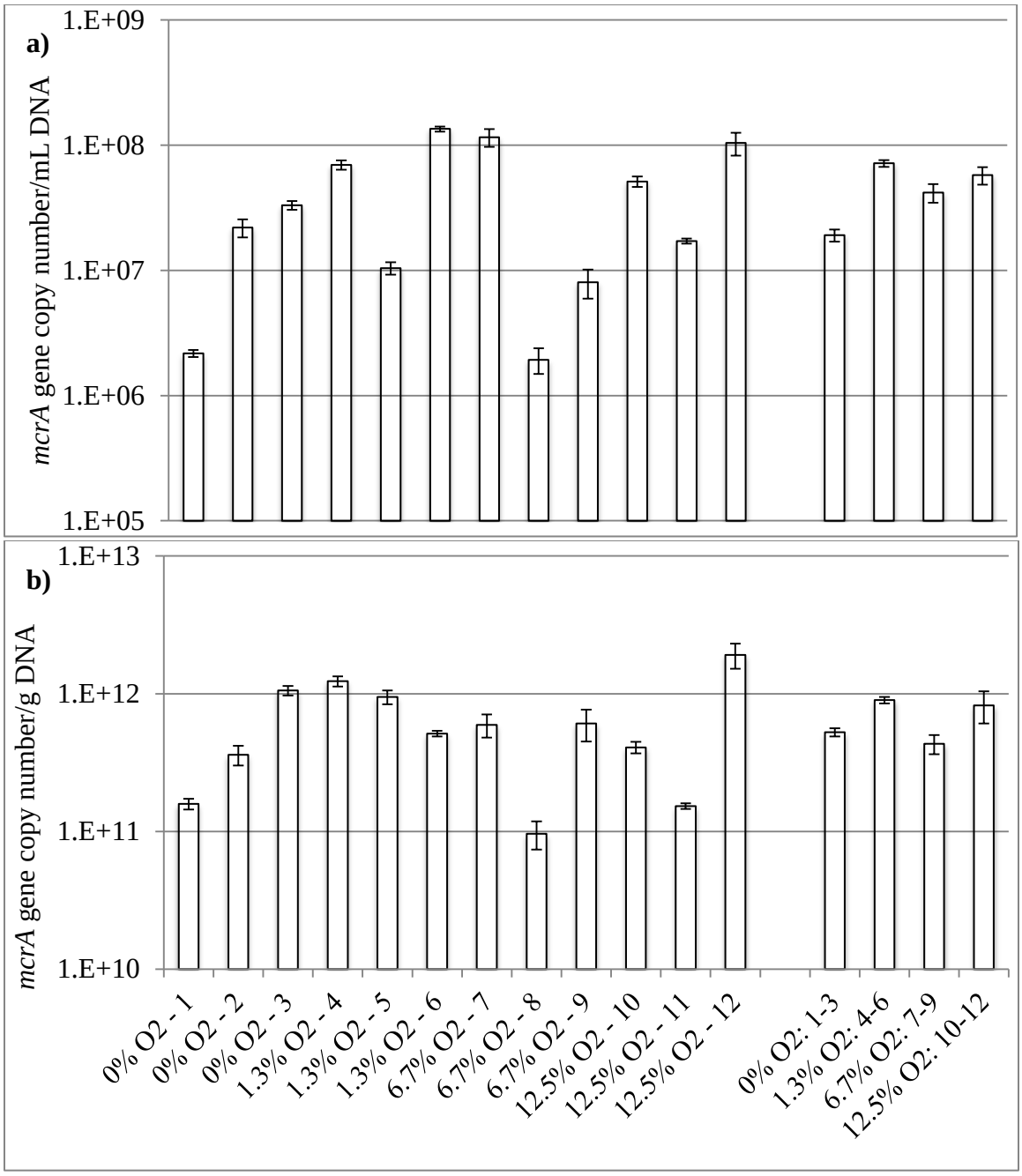
a)
1.E+09
1.E+08
1.E+07
1.E+06
1.E+05
mcrA gene copy number/mL DNA
b)
1.E+13
1.E+12
1.E+11
1.E+10
mcrA gene copy number/g DNA
0% O2 - 1
0% O2 - 2
0% O2 - 3
1.3% O2 - 4
1.3% O2 - 5
1.3% O2 - 6
6.7% O2 - 7
6.7% O2 - 8
6.7% O2 - 9
12.5% O2 - 10
12.5% O2 - 11
12.5% O2 - 12
0% O2: 1-3
1.3% O2: 4-6
6.7% O2: 7-9
12.5% O2: 10-12

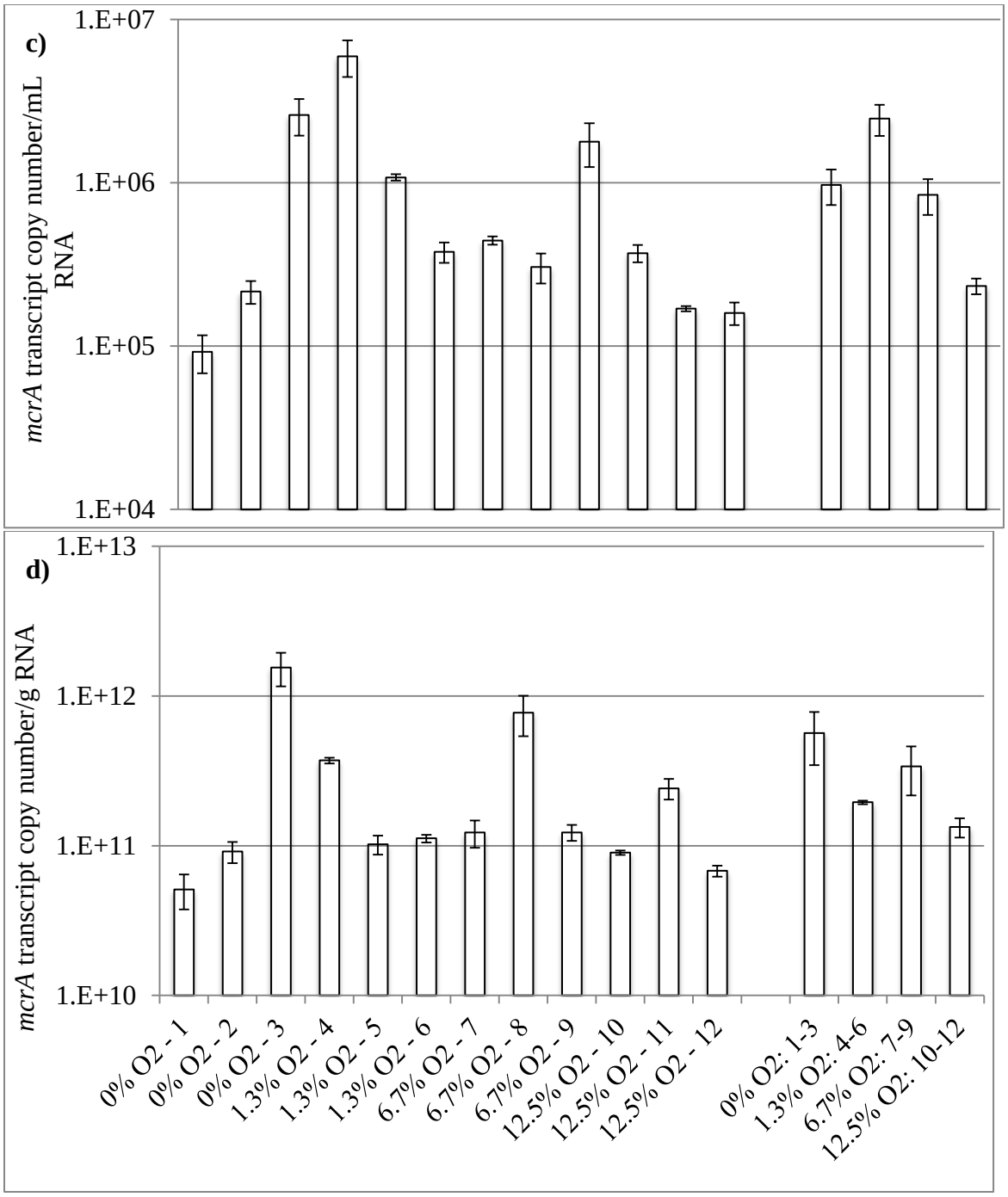

Figure 3F-1. qPCR results for presence of *mcrA* Gene in extracted DNA in terms of *mcrA* gene copy number per mL DNA (a) and per g DNA (b), as well as *mcrA* transcript copy number per mL RNA (c), and per g RNA (d).

3.6 REFERENCES

American Public Health Association (APHA), American Water Works Association (AWWA), Water Environment Federation (WEF) (1998) Standard Methods for the Examination of Water and Wastewater (20th ed.). APHA et al.

American Public Health Association (APHA), American Water Works Association (AWWA), Water Environment Federation (WEF) (2005) Standard Methods for the Examination of Water and Wastewater (21st ed.). APHA et al.

Angelidaki, I., Alves, M., Bolzonella, D., Borzacconi, L., Campos, L., Guwy, A., Jenicek, P., Kalyuzhnui, S., and Van Lier, J. (2007) *Anaerobic Biodegradation, Activity and Inhibition (ABAI) Task Group Meeting Report.* Prague, Czech Republic. October 9-10, 2006.

Bidle, K.A., Kastner, M., and Bartlett, D.H. (1999) "A Plylogenetic Analysis of Microbial Communities Associated With Methane Hydrate Containing Marine Fluids and Sediments in the Cascadia Margin (ODP site 829B)." *FEMS Microbiology Letters*. 177.1:101-108.

Boon, N., Windt, W.D., Verstraete, W., and Top, E.M. (2002) " Evaluation of Nested PCR-DGGE (Denaturing Gradient Gel Electrophoresis) With Group-Specific 16S rRNA Primers for the Analysis of Bacterial Communities from Different Wastewater Treatment Plants." *FEMS Microbiology Ecology*. 39:101-112.

Botheju, D., & Bakke, R. (2011). Oxygen Effects in Anaerobic Digestion – A Review. *Waste Management*, (3901), 1-19.

Botheju, D., Samarakoon, G., Chen, C., and Bakke, R. (2010a) "An experimental study on the effects of oxygen in bio-gasification: Part 1." in proceedings of the International Conference on Renewable Energies and Power Quality (ICREPQ 10), Granada, Spain, March, 2010. Archived in *Renewable Energies & Power Quality Journal* (RE&PQJ), Vol. 8, 2010d.

Botheju, D., Samarakon, G., Chen, C., and Bakke, R. (2010b) "An experimental study on the effects of oxygen in bio-gasification; Part 2" in proceedings of the International Conference on Renewable Energies and Power Quality (ICREPQ 10), Granada, Spain, March, 2010. Archived in *Renewable Energies & Power Quality Journal* (RE&PQJ), Vol. 8, 2010e.

Briones, A. and L. Raskin (2003), "Diversity and dynamics of microbial communities in engineered environments and their implications for process stability," *Current Opinion in Biotechnology*, 14 (3), 270-276.

Bustin, S. a, Benes, V., Garson, J. a, Hellemans, J., Huggett, J., Kubista, M., Mueller, R., et al. (2009). The MIQE guidelines: minimum information for publication of quantitative real-time PCR experiments. *Clinical Chemistry*, *55*(4), 611-22. doi:10.1373/clinchem.2008.112797

Chen, Y., Cheng, J. J., & Creamer, K. S. (2008). Inhibition of anaerobic digestion process: a review. *Bioresource technology*, *99*(10), 4044-64. doi:10.1016/j.biortech.2007.01.057

Chu, L.-bing, Zhang, X.-wen, Li, X., & Yang, F.-lin. (2005). Simultaneous removal of organic substances and nitrogen using a membrane bioreactor seeded with anaerobic granular sludge under oxygen-limited conditions. *Desalination*, *172*, 271-280.

Dalirsefat, S. B., da Silva Meyer, A., & Mirhoseini, S. Z. (2009). Comparison of similarity coefficients used for cluster analysis with amplified fragment length polymorphism markers in the silkworm, Bombyx mori. *Journal of Insect Science*, *9*(71), 1-8. doi:10.1673/031.009.7101

Deublein, D. and Steinhauser, A. *Biogas from Waste and Renewable Resources: An Introduction*. Weinheim: Wiley-VCH Verlag GmbH & Co. KGaA, 2008.

Dogan, T., Ince, O., Oz, N., & Ince, B. (2005). Inhibition of Volatile Fatty Acid Production in Granular Sludge from a UASB Reactor. *Journal of Environmental Science and Health, Part A: Toxic/Hazardous Substances & Environmental Engineering*, *40*(3), 633-644. doi:10.1081/ESE-200046616

Fernandez, A. S., Hashsham, S. A., Dollhopf, S. L., Raskin, L., Glagoleva, O., Dazzo, F. B., Hickey, R. F., et al. (2000). Flexible Community Structure Correlates with Stable Community Function in Methanogenic Bioreactor Communities Perturbed by Glucose. *Applied and Environmental Microbiology*, *66*(9), 4058-4067. doi:10.1128/AEM.66.9.4058-4067.2000.Updated

Freitag, T. E., & Prosser, J. I. (2009). Correlation of methane production and functional gene transcriptional activity in a peat soil. *Applied and Environmental Microbiology*, *75*(21), 6679-87. doi:10.1128/AEM.01021-09

Freitag, T. E., Toet, S., Ineson, P., & Prosser, J. I. (2010). Links between methane flux and transcriptional activities of methanogens and methane oxidizers in a blanket peat bog. *FEMS Microbiology Ecology*, *73*(1), 157-65. doi:10.1111/j.1574-6941.2010.00871.x

Galand, P. E., Saarnio, S., Fritze, H., & Yrjälä, K. (2002). Depth related diversity of methanogen Archaea in Finnish oligotrophic fen. *FEMS Microbiology Ecology*, *42*(3), 441-9. doi:10.1111/j.1574-6941.2002.tb01033.x

Gerritse, J., Schut, F., and Gottschal, J.C. (1990) Mixed chemostat culture of obligately aerobic and fermentative or methanogenic bacteria under oxygen-limiting conditions. *FEMS Microbiology Letters* 66:87-94. "In fact a stimulation of methane production of about 20% was found at low oxygen fluxes"

Goffredi, S. K., Wilpiszeski, R., Lee, R., & Orphan, V. J. (2008). Temporal evolution of methane cycling and phylogenetic diversity of archaea in sediments from a deep-sea whale-fall in Monterey Canyon, California. *The ISME Journal*, *2*(2), 204-20. doi:10.1038/ismej.2007.103

Hanaki, K., T. Mastsuo, and M. Nagase. 1981. Mechanism of inhibition caused by long-chain fatty acids in anaerobic digestion process. Biotechnol. Bioeng. 23:1591–1610.

Hasegawa, S., Shiota, N., Katsura, K., & Akashi, a. (2000). Solubilization of organic sludge by thermophilic aerobic bacteria as a pretreatment for anaerobic digestion. *Water Science and Technology*, *41*(3), 163-9. Retrieved from http://www.ncbi.nlm.nih.gov/pubmed/11381987

Hashsham, S. A., Fernandez, A. S., Dollhopf, S. L., Dazzo, F. B., Hickey, R. F., Tiedje, J. M., & Criddle, C. S. (2000). Parallel processing of substrate correlates with greater functional stability in methanogenic bioreactor communities perturbed by glucose. *Applied and Environmental Microbiology*, *66*(9), 4050-7. Retrieved from http://www.pubmedcentral.nih.gov/articlerender.fcgi?artid=92258&tool=pmcentrez&rendertype=abstract

Hatamoto, M., Imachi, H., Ohashi, A., & Harada, H. (2007). Identification and cultivation of anaerobic, syntrophic long-chain fatty acid-degrading microbes from mesophilic and thermophilic methanogenic sludges. *Applied and Environmental Microbiology*, *73*(4), 1332-40. doi:10.1128/AEM.02053-06

Hao, L., He, P.J., Lu, F., Shao, L. and Zhu, M. (2009). Regulating the hydrolysis of organic waste by micro-aeration and effluent recirculation, *Waste Management*, 29, 2042-2050.

Hungate, R. E. and Macy, J. (1973) The Roll-Tube Method for Cultivation of Strict Anaerobes *Bulletins from the Ecological Research Committee*, No. 17, Modern Methods in the Study of Microbial Ecology, pp. 123-126 Published by: Oikos Editorial Office_Article Stable URL: http://www.jstor.org/stable/20111550 [73]

Jagadabhi, P. S., Kaparaju, P. and Rintala, J. (2009) Effect of micro- aeration and leachate replacement on COD solubilization and VFA production during mono-digestion of grass-silage in one-stage leach-bed reactors, *Bioresource Technology*, 101, 2818- 2824.

Johansen, J.E., and Bakke, R. Enhancing hydrolysis with microaeration. *Water Science and Technology*, vol. 53, no. 8, pp. 43-50, 2006.

Karakashev, D., Batstone, D. J., Trably, E., & Angelidaki, I. (2006). Acetate oxidation is the dominant methanogenic pathway from acetate in the absence of Methanosaetaceae. *Applied and Environmental Microbiology* , *72*(7), 5138-41. doi:10.1128/AEM.00489-06

Kato, M. T., Field, J. A., & Lettinga, G. (1993). High tolerance of methanogens in granular sludge to oxygen. *Biotechnology and Bioengineering*, *42*(11), 1360-1366. Retrieved from http://www.ncbi.nlm.nih.gov/entrez/query.fcgi?cmd=Retrieve&db=PubMed&dopt=Citation&list_uids=18612964

Kato, M.T., Field, J.A., and Lettinga, G. (1997) Anaerobic tolerance to oxygen and the potentials of anaerobic and aerobic cocultures for wastewater treatment. *Brazilian Journal of Chemical Engineering*, vol. 14, no. 4, 1997.

Kida, K., Morimura, S., & Sonoda, Y. (1993). Accumulation of Propionic Acid during Anaerobic Treatment of Distillery Wastewater from Barley-Shochu Making. *Journal of Fermentation and Bioengineering*, *75*(3), 213-216.

Kobayashi, T., Yasuda, D., Li, Y.-Y., Kubota, K., Harada, H., & Yu, H.-Q. (2009). Characterization of start-up performance and archaeal community shifts during anaerobic self-degradation of waste-activated sludge. *Bioresource Technology*, *100*(21), 4981-8. Elsevier Ltd. doi:10.1016/j.biortech.2009.05.043

Koster, I. W., and Cramer, A. (1987). Inhibition of methanogenesis from acetate in granular sludge by long-chain fatty acids. Appl. Environ. Microbiol. 53:403–409.

Kurosawa, H., & Tanaka, H. (1990). Advances in Immobilized Cell Culture: Development of Co-immobilised Mixed Culture System of Aerobic and Anaerobic Micro-organisms. *Process Biochemistry International*, 189-196.

Kosman, E., & Leonard, K. J. (2005). Similarity coefficients for molecular markers in studies of genetic relationships between individuals for haploid, diploid, and polyploid species. *Molecular Ecology*, *14*(2), 415-24. doi:10.1111/j.1365-294X.2005.02416.

Lalman, J. A., & Bagley, D. M. (2001). Anaerobic Degradation and Methanogenic Inhibitory Effects of Oleic and Stearic Acids. *Water Research*, *35*(12), 2975-2983.

Leclerc, M., Delgènes, J.-P., & Godon, J.-J. (2004). Diversity of the archaeal community in 44 anaerobic digesters as determined by single strand conformation polymorphism analysis and 16S rDNA sequencing. *Environmental Microbiology*, *6*(8), 809-19. doi:10.1111/j.1462-2920.2004.00616.x

Lueders, T., Chin, K.-J., Conrad, R., & Friedrich, M. (2001). Molecular analyses of methyl-coenzyme M reductase alpha-subunit (mcrA) genes in rice field soil and enrichment cultures reveal the methanogenic phenotype of a novel archaeal lineage. *Environmental Microbiology*, *3*(3), 194-204.

Luton, P. E., Wayne, J. M., Sharp, R. J., & Riley, P. W. (2002). The mcrA gene as an alternative to 16S rRNA in the phylogenetic analysis of methanogen populations in landfill. *Microbiology*, *148*, 3521-30. Retrieved from http://www.ncbi.nlm.nih.gov/pubmed/12427943

Madigan, M.T. and Martinko, J.M. (2009) Brock Biology of Microorganisms. 12th ed. Pearson Prentice Hall, Pearson Education, Inc. San Francisco, CA.

McCarty, P.L. and Smith, D.P. (1986) Anaerobic Wastewater Treatment. *Environmental Science and Technology*. 20.12: 1200-1206.

McInerney, M. J., Sieber, J. R., & Gunsalus, R. P. (2009). Syntrophy in anaerobic global carbon cycles. *Current Opinion in Biotechnology*, *20*(6), 623-32. doi:10.1016/j.copbio.2009.10.001

Morris, R. (2011). *Relating Methanogen Community Structure to Function in Anaerobic Wastewater Digesters*. Ph.D. Thesis. Biology: Marquette University, Milwaukee, WI.

Navaratnam, N. (2012). *Anaerobic co-digestion for enhanced renewable energy and green house gas emission reduction*, Ph.D. Thesis, Civil, Construction, and Environmental Engineering. Marquette University, Milwaukee.

Ohkuma, M., Noda, S., Horikoshi, K., & Kudo, T. (1995). Phylogeny of symbiotic methanogens in the gut of the termite Reticulitermes speratus. *FEMS Microbiology Letters*, *134*(1), 45-50. Retrieved from http://www.ncbi.nlm.nih.gov/pubmed/8593954

Rastogi, G., Ranade, D. R., Yeole, T. Y., Patole, M. S., & Shouche, Y. S. (2008). Investigation of methanogen population structure in biogas reactor by molecular characterization of methyl-coenzyme M reductase A (mcrA) genes. *Bioresource Technology*, *99*(13), 5317-26. doi:10.1016/j.biortech.2007.11.024

Salminen, E., Rintala, J., Lokshina, L. Y., & Vavilin, V. a. (2000). Anaerobic batch degradation of solid poultry slaughterhouse waste. *Water Science and Technology*, *41*(3), 33-41. Retrieved from http://www.ncbi.nlm.nih.gov/pubmed/11386301

Sawyer, C.N., McCarty, P.L., and Parkin, G.F. (2003) Chemistry for Environmental Engineering and Science 5th ed. McGraw-Hill Companies, Inc. New York, NY.

Schauer-Gimenez, A. E., Zitomer, D. H., Maki, J. S., & Struble, C. A. (2010). Bioaugmentation for improved recovery of anaerobic digesters after toxicant exposure. *Water Research*, *44*(12), 3555-64. Elsevier Ltd. doi:10.1016/j.watres.2010.03.037

Scott, R.I., Williams, T.N., and Lloyd, D. (1983) Oxygen sensitivity of methanogenesis in rumen and anaerobic digester populations using mass spectrometry, *Biotechnology Letters*, 5:6, 375-380. http://www.springerlink.com/content/vt9h226u61r30824/

Shen, C. F., & Guiot, S. R. (1996). Long-term impact of dissolved O(2) on the activity of anaerobic granules. *Biotechnology and Bioengineering*, *49*(6), 611-620. Retrieved from http://www.ncbi.nlm.nih.gov/pubmed/18626856

Smith, C. J., Nedwell, D. B., Dong, L. F., & Osborn, a M. (2006). Evaluation of quantitative polymerase chain reaction-based approaches for determining gene copy and gene transcript numbers in environmental samples. *Environmental Microbiology*, *8*(5), 804-15. doi:10.1111/j.1462-2920.2005.00963.x

Smith, C. J., & Osborn, a M. (2009). Advantages and limitations of quantitative PCR (Q-PCR)-based approaches in microbial ecology. *FEMS Microbiology Ecology*, *67*(1), 6-20. doi:10.1111/j.1574-6941.2008.00629.x

Smith, D.P., and McCarty, P.L. (1990) "Factors Governing Methane Fluctuations Following Shock Loading of Digesters." *Research Journal of the Water Pollution Control Federation*. 62.1: 58-64.

Spearman, C. (1904). The Proof and Measurement of Association between Two Things. *University of Illinois Press*, *15*(1), 72-101.

Speece, R. (2008) *Anaerobic Biotechnology and Odor/Corrosion Control for Municipalities and Industries*. Archae Press. Nashville, TN.

Switzenbaum, M. (2010) *Fundamentals of Anaerobic Treatment* in Conference Proceedings of *Anaerobic Treatment of High-Strength Industrial Wastes*. Marquette University. Milwaukee, WI.

Tale, V. (2010). *Bioaugmentation for Recovery of Anaerobic Digesters Subjected to Organic Overload*, in Ph.D. Thesis. Civil and Environmental Engineering. Marquette University: Milwaukee, WI.

Tale, V. P., Maki, J. S., Struble, C. A., & Zitomer, D. H. (2011). Methanogen community structure-activity relationship and bioaugmentation of overloaded anaerobic digesters. *Water Research*, *45*(16), 5249-5256. Elsevier Ltd. doi:10.1016/j.watres.2011.07.035

Thauer, R.K. (1998) Biochemistry of Methanogenesis: A Tribute to Marjory Stephenson. *Microbiology*. 144: 2377-2406.

Vianna, M. E., Conrads, G., Gomes, B. P. F. A., & Horz, H. P. (2006). Identification and Quantification of Archaea Involved in Primary Endodontic Infections. *Journal of Clinical Microbiology*, *44*(4), 1274-1282. doi:10.1128/JCM.44.4.1274

Wang, Y., Zhang, Y., Wang, J., & Meng, L. (2009). Effects of volatile fatty acid concentrations on methane yield and methanogenic bacteria. *Biomass and Bioenergy*, *33*(5), 848-853. Elsevier Ltd. doi:10.1016/j.biombioe.2009.01.007

Wiegant, W. M., Hennink, M., & Lettinga, G. (1986). Separation of the Propionate Degradation to Improve the Efficiency of Thermophilic Anaerobic Treatment of Acidified Wastewaters. *Water Research*, *20*(4), 517-524.

Werner, J. J., Knights, D., Garcia, M. L., Scalfone, N. B., Smith, S., Yarasheski, K., Cummings, T. A., et al. (2011). Supporting Information. *Proceedings of the National Academy of Sciences of the United States of America*, *108*(10), 1-8.

Wilms, R., Sass, H., Köpke, B., Cypionka, H., & Engelen, B. (2007). Methane and sulfate profiles within the subsurface of a tidal flat are reflected by the distribution of sulfate-reducing bacteria and methanogenic archaea. *FEMS Microbiology Ecology*, *59*(3), 611-21. doi:10.1111/j.1574-6941.2006.00225.x

Wittebolle, L., Marzorati, M., Clement, L., Balloi, A., Daffonchio, D., Heylen, K., De Vos, P., Verstraete, W., Boon, N. (2009). Initial community evenness favours functionality under selective stress. *Nature*, *458*(7238), 623-6. Nature Publishing Group. doi:10.1038/nature07840

Wong, B.-T., Show, K. Y., Lee, D. J., & Lai, J. Y. (2009). Carbon balance of anaerobic granulation process: carbon credit. *Bioresource Technology*, *100*(5), 1734-9. Elsevier Ltd. doi:10.1016/j.biortech.2008.09.045

Zar, J. H. (1972). Significance Testing of the Spearman Rank Correlation Coefficient. *Journal of the American Statistical Association*, *67*(339), 578-580.

van der Zee, F. P., Villaverde, S., García, P. a, & Fdz-Polanco, F. (2007). Sulfide removal by moderate oxygenation of anaerobic sludge environments. *Bioresource Technology*, *98*(3), 518-24. doi:10.1016/j.biortech.2006.02.011

Zhou, W., Imai, T., Ukita, M., Li, F., & Yuasa, A. (2007). Effect of limited aeration on the anaerobic treatment of evaporator condensate from a sulfite pulp mill. *Chemosphere*, *66*(5), 924-9. doi:10.1016/j.chemosphere.2006.06.004

Zitomer, D. H. (1998). Stoichiometry of Combined Aerobic and Methanogenic COD Transformation. *Water Research*, *32*(3), 669-676.

Zitomer, D. H., Johnson, C. C., & Speece, R. E. (2008). Metal Stimulation and Municipal Digester Thermophilic/Mesophilic Activity. *Journal of Environmental Engineering*, *134*(1), 42. doi:10.1061/(ASCE)0733-9372(2008)134:1(42)

Zitomer, D. H., & Shrout, J. D. (1998). Feasibility and benefits of methanogenesis under oxygen-limited conditions. *Waste Management*, *18*, 107-116.

4.0 BIOAUGMENTATION FOR INCREASED METHANE PRODUCTION AND ALTERED MICROBIAL COMMUNITY STRUCTURE IN ANAEROBIC DIGESTERS

4.1 Introduction

4.1.1 Anaerobic Degradation of Propionate

Within the overall anaerobic degradation pathway, propionate ($CH_3CH_2COO^-$) is one of several long chain fatty acids (LCFA) formed, and its degradation is often the rate-limiting step, controlling the rate of methane (CH_4) production from many substrates (Kida et al., 1993; McInerney et al., 2009; Wong et al., 2009). $CH_3CH_2COO^-$ is a key intermediate in the production of CH_4 from complex feedstocks since much of the carbon that is transformed into CH_4 passes through $CH_3CH_2COO^-$ (Speece, 2008). Part of the challenge with $CH_3CH_2COO^-$ degradation is overcoming the energetically unfavorable conversion ($\Delta G^{o\prime}$ = +71.67 kJ/mole $CH_3CH_2COO^-$) into acetate (CH_3COO^-), hydrogen (H_2), and carbon dioxide (CO_2) under standard conditions (Sawyer et al. 2003). Yet, with the concomitant degradation of H_2/CO_2 ($\Delta G^{o\prime}$ = -98.06 kJ/mole $CH_3CH_2COO^-$) as well as acetate (($\Delta G^{o\prime}$ = -35.83 kJ/mole $CH_3CH_2COO^-$), both generating CH_4, the overall reaction becomes favorable (McCarty and Smith, 1986). Additionally, $CH_3CH_2COO^-$ at elevated concentrations is toxic to microorganisms. Thus, both toxicity and thermodynamics can hinder $CH_3CH_2COO^-$ degradation.

Another consideration of this interrelationality is that the H_2 partial pressure must fall between 10^{-4} and 10^{-6} atm for $CH_3CH_2COO^-$ degradation to proceed (McCarty and Smith, 1986). Therefore, $CH_3CH_2COO^-$ can only be degraded as fast as H_2 can be consumed to maintain this ideal range of H_2 partial pressure. When the H_2 concentration is greater than

10^{-4} atm, $CH_3CH_2COO^-$ degradation becomes unfavorable, causing accumulation of $CH_3CH_2COO^-$ and other volatile fatty acids (VFAs); the $CH_3CH_2COO^-$ resists degradation more than ethanol, acetate, n-propanol (Smith and McCarty, 1990). Ultimately, the accumulation of $CH_3CH_2COO^-$ and other reduced products can lead to detrimental pH drops and, subsequently, process upset or digester failure.

$CH_3CH_2COO^-$ is more difficult to degrade and inhibitory than acetate or butyrate. Tested anaerobic cultures were not only less able to produce CH_4 via $CH_3CH_2COO^-$, but also more inhibited at far lower concentrations of it. Maximum CH_4 production rates were 389, 432, and 162 mL/TVS-d at 3000 mg/L acetate, 5000 mg/L butyrate, and only 1000 mg/L $CH_3CH_2COO^-$ (Dogan et al., 2005), respectively. Furthermore, these maximum CH_4 production rates were 50% inhibited at 13,000 mg/L acetate, 15,000 mg/L butyrate, and only 3500 mg/L $CH_3CH_2COO^-$, respectively (Dogan et al., 2005).

Collectively, these factors that contribute to the difficulty of degrading $CH_3CH_2COO^-$ point to the need for more efficient $CH_3CH_2COO^-$ treatment methods, such as the enhanced $CH_3CH_2COO^-$ acid degradation system (EPAD) described by Ma et al. (2009). This system (a membrane to separate liquid with high $CH_3CH_2COO^-$ concentration followed by a UASB to treat the high $CH_3CH_2COO^-$ filtrate) improved recovery from high $CH_3CH_2COO^-$ concentrations that were toxic in a control CSTR that was not connected to an EPAD system. However, the EPAD system necessitated temporarily adding an extra unit onto a treatment system, which could limit use to those facilities that both have the physical space for the added unit (2% of digester volume) and access to this technology (Ma et al., 2009).

Therefore, novel technologies for efficient $CH_3CH_2COO^-$ metabolism that can be achieved at existing facilities regardless of their configuration or geography would be

beneficial to mitigate the challenges associated with $CH_3CH_2COO^-$ degradation. One of these approaches that can enhance anaerobic biotechnologies is bioaugmentation. Bioaugmentation refers to the addition of specialized microbial cultures to improve system function (Rittmann and Whiteman, 1994; Deflaun and Steffan, 2002). Improved $CH_3CH_2COO^-$ degradation rates have been found via bioaugmentation using $CH_3CH_2COO^-$-enriched cultures (Tale, 2010; Cavaleiro et al., 2010). However, bioaugmentation remains a new technology and more research is required before full-scale implementation is possible.

4.1.2 Bioaugmentation of Anaerobic Digester Biomass Samples

Bioaugmentation has been used for decades in numerous applications (Nyer and Bourgeois, 1980; Rittmann and Whitemann, 1994). Traditional approaches include forestry and agricultural soil remediation (Vogel, 1996). More recently, bioaugmentation has enhanced wastewater applications such as nitrification, sludge settling, FOG degradation, transformation of xenobiotic contaminants, and anaerobic digestion (Rittmann and Whitemann, 1994; Abeysinghe, 2002).

In anaerobic cultures, bioaugmentation has been shown to increase CH_4 generation and decrease recovery periods after $CH_3CH_2COO^-$ build-up (Schauer-Gimenez, 2010). In another study, bioaugmentation with *Syntrophomonas zehnderi* increased both CH_4 production from oleate ($CH_3(CH_2)_7CH=CH(CH_2)_7COO^-$), and LCFA degradation (Cavaleiro et al., 2010). Tale et al. (2011) showed that bioaugmentation decreased recovery times after organic overload of anaerobic digesters. Other authors have reviewed bioaugmentation more extensively (Stephenson and Stephenson, 1992; Rittmann and Whiteman, 1994; Tale, 2010). However, the exact mechanisms for enhancement digester function following bioaugmentation often remain unclear.

4.1.3 Microbial Structure and Digester Function

The microbial community structure is described by the identity and relative number of microbes present. Since bioaugmentation involves the addition of a specific microorganism or group of microorganisms designed to accomplish a specific function, it stands to reason that the greater the number of desired organisms, the more the desired function will occur. Thus, bioaugmentation ostensibly exploits beneficial shifts in microbial communities. For example, Angenent et al. (2002) studied methanogenic populations during the start-up of a full-scale, anaerobic sequencing batch reactor (ASBR) treating swine waste. When the organic loading rate was increased from a low start-up rate to the higher design rate, the total ammonia-N concentration also increased from 2 to 3.6 g/L. Simultaneously, *Methanosarcina* decreased from 3.8% to 1.2% of the total 16S ribosomal RNA (rRNA) concentrations and *Methanosaeta concilii* remained below 2.2% (both convert acetate into CH_4 and CO_2), as shown by fluorescence in situ hybridization (FISH). Yet, 16S rRNA concentrations of the order *Methanomicrobiales* (H_2 -utilizing methanogen) increased from 2.3% to 7.0%, thereby enabling consistent CH_4 production and digester performance. Thus, a change in digester conditions increased ammonia concentrations and shifted degradation pathway from acetate to H_2/CO_2.

Furthermore, microbial community structures in full-scale anaerobic digesters, though often assumed to be similar, actually vary greatly (Luton et al., 2002; Werner *et al.*, 2011) and may relate to process function (Angenent et al., 2002; Briones and Raskin, 2003). The maximum rates at which different biomass samples from different full-sale digesters produce CH_4 from $CH_3CH_2COO^-$ also vary greatly (e.g., from <0.1 to >10 mL CH_4/gVS-hr), and microbial community structure was correlated to the rate and extent of CH_4 production (Tale, 2011). Microbial community structure also influences the stability of

digestion during process upsets that occur due to organic overloads or other changes. For example, dissolved oxygen, N or P deficiency, low pH, high VFA, low food:mass (F:M) ratio, and H_2S all impact the presence of different microbes and, therefore, how a digester performs (Hashsham et al., 2000; Fernandez et al., 2000; Madigan and Martinko, 2009; Switzenbaum, 2010; Schauer-Gimenez, 2010; Tale et al., 2011).

Therefore, the microbial community structure in a digester can and should be optimized to produce more CH_4 for a particular set of environmental and operational conditions. Researchers have suggested that digesters containing microbial communities that change more rapidly (i.e., digesters with flexible community structures) can produce CH_4 at a more consistent rate during process upset. When two different digesters containing different groups of microbes were upset, the one in which the community changed the most produced the most CH_4. This occurred even though the physical digester conditions were identical (Fernandez et al., 2000). When considering data from these two digesters, it was suggested that microbial communities with parallel processing capabilities (i.e., cultures that contain many different organisms that can perform the same metabolic function, such as convert acetate into CH_4) are more stable and produced CH_4 more consistently during upset in comparison to less diverse cultures (i.e., less richness) that only contain one or a few organisms performing a given metabolic function (Hashsham et al., 2000).

Evenness is another important community structure parameter that may influence digester function. A microbial community with high evenness contains a mix of different organisms in which each of the different organisms is present in nearly the same number. For example, a community of 3,000 microbes containing three different species with 1000 individual microbes per species has high evenness, whereas a microbial community of 3,000 microbes containing three different species with 1, 100, and 2899 individual microbes per

species, respectively, has lower evenness. Wittebolle et al. (2009) studied over 1000 microbial communities and concluded that communities with high evenness are more resistant to upset after the addition of a toxic chemical. They posited that high evenness provides a higher probability that the specific organism resistant to the toxicant is present in numbers needed to reproduce and proliferate when the toxicant is added. If a culture has low evenness, then there is a chance that the microorganism that is resistant to the toxicant is present in such low numbers that it cannot grow and proliferate in the system, even after the toxicant is added.

4.1.4 Goals of Research

Research to understand the link between anaerobic digester performance and microbial community structure has been limited and technologies to exploit the advantages of optimized microbial structure remain few. Anaerobic digesters are typically designed based on operational parameters such as organic loading rate and residence time. Yet, they could be improved by also designing based on microbial community structure.

The research described herein was performed in an effort to determine a relationship between the rate of conversion of $CH_3CH_2COO^-$ into CH_4 and differences in microbial community structure. It was hypothesized that different anaerobic cultures would have significantly different functional activities as well as exhibit different microbial community structures as characterized by denaturing gradient gel electrophoresis (DGGE).

4.2 Methods and Materials

Nineteen different microbial communities were used: a $CH_3CH_2COO^-$ enrichment, nine diverse anaerobic digester biomass samples, as well as these nine mixed with the $CH_3CH_2COO^-$ enrichment (i.e., nine bioaugmented cultures).

4.2.1 Set-Up and Operation of $CH_3CH_2COO^-$ Enrichment

A methanogenic $CH_3CH_2COO^-$ enrichment was developed to bioaugment anaerobic digester biomass and potentially increase CH_4 production in those digester biomass samples. This $CH_3CH_2COO^-$ enrichment (1-L working volume) was maintained for 317 days in a 2-L, plastic, anaerobic reactor that was continuously mixed on a shaker table and housed in a temperature-controlled incubator (35 ± 1°C). Since diverse seed culture has been correlated to functional benefits (Wittebolle, 2009), the $CH_3CH_2COO^-$ enrichment was seeded with a blend of biomass from eight different mesophilic, anaerobic digesters (Table 4-1).

Table 4-1. Seed Sludge Used

Digester Type*	Substrate	Industry/Municipality	Location
CSTR	Non-Fat Dry Milk	Pilot-scale Digester	Milwaukee, WI
CSTR	Municipal Solids	City of Waukesha, WI WWTP**	Waukesha, WI
CSTR	Municipal Solids	South Shore Water Reclamation Facility	Milwaukee, WI
CSTR	Municipal Solids	City of Brookfield, WI WWTP**	Brookfield, WI
CSTR	Food Additives	Kerry Ingredients & Flavours	Jackson, WI
UASB	Soft Drink Waste	Wis-Pak, Inc.	Watertown, WI
UASB	Brewery Waste	City Brewery Company, LLC	Brewery Waste
CSTR	Cattle Manure	Crave Brothers Farmstead, Inc.	Waterloo, WI

*CSTR - Completely mixed stirred tank reactor. **UASB - Upflow anaerobic sludge blanket.
**WWTP - wastewater treatment plant

Liquid effluent (100 mL) was removed once per day to maintain a solids residence time (SRT) and hydraulic retention time (HRT) of ten days. Effluent was replaced with 100 mL of aerated tap water (to remove residual chlorine) containing $Ca(CH_3CH_2COO^-)_2$ (0.77

±0.03 g COD/L-day), 5 g/L $NaHCO_3$, and the basal nutrient medium described by Schauer-Gimenez et al. (2010). This feed led to a theoretical concentration of 1.5 g Ca^{+2}/L in the $CH_3CH_2COO^-$ enrichments, which was well below the 4.8 g Ca^{+2}/L that caused a 50% reduction in CH_4 production (Switzenbaum, 2010).

4.2.2 Anaerobic Digester Biomass Samples

Nine biomass samples were obtained from various anaerobic digesters treating diverse substrates in an effort to obtain different microbial communities (Table 4-2). The concentrations of chemical constituents in each biomass sample were measured to categorize environmental conditions under which the communities ostensibly developed. Digester constituents measured included total solids (TS), volatile solids (VS), ammonia-nitrogen (NH_3-N), total Kjeldahl nitrogen (TKN), total phosphorus (TP), soluble phosphorus (SP), and a suite of total as well as soluble metals concentrations (Cd^{+2}, Co^{+2}, Ca^{+2}, Cu^{+2}, Pb^{+2}, Ni^{+2}, Zn^{+2}, Mn^{+2}, As^{+2}, Se^{+2}, Ag^{+2}, Mb^{+2}, Hg^{+2}, Be^{+2}, Fe^{+2}, Na^+, K^+, and Mg^{+2}).

Table 4-2. Anaerobic Biomass Samples

Sample Number	Digester Type*	Substrate	Location	Industry/Municipality
1	CSTR	Food Flavorings	Jackson, WI	Kerry Ingredients & Flavours
2	Anaerobic Plug Flow	Brewery Waste	Fort Collins, CO	New Belgium Brewery
3	CSTR	Municipal Solids	Philadelphia, PA	City of Philadelphia WWTP**
4	UASB	Brewery Waste	Chico, CA	Sierra Nevada Brewery
5	CSTR	Non-Fat Dry Milk	Milwaukee, WI	Pilot-scale Digester
6	UASB	Soft Drink Bottling Waste	Watertown, WI	Wis-Pak, Inc.
7	CSTR	Municipal Solids	Des Moines, IA	City of Des Moines WWTP**
8	UASB	Brewery Waste	LaCrosse, WI	City Brewery, LLC
9	CSTR	Cheese Processing Waste	Las Cruces, NM	F & A Dairy

* CSTR - Completely mixed stirred tank reactor, UASB - Upflow anaerobic sludge blanket. **WWTP – Wastewater treatment plant.

4.2.3 Quantification of Microbial Community Activity

Microbial community activity was quantified using specific methanogenic activity (SMA) tests with $CH_3CH_2COO^-$ and organic overload perturbation activity (OOPA) assays with glucose. $CH_3CH_2COO^-$ was chosen because it often has been shown to be the rate-limiting step in the overall anaerobic degradation process, controlling the rate of CH_4 production from many substrates (Kida et al., 1993; McInerney et al., 2009; Wong et al., 2009), and glucose has been used elsewhere to monitor response to organic overload (Hashsham et al., 2000; Fernandez et al., 2000; McHugh et al., 2003; Karakashev et al., 2005; Dearman et al., 2006). Preliminary testing identified the biomass and substrate doses used in these tests.

Because VS or VSS are not accurate measures of active biomass, the biomass in activity tests was quantified based on intracellular adenosine-5'-triphosphate (iATP) concentration, which was measured with a commercial ATP test kit (QuenchGone21™ Wastewater, LuminUltra, Fredericton, New Brunswick, Canada). In order to streamline testing, minimize bias, and maximize the comparability between the two activity parameters, both SMA and OOPA tests were conducted at the same biomass concentration. Previous work has shown SMA tests with $CH_3CH_2COO^-$ yield accurate and precise results at various biomass concentrations, including: 2 g VSS/L or less as well as at 5.0 to 6.0 g VS/L, and both of these studies used 3 g/L $CH_3CH_2COO^-$ as calcium propionate ($Ca(CH_3CH_2COO)_2$) for the substrate (Tale, 2010; Bocher and Zitomer, 2010). Because the OOPA was a novel test, no optimal biomass or substrate (i.e., glucose) concentration was initially known. The purpose of the OOPA was to quantify response to elevated organic loading rates in an anaerobic microbial community. The preliminary testing focused on developing a successful

OOPA by finding an optimal glucose organic overloading rate (i.e., food to microorganism, F:M, ratio) and standard, active biomass concentration such that a distinct response could be observed.

In order to determine a standard, active biomass concentration 57 bottles were set up at 19 F:M ratios (each in triplicate) varying from 0.2 to 33 g COD/g VSS (0.20, 0.62, 1.01, 1.41, 1.44, 1.99, 2.42, 3.10, 3.37, 4.4, 7.03, 10.3, 12.1, 14.2, 15.1, 17.3, 21.6, 23.4, 33.2). The following glucose concentrations were used [g glucose/L]: 1, 3, 7, 10, 12, and 15. Biomass concentrations were as follows [g VSS/L]: 0.1, 0.3, 0.7, 1, and 5. Each mixture was run in triplicate. The initial and final VSS values were averaged and used to calculate SMA values.

4.2.3.1 Specific Methanogenic Activity (SMA) Testing

A modified approach to a standard SMA protocol outlined by Andelicki et al. (2007) was implemented. Biomass samples were collected from nine anaerobic digesters and from the four $CH_3CH_2COO^-$ enrichments and thickened at 6000 rpm (g = 7000) for five minutes in a centrifuge (Clinical 200, VWR International, Radnor, Pennsylvania Germany). Before mixing, granular samples were disrupted to make the biomass flocculant. This allowed a consistent comparison of activity among granular and flocculant biomass samples. Each mixed sample consisted of 80% of one of the nine digester biomass samples and 20% of a $CH_3CH_2COO^-$ enrichment based on iATP concentration. The 80/20 mixed biomass samples were resuspended in DI water that included basal nutrient medium (Table 5-3) to achieve an active biomass concentration of 0.74 mg iATP/L. A 25-mL sample of the active biomass was placed in a 160-mL serum bottle, sparged with O_2-free gas (3:7 v/v mix of CO_2 and N_2), sealed with solid black butyl rubber stoppers, and allowed to produce biogas for three days to determine endogenous biogas production. Excess biogas was removed on day

three to depressurize the headspace, and the sample was then given a non-limiting dose (3 g/L) of $Ca(C_2H_5COO)_2$ (4.6 g COD/L). This substrate concentration has been used elsewhere (Speece, 2008; Zitomer, 2008), is non-toxic to anaerobic microorganisms, and is well above the Monod half-saturation constant values. All 49 samples were run in triplicate at 35±1°C and 150 rpm using a gyratory shaker-incubator (model C25KC, New Brunswick Scientific, Edison, NJ). An additional bottle contained no exogenous substrate and was used to account for endogenous CH_4 production.

The biogas volume produced was measured at ambient pressure and 35°C for 20 days via a displacement method using a glass syringe with a wetted, glass barrel (Perfektum®, Popper & Sons, Inc., New Hyde Park, NY). CH_4 content was measured after 20 days by gas chromatography (GC). Graphs of cumulative biogas production versus time were plotted and the SMA values (mL CH_4/mg iATP-h) were calculated using linear regression on the portion of the curve within the first 60 hours of biogas production with the steepest slope. This initial maximum slope was used because the biomass samples used for molecular analyses were taken on the day the assays were set-up. Thus, the use of initial slopes ensured that the SMA values measured were as representative as possible of the initial microbial community structure and not the community that developed in the SMA bottle after feeding. The average and standard deviation of SMA values were calculated for each sample to yield the average maximum rate of CH_4 production. SMA values with $CH_3CH_2COO^-$ have been shown to vary over two orders of magnitude among biomass samples from different anaerobic digesters (Tale, 2010).

4.2.3.2 Organic Overload Perturbation Activity (OOPA)

For the OOPA test, microbial community samples were diluted to a standard active biomass concentration (0.74 mg iATP/L) based on iATP concentration. A 25-mL sample of standard active biomass was placed in a 160-mL serum bottle, sparged with O_2-free gas (7:3 v/v N_2:CO_2), and allowed to produce biogas for three days, when it stopped producing biogas, to determine the endogenous biogas production. Excess gas was then removed on day three, and a one-time dose of 5.2 g glucose/L (5.6 g COD/L) was added. This dose was within ranges used in other studies, such as 4 g COD/ L-d (Zitomer and Shrout, 1998) and 7.2 g COD/L (Hashsham et al., 2000).

The first and second slopes on the biogas production versus time graph delineated CO_2 production via fermentation, which is known to occur quickly with a sugar substrate like glucose, and methanogenic gas production, respectively (Figure 4-1). The ratio of the respective slopes was defined as the methanogenesis to fermentation (M/F) ratio. A third region of the curve with a slope of zero occurred after the consumption of all substrate. Biogas production was measured for 20 days. Biogas CH_4 content was determined on day 20 using a gas chromatograph (GC), as described below.

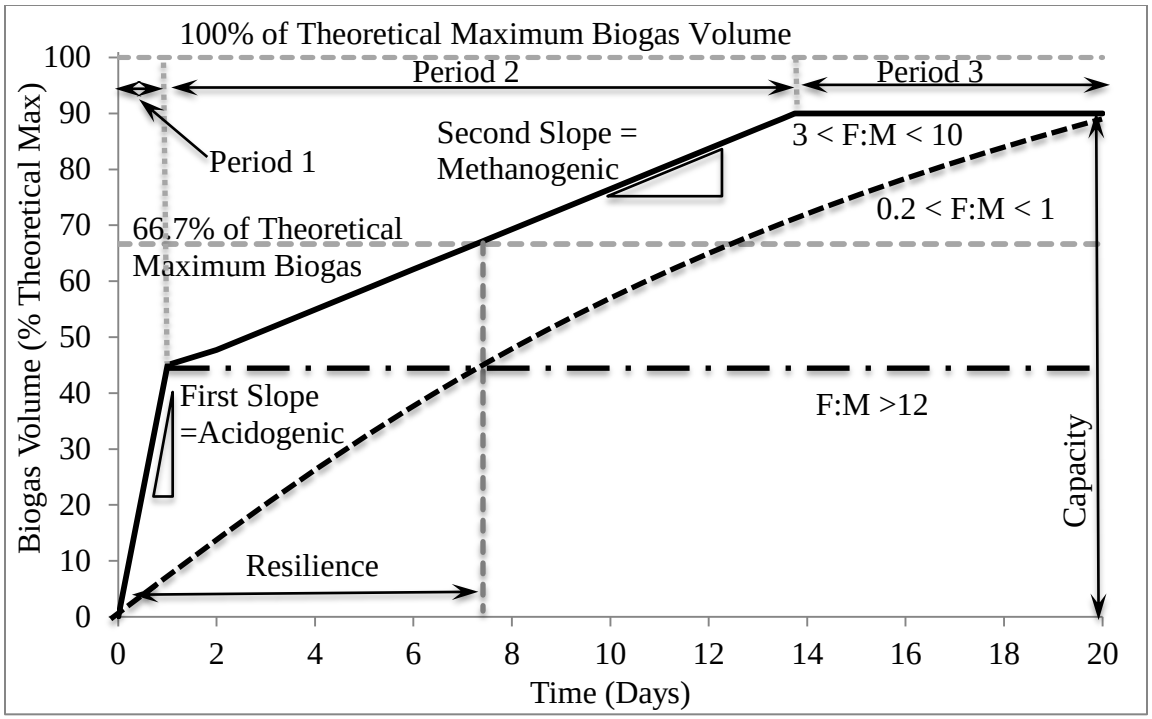

Figure 4-1. Theoretical OOPA graph shown to depict the parameters obtained via overload testing, including resilience, capacity, methanogenesis to fermentation (M/F) ratio (second slope divided by the first slope), and perturbed biogas yield (PBY, maximum biogas volume divided by 100% of theoretical maximum biogas volume). The parameters listed on this graph are for $3 \leq F:M \leq 10$, which is represented with a solid black line. The dashed black line represents $0.2 \leq F:M \leq 1$, and the alternating long dash/short dash represents $F:M \geq 12$.

Resilience was the time required to reach two-thirds (66.7%) of the theoretical maximum biogas production (Figure 4-1). For example, 1 g COD (added as glucose) would yield 800 mL of biogas at 35°C, assuming 50/50 CH_4/CO_2 (v/v) in the biogas (for carbohydrates); thus, the resilience was the number of hours it took to produce 533 mL of biogas. A resilience coefficient was calculated by taking the inverse of resilience and multiplying that by 100. Another parameter, capacity, was the cumulative amount of biogas production after 20 days. The cumulative biogas volume produced after 20 days was divided by the total theoretical volume expected based on the glucose added. This quotient was the 20-day perturbed biogas yield (PBY). Methanogenesis/fermentation (M/F) ratio, resilience, capacity, and PBY were determined in triplicate.

4.2.4 Methanogen Community Analysis

4.2.4.1 DNA Extraction

DNA was extracted using biomass collected when SMA and OOPA testing was performed. Each 50-mL sample was thickened in a centrifuge (AccuSpin Micro 17, Thermo Fischer Scientific, Waltham, MA) for 10 min at 2500 x g. Then DNA was extracted using the DNA Elution Accessory kit with the RNA Powersoil™ Total RNA Isolation Kit (MoBio Laboratories, Carlsbad, CA) according to the manufacturer's instructions. The presence of extracted DNA was confirmed with gel electrophoresis (1% agarose in 1X Tris-Acetate-EDTA, TAE) using ethidium bromide (0.8 μL/mL) stain (Sambrook and Russell, 2001). Prepared gel solution was poured into a gel box and allowed to solidify. A mixture of 3 μL of 6X blue-orange loading dye and 10 μL of DNA was injected into the wells (Hartwell et al., 2004). A λϕ (HindIII, HaeIII) ladder was placed into one of the wells as a marker. This marker had 40 ng/μL Lambda (λ) DNA, HindIII cut and 30 ng/μL phi (ϕ) X174 DNA, HaeIII cut. A 100 millivolt (mV) potential was maintained across the gel for 60 to 90 minutes. This potential caused the DNA to migrate across the gel, which was then illuminated and photographed under ultraviolet light using an imaging system (GDS-8000 Bioimaging System, UVP Inc., Upland, CA). DNA samples were stored at -80°C until further analysis.

4.2.4.2 Polymerase Chain Reaction (PCR)

Extracted DNA was amplified using polymerase chain reaction (PCR) with primers for the methyl coenzyme M reductase (*mcrA*) gene of methanogenic *Archaea* designed by Luton et al. (2002). These are: mcrA1f: 5'-

GGTGGTGTMGGATCACACARTAYGCWACAGC -3', (mcrF); GCmcrA1f: 5'- *GC-clamp-GGTGGTGTMGGA TTCACACARTAYGCWACAGC -3', (mcrA1f), where GC-clamp = 5' – CGCCCGCCGCGCCCCGCGCCCGTGCCGCCGCCCCCGCCCG – 3', (GC-clamp); mcrA500r: 5' – TTCATTGCRTAGTTWGGRTAGTT – 3', (mcrR). The primer product was an approximately 460 -bp long segment of *mcrA*, which codes for the α subunit of methyl coenzyme M reductase (Luton et al., 2002). Since it is a functional gene that is specific to and ubiquitous in methanogens (Thauer, 1998), the *mcrA* gene has been used to compare methanogen community structure and identify the taxonomically distinct methanogens present. Furthermore, numerous studies have exploited the ubiquity of the *mcrA* gene in all known methanogens to find them in various locations, including marine environments (Bidle, 1999; Wilms, 2007), termite guts (Ohkuma, 1995), rice paddies (Lueders, 2001), oligotrophic fen (Galand et al., 2002), and anaerobic digesters (Rastogi, 2008; Tale, 2011).

PCR was performed on the DNA sample using EconoTaq® PLUS 2X Master Mix, which includes the Taq polymerase (Lucigen Corporation, Middleton, WI). Forward and reverse primers were added to the PCR tube with nuclease-free H_2O to make a 100-μL reaction. Nested PCR was performed on the extracted DNA by first amplifying for mcrA1f and mcrA500r primers in the following program: 95°C for 5 min; then six cycles of 95°C for 1 min, 49°C for 1 min, 72°C for 3 min; next 30 cycles of 95°C for 1 min, 49°C for 1 min, 72°C for 3 min; then 95°C for 1 min, 49°C for 1 min, 72°C for 10 min; and then 4°C. Presence of amplified *mcrA* was verified via agarose gel, as described, and then a second cycle was employed to re-amplify with GCmcrA1f (GC clamp) and mcrA500r primers in the following program: 95°C for 5 min; then six cycles of 95°C for 1 min, 58°C for 1 min, 72°C

for 3 min; next 36 cycles of 95°C for 1 min, 58°C for 1 min, 72°C for 3 min; then 95°C for 1 min, 58°C for 1 min, 72°C for 10 min; and then 4°C. The program included a slow ramp in temperature ($0.1°Cs^{-1}$) between the annealing and extension steps of the first five cycles of the protocol to aid in the initial formation of product due to the degenerate nature of the primers, as recommended (Luton et al, 2002). PCR was done on a thermocycler (PTC-200 DNA Engine Cycler, Bio-Rad, Foster City, CA).

4.2.4.3 Denaturing Gradient Gel Electrophoresis (DGGE)

Each microbial community was fingerprinted using denaturing gradient gel electrophoresis (DGGE), which separated amplified genes into bands on a polyacrylamide gel. DGGE has been used with *mcrA* as a target gene (e.g., Galand et al., 2002; Wilms et al., 2007; Morris, 2011; Tale et al., 2011). The denaturant concentration used for DGGE varied linearly over 75 mm and ranged from 40% at the top of the gel to 70% at the bottom of the gel (expressed as v/v of the total gel volume). A detection system (Universal DCode Mutation Detection System, BioRad, Hercules, CA) was used to prepare the DGGE gels. DGGE was performed on 1-mm-thick 8% polyacrylamide gel following the manufacturer's protocol. Approximately 300 ng of DNA product was added to each lane of the polyacrylamide gel with 2X blue loading dye. An electric potential of 100 V was maintained across the gel for 12 hours. A 1% SYBR® gold dye solution (Invitrogen, CA USA) was used to stain the gel. After immersing the gel in the staining solution and rotating it for 30 minutes on a shaker table at a speed sufficient to mix the dye solution, it was viewed under ultraviolet light using an imaging system (GDS-8000 Bioimaging System, UVP Inc., Upland, CA). Densitometric data were obtained using gel viewing software (Lab Works v. 4.6.00.0 Lablogics, Inc., Mission Viejo, CA) with a minimum band height of 0.050, allowed error of

±5%, ten largest bands retained, and the following options activated: dark bands and bright background, rows of equal molecular weight, maximum OD level for the image, and center peak.

4.2.4.4 Principal Component Analysis

Principal component analysis (PCA) was performed with MATLAB (v. R2010bSP1, MathWorks®, Natick, MA) using DGGE banding patterns. Optical densities of the DGGE bands (obtained with Lab Works v. 4.6.00.0) provided dimensional values for community structure. The output of the PCA in MATLAB included the PCA plot as well as equations for each principal component with demeaned X values, which were calculated in MATLAB (Equation 4-1):

Equation 4-1. Demeaned X Values Calculated for Each Principal Component

$$X_m = I_m - \frac{\sum_{i=1}^{n} I_{m,i}}{n}$$

where there are n samples and I_m is the intensity of band m. Thus, X_m is positive if the optical intensity is greater than the average of all samples of a given band and vice versa.

Multiple gels were prepared for this large sample size. Thus, in addition to the equal mass of DNA added to each lane, a ladder was run on each gel to correct for imaging system variations. The band intensities of the ladders on all gels were compared, and their average differences were used to calculate a factor (ranging from 0.8 to 1.4) that was multiplied by each band intensity. These normalized data were used to perform PCA. Though not impacting placement of the data points or the principal components, SMA values were depicted as a third dimension, diameter of the data symbol (larger diameters corresponded to higher SMA values).

4.2.4.5 Cluster Analysis

Pearson's correlation coefficient (Equation 4-2) was used to develop similarities between the banding patterns (i.e., a 0 signified uncorrelated, a +1 was a perfect positive correlation and -1 was a perfect negative correlation) since it accounted for band intensities (i.e., brightness), unlike coefficients like Jaccard that merely account for the presence or absence of bands. This was done using the "pdist" function in MATLAB (v. R2010bSP1, MathWorks®, Natick, MA) and a predefined command entitled "correlation" that calculated one minus the Pearson's correlation coefficient to develop dissimilarities between banding patterns. Dissimilarity values were compiled into a distance matrix using the "squareform" function in MATLAB because the output of "pdist" was a vector variable. This matrix was then uploaded into Plain Text Editor (v. 5.1), formatted to be readable by the Phylogency Inference Package (PHYLIP, v. 3.69) and the unweighted pair group method with arithmetic mean (UPGMA), Fitch-Margolish and Neighbor-joining algorithms were used to build phylogenetic trees. Trees were viewed in FigTree (v. 1.3.1).

Equation 4-2. Pearson's Correlation Coefficient

$$r = \frac{\sum_{i-1}^{n}\left(\left(x_i - \bar{x}\right)^2\left(y_i - \bar{y}\right)^2\right)}{\sqrt{\sum_{i-1}^{n}\left(x_i - \bar{x}\right)^2 \sum_{i-1}^{n}\left(y_i - \bar{y}\right)^2}}$$

Additional statistical analyses were performed. In order to quantify the correlation between the effectiveness of bioaugmentation and methanogenic community structure, SMA values were ranked from highest to lowest. Next, the difference (i.e., dissimilarity distance) among the densitometric data from the samples was calculated using one minus the Pearson's correlation coefficient. These data were then used to rank the biomass samples in ascending order of their pair-wise distances from the $CH_3CH_2COO^-$ enrichment Then the

rank based on SMA values was correlated to the densitometric ranking of distance from the $CH_3CH_2COO^-$ enrichment using Spearman's rank correlation coefficient (Equation 4-2), which measured the monotonic correlation between the similarity of methanogen community structure and SMA values (Spearman, 1904; Zar, 1972). Spearman's rank correlation coefficient is non-parametric in that a higher correlation arises when the independent and dependent variables are related via any monotonic function; thus, it has advantages over methods like Pearson's correlation coefficient and linear regression, which are limited to linear relationships between the independent and dependent variables.

Equation 4-3. Spearman's Rank Correlation Coefficient (Zar, 1972)

$$r_s = 1 - 6\left(\frac{\sum d^2}{\left(n^3 - n\right)}\right)$$

$$\sum d^2 = \sum_{i=1}^{n} d_i^{\,2}$$

where n is the number of samples (e.g., 19) and d_i equals the difference in the ranks of the two parameters being analyzed (e.g., SMA values and densitometric data). Then the Spearman's rank correlation coefficient was used to compare the percent increase in SMA upon bioaugmentation with the densitometric data. A greater correlation between increase in SMA and densitometric data indicated a greater correlation between bioaugmentation efficacy and methanogen community structure.

4.2.4.6 Functional Organization (F_o)

While fingerprinting techniques often have been limited to determining similarity or difference, some parameters have been developed in an attempt to extract quantitative information from DGGE banding patterns for the 16S rRNA gene. Functional organization, (Fo) was calculated in this research to describe how well a community is organized such that,

upon perturbation, it can adapt and remain functionally stable (Marzorati et al., 2008). Functional and structural stability of a microbial community do not always coincide; in fact, structural flexibility (i.e., instability) may be necessary for functional stability in stressed conditions, and structural flexibility may be linked to the evenness of a community (Fernandez et al., 2000). Therefore, quantification of evenness may help provide a better understanding of microbial community response to perturbations. To do this, Pareto-Lorenz (PL) evenness curves were constructed from DGGE banding patterns to graphically represent the methanogenic diversity according to the procedure found in Mertens et al. (2005) and Wittebolle et al. (2008). High Fo values were synonymous with low evenness and vice versa. Thus, a perfectly even community would be graphed as a 45° line through the origin in a PL evenness plot, whereas an increasingly uneven community would have an initial slope much greater than 45° and then a gradually decreasing slope that asymptotically approaches a zero slope.

4.2.5 Metadata Analysis

$CH_3CH_2COO^-$ Enrichment. Temperature and pH were measured using a glass electrode and meter (Orion 4 Star pH-DO Benchtop electrode - 9206BN, Thermo Scientific, Marietta, OH). Feed and effluent were sampled to determine the following parameters (specific method used given in parentheses): total solids (TS) (2540 B), volatile suspended solids (VSS) (filtered as in 2540 D, volatized as in 2540 E), and individual volatile fatty acid (VFA) concentrations (acetic, propionic, butyric, iso-butyric, valeric, and iso-valeric acids) (5560 B) according to standard methods (APHA et al., 1998). For soluble chemical oxygen demand (SCOD) analysis, the samples were thickened at 13,000 rpm for 10 minutes in a centrifuge (Clinical 200 VWR International LLC Radnor, Pennsylvania) and filtered through

a 0.45 μm filter (Whatman International Ltd., Maidstone, England). The filtrate was then tested for COD (5220 D). The biogas volume produced was pressurized in the 2-L vessels, but measured daily at ambient pressure before feeding using a water displacement method (Wet Test Meter, Precision Scientific Petroleum Instruments, San Antonio, TX). Biogas CH_4 content (2720 C) was measured by standard methods (APHA et al., 1998). Biogas CH_4 content as well as the influent and effluent VFA concentrations were determined by gas chromatography (GC) (Series 7890A GC system, Agilent Technologies, Santa Clara, CA, USA) with a thermal conductivity detector (TCD) and flame ionization detector (FID), respectively. For CH_4 content, the carrier gas was helium at a flow of 4.5 mL/min. Temperatures of the injector and detector were 150°C and 250°C, respectively, and the temperature of the oven was 40°C. VFA samples were acidified using 1% phosphoric acid and analyzed as described in Standard Method 5560D (APHA et al., 2005). For VFA analysis, the carrier gas was helium at a flow of 18 mL/min. Temperatures of the injector and detector were 150°C and 300°C, respectively, and the temperature of the column was 40°C (airflow at 400 mL/min, H_2 flow at 30 mL/min). The test results outlined in this section were referred to as metadata.

Biomass Samples. The following were also measured in the nine biomass samples: TS (as described above), as well as volatile solids (VS) (2540 E), ammonia-nitrogen (NH_3-N) (4500-NH3 C. Titrimetric Method), total Kjeldahl nitrogen (TKN) (4500-Norg B.), total phosphorus (TP) (4500-P E. Ascorbic Acid Method), and soluble phosphorus (SP) (4500-P E. with preliminary filtration through 0.45-um membrane filter) (APHA, 1998). A suite of total as well as soluble metals concentrations (Cd^{+2}, Co^{+2}, Ca^{+2}, Cu^{+2}, Pb^{+2}, Ni^{+2}, Zn^{+2}, Mn^{+2}, As^{+2}, Se^{+2}, Ag^{+2}, Mb^{+2}, Hg^{+2}, Be^{+2}, Fe^{+2}, Na^{+}, K^{+}, and Mg^{+2}) was determined using MassHunter software package (Agilent Technologies, Schaumburg, IL) and an inductively

coupled plasma mass spectrophotometer (ICP-MS) with an autosampler (7700x, Agilent Technologies, Schaumburg, IL). The soluble metal fraction was determined by prefiltering via Method 3030 B. Prior to metals analysis, all samples were predigested in nitric acid (3030 E), then diluted into 2% nitric/0.5% hydrochloric acid (APHA et al., 2005). Final metal analysis was performed following Method 3125 B for ICP-MS (APHA et al., 2005).

4.3 Results

Preliminary results for activity test development are presented first. Then the metadata for the $CH_3CH_2COO^-$ enrichment and nine biomass samples are given, followed by the activity test results. Finally, molecular analysis results are provided.

4.3.1 Preliminary Results: Optimization of Activity Tests

4.3.1.1 Mixing Microbial Communities

Because part of this research sought to empirically investigate the relationship between microbial activity and community structure by measuring a large number of different cultures, it was necessary to verify that mixing two or more cultures yielded cultures with statistically different activity values. Furthermore, before different cultures could be mixed to provide a unique microbial community, it was determined if the two cultures provided a unique activity in a linear or non-linear relationship with mixing ratio. Hence, SMA tests were performed using biomass from two continuously mixed stirred tank reactors (CSTR) known to have different SMA values. Biomass from one reactor was fed non-fat dry milk (biomass 1). A second reactor containing biomass with a higher SMA was fed multiple wastes, basal nutrient medium, and 5 g/L $NaHCO_3$ (biomass 2) (Navaratnam, 2012). A linear relationship ($R^2 = 0.95$) was found between CH_4 production rate (mL CH_4/h) and the

mixing ratio (based on VS) of these two cultures with different SMA values (Figure 4-2a). Though with a slightly lower R^2 of 0.75, SMA and mixing ratio (based on VS) also followed a linear model (Figure 4-2b). A theoretical SMA equation was derived (Equations 4-5). This model related SMA to the mass concentration (e.g., g/L) of the high-SMA biomass; the mechanistic model was also linear.

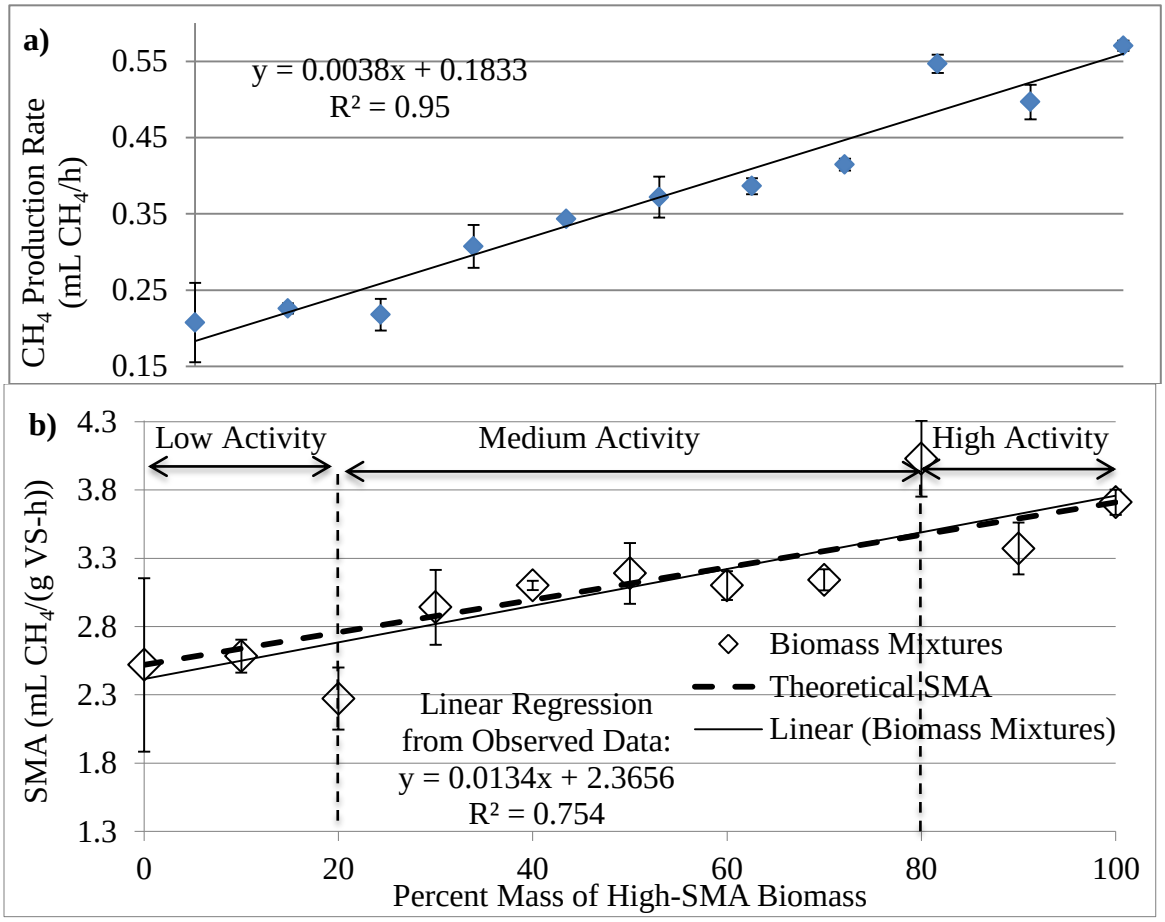

Figure 4-2. The relationship between percent (based on VS mass) of cultures mixed and CH_4 production rate (a) as well as percent of culture mixed and theoretical SMA (b).

Equation 4-4. Theoretical SMA as a function of biomass concentration

$$(a) \quad r_1 = k_1 X_1 V (lowSMA)$$

$$(b) \quad r_2 = k_2 X_2 V (highSMA)$$

$$(c) \quad r_m = k_1 X_1 V + k_2 X_2 V$$

$$(d) \quad X_m = X_1 + X_2$$

Then dividing by X_m, gives:

$$(e) \quad \frac{X_2}{X_m} = z \quad and \quad \frac{X_1}{X_m} = 1 - z$$

$$(f) \quad SMA_m = \frac{r_m}{X_m} = \frac{k_1 X_1 V}{X_m} + \frac{k_2 X_2 V}{X_m}$$

$$(g) \quad SMA_m = k_2 Vz + k_1 V(1 - z)$$

$$(h) \quad SMA_m = k_2 Vz + k_1 V(1) - k_1 Vz$$

$$(i) \quad SMA_m = (k_2 V - k_1 V)z + k_1' V$$

$$(j) \quad m = k_2 V - k_1 V$$

$$(k) \quad b = k_1 V$$

$$(l) \quad SMA_m = mz + b$$

where r_1 and r_2 are the rate of methane production (mL CH_4/h) of biomass samples 1 and 2, respectively. SMA_1 and SMA_2 were defined as the SMA values (mL CH_4/(g VS-h) of biomass 1 and 2, respectively. CH_4 production rate constants, k_1 and k_2 (mL CH_4/(mg VS-h)), for biomass 1 and 2, respectively, were determined from the preliminary mixing experiment at 100% of their respective cultures. X_1 and X_2 were the relative VS masses of biomass 1 and 2, respectively. The initial measured concentrations (mg VS/L) of biomass 1 and 2 before mixing were X_{1^o} and X_{2^o}, respectively; and V_1 and V_2 were the relative volume (L) of biomass 1 and 2, respectively. The total volume, V (L), was 0.015 L; thus, V = 0.015 = V_1 + V_2. Because substrate concentration was non-limiting during the period when SMA was measured, it was not a factor in Equations 4-4a-f. Using Equations 4-4, theoretical SMA was graphed against the percent of each biomass sample (Figure 4-2b).

Three ranges of SMA values (Figure 5-4b) were categorized with the following possible explanation for their presence: (1) low activity (approximately 2.5 mL CH_4/g VS-h) was observed at 0 to 20% of biomass 2 when there was an inadequate amount of the more active biomass, (2) medium activity (approximately 3 mL CH_4/ g VS-h) was observed at 30 to 70% of biomass 2, which resulted in intermediate SMA values, and (3) high activity (approximately 3.75 mL CH_4/ g VS-h) was observed at 80 to 100% of biomass 2 resulting in

relatively high SMA values. The SMA values in the low range were statistically different from those in the medium and high ranges ($p = 0.0106$ and $p = 0.0105$, respectively). The SMA values in the medium range were different from those in the high range ($p = 0.0786$).

4.3.1.2 Defining Appropriate F:M Ratio For OOPA

Preliminary testing to determine an appropriate standard, active biomass concentration yielded three general trends in biogas production. F:M ratios from 0.2 to 1 g COD/g VSS resulted in biogas production rates that quickly stopped, indicating all substrate was consumed. When the F:M ratio was between approximately 3 and 10 g COD/g VSS, the biogas production was initially rapid, then secondarily increased at a moderate rate before finally stopping. Final biogas volumes produced were slightly less than the theoretical maximum in all samples. Lastly, F:M ratios from 12 to 33 g COD/g VSS quickly rose to slightly less than half of the theoretical final biogas volume and did not change for the duration of the testing (more than two weeks), indicating a overloaded condition. Because a clear distinction was evident between the initial and secondary slopes, the optimal overload concentration for OOPA analysis was in the middle range (3 and 10 g COD/g VSS). In particular, the greatest contrast between initial and secondary slopes was found at F:M ratios of 4.4 (Figure 4-3) and 7.0 g COD/g VSS, which had initial average slopes of 1.51 $\pm$0.05 and 3.62 $\pm$0.12 mL biogas h^{-1} as well as secondary slopes of 0.13 $\pm$0.004 and 0.18 $\pm$0.05 mL biogas h^{-1}, respectively. Repeated results from this middle range of F:M ratios showed the same biogas production pattern—an initial increase to half of the 20-day maximum biogas level achieved followed lower secondary rate of biogas production. Therefore, an F:M ratio of 5 was chosen for the OOPA test.

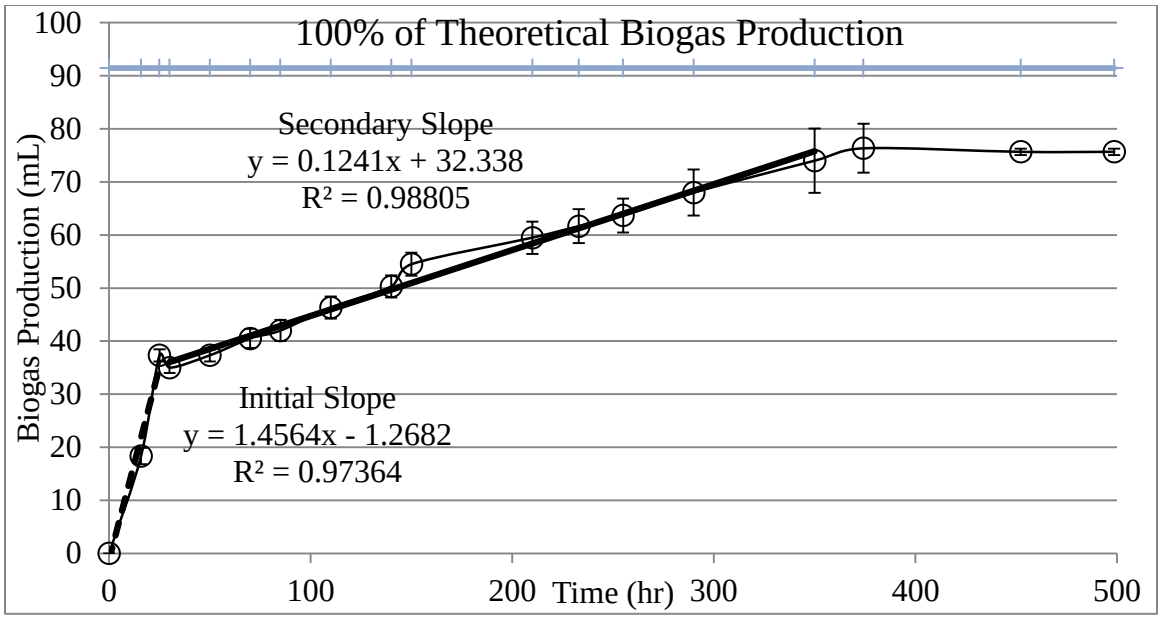

Figure 4-3. OOPA: average for triplicates of F/M ratio at 4.4 g COD/g VSS (3 g Glucose/L and 0.7g VSS/L) distinguishing initial slope ([mL biogas per h] of 1.548, 1.530, and 1.449) from secondary slope ([mL biogas per h] of 0.180, 0.177, and 0.141). Average slopes and standard deviation shown on graph. Horizontal line at 92 mL represented 100% of the theoretical biogas production.

4.3.1.3 Use of Intracellular ATP to Quantify Biomass

Intracellular ATP (iATP) was used to standardize the amount of biomass for SMA and OOPA testing since it has been shown to more accurately quantify active biomass than VSS (Roe and Bhagat, 1982; Cairns et al., 2005; Whalen et al., 2006; Whalen et al., 2006b). For example, the inactive portion of the VSS is included in VSS measurements, yet does not metabolize substrate or intermediates (Perle et al., 1995). Consequently, microbial cultures, especially those with longer sludge ages or recently subjected to stressed conditions, may have a significant portion of inactive VSS (Quirk and Eckenfelder, 1986). Extracellular ATP is often present as cells are lysed; thus, total ATP is less suitable than iATP as an active biomass measurement.

4.3.2 Metadata for $CH_3CH_2COO^-$ Enrichment and Digester Biomass

The quasi steady state metadata collected for the $CH_3CH_2COO^-$ enrichment at the time of activity testing and molecular analysis were as follows: temperature 35 ±1°C; pH 7.09 ±0.07; effluent SCOD: 160 ±10 mg/L (98% SCOD removal); CH_4 production: 0.27 ±0.016 L/d (78 ±0.49% CH_4); VSS concentration: 0.68 ±0.028 g/L; $CH_3CH_2COO^-$ concentration: 48 ±2.9 mg/L; CH_3COO^- concentration: less than the 20-mg/L detection limit. Metadata for nine biomass samples are presented in Appendix A.

4.3.3 Specific Methanogenic Activity (SMA) Testing

There was a statistically significant increase in SMA values after bioaugmenting six of the nine anaerobic biomass cultures (Table 4-3; Figure 4-4). Among these six, the average SMA value increased 29 ±17%. SMA values for anaerobic biomass samples varied more than 500%, from 15 ±0.30 to 77 ±2.3 mL CH_4/mg iATP-h. The SMA of the $CH_3CH_2COO^-$ enrichment used to bioaugment was 50 ±2.1 mL CH_4/mg iATP-h. Furthermore, all bioaugmented cultures exhibited a greater average SMA than the non-bioaugmented biomass; SMA values after bioaugmentation increased from 2 to 57%, and the increase averaged 22 ±17% for all biomass samples tested (Figure 4-4). With the notable exception of sample number 1, cultures with the highest SMA values (samples 2, 3, and 4) did not exhibit a statistical increase in SMA value after bioaugmentation, while those with the mid-range SMA values (samples 5, 6, and 7) showed low improvements and those with the lowest SMA values (samples 8 and 9) showed the greatest improvement after bioaugmentation (Figure 4-4). All SMA values of bioaugmented cultures increased (ranging from 4.2% to 21%) more than expected based on a linear model of 80% digester biomass

mixed with 20% of the $CH_3CH_2COO^-$ enrichment (Table 4-4). The percent increase in SMA for bioaugmented cultures versus the difference between SMA values for the $CH_3CH_2COO^-$ enrichment and digester biomass was graphed to depict little linear correlation among SMA difference and increase in SMA (Figure 4-5).

Table 4-3. SMA Values for Nine Full-Scale and Nine Bioaugmented Cultures

Sample Number	Full-Scale SMA_i (mL CH_4/ iATP-h)	Full-Scale Std. Dev. (mL CH_4/ iATP-h)	Bioaugmented SMA_i (mL CH_4/ iATP-h)	Bioaugmented Std. Dev. (mL CH_4/ iATP-h)	Percent Increase (%)
Bioaugment	50	2.1	N/A	N/A	N/A
1*	77	2.3	87	5.7	13%
2	62	4.4	64	4.0	2%
3	46	3.3	52	4.9	13%
4	39	2.0	43	3.8	10%
5*	35	4.7	44	1.1	25%
6*	35	1.7	40	1.3	14%
7*	30	1.0	38	0.4	26%
8*	26	2.7	36	3.3	39%
9*	15	0.3	24	1.0	57%

*Indicates a statistically significant increase in SMA due to bioaugmentation.

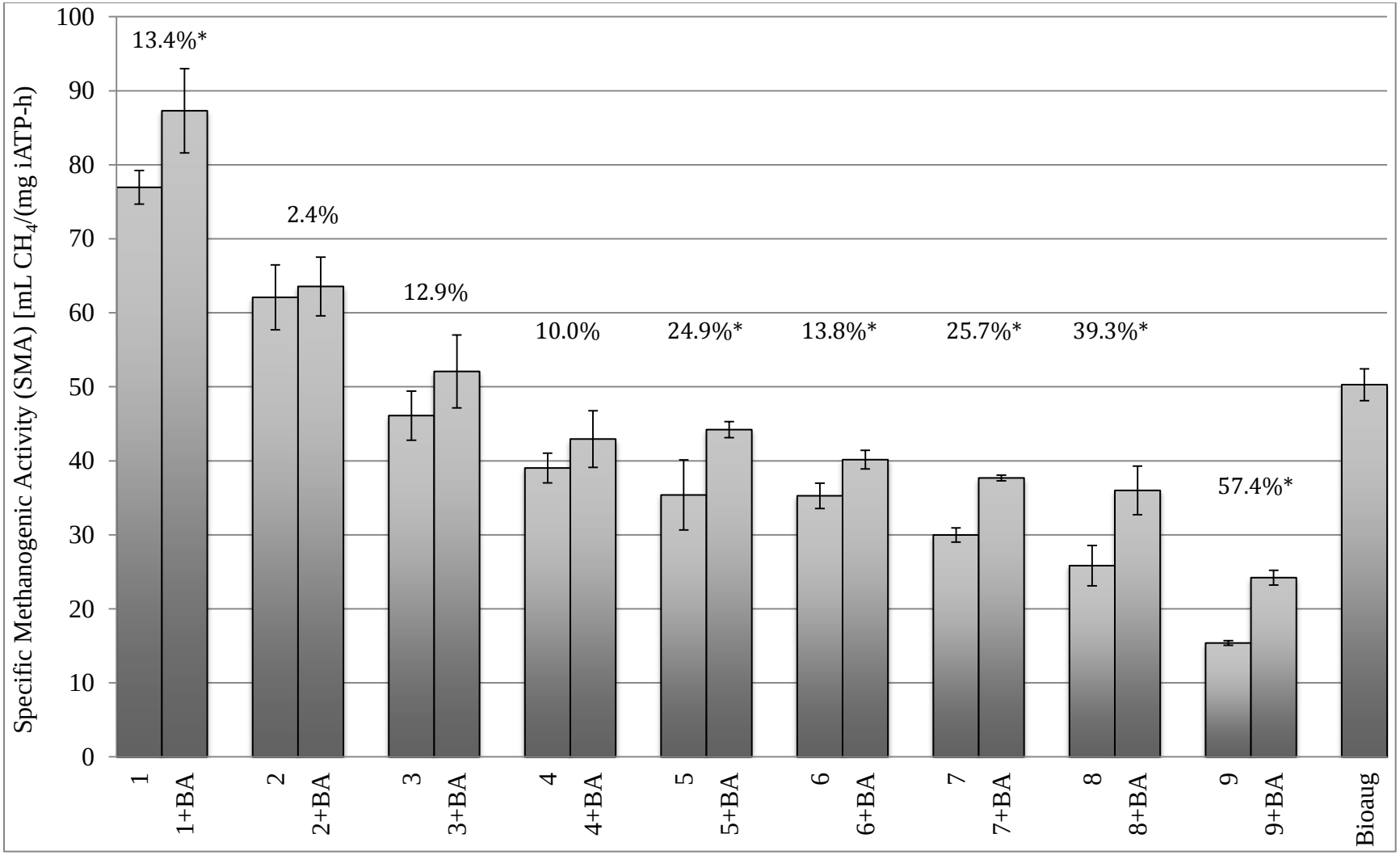

Figure 4-4. SMA for nineteen full-scale anaerobic digester cultures. The bioaugmented culture, a methanogenic culture developed in the lab to potentially increase CH_4 production, is labeled "Bioaug." Pairs are nine digester biomass samples (left; labeled with a sample number) and nine bioaugmented digester biomass samples (labeled "#+BA"). *Indicates statistically greater SMA value upon bioaugmentation.

Table 4-4. Effect of Bioaugmentation on SMA Values

Sample Number	Expected SMA** (mL CH_4/iATP-h)	Measured SMA (mL CH_4/iATP-h)	Increase due to Bioaug.*** Beyond Linear Expected (%)
1*	72	87	21%
2	60	64	7.3%
3	47	52	11%
4	41	43	4.2%
5*	38	44	16%
6*	38	40	5.1%
7*	34	38	12%
8*	31	36	17%
9*	22	24	8.8%

*SMA value statistically increased upon bioaugmentation
** SMA value determined by $0.8*SMA_{digester\ biomass} + 0.2*SMA_{CH3CH3COO-\ enrichment}$
*** Percent greater the measured SMA value was than the expected 80/20 linear SMA value.

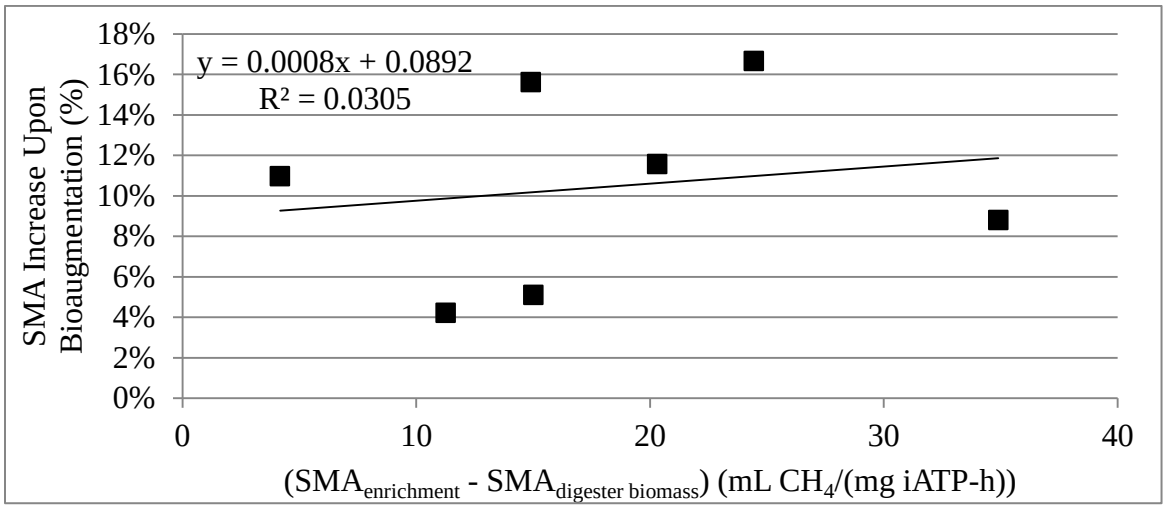

Figure 4-5. Relationship between percent increase in SMA for bioaugmented cultures and the difference between SMA values for the $CH_3CH_2COO^-$ enrichment and digester biomass.

In order to increase the sample size, all SMA values were calculated as the SMA value of the individual replicate divided by the average of all bioaugmented and non-bioaugmented replicates lumped together (triplicates of each for a total of six samples in each pair). The average standardized SMA value (n = 27) of non-bioaugmented samples was 0.90 ±0.083, whereas it was 1.10 ±0.085 for and bioaugmented samples (p = 0.0018). Overall, bioaugmentation statistically increased SMA values.

4.3.4 Organic Overload Perturbation Activity (OOPA) Testing

Upon bioaugmentation, the average M/F ratio increased in one of the nine cultures (culture 6), the one with the lowest M/F (Figure 4-6). Resilience statistically increased in five of the nine bioaugmented cultures (Figure 4-7). Capacity statistically increased in one of the nine biomass samples—the sample with the second lowest SMA (Figure 4-8). A statistical increase was observed in one of the PBY values (Figure 4-9).

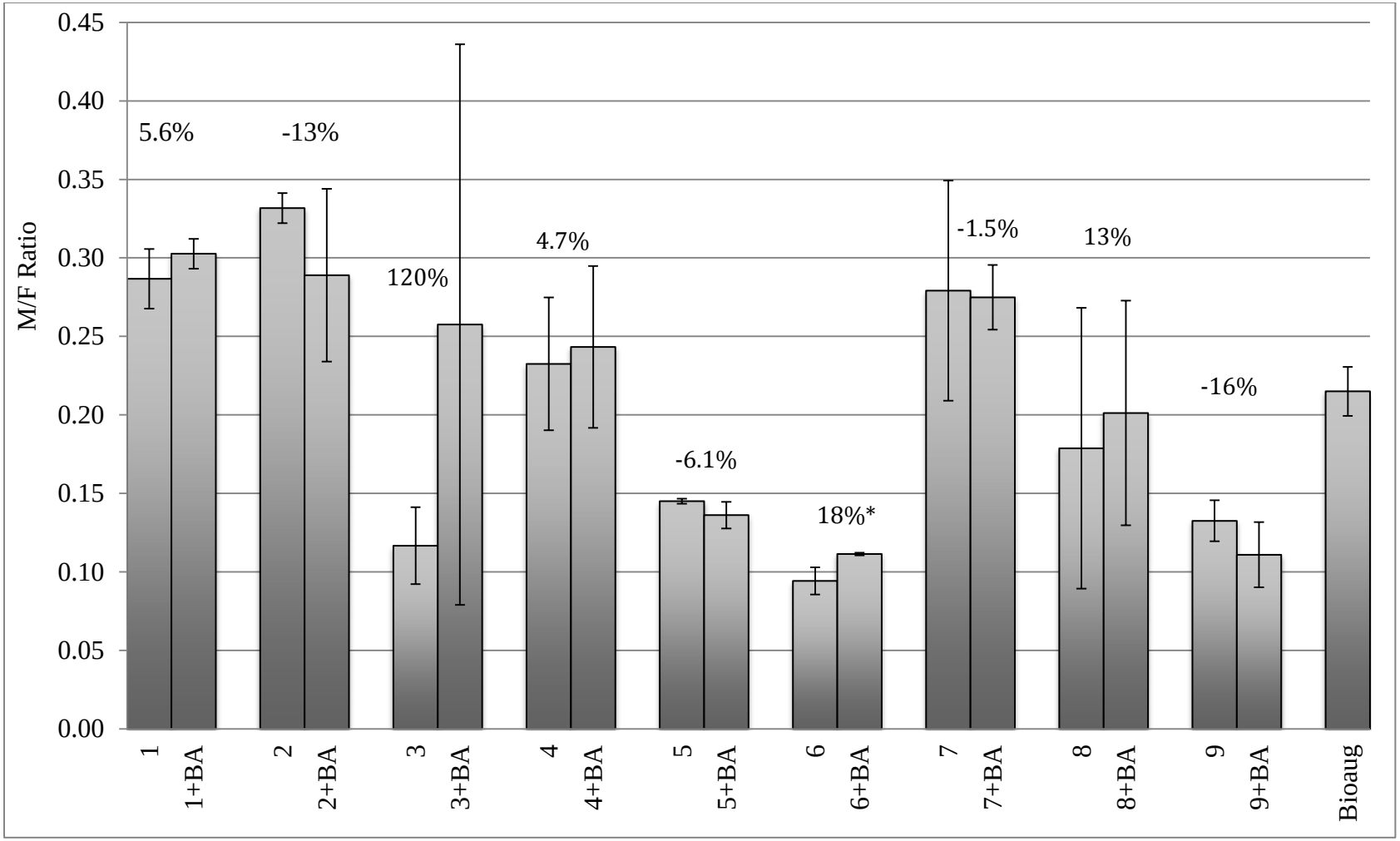

Figure 4-6. Methanogenesis to fermentation (M/F) Ratio. The $CH_3CH_2COO^-$ enrichment, a methanogenic culture developed in the lab to potentially increase CH_4 production, is labeled "Bioaug." Pairs are nine digester biomass samples (left side; labeled with the sample number) and nine bioaugmented digester biomass samples (labeled "#+BA"). *Indicates statistical improvement of bioaugmented culture versus non-bioaugmented culture.

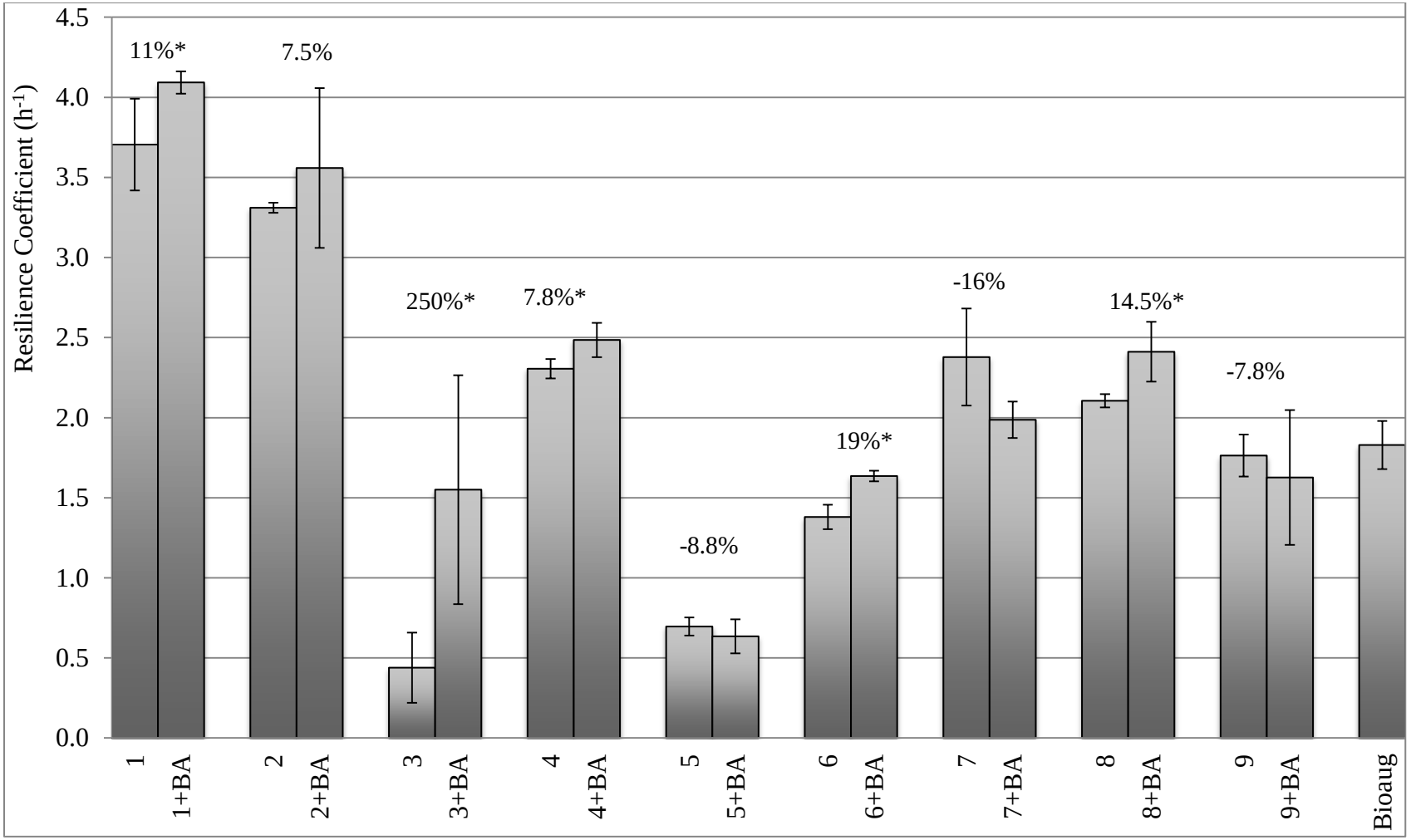

Figure 4-7. Resilience coefficient (time from glucose perturbation to 66.7% of the theoretical maximum biogas production). The $CH_3CH_2COO^-$ enrichment, a methanogenic culture developed in the lab to potentially increase CH_4 production, is labeled "Bioaug." Pairs are nine digester biomass samples (left side; labeled with the sample number) and nine bioaugmented digester biomass samples (labeled "#+BA"). *Indicates statistical improvement of bioaugmented culture versus non-bioaugmented culture.

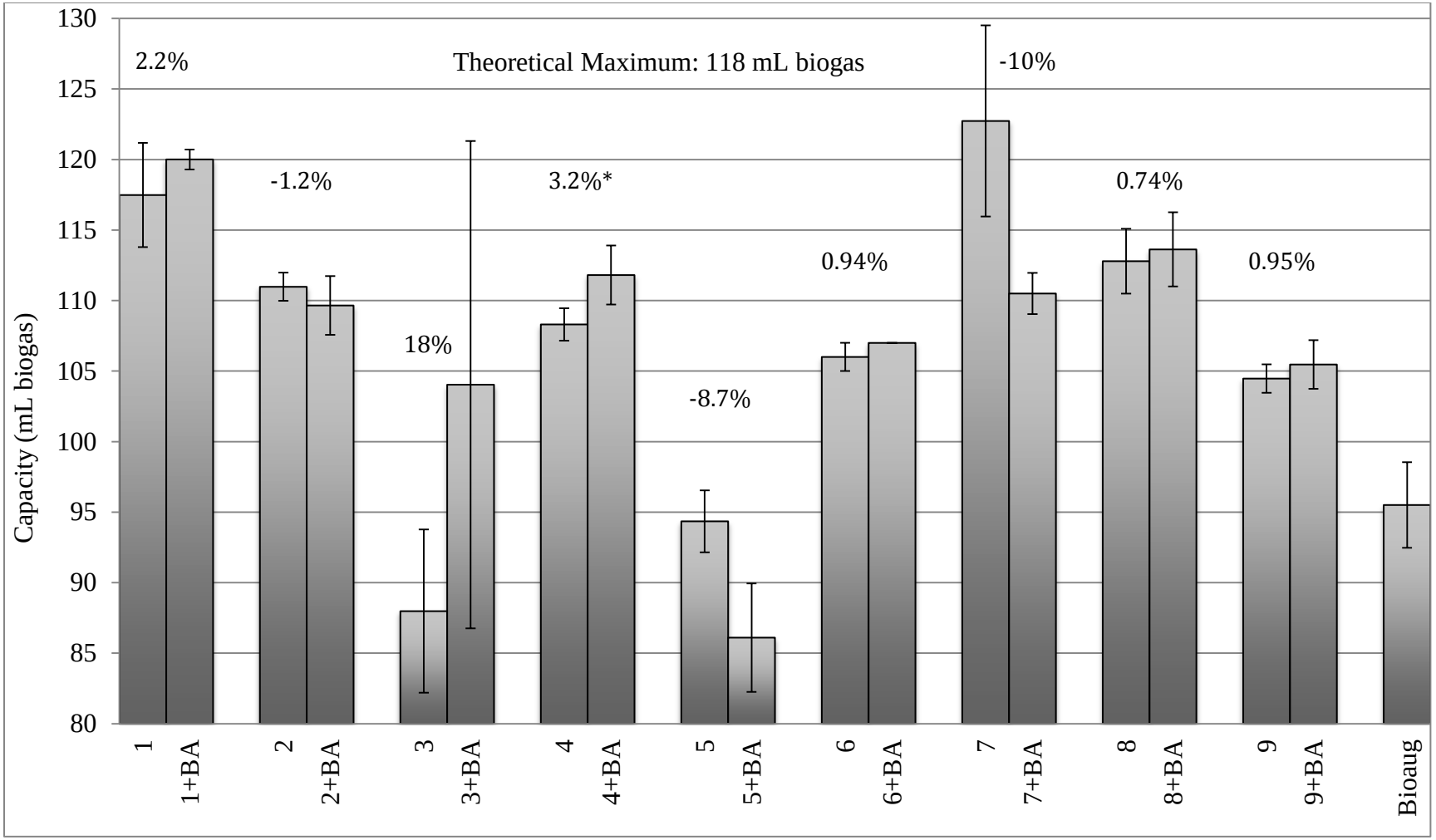

Figure 4-8. Capacity (total 20-day biogas production; theoretical maximum was 118 mL biogas). The $CH_3CH_2COO^-$ enrichment, a methanogenic culture developed in the lab to potentially increase CH_4 production, is labeled "Bioaug." Pairs are nine digester biomass samples (left side; labeled with the sample number) and nine bioaugmented digester biomass samples (labeled "#+BA"). *Indicates statistical improvement of bioaugmented culture versus non-bioaugmented culture.

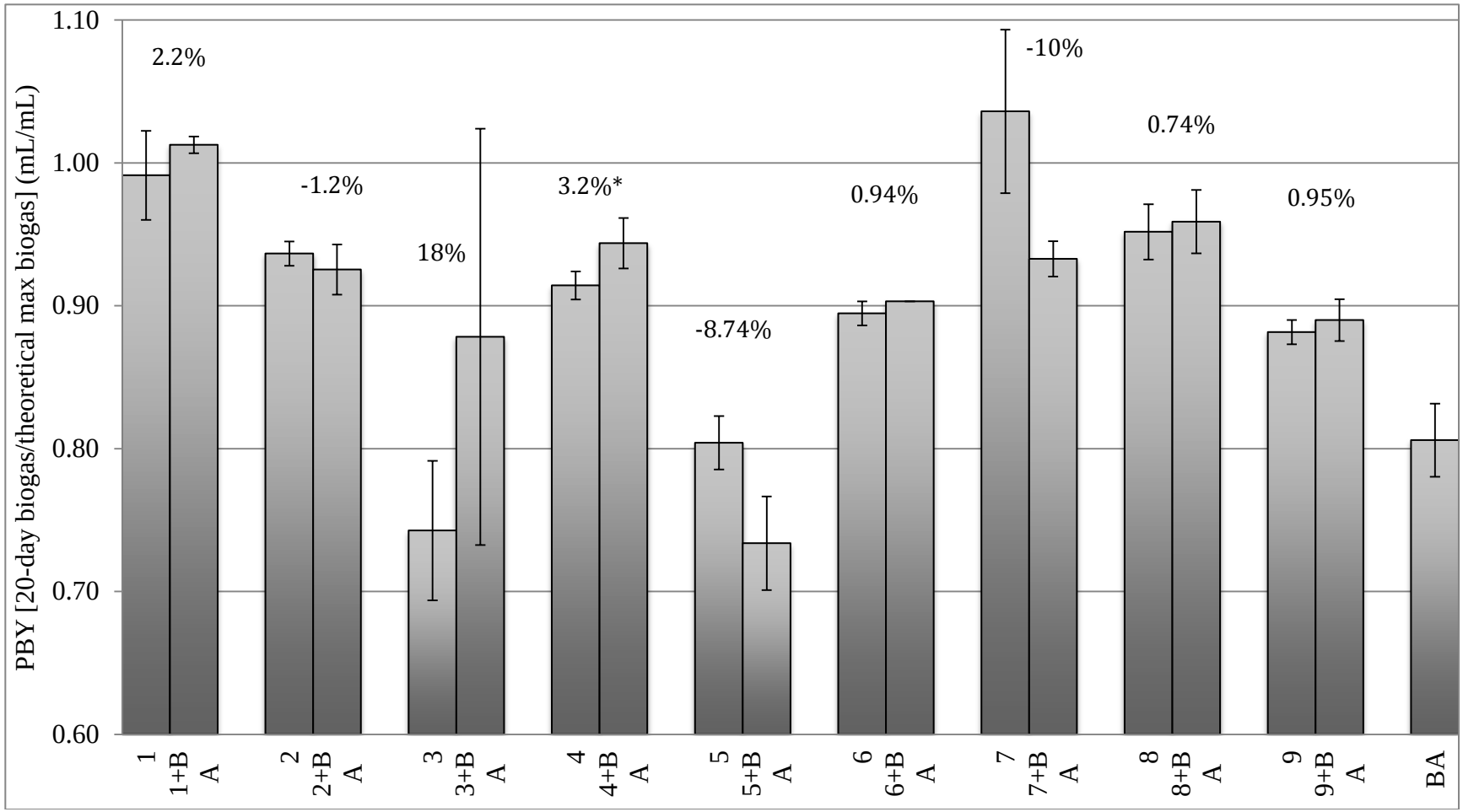

Figure 4-9. Perturbed biogas yield (PBY, cumulative biogas volume produced after 20 days divided by the total theoretical volume expected based on the glucose added). The $CH_3CH_2COO^-$ enrichment, a methanogenic culture developed in the lab to potentially increase CH_4 production, is labeled "Bioaug." Pairs are nine digester biomass samples (left side; labeled with the sample number) and nine bioaugmented digester biomass samples (labeled "#+BA"). *Indicates statistical improvement of bioaugmented culture versus non-bioaugmented culture.

Spearman's Rank Correlation (r_s) Coefficient (Zar, 1972) correlated the following: SMA values and M/F ratio at the 99.5% level (two-tailed) with an r_s value of 0.628 (n = 19) (Table 4-4) as well as SMA values and resilience coefficient correlated at the 90% level (two-tailed) with an r_s value of 0.407 (n = 19) (Table 4-5). The linear relationship with SMA and both M/F ratio and resilience coefficient had R^2 values of 0.40 and 0.41, respectively. The R^2 values found between SMA rank and both M/F ratio rank as well as resilience coefficient rank were 0.395 and 0.166, respectively (Figures 4-10 and 4-11). These linear relationships were in line with the Spearman's Rank Correlation Coefficient results in that SMA and M/F ratio were more significantly correlated than SMA and Resilience coefficient.

Table 4-5. Spearman's Rank Correlation Coefficient correlated SMA and M/F Ratio at the 99.5% level (two-tailed)

	SMA Data		OOPA Data	
Biomass	(mL CH_4/ mg iATP-h)	Rank (a)	M/F Ratio	Rank (b)
1+BA	87.3	1	0.303	2
1	76.9	2	0.287	4
2+BA	63.6	3	0.289	3
2	62.1	4	0.332	1
3+BA	52.1	5	0.258	7
BA	50.3	6	0.215	10
3	46.1	7	0.117	16
5+BA	44.2	8	0.136	14
4+BA	42.9	9	0.243	8
6+BA	40.2	10	0.111	17
4	39.0	11	0.232	9
7+BA	37.7	12	0.275	6
8+BA	36.0	13	0.201	11
5	35.4	14	0.145	13
6	35.3	15	0.094	19
7	30.0	16	0.279	5
8	25.8	17	0.179	12
9+BA	24.2	18	0.111	18
9	15.4	19	0.132	15

Table 4-6. Spearman's Rank Correlation Coefficient correlated SMA and Resilience Coefficient above the 90% level (two-tailed)

	SMA Data		OOPA Data			
Biomass	(mL CH_4/ mg cATP-h)	Rank (a)	Resilience Coefficient	Rank (b)	d_i	d_i^2
1+BA	87.3	1	4.093	1	0	0
1	76.9	2	3.705	2	0	0
2+BA	63.6	3	3.559	3	0	0
2	62.1	4	3.310	4	0	0
3+BA	52.1	5	1.550	15	-10	100
BA	50.3	6	1.821	11	-5	25
3	46.1	7	0.439	19	-12	144
5+BA	44.2	8	0.635	18	-10	100
4+BA	42.9	9	2.485	5	4	16
6+BA	40.2	10	1.635	13	-3	9
4	39.0	11	2.305	8	3	9
7+BA	37.7	12	1.987	10	2	4
8+BA	36.0	13	2.411	6	7	49
5	35.4	14	0.696	17	-3	9
6	35.3	15	1.380	16	-1	1
7	30.0	16	2.378	7	9	81
8	25.8	17	2.105	9	8	64
9+BA	24.2	18	1.626	14	4	16
9	15.4	19	1.763	12	7	49

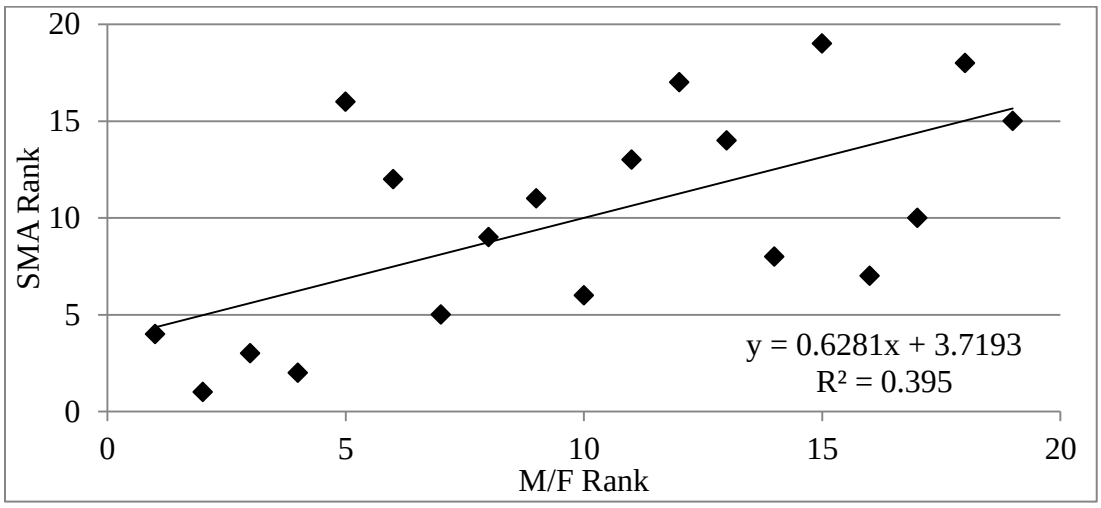

Figure 4-10. Relationship between SMA rank and M/F rank.

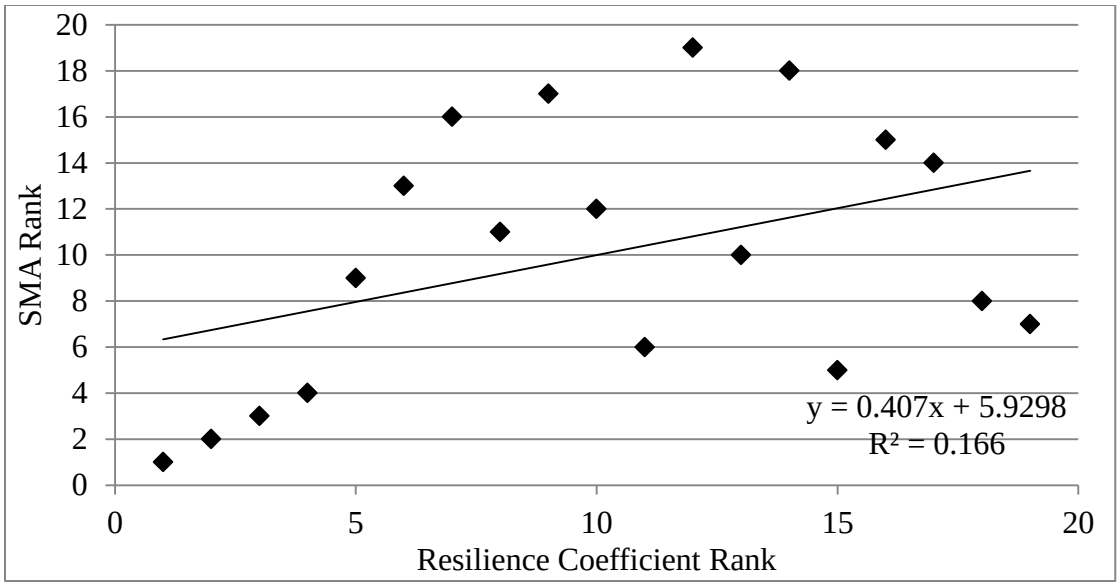

Figure 4-11. Relationship between SMA rank and resilience coefficient rank.

4.3.5 Methanogen Community structure

4.3.5.1 Principal Component Analysis and Clustering

PCA was performed for the nine biomass samples using the eight dominant bands identified (Figure 4-12). Differences were evident in the methanogen community structure of the nine cultures, especially those that had the highest and lowest SMA values with $CH_3CH_2COO^-$. Band 2 had the greatest positive influence on those structures with the highest SMA values, whereas band 4 had greatest positive influence on those structures with the lowest SMA values with $CH_3CH_2COO^-$. These differences showed that diverse methanogen community structures were used to measure the effects of bioaugmentation. Cluster analysis using the UPGMA algorithm showed variability among samples (Figure 4-13), yet depicted some differences from the PCA diagram. The methanogen community structure in digester biomass 1 clustered with digester biomass 7 and then with 5 (Figure 4-13), while the PCA located digester biomass 5 and 7 closer together than digester biomass 1

and 7 (Figure 4-12). Because of the clustering, 1, 5, and 7 are in the same cluster (Figure 4-12).

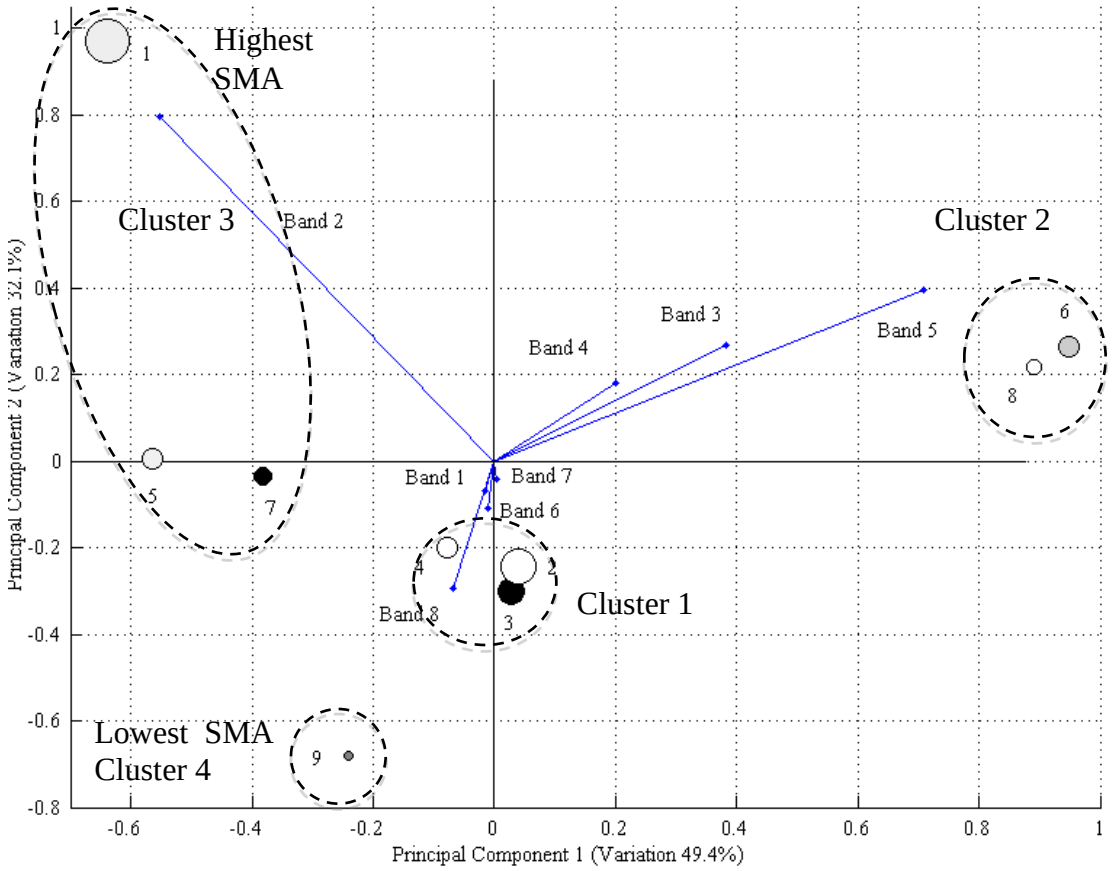

Figure 4-12. PCA plot of the nine biomass samples. Diameter symbols correspond to relative value of the SMA with propionate. Biomass samples from similar substrates are similarly colored (breweries, white; municipalities, black; other, gray). Data from eight common bands were used. Each vector represents one DGGE band and the diameter of each data symbol corresponds to the SMA magnitude. Dashed ovals show clustering based on DGGE banding pattern intensities calculated with UPGMA as well as Neighbor-joining algorithms.

First principal component = $-0.0159(X_1) - 0.0690(X_2) + 0.1396(X_3) + 0.1328(X_4) + 0.1023(X_5) - 0.0104(X_6) + 0.0008(X_7) + 0.9733(X_8)$

Second principal component = $-0.5531(X_1) + 0.7970X_2) + 0.1151(X_3) + 0.1823(X_4) + 0.0661(X_5) + 0.0817(X_6) - 0.0376(X_7) - 0(X_8)$

Where, X_1, X_2, X_3……X_8 are the demeaned optical densities for bands 1, 2, 3,…,8 (1 being top, closest to the well) of the DGGE banding pattern.

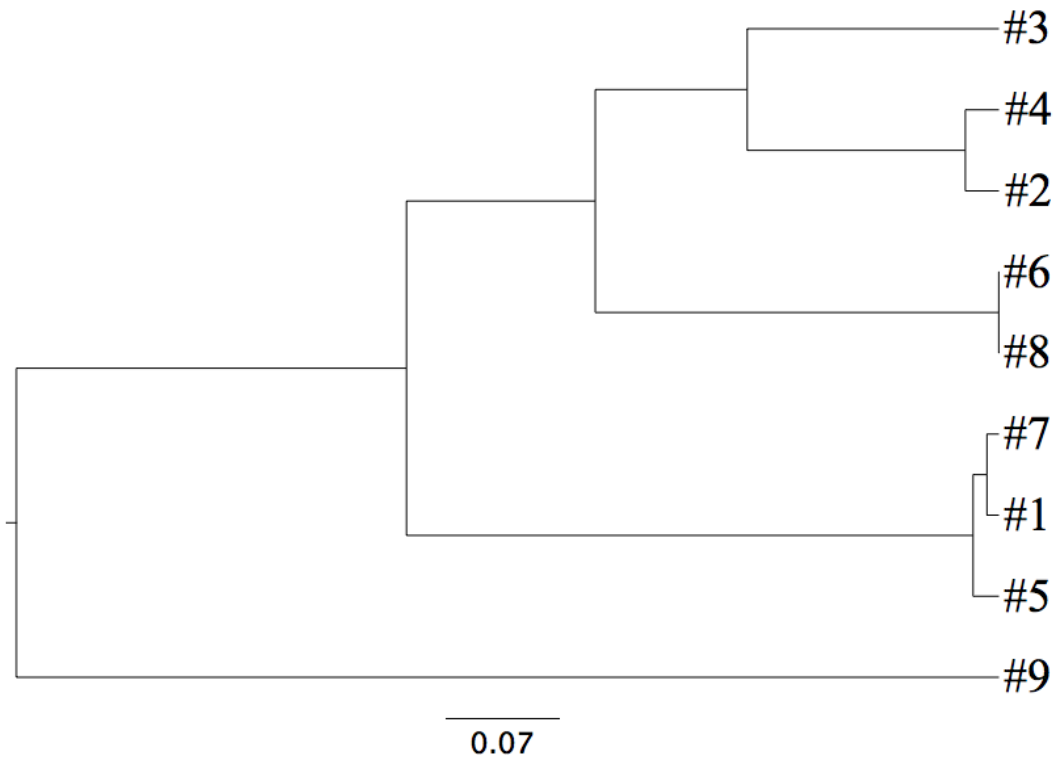

Figure 4-13. UPGMA algorithm used to cluster nine biomass samples (labeled as in Table 4-2).

A second PCA plot of all 19 cultures accounted for 55.8 and 24.7% of the differences in the methanogen community structure (Figure 4-14). Each circle represented one of the nine biomass samples, whereas the squares represented a bioaugmented culture (or the $CH_3CH_2COO^-$ enrichment that was used to bioaugment). The four bands found in all 19 samples were used to construct this PCA.

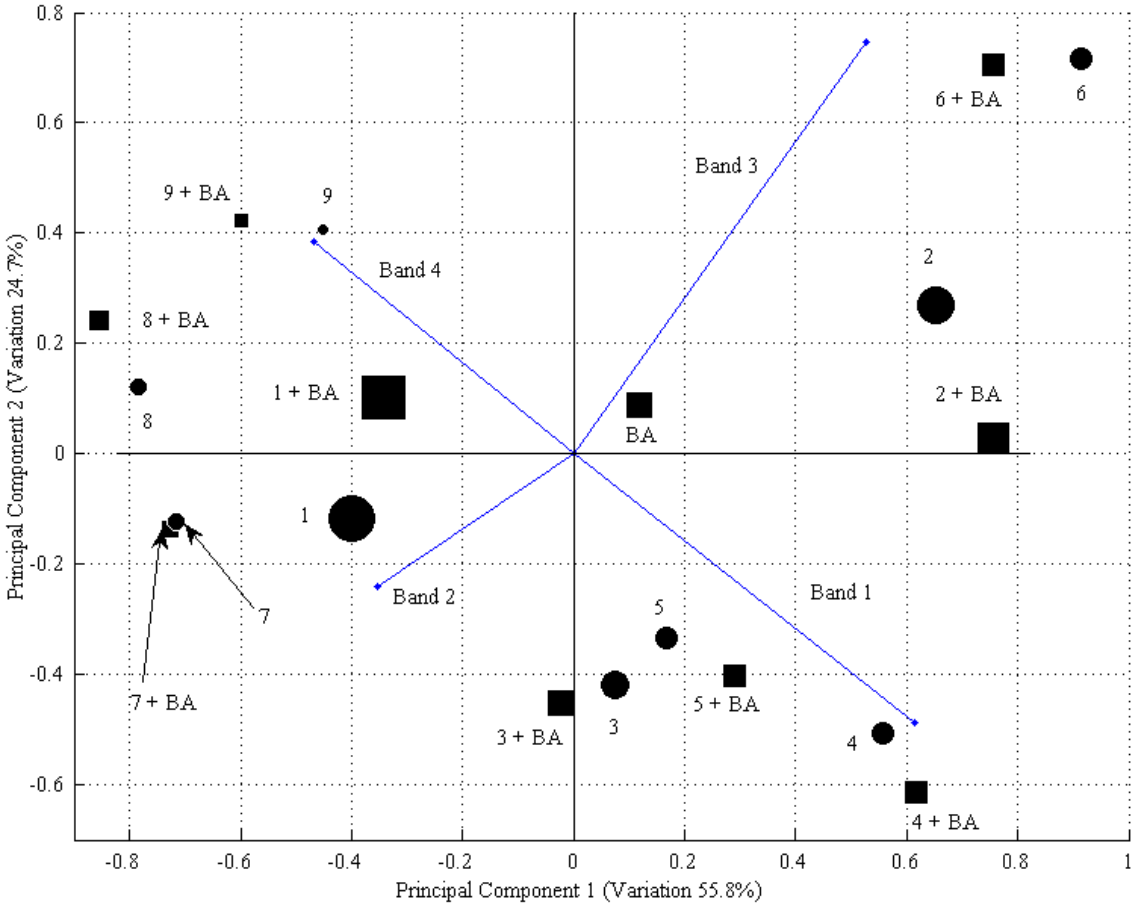

Figure 4-14. PCA of nine biomass samples (DB#), nine bioaugmented samples (DB# + BA), and the $CH_3CH_2COO^-$ enrichment used to bioaugment (BA). Normalized data from four common bands were used. Each vector represents one DGGE band and the diameter of each data point corresponds to the SMA magnitude.
First principal component = 0.6141(X1) - 0.4862(X2) - 0.3307(X3) + 0.5265(X4)
Second principal component = $-0.3548(X_1) - 0.2402(X_2) + 0.6662(X_3) + 0.6104(X_4)$
Where, X_1, X_2, X_3, and X_4 are the normalized optical densities for bands 1, 2, 3, and 4 (1 being top, closest to the well) of the DGGE banding patterns.

The central location of the $CH_3CH_2COO^-$ enrichment on the PCA plot was evidence of the methanogen community common to the bioaugmented cultures. The fact that all non-bioaugmented and bioaugmented pairs were close together depicted that the communities were similar. Cluster analysis using UPGMA further described similarity among the 19 samples (Figure 4-15). In general, SMA increased upon bioaugmentation in communities that had the most dissimilar structures compared to the $CH_3CH_2COO^-$ enrichment. Of the two primary clusters, all those that were more dissimilar to the $CH_3CH_2COO^-$ enrichment had a statistically greater bioaugmented SMA as compared to the non-bioaugmented SMA.

While only two of the five SMA values from samples with communities on the same root-connected branch as the $CH_3CH_2COO^-$ enrichment statistically increased upon bioaugmentation, the two with the closest structures to the $CH_3CH_2COO^-$ enrichment (#8 and 5) also improved. Note that biomass samples 1, 5, 6, 7, 8, and 9 had statistically greater bioaugmented SMA values, and five of these also clustered on the opposite main branch of the Fitch-Margolish phylogenetic tree (Figure 4-16). Thus, biomass samples with greater differences in community structure from the $CH_3CH_2COO^-$ enrichment structure generally exhibited statistically greater SMA values. The relationship between methanogen community structure and improved function via increased SMA values was observed in that greater dissimilarity distance was proportional to the increase in SMA values (Figure 4-17). The two biomass samples with SMA values greater than that of the $CH_3CH_2COO^-$ enrichment were omitted from the graph as other synergistic mechanism might have been present to increase SMA values beyond that of even the higher-SMA biomass.

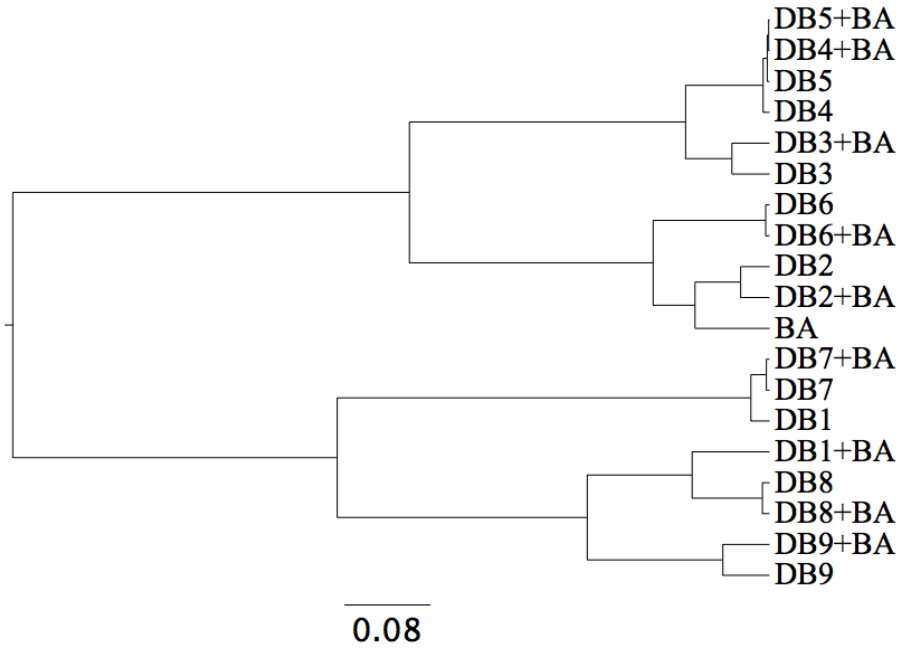

Figure 4-15. UPGMA Tree for nine digester biomass samples (DB#), nine bioaugmented samples (DB#+BA), and the $CH_3CH_2COO^-$ enrichment used to bioaugment (BA). Normalized data from four common bands were used. When biomass samples 1 and 5 through 9 were bioaugmented, they had statistically greater SMA values.

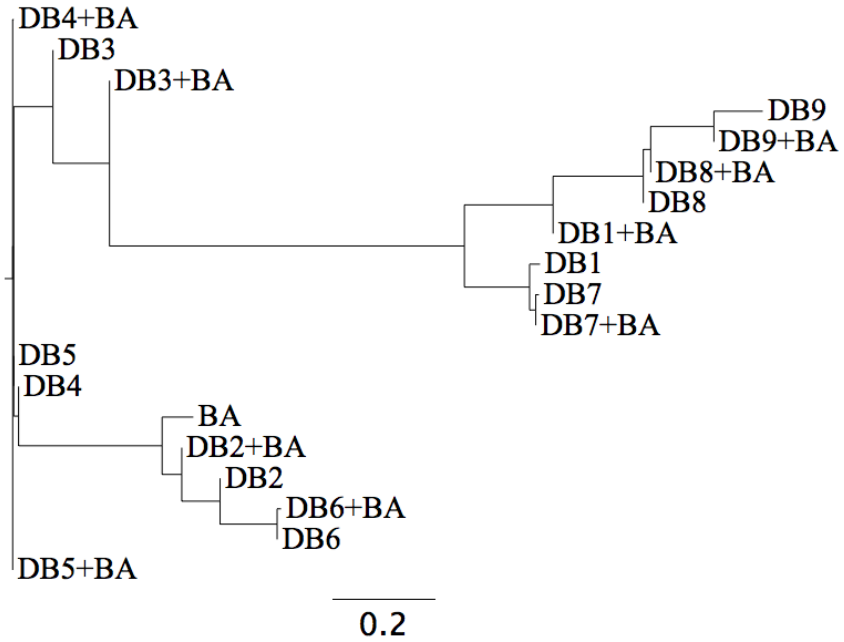

Figure 4-16. Fitch Margolish Tree for nine digester biomass samples (DB#), nine bioaugmented samples (DB#+BA), and the $CH_3CH_2COO^-$ enrichment used to bioaugment (BA). Normalized data from four common bands were used.

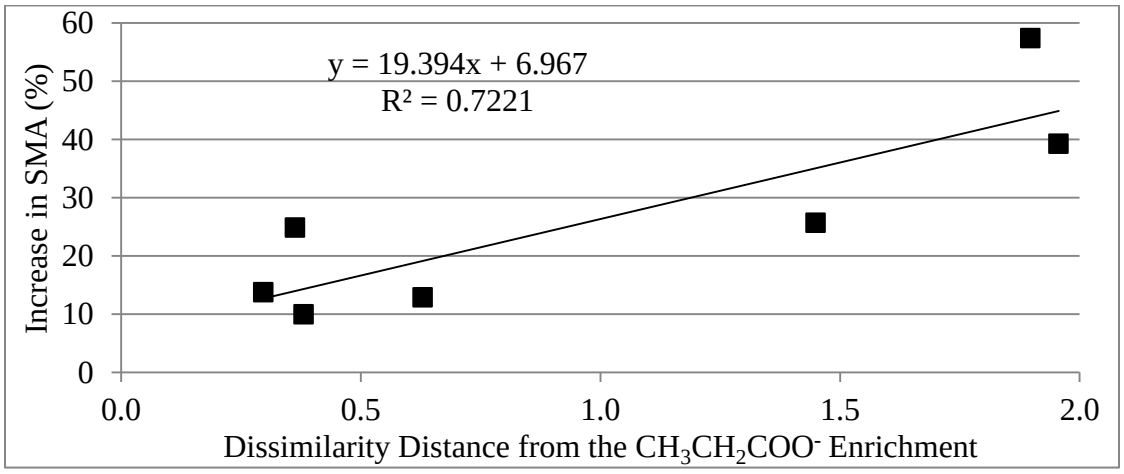

Figure 4-17. Difference between methanogen community structures in the $CH_3CH_2COO^-$ enrichment and digester biomass correlated with percent increase in SMA values. Graph includes biomass samples with SMA values less than those of the $CH_3CH_2COO^-$ enrichment (i.e., digester biomass 1 and 2 are excluded since another mechanism may be responsible for their SMA increasing above that of the $CH_3CH_2COO^-$ enrichment).

Spearman's Rank Correlation Coefficient between the SMA data and the optical density data from DGGE banding patterns (determined as the dissimilarity distance from the $CH_3CH_2COO^-$ enrichment) was 0.396, which is above the 0.391 necessary for a two-tailed 90% confidence interval (Zar, 1972) (Table 4-7). Thus, a correlation between

methanogen community structure data and SMA was also found via Spearman's Rank Correlation Coefficient. Furthermore, methanogen community structure and the likelihood that bioaugmentation will increase SMA value correlated above the 98% level (r_s = 0.770) (Zar, 1972) (Table 4-8). The linear correlation among SMA rank and rank of dissimilarity distance from the $CH_3CH_2COO^-$ enrichment yielded a R^2 of 0.16 and among the rank of the increase in SMA upon bioaugmentation and the same dissimilarity distance yielded a R^2 of 0.59 (Figures 4-18, 4-19). The higher coefficients (r_s and R^2) indicated that there was greater correlation of methanogen community structure with percent increase in SMA values than with SMA values.

Table 4-7. Spearman's Rank Correlation Coefficient for SMA Values and Methanogen Community Structure

	SMA Data		Densitometric Data	
Biomass	(mL CH_4/ mg iATP-h)	Rank (a)	PCC Distance From Bioaug*	Rank (b)
Bioaug	50.3	6	0.000	1
1+BA	87.3	1	1.886	16
1	76.9	2	1.243	12
2+BA	63.6	3	0.149	3
2	62.1	4	0.139	2
3+BA	52.1	5	0.629	11
3	46.1	7	0.550	10
5+BA	44.2	8	0.363	8
4+BA	42.9	9	0.381	9
6+BA	40.2	10	0.297	6
4	39.0	11	0.266	5
7+BA	37.7	12	1.449	14
8+BA	36.0	13	1.956	19
5	35.4	14	0.362	7
6	35.3	15	0.264	4
7	30.0	16	1.400	13
8	25.8	17	1.927	18
9+BA	24.2	18	1.897	17
9	15.4	19	1.748	15

*PCC Distance From Bioaug is the Pearson's Correlation Coefficient distance in the densitometric data from the CH3CH2COO- enrichment to other digester biomass samples.

Table 4-8. Spearman's Rank Correlation Coefficient for Percent Increase in SMA Upon Bioaugmentation and Methanogen Community Structure

Biomass	SMA Data % Increase	Rank (a)	Densitometric Data PCC Distance Bioaug*	Rank (b)
Bioaug	0	1	0.000	1
2+BA	2.4	2	0.149	2
4+BA	10.0	3	0.381	5
3+BA	12.9	4	0.629	6
1+BA	13.4	5	1.886	8
6+BA	13.8	6	0.297	3
5+BA	24.9	7	0.363	4
7+BA	25.7	8	1.449	7
8+BA	39.3	9	1.956	10
9+BA	57.4	10	1.897	9

*PCC Distance From Bioaug is the Pearson's Correlation Coefficient distance in the densitometric data from the CH3CH2COO$^-$ enrichment to other digester biomass samples.

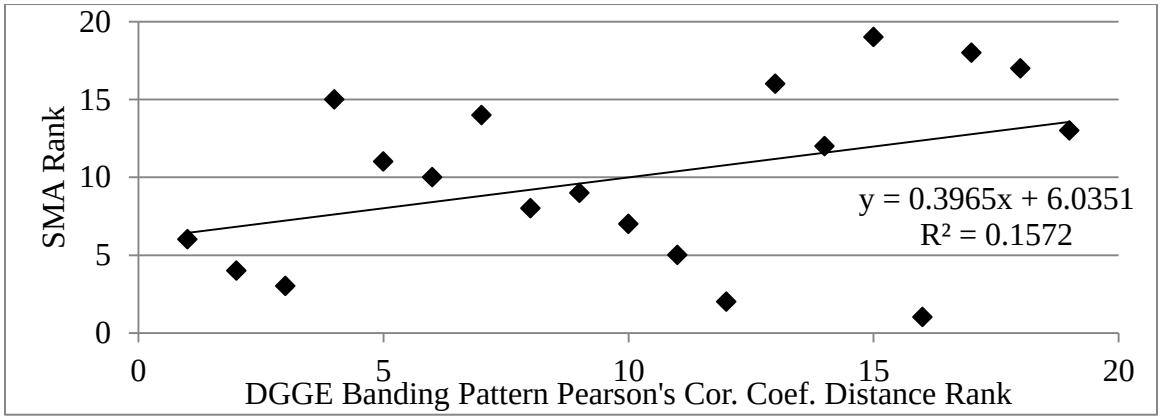

Figure 4-18. Relationship between SMA rank and the rank of DGGE banding pattern dissimilarity distance from the $CH_3CH_2COO^-$ Enrichment (calculated using Pearson's Correlation Coefficient).

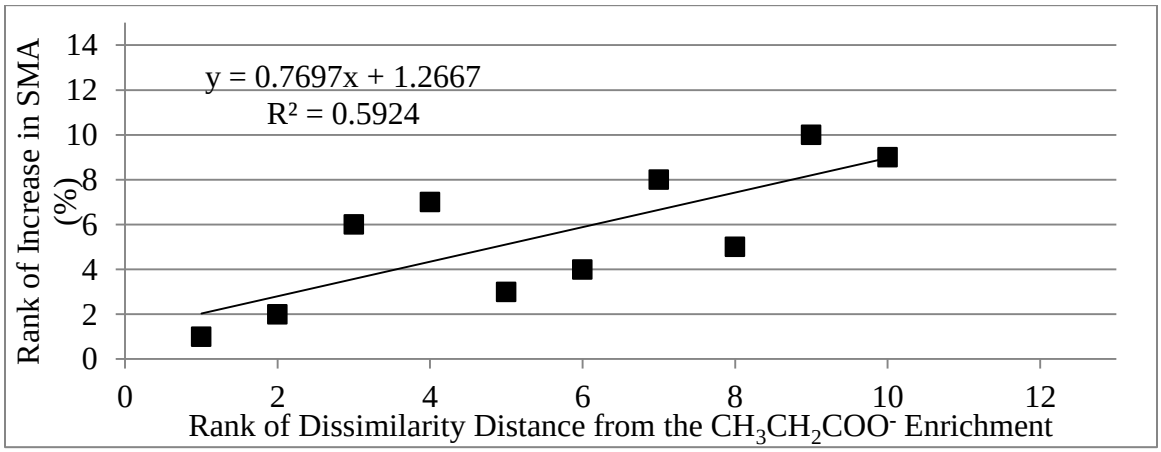

Figure 4-19. Relationship between SMA rank and the rank of DGGE banding pattern dissimilarity distance (calculated using Pearson's Correlation Coefficient) from the $CH_3CH_2COO^-$ Enrichment.

4.3.5.2 Functional Organization

The most even community was the $CH_3CH_2COO^-$ enrichment. This low functional organization (Fo) may be due to the specificity of the substrate (i.e., only two microbial guilds of the anaerobic degradation pathway are present when $CH_3CH_2COO^-$ is fed). The second and third lowest Fo values were found in the bioaugmented digester biomass 1 and digester biomass 1, respectively. This high evenness may be linked to the rapid rate of $CH_3CH_2COO^-$ degradation in digester biomass 1. Given that the $CH_3CH_2COO^-$ enrichment was operated to degrade $CH_3CH_2COO^-$, the highest SMA among samples (obtained in DB1) might be, at least partly, due to the presence of a greater proportion of microorganisms that are well-suited to degrade $CH_3CH_2COO^-$ and its byproducts (e.g., H_2) in DB1. This low Fo culture handling overload well agreed with what Wittebolle et al. (2008) suggested (i.e., communities with high evenness, low Fo, would be best suited to handle stressed conditions) since digester biomass 1 also outperformed all other biomass samples in terms of resilience, and all others except DB7 and DB2 in terms of capacity and M/F ratio, respectively. Those microbes necessary to degrade the high $CH_3CH_2COO^-$ conditions that build up during overload may have dominated the DB1 culture.

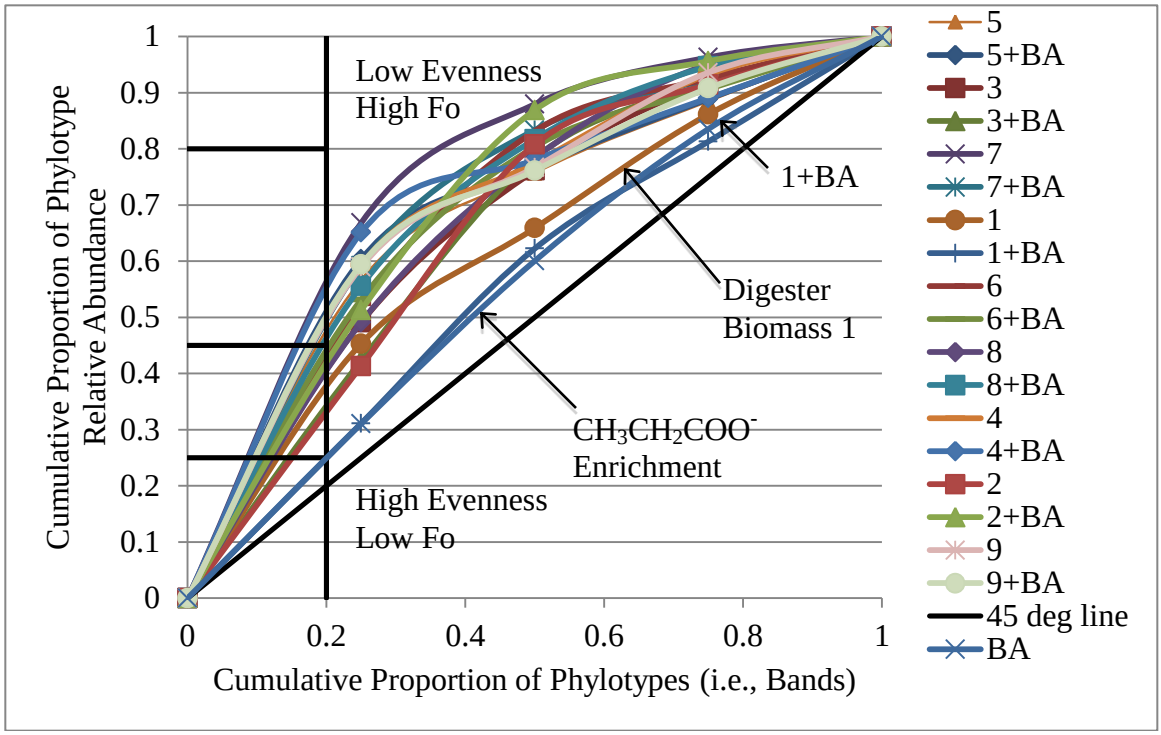

Figure 4-20. Pareto Lorenz Evenness Curve depicting Functional Organization, Fo, for nine biomass samples (labeled numerically), nine bioaugmented samples (#+BA), and $CH_3CH_2COO^-$ enrichment used to bioaugment (BA). The 45° line through the origin represents a perfectly even community, whereas a more uneven community would have an initial slope greater than 45° and then a gradually decreasing slope that asymptotically approaches a slope of zero.

4.4 Discussion

DGGE results showed differences among not only the nine biomass samples, but also the bioaugmented microbial cultures and the non-bioaugmented cultures. PCA (Figures 4-7 and 4-9) and cluster (Figures 4-8, 4-10, and 4-11) analysis results as well as the graph of increase in SMA value versus dissimilarity in densitometric data (Figure 4-12) showed that biomass with methanogen communities that were most structurally different from that of the $CH_3CH_2COO^-$ enrichment exhibited a statistically greater increase in SMA upon bioaugmentation. Likewise, increase in SMA correlated above the 98% level (two-tailed) with densitometric data via Spearman's correlation coefficient with an r_s of 0.770, which exceeded the 98% tolerance of $r_s = 0.745$. Because bioaugmentation with a methanogen community

different from the culture to which it was added improved digester function, these results indicate that digester design and operation should not rely on only operational parameters (e.g., organic loading rate, residence time), but also incorporate methanogen community structure to further improve anaerobic digester treatment efficiency.

In six of the nine biomass samples tested, bioaugmentation increased the SMA with $CH_3CH_2COO^-$. As Werner et al. (2011) suggested, syntrophic organisms (i.e., acidogens) might be less diverse than microbes at other trophic levels and, thus, more essential to healthy digester operation than those organisms involved in other steps of the overall anaerobic degradation pathway. Therefore, the addition of a $CH_3CH_2COO^-$ enrichment to bioaugment would supply a greater proportion of the limited syntrophic species that are necessary for the energetically unfavorable degradation of $CH_3CH_2COO^-$, thereby increasing the overall CH_4 production rate. This would be in alignment with previous bioaugmentation studies using *Syntrophomonas zehnderi* to increase CH_4 production (Cavaleiro et al., 2010).

Spearman's rank correlation coefficient correlated SMA with both resilience (>90%) and M/F ratio (99.5%), a parameter used to quantify resistance to overload. Collectively, these correlations included both CH_4 production rate as well as functional stability during overload, compared to quantifying either methanogen activity or response to perturbation as done elsewhere (e.g., Hashsham et al., 2000; Lerm et al., 2012 or Sorensen and AHring, 1993; Shen and Guiot, 1996; Werner et al., 2011). Particular to this study, biomass 1 was identified as the best functional culture because it had the highest SMA and resilience coefficient as well as the second greatest capacity and M/F ratio.

In biomass samples with a lower SMA than that of the $CH_3CH_2COO^-$ enrichment, bioaugmentation was expected to increase the SMA, and that was consistent with the results found. The anaerobic biomass samples with the five lowest SMA values all had statistically

higher SMA values after bioaugmentation. However, even in biomass samples that had a higher SMA with $CH_3CH_2COO^-$ than the $CH_3CH_2COO^-$ enrichment, adding a culture with a lower activity still increased the activity of the biomass. For example, anaerobic biomass 1 had the highest SMA; yet, addition of the $CH_3CH_2COO^-$ enrichment, which had a SMA that was more than 50% less, still statistically increased the SMA in the bioaugmented culture. While the mechanism for this was not elucidated, a few can be excluded. For example, rate limitations caused by micronutrient deficiencies were not a factor since all samples were centrifuged and re-suspended in a basal nutrient medium (Schauer-Gimenez et al., 2010). Principal component analysis (Figures 4-7 and 4-9) and cluster analysis (Figures 4-8, 4-10 and 4-11) for the nine anaerobic biomass samples, nine bioaugmented cultures, and $CH_3CH_2COO^-$ enrichment depicted that differences in the methanogen community structure may have played a key role. Phenomena like quorum sensing or deficiency of a cofactor could also be a possible cause for this unexpected finding.

One possible difference present in the methanogen community structures may have been linked to H_2 utilization, which is linked to $CH_3CH_2COO^-$ degradation. Given that the culture used to bioaugment was enriched for $CH_3CH_2COO^-$ by feeding $Ca(CH_3CH_2COO^-)_2$, its maximum rate of $CH_3CH_2COO^-$ degradation to acetate and H_2 may have been faster compared to this rate in anaerobic biomass 1. In contrast, the H_2 utilization rate may have been higher in anaerobic biomass 1 than in the $CH_3CH_2COO^-$ enrichment. Therefore, mixing these two cultures could have led to both high rates of $CH_3CH_2COO^-$ degradation via microorganisms from the $CH_3CH_2COO^-$ enrichment as well as high H_2 utilization rates via microbes from digester biomass 1. The fact that biomass 1 had a higher M/F ratio than all biomass samples except biomass 2 might also suggest a high H_2 utilization rate in biomass 1, which would give merit to the aforementioned possibility of synergistic effects.

Biomass samples 7, 8, and 9 all ranked higher in M/F than SMA and, like biomass 1, exhibited statistically increased SMA values upon bioaugmentation. Hence, this synergism may have played a role in improving function.

Greater methanogen community evenness may increase the stability of a digester (i.e., increase resistance and resilience upon organic overload). The relationship between the microbial community structure and digester function must be further elucidated, including identification of the most beneficial and detrimental microbes present. Further investigation that analyzes microbial community structure initially upon bioaugmentation, as done herein, as well as at various time intervals after bioaugmentation (i.e., every SRT) will help determine how the added culture persists.

4.5 Conclusions

Bioaugmentation increased the SMA in six of nine diverse biomass samples, including some that had a greater SMA than the SMA of the $CH_3CH_2COO^-$ enrichment. In all nine cultures, the SMA increased upon bioaugmentation (2 to 57%). Bioaugmentation functioned as a partial re-seeding of the digester, adding organisms needed for more efficient $CH_3CH_2COO^-$ degradation, especially acidogens. Activity was characterized both in terms of specific methanogenic activity (SMA) and overload response. As PCA and cluster analysis suggested, Spearman's Rank Correlation Coefficient and linear regression confirmed that methanogen community structure impacted digester function upon bioaugmentation since there was a correlation among the increase in SMA with $CH_3CH_2COO^-$ and the difference in methanogen community structure in the $CH_3CH_2COO^-$ enrichment and the biomass sample that was bioaugmented ($r_s = 0.770$, which was >98% correlation, two-tailed; $R^2 = 0.059$).

4.6 Supplementary Material

4.6.1 Appendix A: Anaerobic Biomass Samples

Table 4-9. Anaerobic Biomass Sample Characteristics. All metals are in μg/L.

a)	TS (g/L	VS (g/L	NH_3-N (mg/L	TKN (mg/L	$N_{organic}$ (mg/L	PO_4 (mg/L) Total	Sol.
1	12.6	7.33	129	539	410	235	62.0
2	29.4	24.5	29.4	176	147	79.0	66.0
3	20.1	10.9	980	1680	700	240	21.0
4	47.9	42.3	221	4720	4490	134	50.0
5	11.8	8.80	1260	2820	1560	702	82.0
6	31.1	24.9	16.8	2210	2190	7.00	5.50
7	15.6	8.78	680	1320	640	342	85.0
8	45.1	40.3	197	3920	3723	264	58.0
9	22.3	13.7	174	1441	1267	854	71.0

b)	Cadmium		Chromium		Cobalt		Copper	
	Total	Sol.	Total	Sol.	Total	Sol.	Total	Sol.
1	1	0	20	ND	7	5	73	41
2	ND	ND	ND	ND	12	5	ND	ND
3	5	2	125	39	209	167	958	362
4	4	0	117	3	1270	42	1919	ND
5	6	7	177	143	6540	5890	1410	1230
6	2	0	285	12	1760	106	2840	82
7	2	2	52	15	72	147	496	218
8	2	ND	40	ND	22	5	498	29
9	0	ND	57	ND	5	7	22	ND

c)	Lead		Nickel		Zinc		Manganese	
	Total	Sol.	Total	Sol.	Total	Sol.	Total	Sol.
1	12.2	12	17.9	3.5	156	ND	79.3	4.3
2	-0.18	ND	6.1	3.5	ND	ND	27.8	25.2
3	194	103	640	182	4520	3650	2200	104
4	45.4	4.00	2730	71.4	7870	177	124	17.7
5	148	72.8	681	647	4090	3380	942	906
6	87.6	7.9	7680	53.5	8740	14.3	877	18.3
7	89.8	52.8	702	74.8	2790	2070	2680	72.0
8	53.0	4.4	108	24.4	6237	34.4	316	55.3
9	3.3	ND	39.5	1.9	650	ND	559	4.9

d)	Arsenic		Selenium		Silver		Molybdenum	
	Total	Sol.	Total	Sol.	Total	Sol.	Total	Sol.
1	1.4	0.26	1.47	ND	0.55	ND	5.1	0.38
2	ND	ND	7.4	9.1	ND	ND	3.9	0.72
3	15.2	0.68	153	107	96.6	70.2	16.8	7.8
4	17.9	0.05	20.6	10.6	ND	ND	296	7.1
5	1.9	ND	600	460	183	40.2	735	641
6	5.9	0.13	2.79	ND	2.79	ND	302	25.5
7	7.4	1.62	160	83.6	61.2	38.8	10.6	1.2
8	14.4	0.09	17	ND	17.0	ND	55.3	2.71
9	2.9	ND	5.9	11.4	ND	ND	14.0	0.07

e)	Mercury		Beryllium		Iron		Calcium	
	Total	Sol.	Total	Sol.	Total	Sol.	Total	Sol.
1	28.9	18.7	0.76	1.2	87.8	0.9	34.9	3.1
2	ND	ND	ND	ND	0.86	0.1	10.1	4.6
3	14.8	11.6	ND	ND	1506	21.6	85.6	69.6
4	ND	ND	ND	0.7	100	2.6	18.6	7.1
5	ND	ND	ND	ND	31.4	24.7	56.2	49.9
6	81.5	53.0	1.4	1.8	1830	8.8	20	4.3
7	8.8	7.4	ND	ND	262	5.2	84.4	48.8
8	13.7	10.7	0.4	1.4	385	9.6	37.2	10.1
9	ND	ND	0.18	ND	73.8	0.2	266	13.5

f)	Sodium		Potassium		Magnesium	
	Total	Sol.	Total	Sol.	Total	Sol.
1	156	150	15.6	13.1	5.5	2.9
2	85.7	85.1	5.1	5.00	17	17.4
3	156	113	54.6	39.2	13.6	7.6
4	64.8	57.9	56.2	26	11.6	3.8
5	56.3	54.8	46.5	44.6	12	10.9
6	45.4	36.3	14.7	2.1	5.1	1.1
7	43.6	46	24.2	23.6	14.6	5.1
8	43	37	35.6	11.8	16.3	5.1
9	115	110	27.4	22.3	9.00	3.1

4.7 REFERENCES

Abeysinghe, D. H., De Silva, D. G. V., Stahl, D. A., & Rittmann, B. E. (2002). The effectiveness of bioaugmentation in nitrifying systems stressed by a washout condition and cold temperature. *Water Environment Research*, *74*(2), 187-99. Retrieved from http://www.ncbi.nlm.nih.gov/pubmed/12043976

Angelidaki, I., Alves, M., Bolzonella, D., Borzacconi, L., Campos, L., Guwy, A., Jenicek, P., Kalyuzhnui, S., and Van Lier, J. (2007) *Anaerobic Biodegradation, Activity and Inhibition (ABAI) Task Group Meeting Report.* Prague, Czech Republic. October 9-10, 2006.

Angenent, L. T., Zheng, D., Sung, S., & Raskin, L. (2002). Microbial community structure and activity in a compartmentalized, anaerobic bioreactor. *Water Environment Research*, *74*(5), 450-61. Retrieved from http://www.ncbi.nlm.nih.gov/pubmed/12469949

American Public Health Association (APHA), American Water Works Association (AWWA), Water Environment Federation (WEF) (1998) Standard Methods for the Examination of Water and Wastewater (20th ed.). APHA et al.

American Public Health Association (APHA), American Water Works Association (AWWA), Water Environment Federation (WEF) (1998) Standard Methods for the Examination of Water and Wastewater (21st ed.). APHA et al.

Bidle, K.A., Kastner, M., and Bartlett, D.H. (1999) "A Plylogenetic Analysis of Microbial Communities Associated With Methane Hydrate Containing Marine Fluids and Sediments in the Cascadia Margin (ODP site 829B)." *FMES Microbiology Letters*. 177.1:101-108.

Bocher, B., and Zitomer, D. H., Staged Anaerobic Digestion as a Means to Increase Specific Methanogenic Activity, in proceedings of International Water Association (IWA) 12th. World Congress on Anaerobic Digestion, Guadalajara, Mexico, October 31 – November 4, 2010, 5.

Briones, A. and L. Raskin (2003), "Diversity and dynamics of microbial communities in engineered environments and their implications for process stability," *Current Opinion in Biotechnology*, 14 (3), 270-276.

Bustin, S. a, Benes, V., Garson, J. a, Hellemans, J., Huggett, J., Kubista, M., Mueller, R., et al. (2009). The MIQE guidelines: minimum information for publication of quantitative real-time PCR experiments. *Clinical Chemistry*, *55*(4), 611-22. doi:10.1373/clinchem.2008.112797

Cairns, J. E., Whalen, P. A., Whalen, P. J., Tracey, D. R., Palo, R. E., Street, K., & Tower, K. (2005). Dissolved ATP – A New Process Control Parameter for Biological Wastewater Treatment. *WEFTEC, Washington D.C., U.S.A.*

Cavaleiro, a J., Sousa, D. Z., & Alves, M. M. (2010). Methane production from oleate: assessing the bioaugmentation potential of Syntrophomonas zehnderi. *Water Research*, *44*(17), 4940-7. Elsevier Ltd. doi:10.1016/j.watres.2010.07.039

Deflaun, M.F., Steffan, R.J., (2002). Bioaugmentation. In: Bitton, G. (Ed.), Encyclopedia of Environmental Microbiology, vol. 1. Wiley-Interscience, New York, NY, pp. 434-442.

Dogan, T., Ince, O., Oz, N., & Ince, B. (2005). Inhibition of Volatile Fatty Acid Production in Granular Sludge from a UASB Reactor. *Journal of Environmental Science and Health, Part A: Toxic/Hazardous Substances & Environmental Engineering*, *40*(3), 633-644. doi:10.1081/ESE-200046616

Fernandez, A. S., Hashsham, S. A., Dollhopf, S. L., Raskin, L., Glagoleva, O., Dazzo, F. B., Hickey, R. F., et al. (2000). Flexible Community Structure Correlates with Stable Community Function in Methanogenic Bioreactor Communities Perturbed by Glucose. *Applied and Environmental Microbiology*, *66*(9), 4058-4067. doi:10.1128/AEM.66.9.4058-4067.2000.Updated

Freitag, T. E., & Prosser, J. I. (2009). Correlation of methane production and functional gene transcriptional activity in a peat soil. *Applied and Environmental Microbiology*, *75*(21), 6679-87. doi:10.1128/AEM.01021-09

Freitag, T. E., Toet, S., Ineson, P., & Prosser, J. I. (2010). Links between methane flux and transcriptional activities of methanogens and methane oxidizers in a blanket peat bog. *FEMS Microbiology Ecology*, *73*(1), 157-65. doi:10.1111/j.1574-6941.2010.00871.x

Galand, P. E., Saarnio, S., Fritze, H., & Yrjälä, K. (2002). Depth related diversity of methanogen Archaea in Finnish oligotrophic fen. *FEMS Microbiology Ecology*, *42*(3), 441-9. doi:10.1111/j.1574-6941.2002.tb01033.x

Goffredi, S. K., Wilpiszeski, R., Lee, R., & Orphan, V. J. (2008). Temporal evolution of methane cycling and phylogenetic diversity of archaea in sediments from a deep-sea whale-fall in Monterey Canyon, California. *The ISME Journal*, *2*(2), 204-20. doi:10.1038/ismej.2007.103

Hartwell, L.H., Hood L., Goldberg, M.L., Reynolds, A.E., Silver, L.M., and Veres, R.C. (2004) *Genetics: From Genes to Genomes*. 2nd ed. McGraw-Hill Companies, Inc. New York, NY.

Hashsham, S. A., Fernandez, A. S., Dollhopf, S. L., Dazzo, F. B., Hickey, R. F., Tiedje, J. M., & Criddle, C. S. (2000). Parallel processing of substrate correlates with greater functional stability in methanogenic bioreactor communities perturbed by glucose. *Applied and Environmental Microbiology*, *66*(9), 4050-7. Retrieved from http://www.pubmedcentral.nih.gov/articlerender.fcgi?artid=92258&tool=pmcentrez&rendertype=abstract

Kida, K., Morimura, S., & Sonoda, Y. (1993). Accumulation of Propionic Acid during Anaerobic Treatment of Distillery Wastewater from Barley-Shochu Making. *Journal of Fermentation and Bioengineering*, *75*(3), 213-216.

Lerm, S., Kleyböcker, A., Miethling-Graff, R., Alawi, M., Kasina, M., Liebrich, M., & Würdemann, H. (2012). Archaeal community composition affects the function of anaerobic co-digesters in response to organic overload. *Waste Management*, *32*(3), 389-99. Elsevier Ltd. doi:10.1016/j.wasman.2011.11.013

Lettinga, G. (2005). The anaerobic treatment approach towards a more sustainable and robust environmental protection. *Water Science and Technology*, *52*(1-2), 1-11. Retrieved from http://www.ncbi.nlm.nih.gov/pubmed/16180404

Lueders, T., Chin, K.-J., Conrad, R., & Friedrich, M. (2001). Molecular analyses of methyl-coenzyme M reductase alpha-subunit (mcrA) genes in rice field soil and enrichment cultures reveal the methanogenic phenotype of a novel archaeal lineage. *Environmental Microbiology*, *3*(3), 194-204.

Luton, P. E., Wayne, J. M., Sharp, R. J., & Riley, P. W. (2002). The mcrA gene as an alternative to 16S rRNA in the phylogenetic analysis of methanogen populations in landfill. *Microbiology*, *148*, 3521-30. Retrieved from http://www.ncbi.nlm.nih.gov/pubmed/12427943

Ma, J., Carballa, M., Van De Caveye, P., & Verstraete, W. (2009). Enhanced propionic acid degradation (EPAD) system: proof of principle and feasibility. *Water Research*, *43*(13), 3239-48. Elsevier Ltd. doi:10.1016/j.watres.2009.04.046

Madigan, M.T. and Martinko, J.M. (2009) *Brock Biology of Microorganisms*. 12th ed. Pearson Prentice Hall, Pearson Education, Inc. San Francisco, CA.

Marzorati, M., Wittebolle, L., Boon, N., Daffonchio, D., & Verstraete, W. (2008). How to get more out of molecular fingerprints: practical tools for microbial ecology. *Environmental Microbiology*, *10*(6), 1571-1581. Elsevier B.V. Retrieved from http://www.ncbi.nlm.nih.gov/pubmed/18331337

McCarty, P.L. and Smith, D.P. (1986) Anaerobic Wastewater Treatment. *Environmental Science and Technology*. 20.12: 1200-1206.

McInerney, M. J., Sieber, J. R., & Gunsalus, R. P. (2009). Syntrophy in anaerobic global carbon cycles. *Current Opinion in Biotechnology*, *20*(6), 623-32. doi:10.1016/j.copbio.2009.10.001

Mertens, B., Boon, N., and Verstraete, W. (2005). Stereospecific effect of hexachlorocyclohexane on activity and structure of soil methanotrophic communities. *Environmental Microbiology*, *7*, 660-669. doi:10.1111/j.1462-2920.2004.00735.x

Morris, R. (2011). *Relating Methanogen Community Structure to Function in Anaerobic Wastewater Digesters*. Ph.D. Thesis. Biology: Marquette University, Milwaukee, WI.

Navaratnam, N. (2012). *Anaerobic co-digestion for enhanced renewable energy and green house gas emission reduction*, Ph.D. Thesis, Civil, Construction, and Environmental Engineering. Marquette University, Milwaukee.

Nyer, E. K. and Bourgeois, H. J., Jr. (1980) "Operational Troubleshooting in Industrial Biological Treatment Systems." Proceedings of the 35th Industrial Waste Conference. (pp. 849-854). West Lafayette, Indiana: Purdue University

Ohkuma, M., Noda, S., Horikoshi, K., & Kudo, T. (1995). Phylogeny of symbiotic methanogens in the gut of the termite Reticulitermes speratus. *FEMS Microbiology Letters*, *134*(1), 45-50. Retrieved from http://www.ncbi.nlm.nih.gov/pubmed/8593954

Perle, M., Kimchie, S., & Shelef, G. (1995). Some Biochemical Aspects of the Anaerobic Degradation of Dairy Wastewater. *Water Research*, *29*(6), 1549-1554.

Quirk T. and Eckenfelder, W.W. (1986). Active biomass in activated sludge analysis and design. *Journal of Water Pollution Control Federation* 58 (9), 932.

Rastogi, G., Ranade, D. R., Yeole, T. Y., Patole, M. S., & Shouche, Y. S. (2008). Investigation of methanogen population structure in biogas reactor by molecular characterization of methyl-coenzyme M reductase A (mcrA) genes. *Bioresource Technology*, *99*(13), 5317-26. doi:10.1016/j.biortech.2007.11.024

Rittmann, B.E., Whiteman, R., 1994. Bioaugmentation: a coming of age. Water Quality International 1, 12e16.

Roe, P.C. and Bhagat, S.K. (1982). Adenosine Triphosphate as a Control Parameter for Activated Sludge Processes *Journal of the Water Pollution Control Federation* 54(3), 244-254 Water Environment Federation http://www.jstor.org/stable/25041280

Sambrook, J. and Russell, D.W., 2001. Molecular Cloning: A Laboratory Manual, 3rd ed. Cold Spring Harbor Laboratory Press, Cold Spring Harbor, NY.

Schauer-Gimenez, A. E., Zitomer, D. H., Maki, J. S., & Struble, C. A. (2010). Bioaugmentation for improved recovery of anaerobic digesters after toxicant exposure. *Water Research*, *44*(12), 3555-64. Elsevier Ltd. doi:10.1016/j.watres.2010.03.037

Shen, C. F., & Guiot, S. R. (1996). Long-term impact of dissolved O(2) on the activity of anaerobic granules. *Biotechnology and Bioengineering*, *49*(6), 611-620. Retrieved from http://www.ncbi.nlm.nih.gov/pubmed/18626856

Smith, D.P., and McCarty, P.L. (1990) Factors Governing Methane Fluctuations Following Shock Loading of Digesters. *Research Journal of the Water Pollution Control Federation*. 62.1: 58-64.

Smith, C. J., & Osborn, a M. (2009). Advantages and limitations of quantitative PCR (Q-PCR)-based approaches in microbial ecology. *FEMS Microbiology Ecology*, *67*(1), 6-20. doi:10.1111/j.1574-6941.2008.00629.x

Smith, C. J., Nedwell, D. B., Dong, L. F., & Osborn, M. (2006). Evaluation of quantitative polymerase chain reaction-based approaches for determining gene copy and gene transcript numbers in environmental samples. *Environmental Microbiology*, *8*(5), 804-15. doi:10.1111/j.1462-2920.2005.00963.x

Sorensen, A. H., & Ahring, B. K. (1993). Applied Biotechnology Measurements of the specific methanogenic activity of anaerobic digestor biomass. *Environmental Microbiology*, 427-431.

Spearman, C. (1904). The Proof and Measurement of Association between Two Things. *University of Illinois Press*, *15*(1), 72-101.

Speece, R. (2008) *Anaerobic Biotechnology and Odor/Corrosion Control for Municipalities and Industries*. Archae Press. Nashville, TN.

Stephenson, D. and Stephenson, T. (1992). Bioaugmentation for enhancing biological wastewater treatment. *Biotechnology Advances* 10, 549 - 559.

Switzenbaum, M., *Environmental Engineering Microbiology: Wastewater Treatment*, B. Bocher, Editor. 2010: Milwaukee, WI.

Tale, V. P., Maki, J. S., Struble, C. A., & Zitomer, D. H. (2011). Methanogen community structure-activity relationship and bioaugmentation of overloaded anaerobic digesters. *Water Research*, *45*(16), 5249-5256. Elsevier Ltd. doi:10.1016/j.watres.2011.07.035

Tale, V., *Bioaugmentation Can Improve Anaerobic Digester Performance After Organic Overload* in *International Water Association: 12th World Congress on Anaerobic Digestion*. 2010b: Guadalajara, Mexico.

Tale, V. (2010). *Bioaugmentation for Recovery of Anaerobic Digesters Subjected to Organic Overload*, in Ph.D. Thesis. Civil and Environmental Engineering. Marquette University: Milwaukee, WI.

Tale, V. P., Maki, J. S., Struble, C. A., & Zitomer, D. H. (2011). Methanogen community structure-activity relationship and bioaugmentation of overloaded anaerobic digesters. *Water Research*, *45*(16), 5249-5256. Elsevier Ltd. doi:10.1016/j.watres.2011.07.035

Thauer, R.K. (1998) Biochemistry of Methanogenesis: A Tribute to Marjory Stephenson. *Microbiology*. 144:2377-2406.

Vianna, M. E., Conrads, G., Gomes, B. P. F. A., & Horz, H. P. (2006). Identification and Quantification of Archaea Involved in Primary Endodontic Infections. *Journal of Clinical Microbiology*, *44*(4), 1274-1282. doi:10.1128/JCM.44.4.1274

Vogel, T. M. (1996). Bioaugmentation as a soil bioremediation approach. *Current Opinion in Biotechnology*, *7*(3), 311-6. Retrieved from http://www.ncbi.nlm.nih.gov/pubmed/8785436

Werner, J. J., Knights, D., Garcia, M. L., Scalfone, N. B., Smith, S., Yarasheski, K., Cummings, T. A., et al. (2011). Supporting Information. *Proceedings of the National Academy of Sciences of the United States of America*, *108*(10), 1-8.

Whalen, P. A., Whalen, P. J., & Tracey, D. R. (2006a). Cellular ATP - A Superior Measure of Active Biomass for Biological Wastewater Treatment Processes. *WEFTEC* (Vol. 4, pp. 3025-3037).

Whalen, P. A., Whalen, P. J., & Tracey, D. R. (2006b). Improving Biological Wastewater Treatment Process Control Through ATP-based Parameters. *WEFTEC* (pp. 5949-5965).

Wilms, R., Sass, H., Köpke, B., Cypionka, H., & Engelen, B. (2007). Methane and sulfate profiles within the subsurface of a tidal flat are reflected by the distribution of sulfate-reducing bacteria and methanogenic archaea. *FEMS Microbiology Ecology*, *59*(3), 611-21. doi:10.1111/j.1574-6941.2006.00225.x

Wittebolle, L., Marzorati, M., Clement, L., Balloi, A., Daffonchio, D., Heylen, K., De Vos, P., Verstraete, W., Boon, N. (2009). Initial community evenness favours functionality under selective stress. *Nature*, *458*(7238), 623-6. Nature Publishing Group. doi:10.1038/nature07840

Wittebolle, L., Vervaeren, H., Verstraete, W., and Boon, N. (2008) Quantifying community dynamics of nitrifiers in functionally stable reactors. *Applied and Environmental Microbiology* 74: 286–293.

Wittebolle, L., Marzorati, M., Clement, L., Balloi, A., Daffonchio, D., Heylen, K., De Vos, P., et al. (2009). Initial community evenness favours functionality under selective stress. *Nature*, *458*(7238), 623-6. Nature Publishing Group. doi:10.1038/nature07840

Wong, B.-T., Show, K. Y., Lee, D. J., & Lai, J. Y. (2009). Carbon balance of anaerobic granulation process: carbon credit. *Bioresource Technology*, *100*(5), 1734-9. Elsevier Ltd. doi:10.1016/j.biortech.2008.09.045

Zar, J. H. (1972). Significance Testing of the Spearman Rank Correlation Coefficient. *Journal of the American Statistical Association*, *67*(339), 578-580.

Zitomer, D. H., & Shrout, J. D. (1998). Feasibility and benefits of methanogenesis under oxygen-limited conditions. *Waste Management*, *18*, 107-116.

Zitomer, D. H., Johnson, C. C., & Speece, R. E. (2008). Metal Stimulation and Municipal Digester Thermophilic/Mesophilic Activity. *Journal of Environmental Engineering*, *134*(1), 42. doi:10.1061/(ASCE)0733-9372(2008)134:1(42)

5.0 RELATING METHANOGEN COMMUNITY STRUCTURE AND DIGESTER FUNCTION

5.1 Introduction

A growing emphasis exists among industries and municipalities to achieve sustainability goals (Holm-Nielsen et al., 2009) and to shift from wastewater treatment to resource recovery (Angenent et al., 2004; Novotny et al., 2010). This, combined with the economic benefits from renewable energy generation via anaerobic biotechnologies, is making anaerobic digestion increasingly attractive (Speece, 2008), thereby adding pressure to make technological advances that optimize methane production.

One challenge with the appropriation of anaerobic bioprocesses is that much remains unknown about the distinguishing factors between well and poorly performing digesters (Leitão et al., 2006). Although interdependent microbial populations accomplish the overall anaerobic degradation process (Batstone et al., 2002), the microbial community is almost always unaccounted for in design. Current wastewater treatment system engineering continues to rely on theories developed in the 1960s that consider biomass to be one independent population that is viewed as a "black box" (Downing et al., 1964; Knowles et al., 1965; Lawrence and McCarty, 1970). Röling et al. (2010) have pointed out a need to improve models of complex microbial communities via "extensive experimental validation by a number of methods…" One next step to improve design, then, is to deepen the understanding of the microbial community behind anaerobic digestion and how microbial community structure relates to process function, such as volatile solids destruction and methane generation (Curtis et al., 2003).

5.1.1 Past Studies of Microbial Community Structure and Function

Some studies have started to link biological function to microbial community structure. For example, improved trichloroethylene (TCE) degradation directly resulted from understanding the functional diversity of a microbial community and designing a (aerobic) bioreactor based on that knowledge of microbial community structure (Watanabe et al, 2002). Hashsham et al. (2000) showed that greater functional stability after glucose overload was exhibited by anaerobic digesters with greater parallel process pathways (i.e., multiple microorganisms performing the same function). They concluded that more species performing the same function (e.g., propionate degradation) increased the likelihood of continued, stable function. Fernandez et al. (2000) observed that less stable community structure enhanced functional stability since microbial cultures were able to adapt to stresses. Compared to continuously mixed conditions, pulsed loadings resulted in more propionate degrading organisms in digesters fed a mixture of organic fraction municipal solids waste, primary sludge, and waste activated sludge (McMahon et al., 2001). In a study of over 1000 different denitrifying communities, even communities (i.e., various microbial populations present in similar amounts) were more functionally resistant to a selective stress (e.g., salt toxicity) than uneven ones. Highly uneven communities (i.e., where one or a few species dominate) were less functionally stable (Wittebolle et al., 2009). The theory was that in highly even communities there was a higher probability that an organism (or a few organisms) resistant to the selective stress would be present in significant enough numbers to proliferate during and after the stress, whereas low evenness may result in an organism that is resistant to the stress, but present in too low of numbers to proliferate.

More research is necessary to establish a predictive link between microbial community structure and anaerobic digester function. Allison and Martiny (2008) stated that research should provide greater empirical knowledge of the relationship between microbial community structure and function, especially as it pertains to system perturbations. Thus, more empirical data, especially for perturbations and key steps like propionate degradation, are necessary to better understand the link between process function and microbial community structure. These data would allow anaerobic digesters, which are typically designed based on operational parameters such as organic loading rate and residence time, to be further improved by also designing based on microbial community structure.

5.1.2 Multiple Linear Regression (MLR) for Structure-Activity Relationships

Multiple linear regression (MLR) has been used to determine structure-activity relationships between chemical structure descriptors and biological or physiochemical activities, such as toxicity values or Henry's Constant values (Nirmalakhandan and Speece, 1988; Robinson et al., 2004; Freitag and Prosser, 2009; Undas et al., 2009). Tale et al. (2011) applied MLR to anaerobic digester data, finding similar specific methanogenic activity (SMA) values related to similar community structures, as defined by DGGE banding patterns of methyl coenzyme A (*mcrA*) amplicons. However, the microbial community data were overrepresented in a MLR model with ten independent variables (i.e., band intensities) that described 14 dependent variables (i.e., SMA values of individual biomass samples). Principal components analysis (PCA) depicted a relationship between microbial community structure defined by DGGE banding pattern and SMA value in that biomass with high SMA values clustered on a PCA plot developed using only DGGE banding patterns, whereas biomass with low SMA values clustered in a different location (Figure 5-1). Other researchers have

also demonstrated a correlation between densitometric data and SMA values (Navaratnam, 2012). Even though preliminary data suggest a relationship exists, an insufficient number of different biomass samples previously prevented determination of a predictive relationship between microbial community structure and digester function.

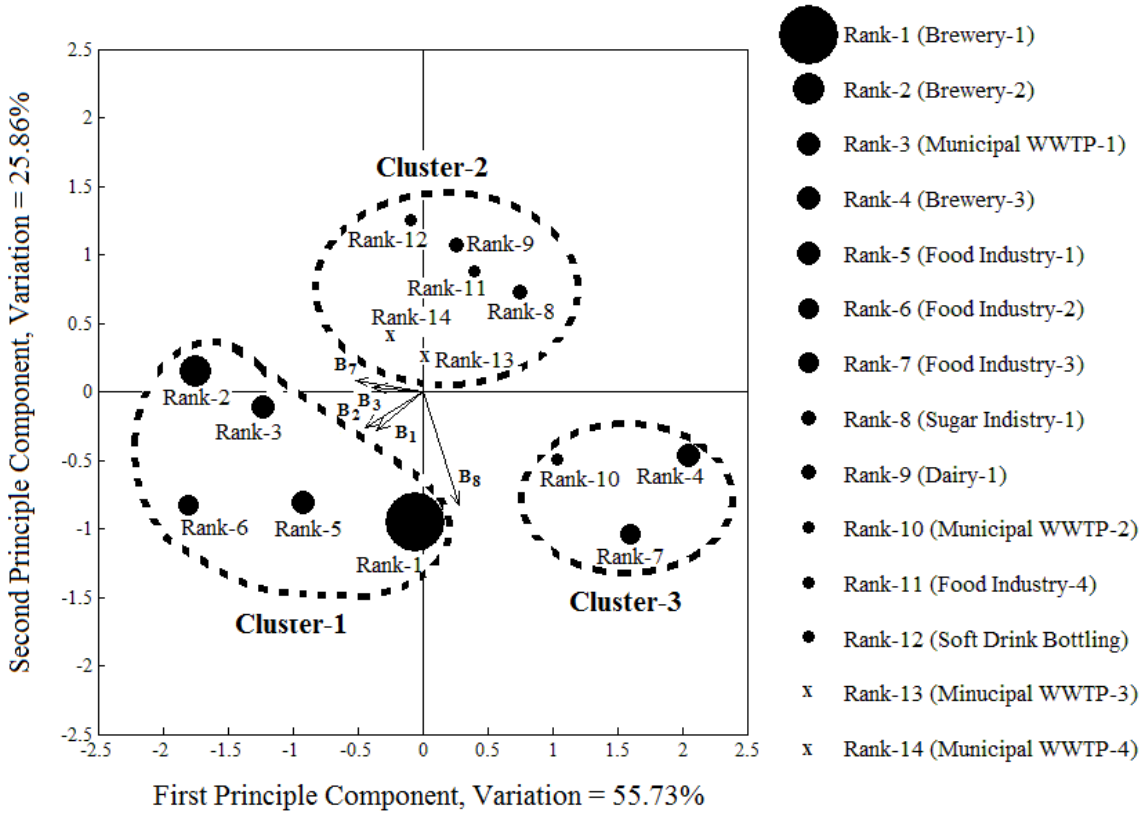

Figure 5-1. Principal Component analysis (PCA) using DGGE band intensities of methanogen community structures for 14 biomass samples. The diameter of each point is proportional to the SMA value. Vectors B1, B2, B3, B7, and B8 represent DGGE bands with the greatest influence on differences in methanogen community structure. Clones from bands B1 and B2 were most similar to *Methanospirillum hungatei* and *Methanobacterium beijingense*, respectively (Tale et al., 2011).

In this study, it was hypothesized that different anaerobic cultures would have different functional responses and result in different functional activities as well as exhibit different microbial community structures. Forty-nine anaerobic cultures were used to establish a quantitative structure-activity relationship (QSAR) between microbial community structure and biomass function.

5.2 Methods and Materials

Different microbial communities were examined: four propionate enrichments, nine anaerobic digester biomass samples, and the nine digester biomass samples mixed with each of the four propionate enrichments. Three fundamental tasks were performed: (1) develop and maintain four propionate enrichment cultures in triplicate and collect anaerobic biomass samples, (2) measure methanogenic activity and response to organic overload for all cultures, and (3) relate biomass function to microbial community structure.

5.2.1 Propionate Enrichments

Twelve propionate enrichment cultures with a working volume of 1 L were maintained for 317 days in 2-L, polyethylene terephthalate (PETE) plastic, anaerobic reactors that were continuously shaken on a shaker table housed in a temperature-controlled (35 ± 1°C) incubator (Model 4350, Thermo Scientific, Marietta, OH) (Table 5-1). In an effort to obtain a range of significantly different cultures, each propionate enrichment was fed a different O_2 dose, calculated to satisfy a portion of the added total chemical oxygen demand (TCOD) (Table 3-4). Enrichment conditions were maintained in triplicate to determine statistical differences in digester operation for each condition. Thus, enrichments that received 0, 1.3, 6.7, and 12.5% of the total chemical oxygen demand (TCOD) added as O_2 are referred to as 0%, 1.3%, 6.7%, and 12.5%, respectively, throughout this chapter. Up to 75 mL of O_2 (aviator's breathing grade; 99.9% purity; approximately 1 atm and 22°C) per L of liquid was added by injecting it directly into the bottle headspace with a wetted-barrel,

glass syringe immediately after being fed.[2] Propionate enrichment cultures 1 through 3, which received no O_2, served as controls.

Table 5-1. Propionate O_2 Additions

Propionate Enrichment Numbers	1,2, 3	4, 5, 6	7, 8, 9	10, 11, 12
Liquid O_2 Dose (mL O_2/L-d)	0	8	40	75
Headspace O_2 Dose (mg O_2/L-d)*	0	11	53	99
Percent of COD_{total} (%)	0.0	1.3	6.7	12.5

*O_2 concentration in headspace, based on dose at 22°C and 1 atm

Since seed cultures with diverse microbial communities have been shown to be functionally beneficial (Wittebolle, 2009), each of these 12 propionate enrichment cultures was seeded with a blend of eight biomass samples: two municipal, two brewery, one agricultural, one beverage industry, one food industry, and one pilot scale anaerobic digester (Table 5-2).

Table 5-2. Seed Biomass Used for Propionate Enrichment Cultures

Digester Type*	**Substrate**	**Industry/Municipality**	**Location**
CSTR	Non-Fat Dry Milk	Pilot-scale CSTR, Marquette University	Milwaukee, WI
CSTR	Municipal Solids	City of Waukesha, WI WWTP**	Waukesha, WI
CSTR	Municipal Solids	South Shore Water Reclamation Facility	Milwaukee, WI
CSTR	Municipal Solids	City of Brookfield, WI WWTP**	Brookfield, WI
CSTR	Food Additives	Kerry Ingredients & Flavours	Jackson, WI
UASB	Soft Drink Waste	Wis-Pak, Inc.	Watertown, WI
UASB	Brewery Waste	City Brewery Company, LLC	Brewery Waste
CSTR	Cattle Manure	Crave Brothers Farmstead, Inc.	Waterloo, WI

*CSTR - Completely mixed stirred tank reactor, UASB - Upflow anaerobic sludge blanket
**WWTP - wastewater treatment plant

Liquid effluent (100 mL) was removed once per day to maintain a solids residence time (SRT) and hydraulic retention time (HRT) of ten days. Effluent was replaced with 100

[2] Pure O_2, rather than air, was used in this study. The volume of O_2 in air (assuming 21%) needed to satisfy 12.5% of the influent TCOD (~280 mL air) and the resulting pressure would have been too great to perform daily lab procedures. Also, use of pure O_2 avoided the disadvantage of diluting biogas with N_2 in air. Some studies have yielded different results between air and pure O_2. For example, Stephenson, et al. (1999) added air without a significant change in methane production rate in a UASB reactor, whereas pure O_2 reduced methane production.

mL of aerated (to remove residual chlorine) tap water containing calcium propionate (0.77 ±0.03 g COD/L-day), 5 g/L $NaHCO_3$, and basal nutrient medium (Table 5-3). This feed led to a theoretical maximum of 1.5 g Ca^{+2}/L in the propionate enrichments, which is well below the 4.8 g Ca^{+2}/L that caused a 50% reduction in methane production (Switzenbaum, 2010).

Table 5-3. Basal Nutrient Medium Added Daily to Propionate Enrichment Cultures

Constituent	Concentration* (mg/L)
NH_4Cl	400
$MgSO_4$	250
KCl	400
$CaCl_2$	120
$(NH_4)_2HPO_4$	80
$FeCl_3.6H_2O$	55
$CoCl2.6H_2O$	10
KI	10
Metals**	0.5
Alkalinity ($NaHCO_3$)	5000

*Concentrations given as those present in the propionate enrichments
**The following metals were added together in solution (each at 0.5mg/L): $MnCl_2.4H_2O$, NH_4VO_3, $CuCl_2.2H_2O$, $Zn(C_2H_3O_2)_2.2H_2O$, $AlCl_3.6H_2O$, $NaMoO_4.2H_2O$, H_3BO_3, $NiCl_2.6H_2O$, $NaWO_4.2H_2O$ and Na_2SeO_3

5.2.2 Anaerobic Biomass Samples

Nine biomass samples were obtained from various anaerobic digesters treating diverse substrates in an effort to obtain different microbial communities (Table 5-4). As described below, the concentrations of chemical constituents in each biomass sample were measured to categorize environmental conditions under which the communities ostensibly developed.

Table 5-4. Anaerobic Biomass Samples

Sample Number	Digester Type*	Substrate	Location	Industry/Municipality
1	CSTR	Food Flavorings	Jackson, WI	Kerry Ingredients & Flavours
2	Anaerobic Plug Flow	Brewery Waste	Fort Collins, CO	New Belgium Brewery
3	CSTR	Municipal Wastewater Solids	Philadelphia, PA	City of Philadelphia WWTP**
4	UASB	Brewery Waste	Chico, CA	Sierra Nevada Brewery
5	CSTR	Non-Fat Dry Milk	Milwaukee, WI	Pilot-scale Digester
6	UASB	Soft Drink Bottling Waste	Watertown, WI	Wis-Pak, Inc.
7	CSTR	Municipal Wastewater Solids	Des Moines, IA	City of Des Moines WWTP**
8	UASB	Brewery Waste	LaCrosse, WI	City Brewery, LLC
9	CSTR	Cheese Processing Waste	Las Cruces, NM	F & A Dairy

* CSTR - Completely mixed stirred tank reactor, UASB - Upflow anaerobic sludge sludge blanket
**WWTP – Wastewater treatment plant

5.2.3 Quantification of Microbial Community Activity

Microbial community activity was quantified using organic overload perturbation activity (OOPA) assays with glucose and specific methanogenic activity (SMA) tests with propionate.

5.2.3.1 Mixing Microbial Cultures

Because part of this research sought to investigate the relationship between microbial activity and community structure, it was necessary to verify that mixed cultures yielded statistically different activity values. Furthermore, before different cultures could be mixed to provide a unique microbial community, it was determined if the two cultures provided a unique activity in a linear or non-linear relationship with mixing ratio. Hence, SMA tests were performed using a mix of biomass from two continuously mixed stirred tank reactors (CSTR) known to have different SMA values. Biomass from one digester was fed non-fat dry milk (biomass 1). A second digester containing biomass with a higher SMA was fed multiple wastes, basal nutrient medium, and 5 g/L $NaHCO_3$ (biomass 2) (Navaratnam, 2012).

5.2.3.2 Organic Overload Perturbation Assays (OOPA)

The purpose of the OOPA was to quantify the ability of an anaerobic culture to produce methane at elevated organic loading rates. Preliminary testing focused on developing a successful OOPA by finding an optimal glucose organic overloading rate and standard, active biomass concentration such that a distinct response could be observed.

Though glucose has been used elsewhere to monitor response to organic overload (Hashsham et al., 2000; Fernandez et al., 2000; McHugh et al., 2003; Karakashev et al., 2005; Dearman et al., 2006), the OOPA was a novel test so no optimal biomass or substrate (i.e., glucose) concentrations were initially known. Therefore, preliminary testing was performed to identify the biomass and substrate doses used in OOPA tests. In order to determine a standard, active biomass concentration, 57 bottles were set up at 19 food-to-microorganism (F:M) ratios (each in triplicate) varying from 0.2 to 33 g COD/g VSS (0.20, 0.62, 1.01, 1.41, 1.44, 1.99, 2.42, 3.10, 3.37, 4.4, 7.03, 10.3, 12.1, 14.2, 15.1, 17.3, 21.6, 23.4, 33.2). The following glucose concentrations were used [g glucose/L]: 1, 3, 7, 10, 12, and 15. Biomass concentrations were as follows [g VSS/L]: 0.1, 0.3, 0.7, 1, and 5. Each mixture was run in triplicate. The initial and final VSS measurements were averaged and used to calculate SMA values.

Because VS or VSS values are not accurate measures of active biomass, the active biomass concentration was measured using intracellular adenosine-5'-triphosphate (iATP) concentration, which was determined with a commercial ATP test kit (QuenchGone21^{TM} Wastewater, LuminUltra, Fredericton, New Brunswick, Canada). Additionally, in order to streamline testing, minimize bias, and maximize the comparability between the two activity parameters, both SMA and OOPA tests were conducted using the same biomass concentration.

For the OOPA test, microbial community samples were diluted to a standard active biomass concentration (0.74 mg iATP/L). A 25-mL sample of standard active biomass was placed in a 160-mL serum bottle, sparged with O_2-free gas (7:3 v/v N_2:CO_2), and allowed to produce biogas for three days, when it stopped producing biogas, to determine the endogenous biogas production. Excess gas was then removed on day three, and a one-time

dose of 5.2 g glucose/L (5.6 g COD/L) was added. This dose was within ranges used in other studies, such as 4 g COD/ L-d (Zitomer and Shrout, 1998) and 7.2 g COD/L (Hashsham et al., 2000). All OOPA tests were run in triplicate.

The first and second slopes on the biogas production versus time graph delineated CO_2 production via acidogenesis, which is known to occur quickly with a sugar substrate like glucose (Period 1), and methanogenic gas production (Period 2), respectively (Figure 5-2). The ratio of the respective slopes was defined as the methanogenesis-to-fermentation ratio (M/F). A third region of the curve with a slope of zero occurred after the consumption of all substrate (Period 3) (Figure 5-2). Biogas production was measured for 20 days. Biogas methane content was determined on day 20 using a gas chromatograph (GC), as described below.

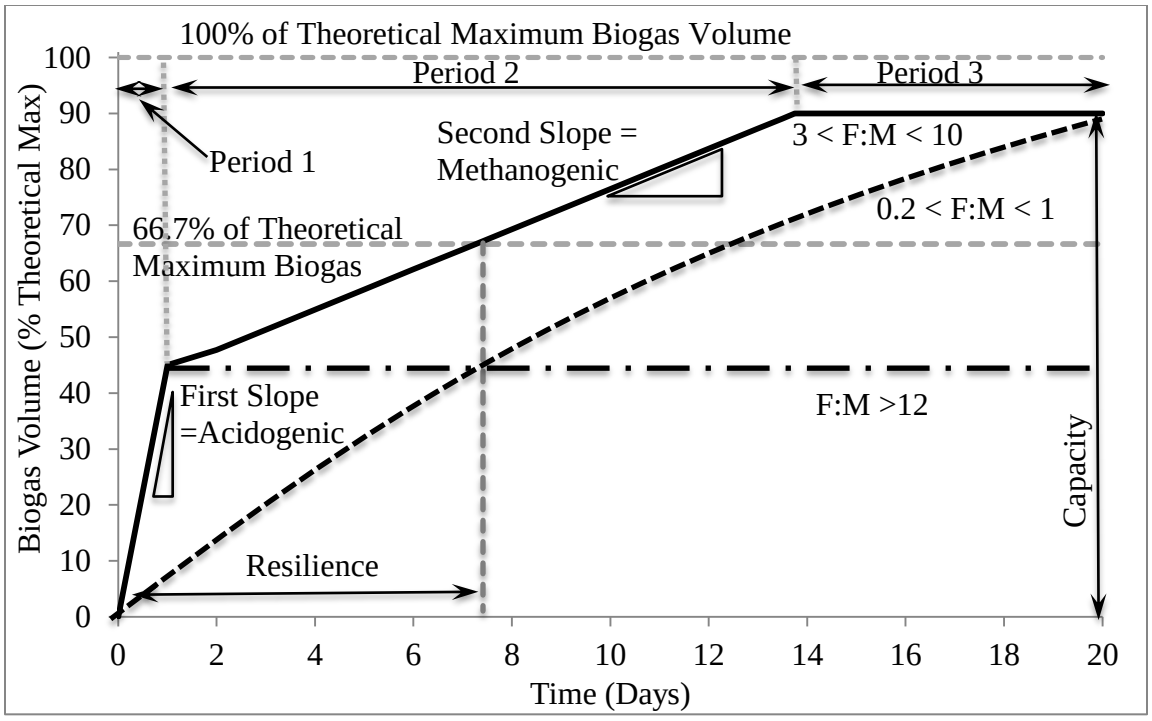

Figure 5-2. Theoretical OOPA graph shown to depict the parameters obtained via overload testing, including resilience, capacity, methanogenesis to fermentation (M/F) ratio (second slope divided by the first slope), and perturbed biogas yield (PBY, maximum biogas volume divided by 100% of theoretical maximum biogas volume). The parameters listed on this graph are for $3 \leq F:M \leq 10$, which is represented with a solid black line. The dashed black line represents $0.2 \leq F:M \leq 1$, and the alternating long dash/short dash represents $F:M \geq 12$.

Resilience was defined as the time required to reach two-thirds (66.7%) of the theoretical maximum biogas production (Figure 5-2). For example, 1 g COD/L (added as glucose) would yield 800 mL of biogas at 35°C, assuming 50/50 CH_4/CO_2 (v/v) in the biogas (for carbohydrates); thus, the resilience was the number of hours it took to produce 533 mL of biogas. A resilience coefficient was calculated by taking the inverse of resilience and multiplying that by 100. Not all samples reached 100%, and some make significantly less biogas, making even 75% of the theoretical maximum less suitable than 66.7%. Also, 50% of the biogas from carbohydrate breakdown is theoretically CO_2, produced quickly upon the addition of glucose from fermentation; thus, the percentage chosen had to exceed 50% of the theoretical maximum. Therefore, resilience was measured at 66.7%.

Another parameter, capacity, characterized both resistance and resilience by identifying the cumulative amount of biogas production after 20 days. For example, a biomass that is less able to handle organic overload would consume less of the total substrate added due to greater inhibition, thereby, producing proportionally less of the theoretical maximum biogas. The cumulative biogas volume produced after 20 days was divided by the total theoretical maximum volume expected based on the glucose added. This quotient was the 20-day perturbed biogas yield (PBY). M/F ratio, resilience, capacity, and PBY were determined in triplicate for all 49 samples.

5.2.3.3 Specific Methanogenic Activity (SMA) Tests

Specific methanogenic activity tests were conducted to determine the maximum rate that a microbial culture generated methane when fed propionate. Propionate was chosen because its degradation has been shown often to be the rate-limiting step in the overall anaerobic degradation process, controlling the rate of methane production from many

substrates (Kida et al., 1993; McInerney et al., 2009; Wong et al., 2009). A modified approach to a standard SMA protocol outlined by Andelicki et al. (2007) was implemented. Biomass samples were thickened at 6000 rpm (g = 7000) for five minutes in a centrifuge (Clinical 200, VWR International, Radnor, Pennsylvania Germany). Before mixing, granular samples were disrupted to make the biomass flocculant. This allowed a consistent comparison of activity among granular and flocculant biomass samples. Each mixed sample consisted of 80% of one of the nine biomass samples and 20% of a propionate enrichment based on iATP concentration. Previous work has shown SMA tests with propionate yield precise results at various biomass concentrations, including: 2 g VSS/L or less as well as at 5.0 to 6.0 g VS/L, which typically fall within the range observed herein. Biomass samples were resuspended in DI water that included basal nutrient medium (Table 5-3) to achieve an active biomass concentration of 0.74 mg iATP/L. A 25-mL sample of the active biomass was placed in a 160-mL serum bottle, sparged with O_2-free gas (3:7 v/v mix of CO_2 and N_2), sealed with solid black butyl rubber stoppers, and allowed to produce biogas for three days to determine endogenous biogas production. Excess biogas was removed on day three to depressurize the headspace, and the sample was then given a non-limiting dose (3 g/L) of calcium propionate ($Ca(C_2H_5COO)_2$) (4.6 g COD/L). This substrate concentration has been used elsewhere (Speece, 2008; Zitomer, 2008), is non-toxic to anaerobic microorganisms, and is well above the Monod half-saturation constant values. All 49 samples were run in triplicate at 35±1°C and 150 rpm using a gyratory shaker-incubator (model C25KC, New Brunswick Scientific, Edison, NJ). An additional bottle contained no exogenous substrate and was used to account for endogenous methane production.

The biogas volume produced was measured at ambient pressure and 35°C for 20 days via a displacement method using a glass syringe with a wetted, glass barrel

(Perfektum®, Popper & Sons, Inc., New Hyde Park, NY). Methane content was measured after 20 days by gas chromatography (GC). Graphs of cumulative biogas production versus time were plotted and the SMA values (mL CH_4/mg iATP-h) were calculated using linear regression on the portion of the curve within the first 60 hours of biogas production with the steepest slope. This initial maximum slope was used because the biomass samples used for molecular analyses were taken on the day the assays were set up. Thus, the use of initial slopes ensured that the SMA values measured were as representative as possible of the microbial community structure that was analyzed and not the community that developed in the SMA bottle after feeding. The average and standard deviation of SMA values were calculated for each sample to yield the average maximum rate of methane production. Average SMA values with propionate have been shown to vary over two orders of magnitude among biomass samples from different anaerobic digesters (Tale, 2010).

5.2.4 Microbial Community Analysis

5.2.4.1 DNA Extraction

DNA was extracted from the biomass that was collected when SMA and OOPA testing was performed. Each 50-mL sample was thickened in a centrifuge (AccuSpin Micro 17, Thermo Fischer Scientific, Waltham, MA) for 10 min at 2500 x g. Then DNA was extracted from 0.75 mL of thickened biomassed using the DNA Elution Accessory kit with the RNA Powersoil™ Total RNA Isolation Kit (MoBio Laboratories, Carlsbad, CA) according to the manufacturer's instructions. The presence of extracted DNA was confirmed with gel electrophoresis (1% agarose in 1X Tris-Acetate-EDTA, TAE) using ethidium bromide (0.8 μL/mL) stain (Sambrook and Russell, 2001). Prepared gel solution was poured into a gel box and allowed to solidify. A mixture of 3 μL of 6X blue-orange

loading dye and 10 μL of DNA was injected into the wells (Hartwell et al., 2004). A λϕ (HindIII, HaeIII) ladder was placed into one of the wells as a marker. This marker had 40 ng/μL Lambda (λ) DNA, HindIII cut and 30 ng/μL phi (ϕ) X174 DNA, HaeIII cut. A 100-millivolt (mV) potential was maintained across the gel for 60 to 90 minutes. This potential caused the DNA to migrate across the gel, which was then illuminated and photographed under ultraviolet light using an imaging system (GDS-8000 Bioimaging System, UVP Inc., Upland, CA). DNA samples were stored at -80°C until further analysis.

5.2.4.2 Polymerase Chain Reaction (PCR)

Extracted DNA was amplified using polymerase chain reaction (PCR) with primers for the methyl coenzyme M reductase (*mcrA*) gene of methanogenic *Archaea* designed by Luton et al. (2002). These are: mcrA1f: 5'-GGTGGTGTMGGATCACACARTAYGCWACAGC -3', (mcrF); GCmcrA1f: 5'- *GC-clamp-GGTGGTGTMGGA TTCACACARTAYGCWACAGC -3', (mcrA1f), where GC-clamp = 5' – CGCCCGCCGCGCCCCGCGCCCGTGCCGCCGCCCCCGCCCG – 3', (GC-clamp); mcrA500r: 5' – TTCATTGCRTAGTTWGGRTAGTT – 3', (mcrR). The primer product was an approximately 460-bp-long segment of *mcrA*, which codes for the α subunit of methyl coenzyme M reductase (Luton et al., 2002). Since it is a functional gene that is specific to and ubiquitous in methanogens (Thauer, 1998), the *mcrA* gene has been used to compare methanogen community structure and identify the taxonomically distinct methanogens present. Furthermore, numerous studies have exploited the ubiquity of the *mcrA* gene in all known methanogens to find them in various locations, including marine environments (Bidle, 1999; Wilms, 2007), termite guts (Ohkuma, 1995), rice paddies

(Lueders, 2001), oligotrophic fen (Galand et al., 2002), and anaerobic digesters (Rastogi, 2008; Tale, 2011).

PCR was performed using EconoTaq® PLUS 2X Master Mix, which included the Taq polymerase (Lucigen Corporation, Middleton, WI). Forward and reverse primers were added to the PCR tube with nuclease-free H_2O to make a 100-µL reaction. Nested PCR was performed on the extracted DNA by first amplifying for mcrA1f and mcrA500r primers in the following program: 95°C for 5 min; then six cycles of 95°C for 1 min, 49°C for 1 min, 72°C for 3 min; next 30 cycles of 95°C for 1 min, 49°C for 1 min, 72°C for 3 min; then 95°C for 1 min, 49°C for 1 min, 72°C for 10 min; and then 4°C. Presence of amplified *mcrA* was verified via agarose gel, as described, and then a second cycle was employed to re-amplify with GCmcrA1f (GC clamp) and mcrA500r primers in the following program: 95°C for 5 min; then six cycles of 95°C for 1 min, 58°C for 1 min, 72°C for 3 min; next 36 cycles of 95°C for 1 min, 58°C for 1 min, 72°C for 3 min; then 95°C for 1 min, 58°C for 1 min, 72°C for 10 min; and then 4°C. The program included a slow ramp in temperature ($0.1°Cs^{-1}$) between the annealing and extension steps of the first five cycles of the protocol to aid in the initial formation of product due to the degenerate nature of the primers, as recommended (Luton et al, 2002). PCR was done on a thermocycler (PTC-200 DNA Engine Cycler, Bio-Rad, Foster City, CA).

5.2.4.3 Denaturing Gradient Gel Electrophoresis (DGGE)

Each microbial community was fingerprinted using denaturing gradient gel electrophoresis (DGGE), which separated amplified genes into bands on a polyacrylamide gel. DGGE has been used with *mcrA* as a target gene (e.g., Galand, 2002; Wilms et al., 2007;

Morris, 2011; Tale et al., 2011). The denaturant concentration used for DGGE varied linearly over 75 mm and ranged from 40% at the top of the gel to 70% at the bottom of the gel (expressed as v/v of the total gel volume). A detection system (BioRad Universal DCode Mutation Detection System, Richmond, CA) was used to run the DGGE gels. DGGE was performed on 1-mm-thick 8% polyacrylamide gel following the manufacturer's protocol. Approximately, 300 ng of DNA product was added to each lane of the polyacrylamide gel with 2X blue loading dye. An electric potential of 100 V was maintained across the gel for 12 hours. A 1% SYBR® gold dye solution (Invitrogen, CA USA) was used to stain the gel. After immersing the gel in the staining solution and rotating it for 30 minutes on a shaker table at a speed sufficient to mix the dye solution, it was viewed under ultraviolet light using an imaging system (GDS-8000 Bioimaging System, UVP Inc., Upland, CA). Densitometric data were obtained using gel viewing software (Lab Works v. 4.6.00.0 Lablogics, Inc., Mission Viejo, CA) with a minimum band height of 0.050, allowed error of ±5%, ten largest bands retained, and the following options activated: dark bands and bright background, rows of equal molecular weight, maximum OD level for the image, and center peak.

Multiple DGGE gels were prepared to accommodate all 49 biomass samples. Thus, in addition to the equal mass of DNA added to each lane, a ladder was run on each gel to correct for imaging system variations. The band intensities of the ladders on all gels were compared, and their average differences were used to calculate a factor (ranging from 0.8 to 1.4) that was multiplied by each band intensity. These normalized data were used to perform principal components analysis (PCA). Though not impacting placement of the data points or the principal components, SMA values were depicted as a third dimension, diameter of the data symbol (larger diameters corresponded to higher SMA values).

5.2.4.4 Principal Component Analysis (PCA)

Principal component analysis (PCA) was performed with MATLAB (v. R2010bSP1, MathWorks®, Natick, MA) using DGGE banding patterns. Optical densities of the DGGE bands (obtained with Lab Works v. 4.6.00.0, Lablogics, Inc., Mission Viejo, CA) provided dimensional values for community structure. The output of the PCA in MATLAB included the PCA plot as well as equations for each principal component with demeaned X values, which were calculated in MATLAB as follows:

Equation 5-1. Demeaned X Values Calculated for Each Principal Component

$$X_m = I_m - \frac{\sum_{i=1}^{n} I_{m,i}}{n}$$

where there are n samples and I_m is the intensity of band m in biomass j. Thus, X_m is positive if the optical intensity is greater than the average of all samples of a given band and vice versa.

5.2.4.5 Cluster Analysis

Similarity coefficients (e.g., Dice, Jaccard), simple mismatch coefficients, the squared Euclidean distance (Kosman and Leonard, 2005), the Shannon Index (Boon et al., 2002), as well as Pearson correlation coefficients (Dalirsefat, 2009) have been used in molecular ecology to analyze phylogenetic similarity. Pearson's correlation coefficient (Equation 5-2) was used to develop similarities between the banding patterns (i.e., a 0 signified uncorrelated, a +1 was a perfect positive correlation and -1 was a perfect negative correlation) since it accounted for band intensities (i.e., brightness). This was done using the "pdist" function in MATLAB (v. R2010bSP1, MathWorks®, Natick, MA) and a predefined command entitled "correlation" that calculated one minus the Pearson's correlation coefficient to develop

dissimilarities between banding patterns. Dissimilarity distances were compiled into a matrix using the "squareform" function in MATLAB because the output of "pdist" was a vector variable. This matrix was then uploaded into Plain Text Editor (v. 5.1), formatted to be readable by the Phylogency Inference Package (PHYLIP, v. 3.69) and the unweighted pair group method with arithmetic mean (UPGMA), Fitch-Margolish and Neighbor-joining algorithms were used to build phylogenetic trees. Trees were viewed in FigTree (v. 1.3.1).

Equation 5-2. Pearson's Correlation Coefficient

$$r = \frac{\sum_{i-1}^{n}\left(\left(x_i - \bar{x}\right)^2\left(y_i - \bar{y}\right)^2\right)}{\sqrt{\sum_{i-1}^{n}\left(x_i - \bar{x}\right)^2 \sum_{i-1}^{n}\left(y_i - \bar{y}\right)^2}}$$

5.2.4.6 Spearman's Rank Correlation Coefficient

Additional statistical analyses were performed. In order to quantify the correlation between the effectiveness of bioaugmentation and methanogenic community structure, SMA values were ranked from highest to lowest. Next, the difference (i.e., dissimilarity distance) among the densitometric data from the samples was calculated using one minus the Pearson's correlation coefficient. These data were then used to rank the biomass samples in ascending order of their pair-wise distances from the sample with the greatest SMA value. Then the rank based on SMA values was correlated to the densitometric ranking of distance from this sample using Spearman's rank correlation coefficient (Equation 5-3), which measured the monotonic correlation between the similarity of methanogen community structure and SMA values (Spearman, 1904; Zar, 1972). Spearman's rank correlation coefficient is non-parametric in that a higher correlation arises when the independent and dependent variables are related via any monotonic function; thus, it has advantages over methods like Pearson's correlation coefficient and linear regression, which are limited to

linear relationships between the independent and dependent variables. Spearman's Rank Correlation Coefficient was also used to correlate different paired combinations of OOPA parameters (e.g., resilience coefficient and capacity), SMA with individual OOPA parameters (e.g., SMA and M/F ratio), SMA with densitometric data, M/F ratio with densitometric data, and methanogenic slope in the OOPA with densitometric data.

Equation 5-3. Spearman's Rank Correlation Coefficient (Zar, 1972)

$$r_s = 1 - 6\left(\frac{\sum_{i=1}^{n} d_i^{\,2}}{\left(n^3 - n\right)}\right)$$

where n is the number of samples (e.g., 19) and d_i equals the difference in the ranks of the two parameters being analyzed (e.g., SMA values and densitometric data).

5.2.4.7 Multiple Linear Regression (MLR)

The densitometric data obtained by the DGGE image analysis were used to fit a MLR equation expressing SMA with propionate (dependent variable) as a function of band intensities (independent variables) for 30 samples. Microsoft Excel® (v.2010) software was used for this regression analysis by the least squares method, and the results obtained were used to test the significance of the regression equation. Four bands were present in all 49 samples. Thus, these were used as four X variables, along with a fifth X variable that was determined based on its significant contribution to the "R Square" value calculated in Excel® (See Results for details). A MLR equation was also found for the secondary slope of the OOPA data using the Bottom-up algorithm (Keogh et al., 2001) to select the five bands that yielded the highest "R Square" (R^2) and "Adjusted R square" (adjusted R^2) values in Microsoft Excel®. The Bottom-up algorithm entailed measuring the R^2 value of each X variable (i.e., band intensity) with Y variable (i.e., SMA or second slope of the OOPA). The

single X variable with the highest R^2 was then used in combination with all other potential X variables to generate a MLR model based on two X variables. The pair with the highest R^2 value was then used with all other potential X variables until the greatest MLR R^2 value from three different X variables was found. This was done until five X variables were selected. In addition to the factor mentioned in 5.2.4, all DGGE band intensities used were input into the MLR as the band intensity divided by the total lane intensity.

Once these two combinations of bands were found, a random number generator (www.random.org/integer-sets/) was used to provide a data set (n = 30) on which MLR equations could be calculated for a portion of each data set (i.e., training set) while the remaining samples in each data set were used to test (i.e., test set) the training set equation. All 49 samples from the combination of bands that yielded the highest "R Square" and "Adjusted R Square" were then used to calculate a final MLR equation using all 49 points. This was done for both SMA with propionate and the secondary slope of the OOPA tests. This jackknifing method has been used previously to examine structure function relationships (Nirmalakhandan and Speece, 1988b; Eriksson et al., 2003; Konovalov et al., 2008).

5.2.5 Physical and Chemical Analysis

A luciferase-based test kit (QuenchGone21™ Wastewater test kit, LuminUltra, Fredericton, New Brunswick, Canada) was used to measure iATP concentration. Briefly, this protocol included measuring each biomass sample both for extracellular ATP using a proprietary stabilizing agent and for total ATP using a proprietary NaOH-based lysing agent. The difference between total ATP and extracellular ATP was calculated as iATP.

Propionate Enrichments. The temperature and pH of propionate enrichments were measured daily using a glass electrode and meter (Orion 4 Star pH-DO Benchtop electrode - 9206BN, Thermo Scientific, Marietta, OH). Two samples of feed and effluent per week were used to determine the following parameters (specific method used given in parentheses): total solids (TS) (2540 B), volatile solids (VS) (2540 E), volatile suspended solids (VSS) (filtered as in 2540 D, volatized as in 2540 E), soluble chemical oxygen demand (SCOD) (5220 D), and individual volatile fatty acid (VFA) concentrations (acetic, propionic, butyric, iso-butyric, valeric, and iso-valeric acids) (5560 B) according to standard methods (APHA et al., 1998). From the beginning of the study until day 280, effluent SCOD was measured and from day 280 until the end of the study effluent TCOD was monitored. For SCOD analysis, the samples were thickened at 13,000 rpm for 10 minutes in a centrifuge (Clinical 200 VWR International LLC Radnor, Pennsylvania) and the supernatant filtered through a 0.45 μm filter (Whatman International Ltd., Maidstone, England). The filtrate was then tested for COD. The biogas volume produced was measured daily at ambient pressure before feeding using a water displacement method (Wet Test Meter, Precision Scientific Petroleum Instruments, San Antonio, TX), and biogas methane content (2720 C) was measured by standard methods (APHA et al., 1998). Methane content in the biogas as well as the influent and effluent VFA concentrations were determined by gas chromatography (GC) (Series 7890A GC system, Agilent Technologies, Santa Clara, CA, USA) with a thermal conductivity detector (TCD) and flame ionization detector (FID), respectively. For methane content, the carrier gas was helium at a flow of 4.5 mL/ min. Temperatures of the injector and detector were 150°C and 250°C, respectively, and the temperature of the oven was 40°C. VFA samples were acidified using 1% phosphoric acid and analyzed as described in Standard Method 5560D (APHA et al., 2005). For VFA analysis, the carrier gas was helium at a flow

of 18 mL/min. Temperatures of the injector and detector were 150 °C and 300°C, respectively, and the temperature of the column was 40°C (detector airflow at 400 mL/min, H_2 flow at 30 mL/min). The test results outlined in this section were referred to as metadata.

Biomass Samples. The following were also measured in the nine biomass samples: TS (2540 B), as well as volatile solids (VS) (2540 E), ammonia-nitrogen (NH_3-N) (4500-NH3 C. Titrimetric method), total Kjeldahl nitrogen (TKN) (4500-Norg B.), total phosphorus (TP) (4500-P E. Ascorbic Acid Method), soluble phosphorus (SP) (4500-P E. with preliminary filtration through 0.45-um membrane filter) (APHA, 1998). A suite of total as well as soluble metal ion concentrations (Cd^{+2}, Co^{+2}, Ca^{+2}, Cu^{+2}, Pb^{+2}, Ni^{+2}, Zn^{+2}, Mn^{+2}, As^{+2}, Se^{+2}, Ag^{+2}, Mb^{+2}, Hg^{+2}, Be^{+2}, Fe^{+2}, Na^{+}, K^{+}, and Mg^{+2}) was determined using a MassHunter (Agilent Technologies, Schaumburg, IL) software package and an inductively coupled plasma mass spectrophotometer (ICP-MS) with an autosampler (7700x, Agilent Technologies, Schaumburg, IL). The soluble metal fraction was determined by prefiltering via Method 3030 B. Prior to metals analysis, all samples were predigested in nitric acid (3030 E), then diluted into 2% nitric/0.5% hydrochloric acid (APHA et al., 2005). Final metal analysis was performed following Method 3125 B for inductively coupled plasma-mass spectrophotometer (ICP-MS) (APHA et al., 2005).

5.3 Results

5.3.1 Preliminary Results: Optimization of Activity Tests

Preliminary results for activity test development are presented first. Then the digester operational data for the propionate enrichments are presented. Activity test results, and, finally, molecular analysis results are provided.

5.3.1.1 Linearity Upon Mixing Microbial Cultures

A linear relationship (R^2 = 0.95) was found between methane production rate (mL CH_4/h) and the mixing ratio (based on VS) when two cultures with different SMA values were mixed (Figure 5-3a). Though with a slightly lower R^2 of 0.75 (attributable, at least in part, to variations due to inactive VSS discussed below), SMA and mixing ratio also followed a linear model (Figure 5-3b). Because of the less precise fit of the linear regression, a theoretical SMA equation was derived to determine if a more appropriate model could more accurately estimate SMA in the mixed cultures (Equations 5-4). SMA linearly increased with increased VS mass of the high-SMA biomass.

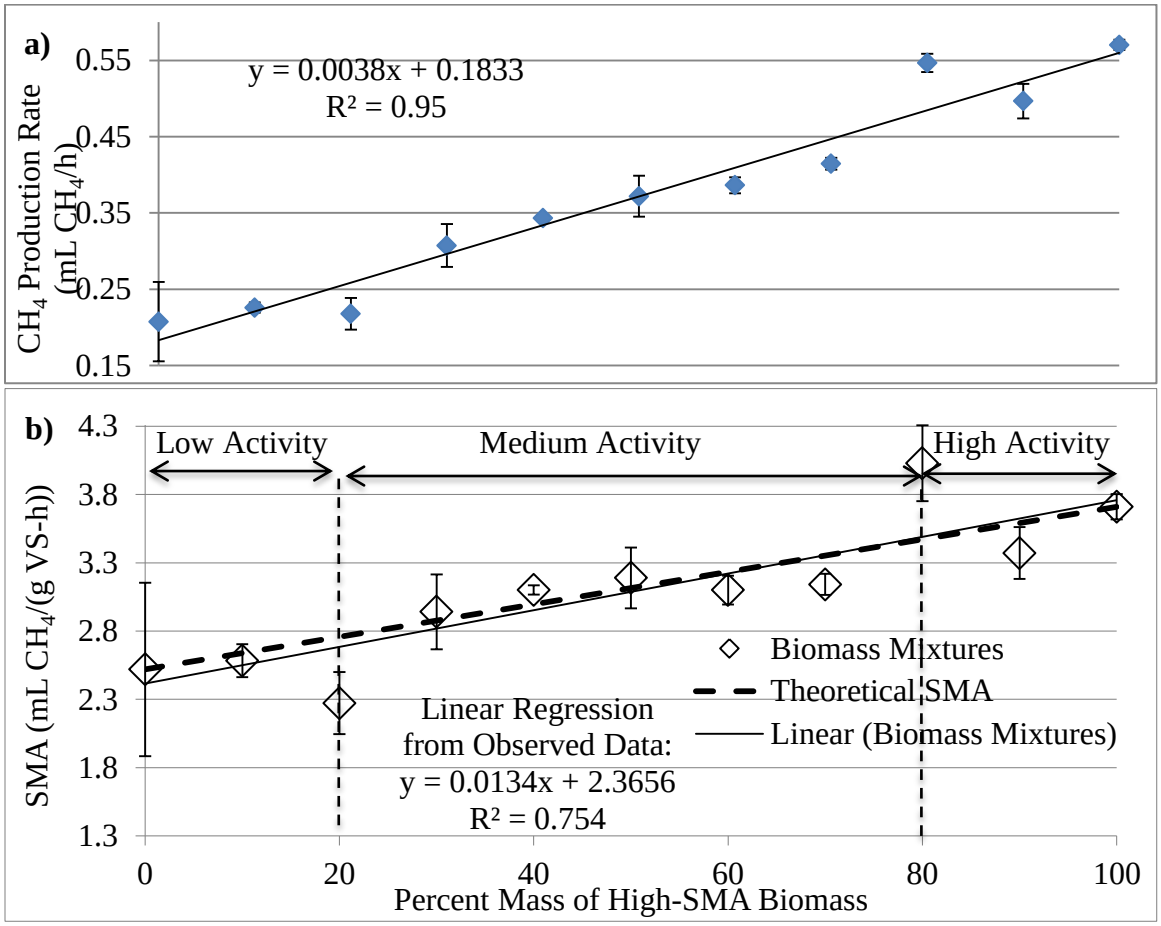

Figure 5-3. The relationship between percent (based on mass) of two cultures mixed and methane production rate of the mixture (a) as well as percent of culture mixed and theoretical SMA (b).

Equation 5-4. Theoretical SMA as a function of biomass concentration

$$(a) \quad r_1 = k_1 X_1 V \,(low\ SMA)$$

$$(b) \quad r_2 = k_2 X_2 V \,(high\ SMA)$$

$$(c) \quad r_m = k_1 X_1 V + k_2 X_2 V$$

$$(d) \quad X_m = X_1 + X_2$$

Then dividing by X_m, gives:

$$(e) \quad \frac{X_2}{X_m} = z \quad and \quad \frac{X_1}{X_m} = 1 - z$$

$$(f) \quad SMA_m = \frac{r_m}{X_m} = \frac{k_1 X_1 V}{X_m} + \frac{k_2 X_2 V}{X_m}$$

$$(g) \quad SMA_m = k_2 V z + k_1 V (1 - z)$$

$$(h) \quad SMA_m = k_2 V z + k_1 V (1) - k_1 V z$$

$$(i) \quad SMA_m = (k_2 V - k_1 V) z + k_1' V$$

$$(j) \quad m = k_2 V - k_1 V$$

$$(k) \quad b = k_1 V$$

$$(l) \quad SMA_m = mz + b$$

where r_1 and r_2 are the rate of methane production (mL CH_4/h) of biomass samples 1 and 2, respectively. SMA_1 and SMA_2 were defined as the SMA values (mL CH_4/(g VS-h) of biomass 1 and 2, respectively. CH_4 production rate constants, k_1 and k_2 (mL CH_4/(mg VS-h)), for biomass 1 and 2, respectively, were determined from the preliminary mixing experiment at 100% of their respective cultures. X_1 and X_2 were the relative VS masses of biomass 1 and 2, respectively. The initial measured concentrations (mg VS/L) of biomass 1 and 2 before mixing were X_{1° and X_{2°, respectively; and V_1 and V_2 were the relative volume (L) of biomass 1 and 2, respectively. The total volume, V (L), was 0.015 L; thus, V = 0.015 = V_1 + V_2. Because substrate concentration was non-limiting during the period when SMA was measured, it was not a factor in Equations 5-4a-f. Using Equations 5-4, theoretical SMA was graphed against the percent of each biomass sample (Figure 5-4b).

Three ranges of SMA values (Figure 5-4b) were categorized with the following possible explanation for their presence: (1) low activity (approximately 2.5 mL CH_4/g VS-h) was

observed at 0 to 20% of biomass 2 when there was an inadequate amount of the more active biomass, (2) medium activity (approximately 3 mL CH_4/ g VS-h) was observed at 30 to 70% of biomass 2, which resulted in intermediate SMA values, and (3) high activity (approximately 3.75 mL CH_4/ g VS-h) was observed at 80 to 100% of biomass 2 resulting in relatively high SMA values. The SMA values in the low range were statistically different from those in the medium and high ranges ($p = 0.0106$ and $p = 0.0105$, respectively). The SMA values in the medium range were different from those in the high range ($p = 0.0786$).

5.3.1.2 Defining Appropriate F:M Ratio for OOPA

Preliminary testing to determine an appropriate standard, active biomass concentration yielded three general trends in biogas production. F:M ratios from 0.2 to 1 g COD/g VSS resulted in biogas production rates that quickly stopped, indicating all substrate was consumed. When the F:M ratio was between approximately 3 and 10 g COD/g VSS, the biogas production was initially rapid, then secondarily increased at a moderate rate before finally stopping. Final biogas volumes produced were slightly less than the theoretical maximum in all samples. Lastly, F:M ratios from 12 to 33 g COD/g VSS quickly rose to slightly less than half of the theoretical final biogas volume and did not change for the duration of the testing (more than two weeks), indicating an overloaded condition. Because a clear distinction was evident between the initial and secondary slopes, the optimal overload concentration for OOPA analysis was in the middle range (3 and 10 g COD/g VSS). In particular, the greatest contrast between initial and secondary slopes was found at F:M ratios of 4.4 (Figure 5-5) and 7.0 g COD/g VSS, which had initial average slopes of 1.51 $\pm$0.05 and 3.62 $\pm$0.12 mL biogas h^{-1} as well as secondary slopes of 0.13 $\pm$0.004 and 0.18 $\pm$0.05 mL biogas h^{-1}, respectively. Repeated results from this middle range of F:M ratios showed the

same biogas production pattern—an initial increase to half of the 20-day maximum biogas level achieved followed lower secondary rate of biogas production. Therefore, an F:M ratio of 5 was chosen for the OOPA test.

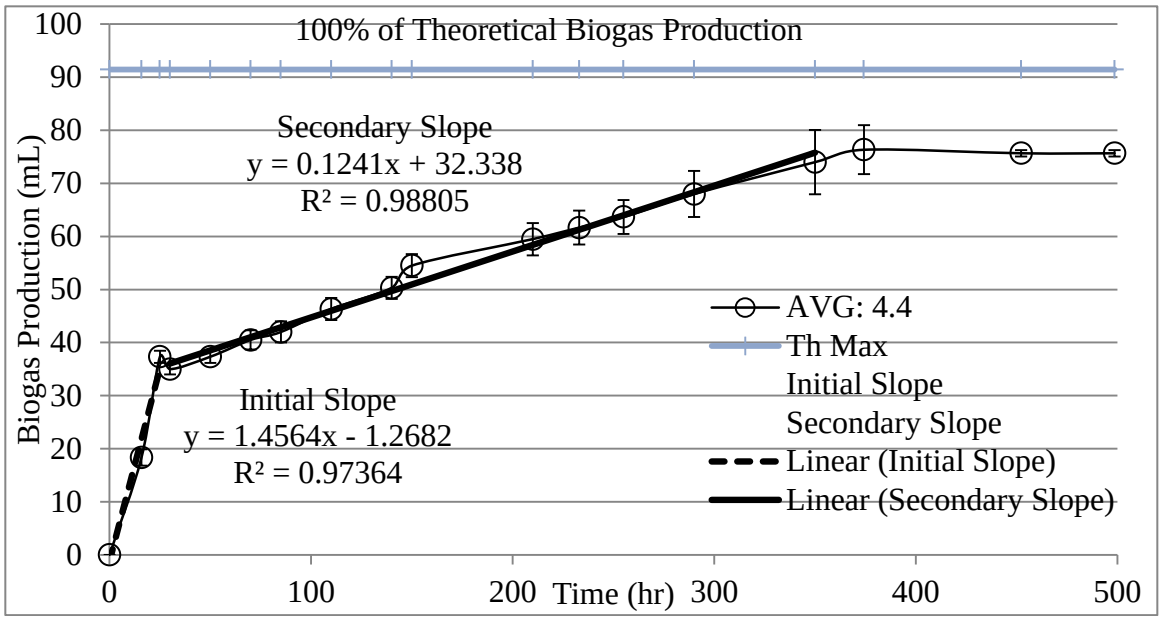

Figure 5-4. OOPA: average for triplicates of F/M ratio at 4.4 g COD/g VSS (3 g Glucose/L and 0.7g VSS/L) distinguishing initial slope ([mL biogas per h] of 1.548, 1.530, and 1.449) from secondary slope ([mL biogas per h] of 0.180, 0.177, and 0.141). Average slopes and standard deviation shown on graph. Horizontal line at 92 mL represented 100% of the theoretical biogas production.

5.3.1.3 Use of Intracellular ATP to Quantify Biomass

Intracellular ATP was used to standardize the amount of biomass for SMA and OOPA data since it has been shown to more accurately quantify active biomass than VSS (Roe and Bhagat, 1982; Cairns et al., 2005; Whalen et al., 2006a, b). For example, the inactive portion of the VSS is included in VSS measurements, yet does not metabolize substrate or intermediates (Perle et al., 1995). Consequently, microbial cultures, especially those with longer sludge ages or recently subjected to stressed conditions, may have a significant portion of inactive VSS (Quirk and Eckenfelder, 1986). Extracellular ATP is often present as cells are lysed; thus, total ATP is less suitable than iATP as an active biomass measurement.

5.3.2 Propionate Enrichment and Biomass Sample Metadata

The quasi steady state metadata collected for propionate enrichments at the time of activity testing and molecular analysis are presented below (Table 5-5). Metadata for the nine biomass samples are presented in Appendix A.

Table 5-5. Metadata for Propionate Enrichments at Quasi Steady State

Enrichment	0%	1.3%	6.7%	12.5%
pH	7.09 ±0.07	7.11 ±0.04	7.04 ±0.03	6.99 ±0.05
$SCOD_{effluent}$ (mg/L)	160 ±10	170 ±10	210 ±30	160 ±30
$SCOD_{removal}$ (%)	98 ±1.7	97 ±1.3	97 ±1.3	98 ±1.9
CH_4 (L/d)	0.21 ±0.023	0.22 ±0.02	0.21 ±0.03	0.19 ±0.03
CH_4 Content (%)	78 ±0.51	76 ±6.0	73 ±0.50	73 ±2.5
$VSS_{effluent}$ (g/L)	0.76 ±0.14	0.73 ±0.06	0.84 ±0.02	0.95 ±0.03
$CH_3CH_2COO^-_{effluent}$ (mg/L)	49 ±1.3	86 ±28	52 ±15	47 ±14
$CH_3COO^-_{effluent}$ (mg/L)	< 20*	< 20*	< 20*	57 24

*Below 20-mg/L detection limit

5.3.3 Function of 49 Methanogenic Cultures

5.3.3.1 Organic Overload Perturbation Activity (OOPA) Tests

Initial acidogenesis rates in the OOPA tests varied over 200%, between 3.14 and 6.32 mL biogas/h, while secondary methanogenesis rates varied 370%, ranging from 1.6 to 0.44 mL biogas/h (Appendix B). M/F ratios varied more than 350%, ranging from 0.09 to 0.34 (Figure 5-5). The lowest resilience was 0.34 h^{-1} and the greatest was 1.1 h^{-1} (320% difference) (Figure 5-6). The capacity varied 120%, from 86 to 120 h (Figure 5-7), and the PBY spanned 140%, from 0.73 to 1.0 mL biogas measured/mL biogas theoretically produced (Figure 5-8). Among the samples, digester biomass 1 had the highest resilience and second greatest M/F ratio, capacity, and PBY, while digester biomass 7 had the highest capacity and PBY.

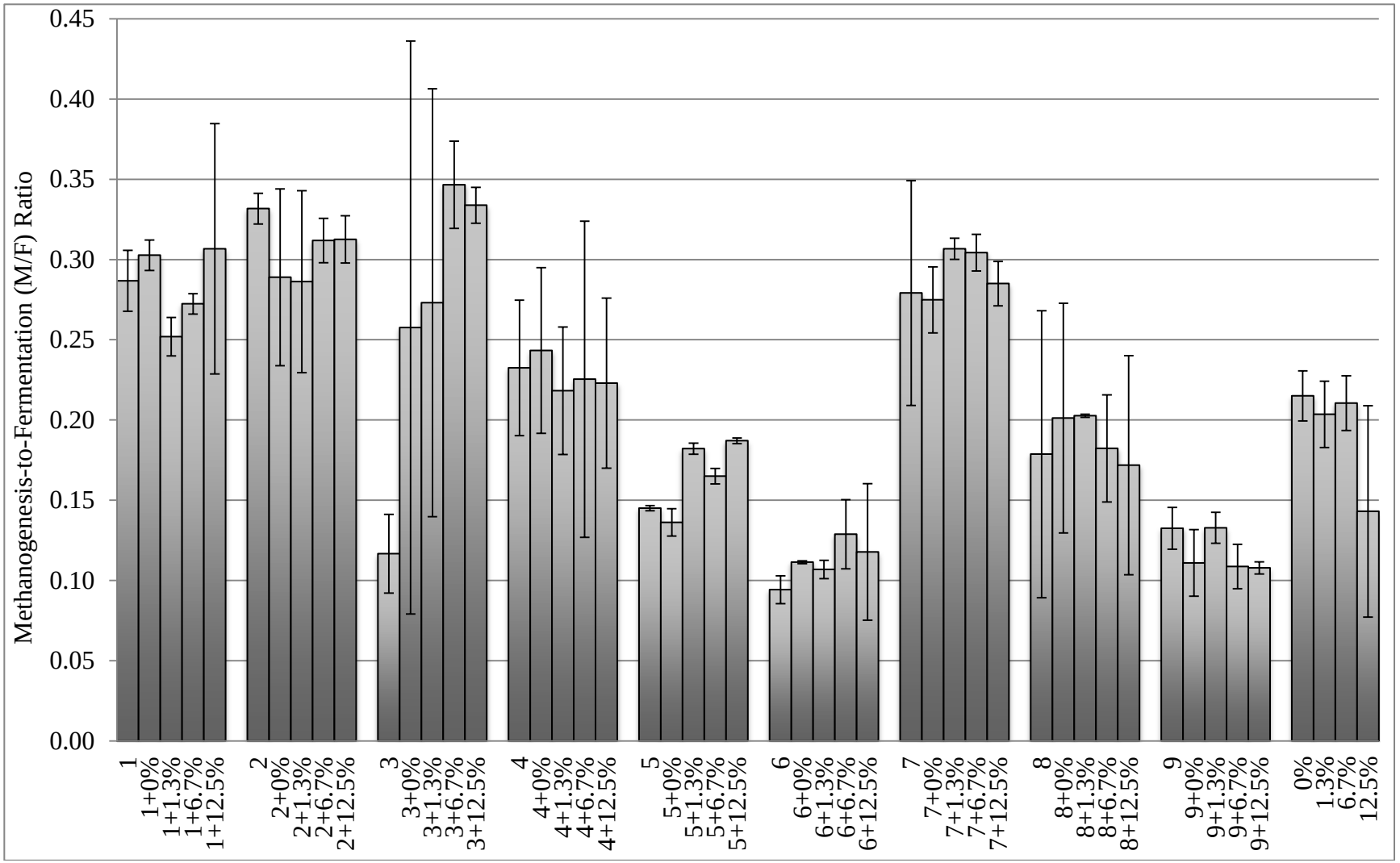

Figure 5-5. Methanogenesis to Fermentation (M/F) Ratio. Each group of five consists of (left to right) an unmixed biomass sample (labeled #) and, subsequently, biomass samples mixed with enrichments 0, 1.3, 6.7, and 12.5%. The right most group of four is the enrichments, labeled accordingly.

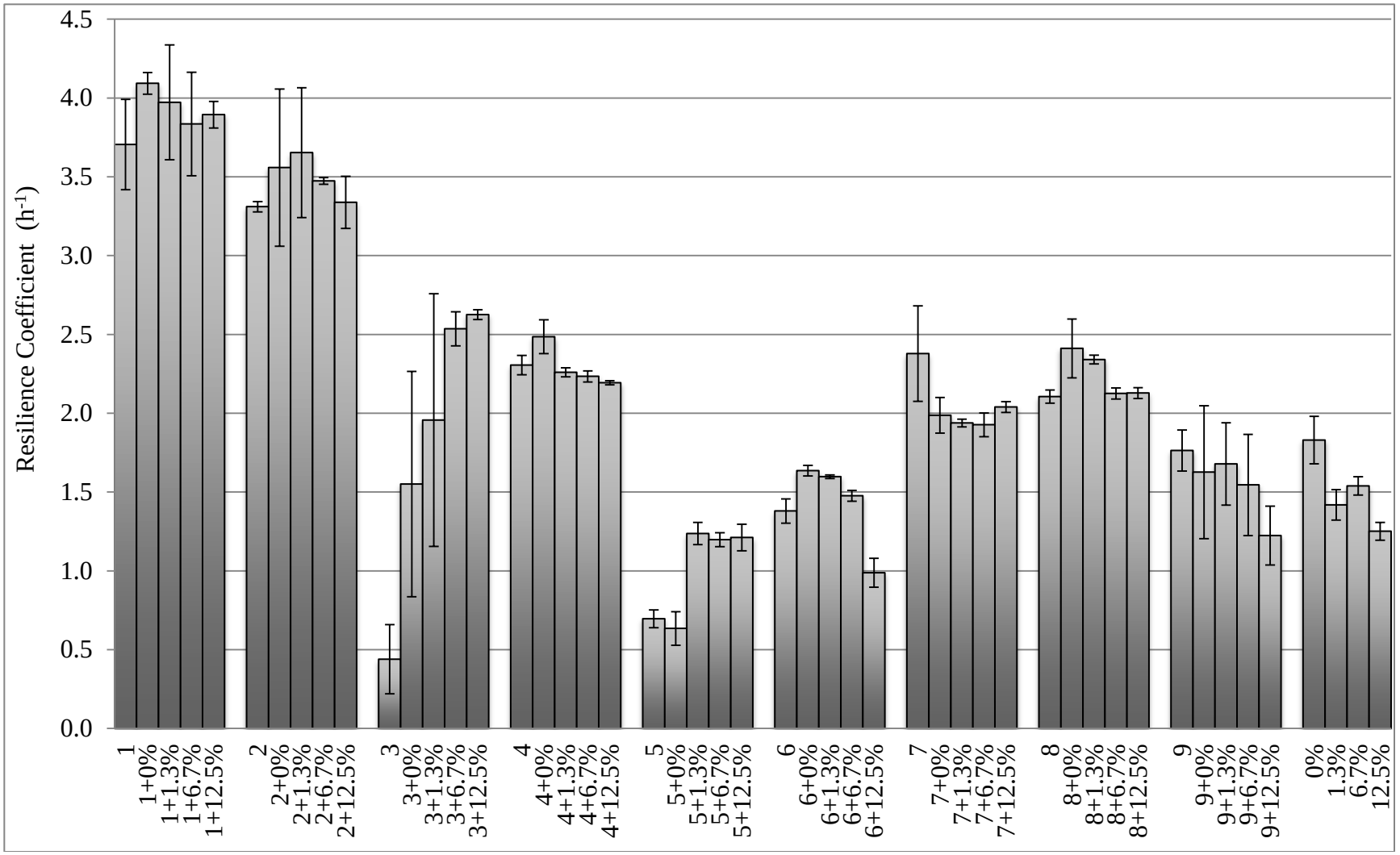

Figure 5-6. Resilience Coefficient from time of glucose perturbation to 66.7% of the theoretical maximum biogas production. Each group of five consists of (left to right) an unmixed biomass sample (labeled #) and, subsequently, biomass samples mixed with enrichments 0, 1.3, 6.7, and 12.5%. The right most group of four is the enrichments, labeled accordingly.

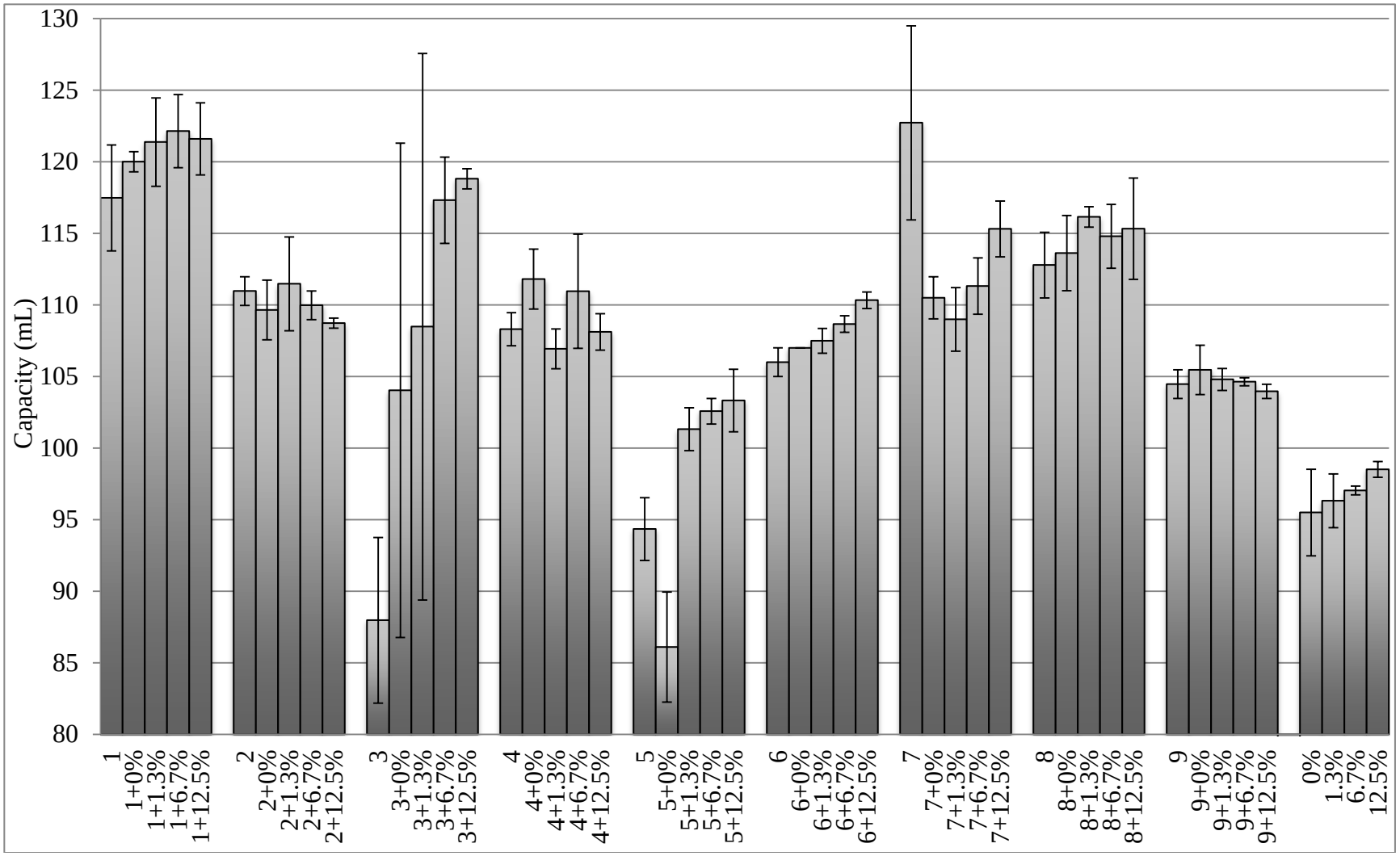

Figure 5-7. Capacity, defined as the cumulative 20-day biogas production, for 49 biomass samples. Each group of five consists of (left to right) an unmixed biomass sample (labeled #) and, subsequently, biomass samples mixed with enrichments 0, 1.3, 6.7, and 12.5%. The right most group of four is the enrichments, labeled accordingly.

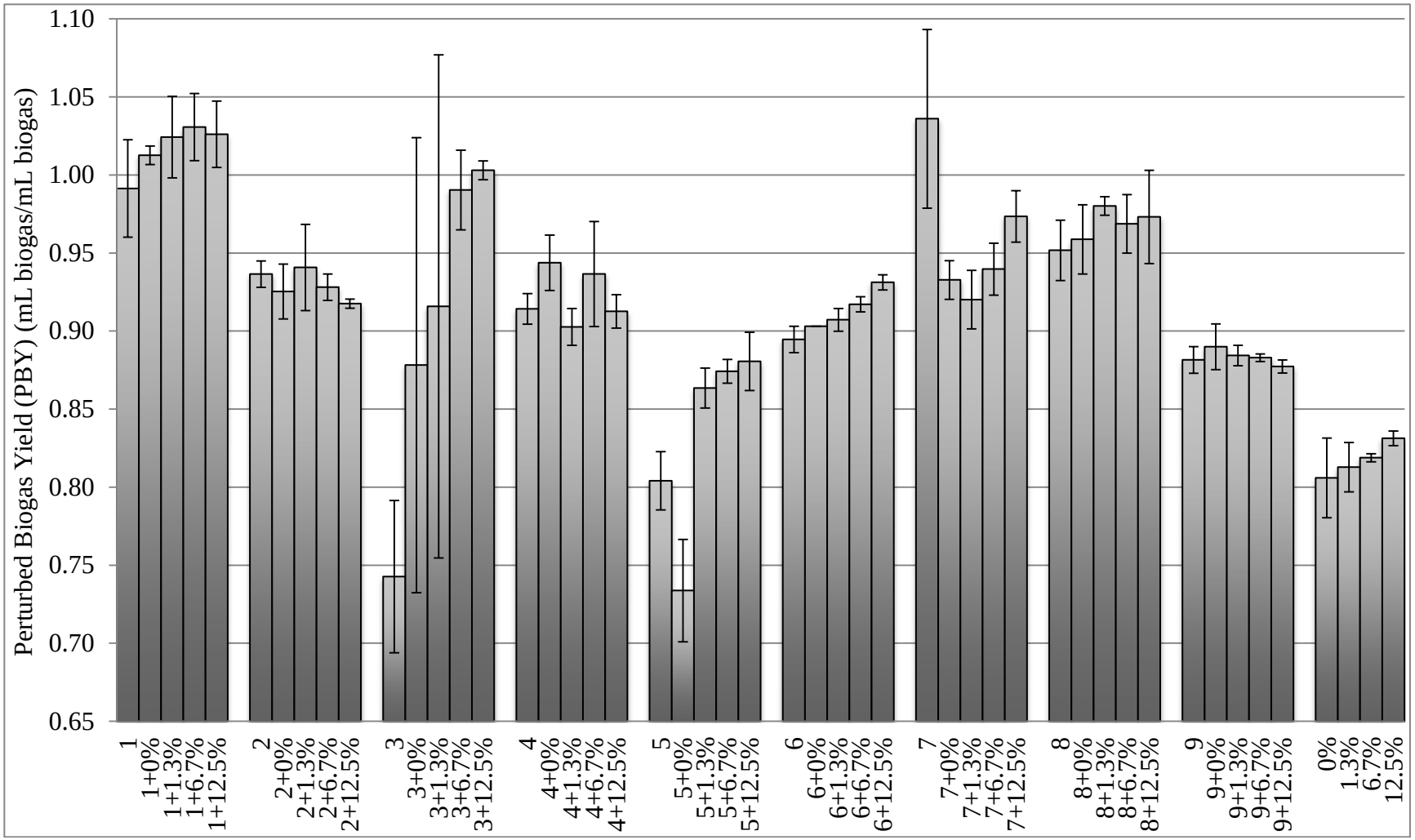

Figure 5-8. Perturbed Biogas Yield (PBY) for 49 biomass samples, defined as 20-day biogas production divided by theoretical maximum biogas production. Each group of five consists of (left to right) an unmixed biomass sample (labeled #) and, subsequently, biomass samples mixed with enrichments 0, 1.3, 6.7, and 12.5%. The right most group of four is the enrichments, labeled accordingly.

M/F ratio, resilience coefficient, capacity, and perturbed biogas yield were correlated pair-wise with one another in the six possible combinations using Spearman's rank correlation coefficient. All combinations had a $r_s \geq 0.578$, which was above the 0.460 needed for a 99.9% correlation for 49 samples (Zar, 1972) (Appendix C).

5.3.3.2 Specific Methanogenic Activity (SMA) Testing

Average SMA values for anaerobic biomass samples varied more than 650%, from 15 ±0.30 to 91 ±4.2 mL CH_4/mg iATP-h (Figure 5-9). This affirmed previous findings that showed SMA values with propionate vary greatly among biomass samples from different anaerobic digesters (Tale et al., 2011).

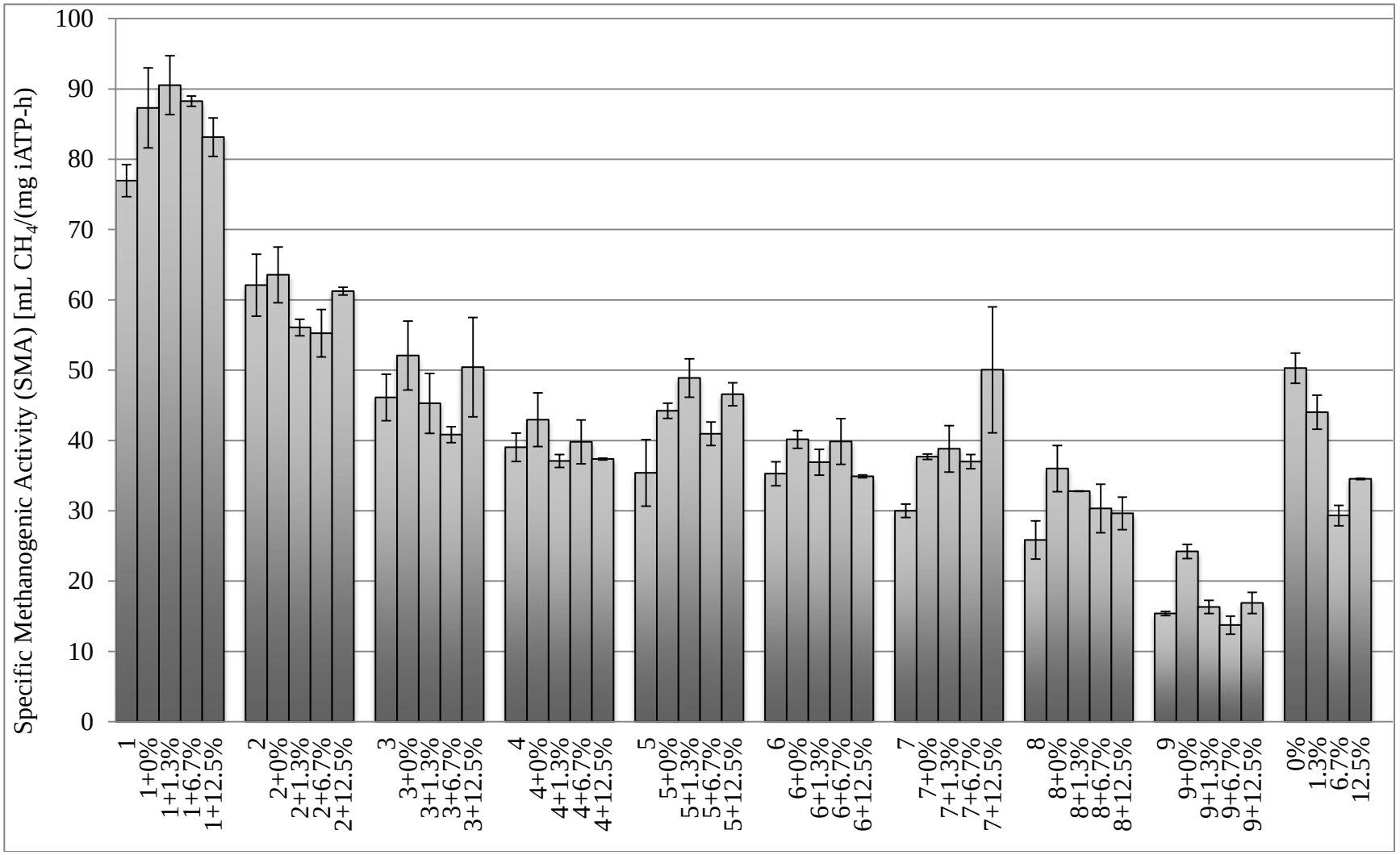

Figure 5-9. Average SMA values for 49 biomass samples. Each group of five consists of (left to right) an unmixed biomass sample (labeled #) and, subsequently, biomass samples mixed with enrichments 0, 1.3, 6.7, and 12.5%. The right most group of four is the enrichments, labeled accordingly.

SMA values from the 36 mixed cultures were calculated by multiplying by the percent added (i.e., 0.8 times the SMA value of one of the nine biomass samples plus 0.2 times the SMA value of the propionate enrichment used); these estimates were then graphed on the x-axis and the observed SMA values on the y-axis to show that mixing two microbial communities had a linear relationship with SMA values ($R^2 = 0.905$) (Figure 5-10). This linear fit further confirmed the accuracy of applying a linear model to describe the relationship between methanogen community structure and digester function. However, it was not predictive based on known microbial communities, but rather only possible for mixtures of two biomass samples with known SMA values.

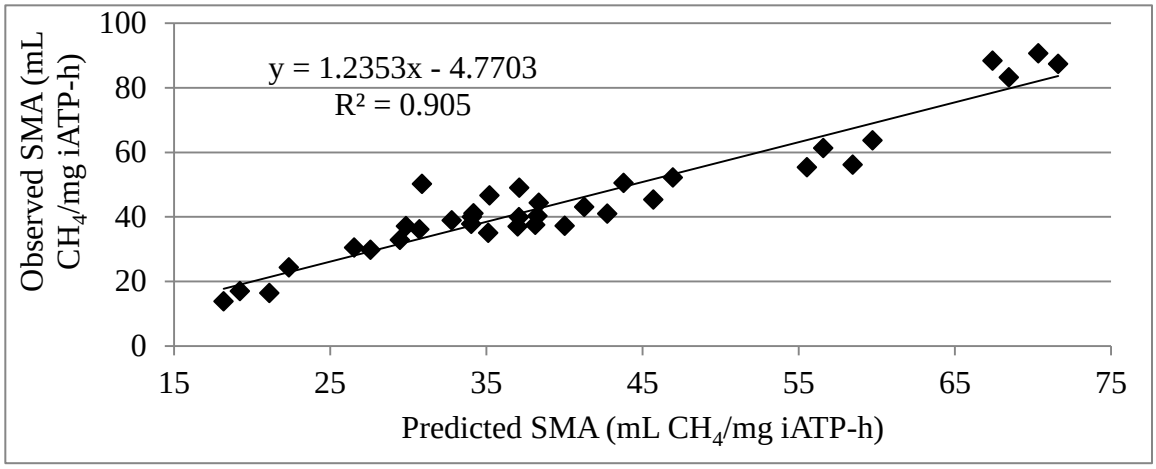

Figure 5-10. Observed SMA values (i.e., x = measured laboratory SMA) compared to SMA values predicted by a linear transformation of 80% biomass sample and 20% propionate enrichment (Y = 0.8Biomass sample + 0.2 Propionate enrichment).

When the leave-group-out (LGO) model is utilized (here 18 were left out), the q^2 value (Equation 5-5) is generally accepted as a means to determine if a model is predictive (Benigni and Bossa, 2008). In this equation: y_i was the sample SMA value; $\hat{y}$ was the predicted SMA value, $\bar{y}$ is the average measured SMA value; and n was the number of samples. Therefore, q^2 was calculated as 0.80, which is considered to be a value indicating very good predictability (Eriksson et al., 2003). This level of predictability using a linear

transformation (80/20 mixing ratio based on iATP) helped affirm the use of a linear model to relate SMA values.

Equation 5-5. q^2 value

$$q^2 = \frac{\sum_{i=1}^{n}\left(y_i - \hat{y}_i\right)^2}{\sum_{i=1}^{n}\left(y_i - \bar{y}_i\right)^2}$$

5.3.3.3 Spearman's Rank Correlation Between OOPA and SMA

SMA was plotted against the initial methanogenesis slope in the OOPA, M/F ratio, resilience coefficient, capacity, and PBY on a scatter plot to determine if they were linearly related; R^2 values suggested a weak linear correlation between each pair of parameters (Figure 5-11). Thus, function data (i.e., SMA and OOPA parameters) were also correlated with Spearman's Rank Correlation Coefficient (Appendix D). SMA values correlated with the initial methanogenesis slope in the OOPA (r_s = 0.561) (Table 5D-2), M/F ratio (r_s = 0.628) (Table 5D-3), and resilience coefficient (r_s = 0.481) (Table 5D-4) above the 99.9% for a two-tailed test (Zar, 1972). SMA correlated above the 90% level with capacity (r_s = 0.267) (Table 5D-5) and PBY (r_s = 0.269) (Table 5D-6) (Zar, 1972).

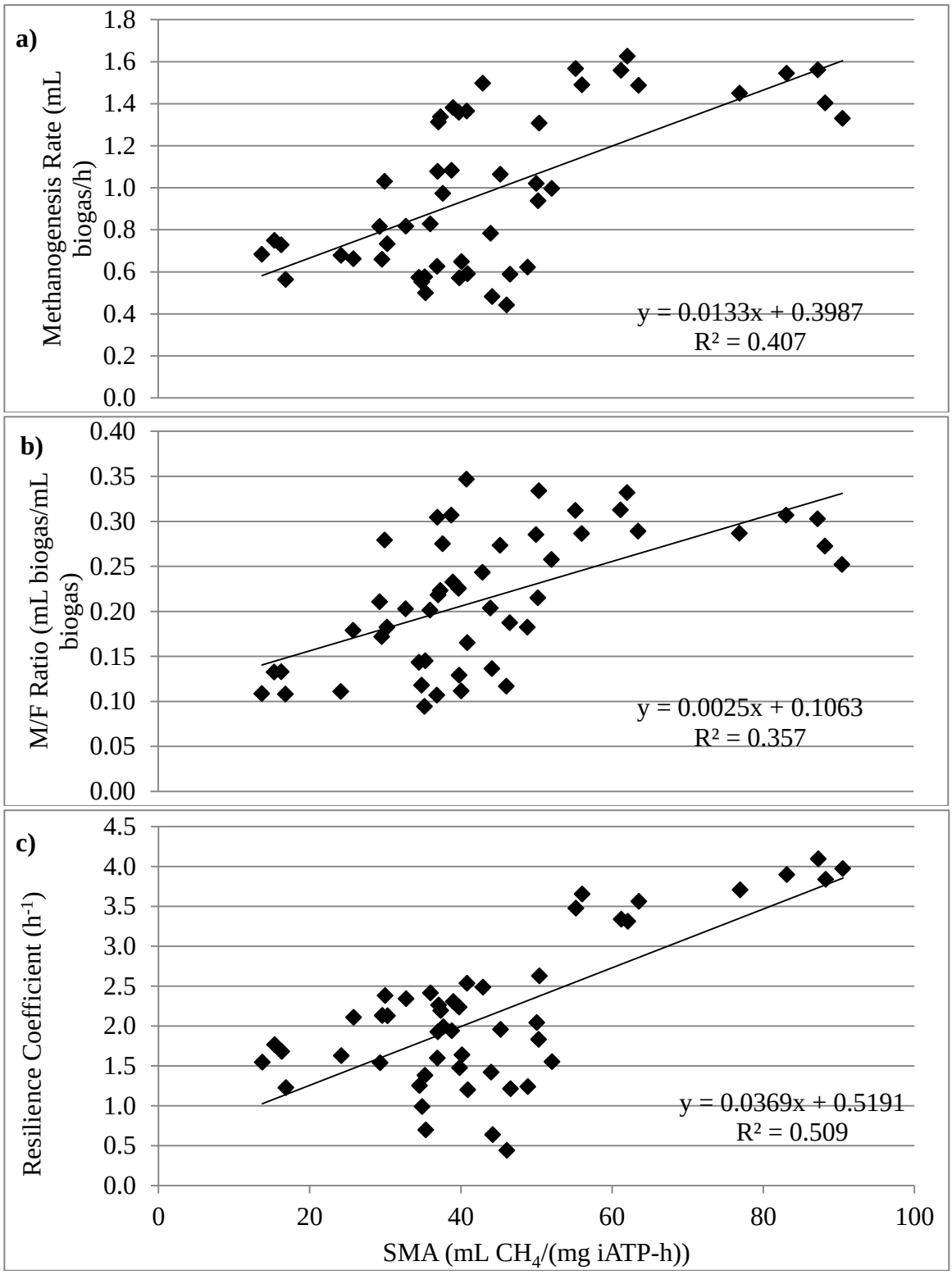
a)
Methanogenesis Rate (mL biogas/h)
1.8
1.6
1.4
1.2
1.0
0.8
0.6
0.4
0.2
0.0
y = 0.0133x + 0.3987
R² = 0.407
b)
M/F Ratio (mL biogas/mL biogas)
0.40
0.35
0.30
0.25
0.20
0.15
0.10
0.05
0.00
y = 0.0025x + 0.1063
R² = 0.357
c)
Resilience Coefficient (h-1)
4.5
4.0
3.5
3.0
2.5
2.0
1.5
1.0
0.5
0.0
y = 0.0369x + 0.5191
R² = 0.509
0
20
40
60
80
100
SMA (mL CH4/(mg iATP-h))

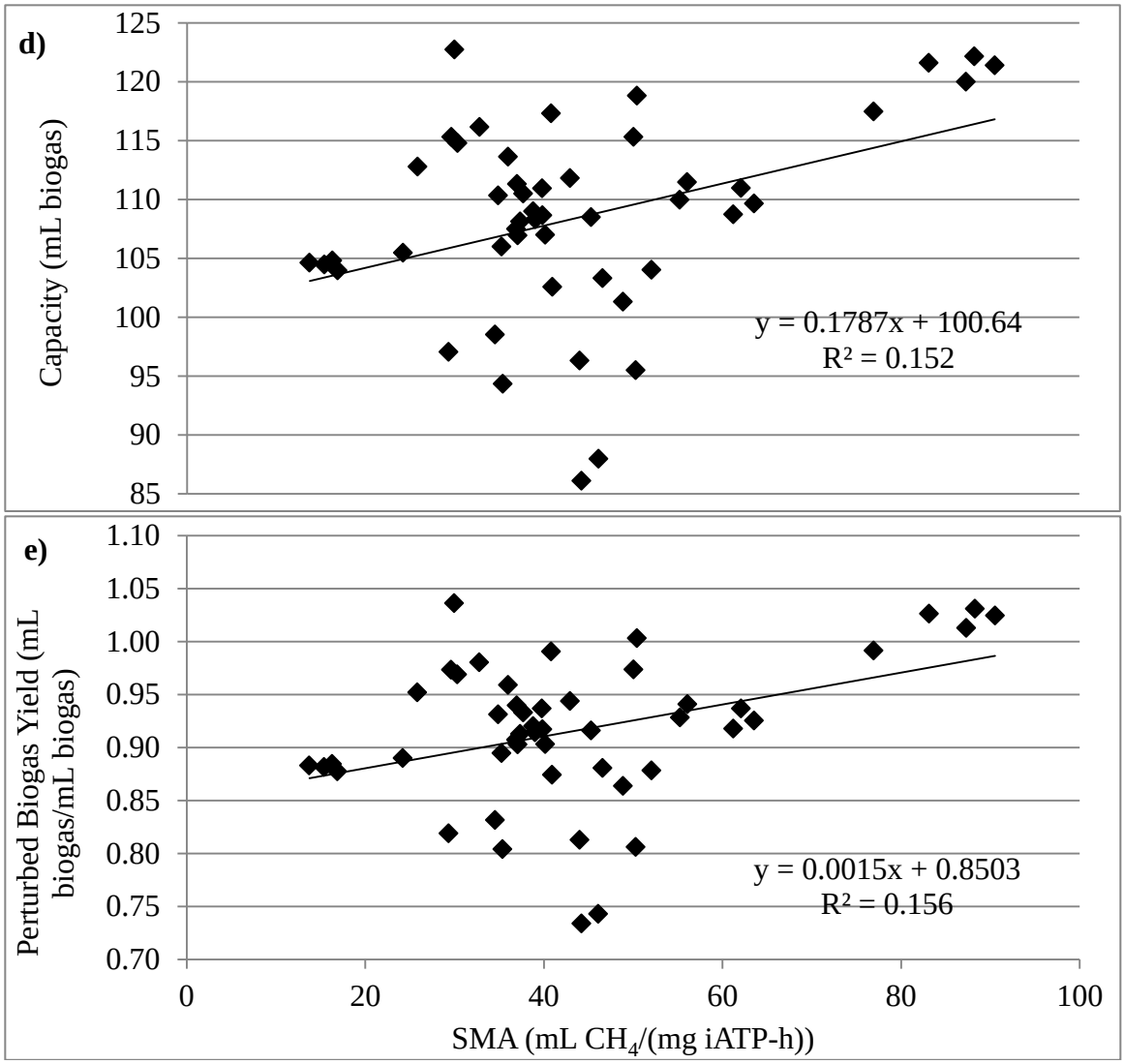

Figure 5-11. SMA values plotted against the following: methane production rate in OOPA tests (a), M/F ratio (b), resilience coefficient (c), capacity (d), and perturbed biogas yield (PBY) (e). Each point is an average of three triplicate OOPA tests and three SMA tests.

5.3.4 Community Structure

5.3.4.1 Principal Components Analysis

PCA was performed for the nine biomass samples using the eight dominant bands identified (Figure 5-12). Differences were evident in the methanogen community structure of the nine cultures, especially those that had the highest and lowest SMA values with $CH_3CH_2COO^-$. Band 2 had the greatest positive influence on those structures with the

highest SMA values, whereas band 4 had greatest positive influence on those structures with the lowest SMA values with $CH_3CH_2COO^-$.

These differences showed that diverse methanogen community structures were used to measure the effects of bioaugmentation. Cluster analysis using the UPGMA (Figure 5-13a) and Neighbor-joining (Figure 5-13b) algorithms showed variability among samples; yet, both algorithms depicted some differences from the PCA diagram. The methanogen community structure in biomass 1 was most similar to biomass 7 and then to 5 using the UPGMA algorithm and was most similar to biomass 5 and then to 7 using the Neighbor-joining algorithm. Hence, 1, 5, and 7 are shown in the same cluster in the PCA plot.

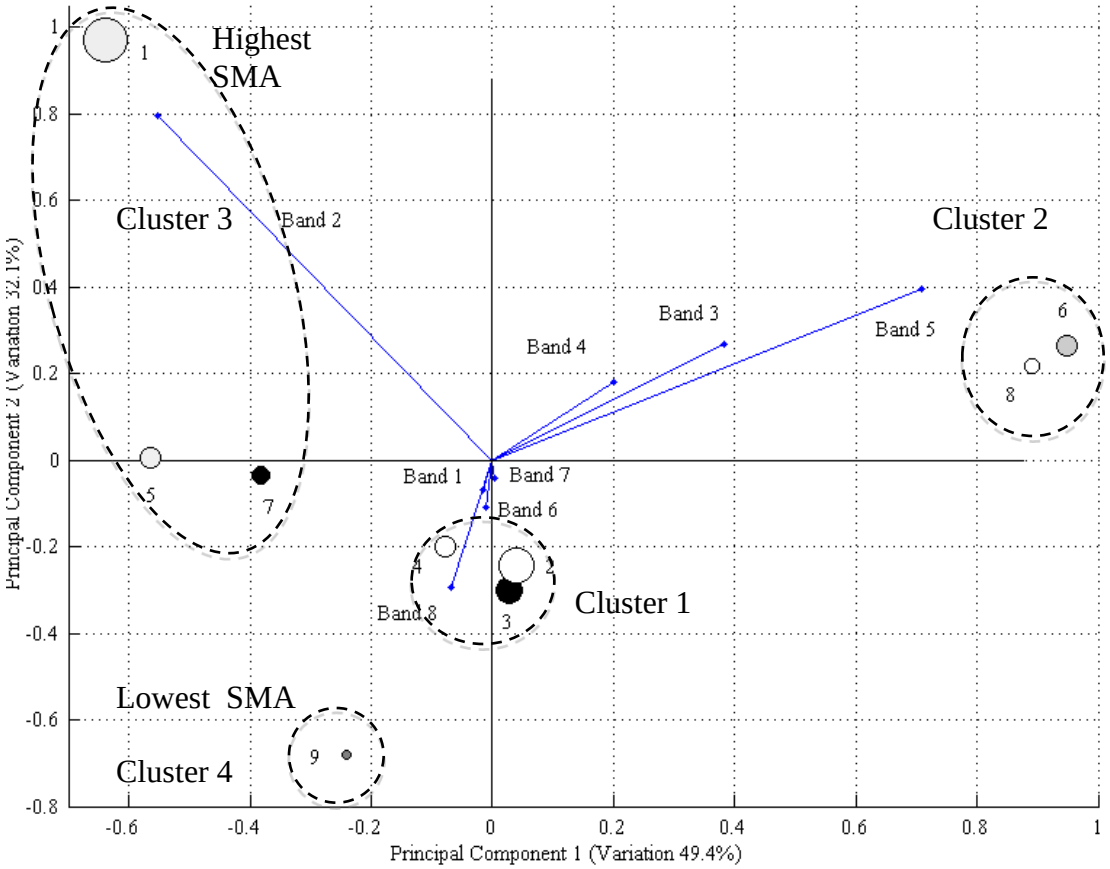

Figure 5-12. PCA plot of the nine biomass samples. Diameter symbols correspond to relative value of the SMA with propionate. Biomass samples from similar substrates are similarly colored (breweries, white; municipalities, black; other, gray). Data from eight common bands were used. Each vector represents one DGGE band and the diameter of each data symbol corresponds to the SMA magnitude. Dashed ovals show clustering based on DGGE banding pattern intensities calculated with UPGMA as well as Neighbor-joining algorithms.

First principal component = – 0.0159(X_1) – 0.0690(X_2) + 0.1396(X_3) + 0.1328(X_4) + 0.1023(X_5) – 0.0104(X_6) + 0.0008(X_7) + 0.9733(X_8)

Second principal component = – 0.5531(X_1) + 0.7970X_2) + 0.1151(X_3) + 0.1823(X_4) + 0.0661(X_5) + 0.0817 (X_6) – 0.0376(X_7) – 0(X_8)

Where, X_1, X_2, X_3……X_8 are the demeaned optical densities for bands 1, 2, 3,…,8 (1 being top, closest to the well) of the DGGE banding pattern.

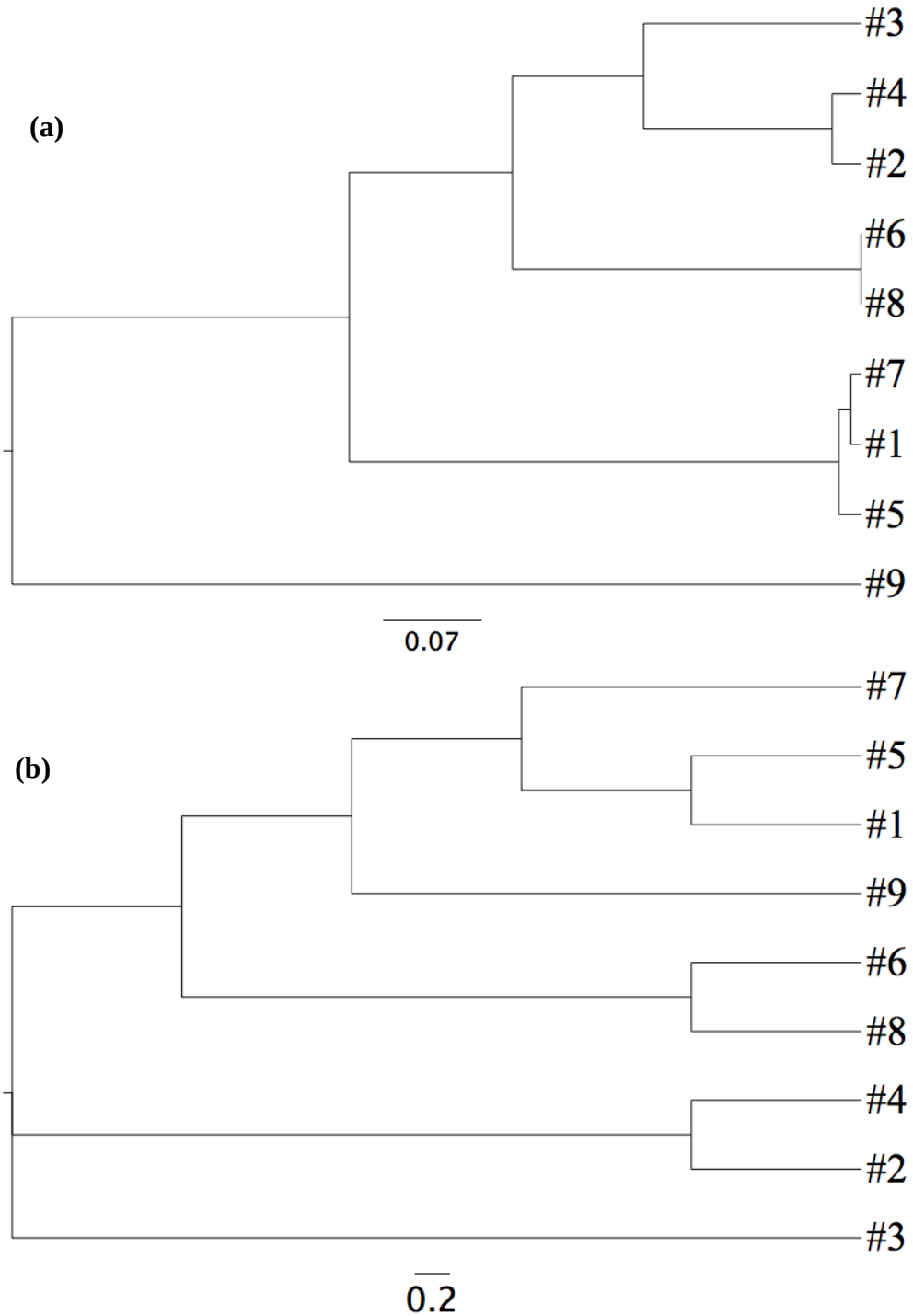

Figure 5-13. UPGMA (a) and Neighbor-joining (b) algorithms used to cluster nine biomass samples (labeled as in Table 4-2).

A second PCA plot of all 49 cultures using the five dominant bands accounted for 51.4 and 35.2% of the differences in the methanogen community structure (Figure 5-14). A different shape was used to represent each one of the nine biomass samples and its mixed samples. Color ranged from dark to light (black: biomass samples and mixed cultures with 0% O_2; white: mixed cultures with 12.5% O_2). The symbol size depicted the relative magnitude of the SMA with propionate. The central location of all four propionate enrichments on the PCA plot evidenced the methanogen community common to the mixed cultures. Each biomass sample and those cultures mixed with that biomass sample were close together, depicting similarity among those communities. Of the five bands used, bands 11, 12 and 14 captured the majority of the differences

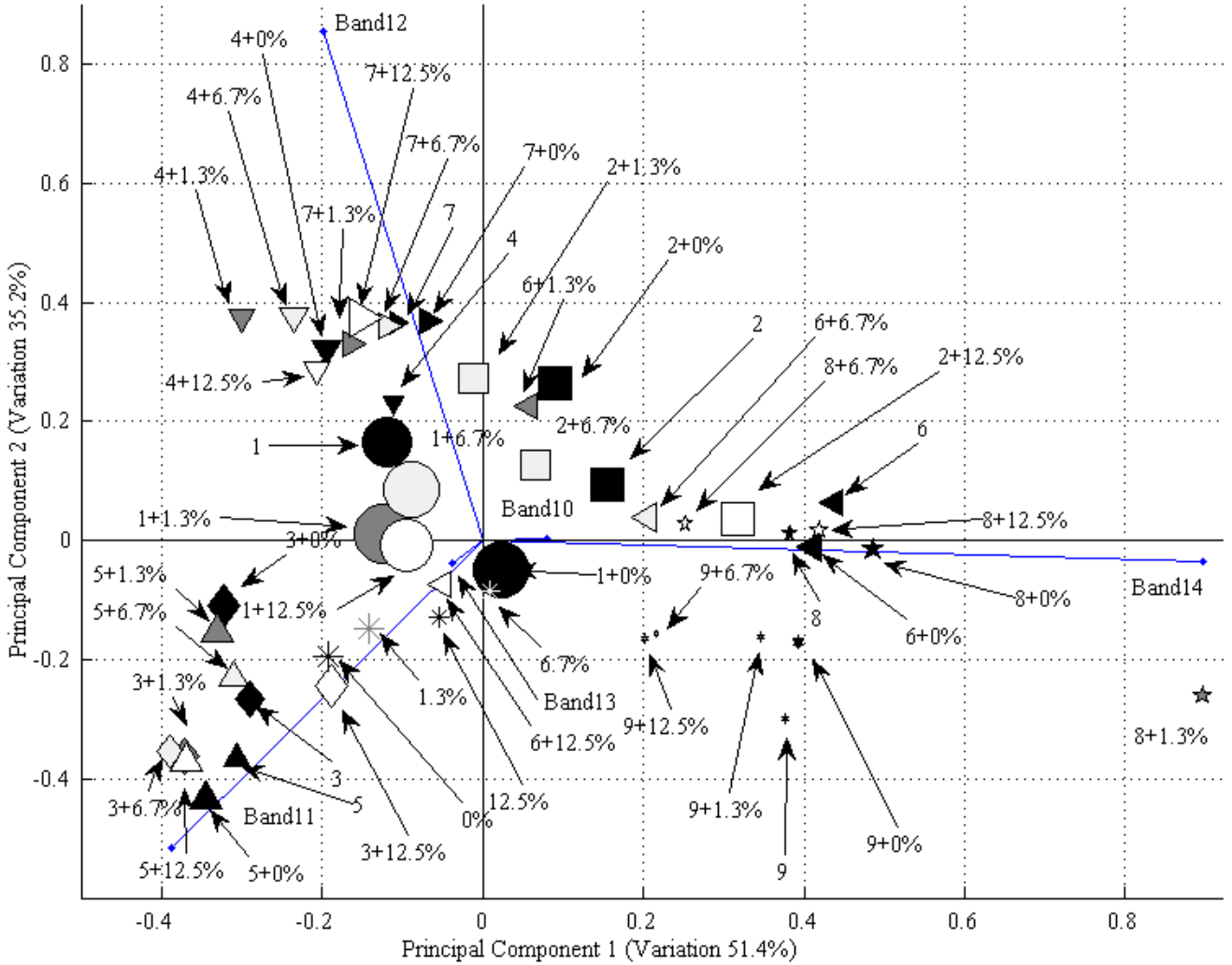

Figure 5-14. PCA of 49 biomass samples showing diversity of methanogen community structures of biomass samples. Labeled as digester biomass # and where appropriate "+ X%" (where X% is TCOD added as O_2 to propionate enrichment that was mixed with the digester biomass samples).

Normalized data from four common bands were used. Each vector represents one DGGE band and the diameter of each data symbol corresponds to the SMA magnitude.
First principal component = $0.0806(X_1) + 0.0019(X_2) + 0.1554(X_3) + 0.1501(X_4) + 0.9730(X_5)$
Second principal component = $-0.3877(X_1) - 0.5149 (X_2) + 0.7426(X_3) + 0.1465(X_4) - 0.1081(X_5)$
Where, X_1, X_2, X_3, X_4, and X_5 are the normalized optical densities for bands 1, 2, 3, 4, and 5 (1 being top, closest to the well) of the DGGE banding patterns.

The UPGMA algorithm was used to describe similarity among all 49 samples (Figure 5-15). Propionate enrichments 0, 1.3, and 12.5% clustered, with 6.7% on the opposite main branch. The SMA value of enrichment 6.7% was statistically lower than the other three enrichments, and it more closely clustered with samples containing biomass 8 and 9, which had some of the lowest SMA values. Biomass 1 and 7 clustered closely and were the only two biomass samples that statistically increased SMA values upon the addition of all four propionate enrichments, suggesting that the increase may have been due to the addition of a population(s) that was (more) present in the propionate enrichments and enhanced maximum methane production rate. Thus, greater differences in community structures between samples may have increased SMA values.

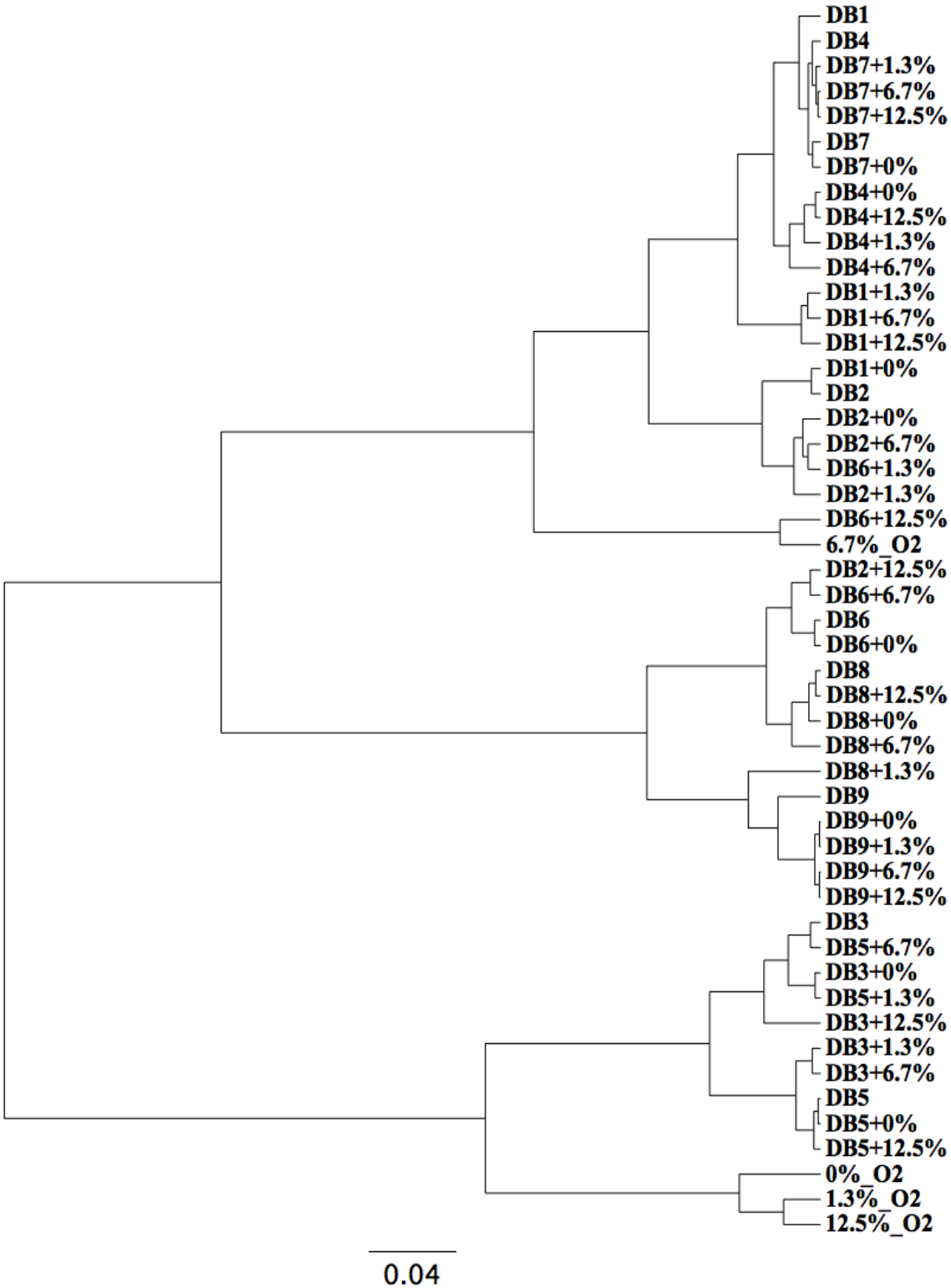

Figure 5-15. Phylogenetic tree of 49 biomass samples using one minus Pearson's Correlation Coefficient to calculate dissimilarity distance between densitometric data of the samples and the UPGMA algorithm to construct the tree.

5.3.4.2 Spearman's Rank Correlation Between Functional Parameters and Community Structure Data

Since SMA, M/F, and resilience coefficient had the greatest Spearman's rank correlation among functional parameters, they were correlated with densitometric data from DGGE banding patterns to determine if a link between digester function and methanogen community structure was present according to Spearman's Rank Correlation Coefficient. Since an r_s of 0.460, 0.282, 0.238, and 0.186 are needed to correlate at the 99.9, 95, 90, and 80% level (two-tailed), densitometric data correlated with SMA correlated at above 99.9% (r_s = 0.486) and with M/F above 80% (r_s = 0.223) (Zar, 1972). Additionally, the second slope of the OOPA test correlated to the densitometric data above the 90% level (r_s = 0.254). Results are tabulated in Appendix E.

5.3.5 Quantitative Structure-Activity Relationship

A predictive relationship between methanogen community structure and digester function was determined using MLR for DGGE banding pattern intensities and both SMA values. The four bands (X = 3, 4, 5, and 6 in Figure 5-16) that were present in all 49 samples were used in the MLR model. The fifth X variable in the MLR for SMA with propionate was determined by testing different DGGE bands in the order they appeared in the gel (i.e., bottom to top of the gel) and evaluating them based on their "R Square" values in Excel® (Figure 5-16). Starting from the top of the DGGE gel with 16 bands (i.e., X variables) one band was progressively eliminated in each successive MLR equation model such that every subset contained bands that were present in the superset. Exclusion of some bands that were both higher and lower on the DGGE gel had little effect on the accuracy of the model as described by R^2. However, a steep drop in R^2 was observed when X = 7 was eliminated from

the MLR model; thus, this analysis identified that the 7th band from the top of the DGGE gel was vital to develop a predictive MLR model (Figure 5-16). Therefore, the final model incorporated bands present at X = 3 through 7 in Figure 5-16.

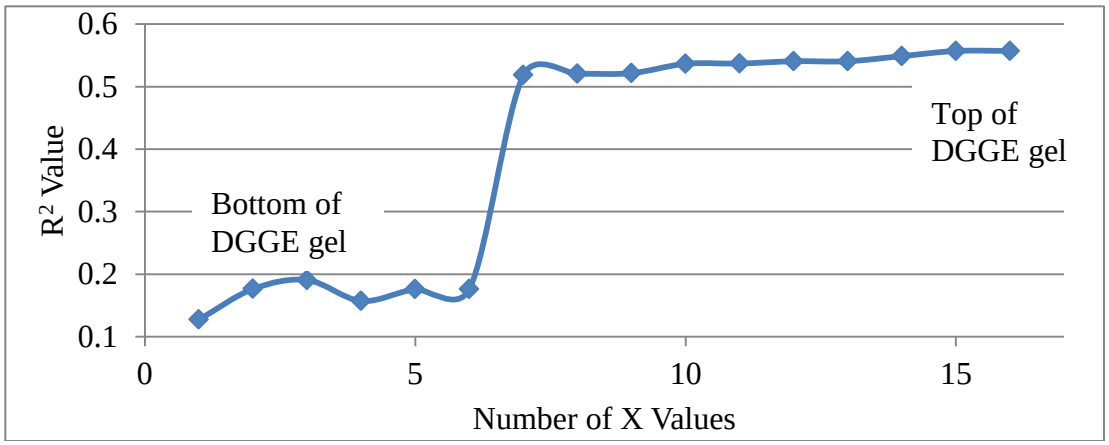

Figure 5-16. "R Square" value versus number of X values (independent variables). X values were bands, beginning with 17, which included all and progressively eliminating one band such that every subset contained bands in the superset with a greater number of X values.

A sample size of 30 has been shown to accurately test five independent variables at the recommended $r^2 = 0.4$ (Topliss and Costello, 1972). Therefore, the leave group out (LGO) method was applied by randomly selecting 30 samples and using them as a training set to develop a MLR model (Equation 5-6; Figure 5-17). The y-intercept was zero, Significance F was 9.94×10^{-12} and adjusted R^2 was 0.851. The adjusted R^2 is a metric that describes the likelihood of the model to improve if another variable were added (Konovalov et al., 2008).

Equation 5-6. Multiple Linear Regression Model from Five DGGE Bands Using 30 Samples

$$SMA = 306.9(X_1) + 41.15\ (X_2) + 40.36(X_3) + 139.8\ (X_4) + 29.55(X_5),\ n = 30,\ R^2 = 0.906$$

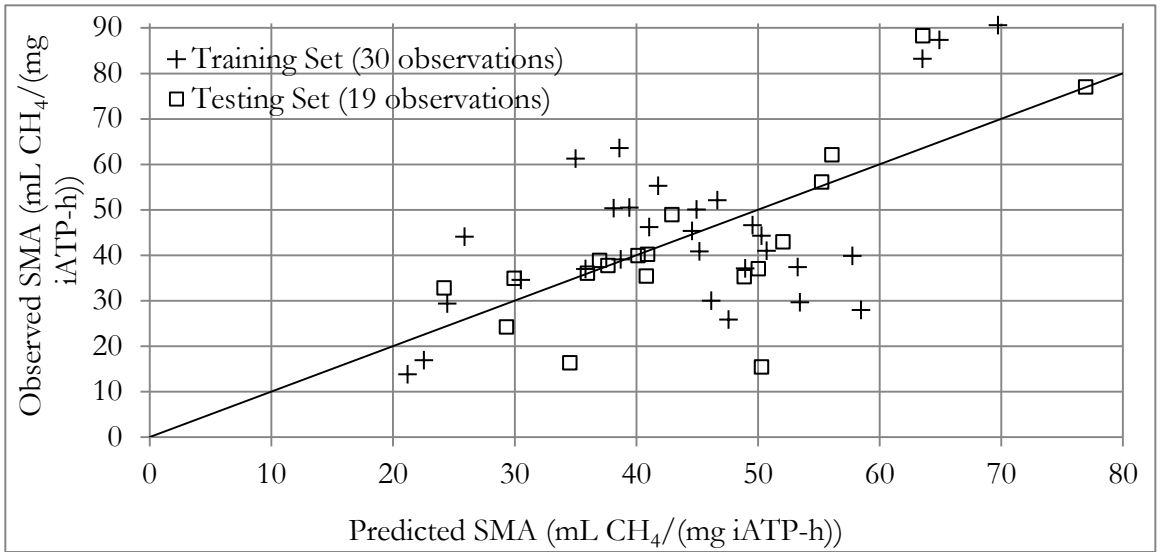

Figure 5-17. Comparison between experimentally determined (observed) SMA values with SMA values predicted by a multiple linear regression equation from 30-sample training set with R^2 = 0.906, n = 30, and q^2 = 0.52.

The q^2 value was used to assess predictability, but in this case, it was the predictability of the MLR equation (Equation 5-6). Limitations, such as uniformity of error, can be present with this metric, but residuals as well as p-values were analyzed to compensate for these limitations (Eriksson et al., 2003). Therefore, q^2 was calculated as 0.52, which is considered to be a value indicating good predictability (Eriksson et al., 2003). Furthermore, the theoretical linear regression performed on various mixes of two different cultures (Figure 5-3b; R^2 = 0.75) may suggest that the variability in SMA data is such that a model may be limited to a best fit with an R^2 = 0.75. This was an added reason that this q^2 value is reasonably high based on expected experimental inaccuracies.

Because this LGO model predicted SMA value using the intensities of the five bands (q^2 > 0.5), a MLR model was determined using all 49 samples to develop a predictive equation (Equation 5-7; Figure 5-18). The Significance F of this Equation was 4.3 x10^{-22} and the adjusted R^2 was 0.885, indicating an improved fit using all 49 samples over that of the 30 that were used as a training set.

Equation 5-7. Multiple Linear Regression Model from Five DGGE Bands Using 49 Samples

$SMA = 329.7(X_1) + 42.07(X_2) + 50.63(X_3) + 116.6(X_4) + 20.57(X_5)$, $n = 49$, $R^2 = 0.915$

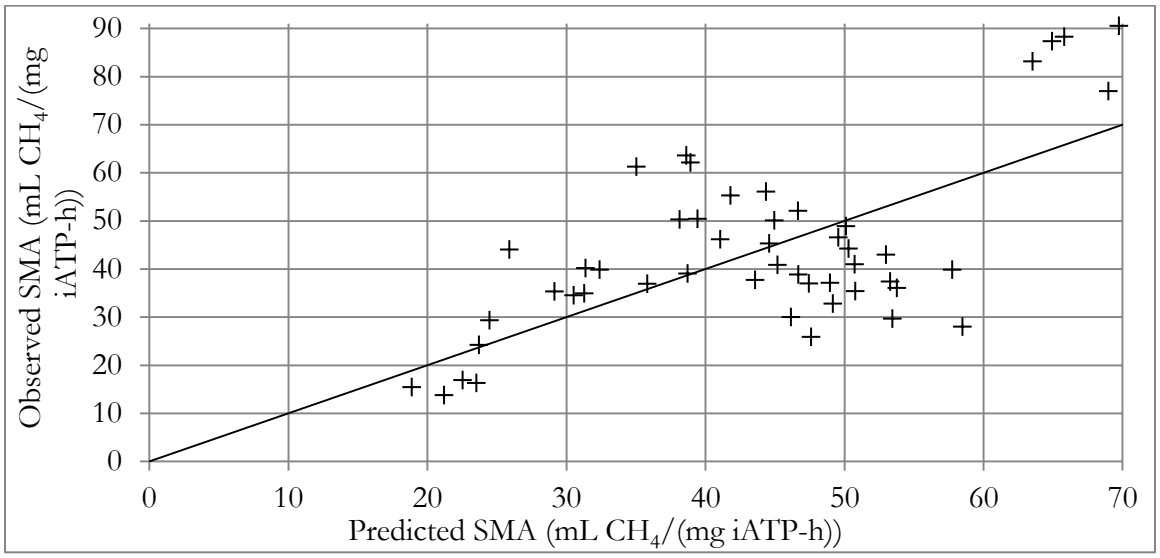

Figure 5-18. Comparison between experimentally determined (observed) SMA values with SMA values predicted by a multiple linear regression equation generated from all 49 samples with R^2 = 0.915 and n = 49.

A predictive relationship between methanogen community structure and digester function was also determined using MLR for DGGE banding pattern intensities and the secondary slope from OOPA tests. As described above, a MLR equation was developed from a 30-sample training set (Equation 5-8; Figure 5-19). The adjusted R^2 value was 0.870, and the Significance F was 1.02×10^{-12}.

Equation 5-8. Multiple Linear Regression Model from Five DGGE Bands for the Secondary Slope of the OOPA Tests

$SMA = 1.07(X_1) + 4.09(X_2) + 3.49(X_3) + 6.60(X_4) + 3.04(X_5)$, $n = 30$, $R^2 = 0.922$

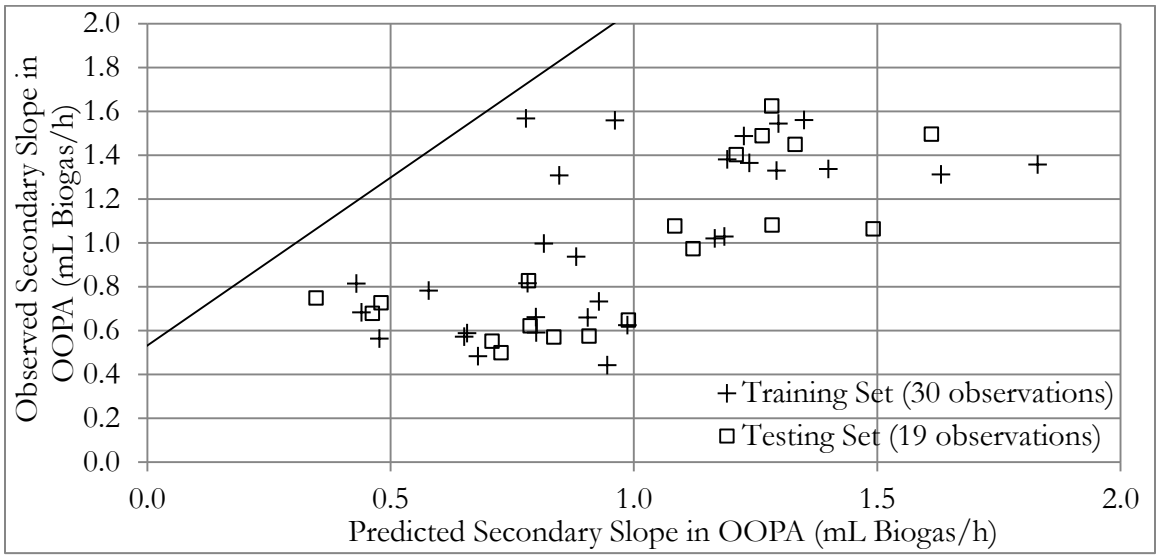

Figure 5-19. Comparison between experimentally determined (observed) secondary slope in OOPA Tests with slope predicted by a multiple linear regression equation from 30-sample training set with the following: R^2 = 0.922, n = 30, and q^2 = 0.56.

An LGO model again predicted function, secondary slope of the OOPA test, using the intensities of the five bands ($q^2 > 0.5$); thus, a MLR model was determined using all 49 samples to develop a quantitatively predictive equation (Equation 5-9; Figure 5-20). The Significance F was 3.49 $x10^{-24}$ and the adjusted R^2 was 0.903, which indicated an improved fit using all 49 samples over that of the 30 that were used as a training set.

Equation 5-9. Multiple Linear Regression Model from Five DGGE Bands for the Secondary Slope of the OOPA Tests

$$SMA = 1.11 (X_1) + 4.13 (X_2) + 4.66 (X_3) + 5.82 (X_4) + 2.01 (X_5), n = 49, R^2 = 0.932$$

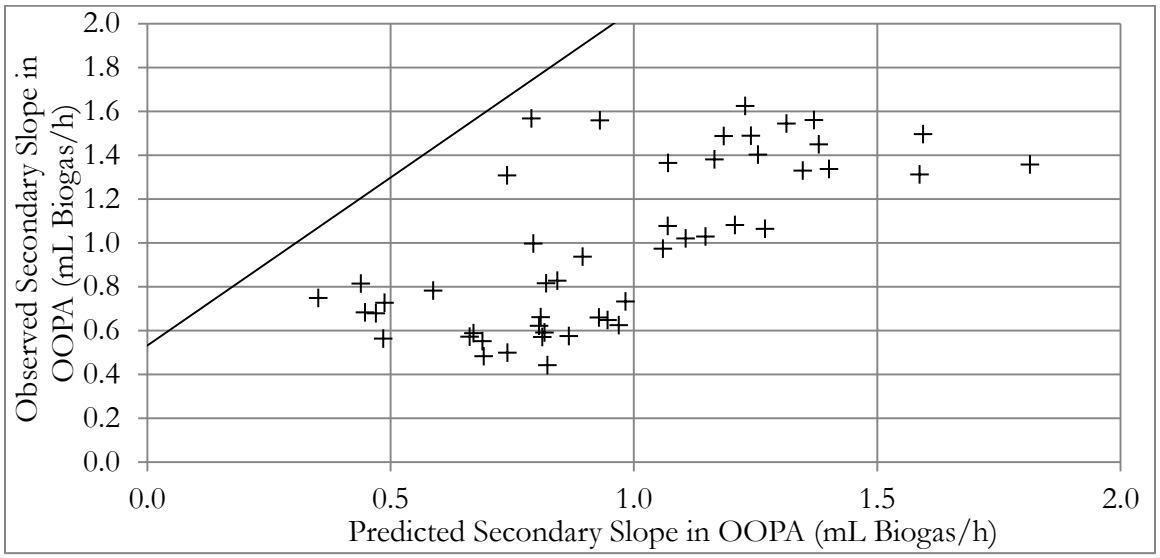

Figure 5-20. Comparison between experimentally determined (observed) secondary slope in OOPA Tests with slope predicted by a multiple linear regression equation generated from all 49 samples with R^2 = 0.932 and n = 49.

5.3.5.1 Extended Application of QSARS

A quantitative and predictive relationship between methanogen community structure and digester function was developed (Equations 5-7, 5-9). Greater understanding of anaerobic digester microbial communities is possible using these QSARs. A MLR model may be applicable to other biological communities when trophic redundancy and a ubiquitous gene are present and when a linear model is appropriate. Furthermore, this research serves as a template that can be used to construct additional quantitative and predictive QSARs for other complex microbial communities in engineered systems (e.g., nitrification, denitrification, $CH_3CH_3COO^-$ degradation by syntrophs).

5.4 Conclusions

Forty-nine, anaerobic digester biomass samples were used to establish two quantitative structure-activity relationships (QSARs) between methanogen community

structure (i.e., intensities of DGGE banding patterns) and two activities using multiple linear regression (MLR). Two different QSARs were predictive of specific methanogenic activity (SMA) values with propionate ($q^2 = 0.52$) and methanogenic activity with glucose via OOPA tests ($q^2 = 0.56$), respectively. A MLR model may be applicable to other biological communities when trophic redundancy and a ubiquitous gene are present and when a linear model is appropriate. Thus, these models constitute an initial step toward using microbial community descriptors to increase the rate and extent of VS destruction and methane production, for example. Greater understanding of anaerobic digester microbial communities is possible using these QSARs. This research serves as a template that can be used to construct additional QSARs for other complex microbial communities in engineered systems. Even with differences in banding pattern intensities between DGGE ladders run on different gels and inherent variability in activity testing, these models were still predictive. Future research ought to include optimization of ladders to decrease variability among DGGE gels as well as development of other QSARs.

5.5 Supplementary Material

5.5.1 Appendix A: Metadata for Anaerobic Biomass Samples

Table 5-6. Anaerobic Biomass Sample Characteristics. Iron, Calcium, Sodium, Potassium, and Magnesium are in mg/kg wet weight. Other metals are in µg/kg wet weight.

a) Biomass	TS (g/L	VS (g/L	NH_3-N (mg/L	TKN (mg/L	$N_{organic}$ (mg/L	PO_4 (mg/L) Total	Sol.
1	12.6	7.33	129	539	410	235	62.0
2	29.4	24.5	29.4	176	147	79.0	66.0
3	20.1	10.9	980	1680	700	240	21.0
4	47.9	42.3	221	4720	4490	134	50.0
5	11.8	8.80	1260	2820	1560	702	82.0
6	31.1	24.9	16.8	2210	2190	7.00	5.50
7	15.6	8.78	680	1320	640	342	85.0
8	45.1	40.3	197	3920	3723	264	58.0
9	22.3	13.7	174	1441	1267	854	71.0

b)	Cadmium		Chromium		Cobalt		Copper	
Biomass	Total	Sol.	Total	Sol.	Total	Sol.	Total	Sol.
1	1	0	20	ND	7	5	73	41
2	ND	ND	ND	ND	12	5	ND	ND
3	5	2	125	39	209	167	958	362
4	4	0	117	3	1270	42	1919	ND
5	6	7	177	143	6540	5890	1410	1230
6	2	0	285	12	1760	106	2840	82
7	2	2	52	15	72	147	496	218
8	2	ND	40	ND	22	5	498	29
9	0	ND	57	ND	5	7	22	ND

c)	Lead		Nickel		Zinc		Manganese	
Biomass	Total	Sol.	Total	Sol.	Total	Sol.	Total	Sol.
1	12.2	12	17.9	3.5	156	ND	79.3	4.3
2	< LOD[b]	ND	6.1	3.5	ND	ND	27.8	25.2
3	194	103	640	182	4520	3650	2200	104
4	45.4	4.00	2730	71.4	7870	177	124	17.7
5	148	72.8	681	647	4090	3380	942	906
6	87.6	7.9	7680	53.5	8740	14.3	877	18.3
7	89.8	52.8	702	74.8	2790	2070	2680	72.0
8	53.0	4.4	108	24.4	6237	34.4	316	55.3
9	3.3	ND	39.5	1.9	650	ND	559	4.9

d)	Arsenic		Selenium		Silver		Molybdenum	
Biomass	Total	Sol.	Total	Sol.	Total	Sol.	Total	Sol.
1	1.4	0.26	1.47	ND	0.55	ND	5.1	0.38
2	ND	ND	7.4	9.1	ND	ND	3.9	0.72
3	15.2	0.68	153	107	96.6	70.2	16.8	7.8
4	17.9	0.05	20.6	10.6	ND	ND	296	7.1
5	1.9	ND	600	460	183	40.2	735	641
6	5.9	0.13	2.79	ND	2.79	ND	302	25.5
7	7.4	1.62	160	83.6	61.2	38.8	10.6	1.2
8	14.4	0.09	17	ND	17.0	ND	55.3	2.71
9	2.9	ND	5.9	11.4	ND	ND	14.0	0.07

e)	Mercury		Beryllium		Iron		Calcium	
Biomass	Total	Sol.	Total	Sol.	Total	Sol.	Total	Sol.
1	28.9	18.7	0.76	1.2	87.8	0.9	34.9	3.1
2	ND	ND	ND	ND	0.86	0.1	10.1	4.6
3	14.8	11.6	ND	ND	1506	21.6	85.6	69.6
4	ND	ND	ND	0.7	100	2.6	18.6	7.1
5	ND	ND	ND	ND	31.4	24.7	56.2	49.9
6	81.5	53.0	1.4	1.8	1830	8.8	20	4.3
7	8.8	7.4	ND	ND	262	5.2	84.4	48.8
8	13.7	10.7	0.4	1.4	385	9.6	37.2	10.1
9	ND	ND	0.18	ND	73.8	0.2	266	13.5

f)	Sodium		Potassium		Magnesium	
Biomass	Total	Sol.	Total	Sol.	Total	Sol.
1	156	150	15.6	13.1	5.5	2.9
2	85.7	85.1	5.1	5.00	17	17.4
3	156	113	54.6	39.2	13.6	7.6
4	64.8	57.9	56.2	26	11.6	3.8
5	56.3	54.8	46.5	44.6	12	10.9
6	45.4	36.3	14.7	2.1	5.1	1.1
7	43.6	46	24.2	23.6	14.6	5.1
8	43	37	35.6	11.8	16.3	5.1
9	115	110	27.4	22.3	9.00	3.1

[a]ND = not detected
[b]LOD = level of detection

5.5.2 Appendix B: Initial and Secondary OOPA Slopes

Initial acidogenesis rates and secondary methanogenesis rates from OOPA tests are presented below.

Table 5B-1. Initial and Secondary Slopes from OOPA Tests

	Initial Slope		Secondary Slope	
	Average	Std. Dev.	Average	Std. Dev.
	mL biogas/h		mL biogas/h	
1	5.05	0.18	1.45	0.14
1+0%	5.16	0.16	1.56	0.00
1+1.3%	5.29	0.30	1.33	0.03
1+6.7%	5.15	0.24	1.40	0.04
1+12.5%	5.05	0.12	1.54	0.35
2	4.90	0.07	1.63	0.03
2+0%	5.21	0.52	1.49	0.16
2+1.3%	5.26	0.45	1.49	0.17
2+6.7%	5.03	0.12	1.57	0.03
2+12.5%	4.99	0.04	1.56	0.06
3	3.78	0.05	0.44	0.10
3+0%	3.89	0.04	1.00	0.68
3+1.3%	3.89	0.01	1.06	0.52
3+6.7%	3.94	0.00	1.36	0.11
3+12.5%	3.92	0.01	1.31	0.05
4	5.95	0.20	1.38	0.04
4+0%	6.15	0.22	1.50	0.06
4+1.3%	6.01	0.05	1.31	0.05
4+6.7%	6.02	0.27	1.36	0.12
4+12.5%	6.00	0.13	1.34	0.06
5	3.44	0.03	0.50	0.01
5+0%	3.54	0.03	0.48	0.03
5+1.3%	3.41	0.03	0.62	0.01
5+6.7%	3.58	0.06	0.59	0.01
5+12.5%	3.14	0.03	0.59	0.01
6	6.09	0.07	0.57	0.00
6+0%	5.81	0.09	0.65	0.01
6+1.3%	5.85	0.27	0.62	0.01
6+6.7%	4.46	0.53	0.57	0.01
6+12.5%	4.65	0.13	0.55	0.21
7	3.68	0.02	1.03	0.26
7+0%	3.54	0.05	0.97	0.06
7+1.3%	3.53	0.05	1.08	0.01

7+6.7%	3.54	0.06	1.08	0.03
7+12.5%	3.58	0.04	1.02	0.06
8	3.71	0.20	0.66	0.05
8+0%	4.12	0.20	0.83	0.04
8+1.3%	4.02	0.00	0.82	0.00
8+6.7%	4.02	0.13	0.73	0.00
8+12.5%	3.84	0.06	0.66	0.04
9	5.71	1.07	0.75	0.10
9+0%	6.05	0.91	0.68	0.20
9+1.3%	5.52	1.07	0.73	0.10
9+6.7%	6.32	1.01	0.68	0.12
9+12.5%	5.21	0.57	0.56	0.08
0%	4.36	0.15	0.94	0.06
1.3%	3.85	0.08	0.78	0.06
6.7%	3.88	0.15	0.81	0.04
12.5%	4.23	0.74	0.57	0.14

5.5.3 Appendix C: Spearman's Rank Correlation: OOPA Data

The M/F ratio, resilience coefficient, capacity, and perturbed biogas yield (PBY) from OOPA tests were correlated among one another using Spearman's Correlation Coefficient and previously established correlation criteria (Zar, 1972).

Table 5C-1. Critical Values of the Spearman's Rank Correlation Coefficients for Two-Tailed Probabilities at n = 49 (Zar, 1972)

Probability	**0.50**	**0.20**	**0.10**	**0.05**	**0.02**	**0.01**	**0.005**	**0.002**	**0.001**
$\mathbf{r_s}$	0.098	0.186	0.238	0.282	0.333	0.366	0.397	0.434	0.460

Table 5C-2. Spearman's Rank Correlation Between M/F Ratio and Resilience Coefficient (a), M/F Ratio and Capacity (b), M/F Ratio and Perturbed Biogas Yield (PBY) (c), Resilience Coefficient and Capacity (d), Resilience Coefficient and PBY (e), and PBY and Capacity (f)

a)

Biomass	M/F Ratio		Resilience Coef.		Spearman's Correlation		
Sample	M/F Ratio	Rank (a)	Resil. Coef.	Rank (b)	d_i	d_i^2	Rank Corr. Coef. (r_s)
1	0.29	11	3.705	5	6	36	
1+0%	0.30	9	4.093	1	8	64	
1+1.3%	0.25	19	3.972	2	17	289	
1+6.7%	0.27	17	3.835	4	13	169	
1+12.5%	0.31	7	3.894	3	4	16	
2	0.33	3	3.310	10	-7	49	

2+0%	0.29	10	3.559	7	3	9	
2+1.3%	0.29	12	3.653	6	6	36	
2+6.7%	0.31	5	3.474	8	-3	9	
2+12.5%	0.31	4	3.338	9	-5	25	
3	0.12	43	0.439	49	-6	36	
3+0%	0.26	18	1.550	35	-17	289	
3+1.3%	0.27	16	1.956	26	-10	100	
3+6.7%	0.35	1	2.536	12	-11	121	
3+12.5%	0.33	2	2.625	11	-9	81	
4	0.23	21	2.305	17	4	16	
4+0%	0.24	20	2.485	13	7	49	
4+1.3%	0.22	24	2.259	18	6	36	
4+6.7%	0.23	22	2.234	19	3	9	
4+12.5%	0.22	23	2.193	20	3	9	
5	0.15	36	0.696	47	-11	121	
5+0%	0.14	38	0.635	48	-10	100	0.744
5+1.3%	0.18	32	1.237	42	-10	100	
5+6.7%	0.16	35	1.198	45	-10	100	
5+12.5%	0.19	30	1.211	44	-14	196	
6	0.09	49	1.380	40	9	81	
6+0%	0.11	44	1.635	32	12	144	
6+1.3%	0.11	48	1.597	34	14	196	
6+6.7%	0.13	41	1.476	38	3	9	
6+12.5%	0.12	42	0.988	46	-4	16	
7	0.28	14	2.378	15	-1	1	
7+0%	0.27	15	1.987	25	-10	100	
7+1.3%	0.31	6	1.938	27	-21	441	
7+6.7%	0.30	8	1.927	28	-20	400	
7+12.5%	0.29	13	2.039	24	-11	121	
8	0.18	33	2.105	23	10	100	
8+0%	0.20	29	2.411	14	15	225	
8+1.3%	0.20	28	2.340	16	12	144	
8+6.7%	0.18	31	2.125	22	9	81	
8+12.5%	0.17	34	2.128	21	13	169	
9	0.13	40	1.763	30	10	100	
9+0%	0.11	45	1.626	33	12	144	
9+1.3%	0.13	39	1.678	31	8	64	
9+6.7%	0.11	46	1.545	36	10	100	
9+12.5%	0.11	47	1.224	43	4	16	
0.0%	0.22	25	1.829	29	-4	16	
1.3%	0.20	27	1.418	39	-12	144	
6.7%	0.21	26	1.539	37	-11	121	
12.5%	0.14	37	1.251	41	-4	16	

				Sum	0	5014	

b)

Biomass	M/F Ratio		Capacity		Spearman's Correlation		
Sample	M/F Ratio	Rank (a)	Cap. (mL)	Rank (b)	d_i	d_i^2	Rank Corr. Coef. (r_s)
1	0.29	11	117	7	4	16	
1+0%	0.30	9	120	5	4	16	
1+1.3%	0.25	19	121	4	15	225	
1+6.7%	0.27	17	122	2	15	225	
1+12.5%	0.31	7	122	3	4	16	
2	0.33	3	111	18	-15	225	
2+0%	0.29	10	110	23	-13	169	
2+1.3%	0.29	12	111	16	-4	16	
2+6.7%	0.31	5	110	22	-17	289	
2+12.5%	0.31	4	109	25	-21	441	
3	0.12	43	88	48	-5	25	
3+0%	0.26	18	104	38	-20	400	
3+1.3%	0.27	16	108	27	-11	121	
3+6.7%	0.35	1	117	8	-7	49	
3+12.5%	0.33	2	119	6	-4	16	
4	0.23	21	108	28	-7	49	
4+0%	0.24	20	112	15	5	25	
4+1.3%	0.22	24	107	32	-8	64	
4+6.7%	0.23	22	111	19	3	9	
4+12.5%	0.22	23	108	29	-6	36	
5	0.15	36	94	47	-11	121	
5+0%	0.14	38	86	49	-11	121	0.578
5+1.3%	0.18	32	101	42	-10	100	
5+6.7%	0.16	35	103	41	-6	36	
5+12.5%	0.19	30	103	40	-10	100	
6	0.09	49	106	33	16	256	
6+0%	0.11	44	107	31	13	169	
6+1.3%	0.11	48	107	30	18	324	
6+6.7%	0.13	41	109	26	15	225	
6+12.5%	0.12	42	110	21	21	441	
7	0.28	14	123	1	13	169	
7+0%	0.27	15	110	20	-5	25	
7+1.3%	0.31	6	109	24	-18	324	
7+6.7%	0.30	8	111	17	-9	81	
7+12.5%	0.29	13	115	11	2	4	
8	0.18	33	113	14	19	361	

8+0%	0.20	29	114	13	16	256
8+1.3%	0.20	28	116	9	19	361
8+6.7%	0.18	31	115	12	19	361
8+12.5%	0.17	34	115	10	24	576
9	0.13	40	104	37	3	9
9+0%	0.11	45	105	34	11	121
9+1.3%	0.13	39	105	35	4	16
9+6.7%	0.11	46	105	36	10	100
9+12.5%	0.11	47	104	39	8	64
0.0%	0.22	25	96	46	-21	441
1.3%	0.20	27	96	45	-18	324
6.7%	0.21	26	97	44	-18	324
12.5%	0.14	37	99	43	-6	36
				Sum	0	8278

c)

Biomass	M/F Ratio		Perturbed Biogas Yield		Spearman's Correlation		
Sample	M/F Ratio	Rank (a)	PBY (mL/mL)	Rank (b)	d_i	d_i^2	Rank Corr. Coef. (r_s)
1	0.29	11	0.991	7	4	16	
1+0%	0.30	9	1.013	5	4	16	
1+1.3%	0.25	19	1.024	4	15	225	
1+6.7%	0.27	17	1.031	2	15	225	
1+12.5%	0.31	7	1.026	3	4	16	
2	0.33	3	0.937	19	-16	256	
2+0%	0.29	10	0.925	23	-13	169	
2+1.3%	0.29	12	0.941	16	-4	16	
2+6.7%	0.31	5	0.928	22	-17	289	
2+12.5%	0.31	4	0.918	25	-21	441	
3	0.12	43	0.743	48	-5	25	
3+0%	0.26	18	0.878	39	-21	441	
3+1.3%	0.27	16	0.916	27	-11	121	
3+6.7%	0.35	1	0.990	8	-7	49	
3+12.5%	0.33	2	1.003	6	-4	16	
4	0.23	21	0.914	28	-7	49	
4+0%	0.24	20	0.944	15	5	25	
4+1.3%	0.22	24	0.903	32	-8	64	
4+6.7%	0.23	22	0.937	18	4	16	
4+12.5%	0.22	23	0.913	29	-6	36	
5	0.15	36	0.804	47	-11	121	
5+0%	0.14	38	0.734	49	-11	121	0.578

5+1.3%	0.18	32	0.863	42	-10	100
5+6.7%	0.16	35	0.874	41	-6	36
5+12.5%	0.19	30	0.881	38	-8	64
6	0.09	49	0.895	33	16	256
6+0%	0.11	44	0.903	31	13	169
6+1.3%	0.11	48	0.907	30	18	324
6+6.7%	0.13	41	0.917	26	15	225
6+12.5%	0.12	42	0.931	21	21	441
7	0.28	14	1.036	1	13	169
7+0%	0.27	15	0.933	20	-5	25
7+1.3%	0.31	6	0.920	24	-18	324
7+6.7%	0.30	8	0.940	17	-9	81
7+12.5%	0.29	13	0.973	10	3	9
8	0.18	33	0.952	14	19	361
8+0%	0.20	29	0.959	13	16	256
8+1.3%	0.20	28	0.980	9	19	361
8+6.7%	0.18	31	0.969	12	19	361
8+12.5%	0.17	34	0.973	11	23	529
9	0.13	40	0.882	37	3	9
9+0%	0.11	45	0.890	34	11	121
9+1.3%	0.13	39	0.884	35	4	16
9+6.7%	0.11	46	0.883	36	10	100
9+12.5%	0.11	47	0.877	40	7	49
0.0%	0.22	25	0.806	46	-21	441
1.3%	0.20	27	0.813	45	-18	324
6.7%	0.21	26	0.819	44	-18	324
12.5%	0.14	37	0.831	43	-6	36
				Sum	0	8264

d)

Biomass	Resilience Coef.		Capacity		Spearman's Correlation		
Sample	Resil. Coef.	Rank (a)	Cap (mL)	Rank (b)	d_i	d_i^2	Rank Corr. Coef. (r_s)
1	3.70	5	117	7	-2	4	
1+0%	4.09	1	120	5	-4	16	
1+1.3%	3.97	2	121	4	-2	4	
1+6.7%	3.84	4	122	2	2	4	
1+12.5%	3.89	3	122	3	0	0	
2	3.31	10	111	18	-8	64	
2+0%	3.56	7	110	23	-16	256	
2+1.3%	3.65	6	111	16	-10	100	
2+6.7%	3.47	8	110	22	-14	196	

2+12.5%	3.34	9	109	25	-16	256	
3	0.44	49	88	48	1	1	
3+0%	1.55	35	104	38	-3	9	
3+1.3%	1.96	26	108	27	-1	1	
3+6.7%	2.54	12	117	8	4	16	
3+12.5%	2.63	11	119	6	5	25	
4	2.31	17	108	28	-11	121	
4+0%	2.49	13	112	15	-2	4	
4+1.3%	2.26	18	107	32	-14	196	
4+6.7%	2.23	19	111	19	0	0	
4+12.5%	2.19	20	108	29	-9	81	
5	0.70	47	94	47	0	0	
5+0%	0.63	48	86	49	-1	1	0.819
5+1.3%	1.24	42	101	42	0	0	
5+6.7%	1.20	45	103	41	4	16	
5+12.5%	1.21	44	103	40	4	16	
6	1.38	40	106	33	7	49	
6+0%	1.64	32	107	31	1	1	
6+1.3%	1.60	34	107	30	4	16	
6+6.7%	1.48	38	109	26	12	144	
6+12.5%	0.99	46	110	21	25	625	
7	2.38	15	123	1	14	196	
7+0%	1.99	25	110	20	5	25	
7+1.3%	1.94	27	109	24	3	9	
7+6.7%	1.93	28	111	17	11	121	
7+12.5%	2.04	24	115	11	13	169	
8	2.11	23	113	14	9	81	
8+0%	2.41	14	114	13	1	1	
8+1.3%	2.34	16	116	9	7	49	
8+6.7%	2.13	22	115	12	10	100	
8+12.5%	2.13	21	115	10	11	121	
9	1.76	30	104	37	-7	49	
9+0%	1.63	33	105	34	-1	1	
9+1.3%	1.68	31	105	35	-4	16	
9+6.7%	1.55	36	105	36	0	0	
9+12.5%	1.22	43	104	39	4	16	
0.0%	1.83	29	96	46	-17	289	
1.3%	1.42	39	96	45	-6	36	
6.7%	1.54	37	97	44	-7	49	
12.5%	1.25	41	99	43	-2	4	
				Sum	0	3554	

e)

Biomass	Resil. Coef.		Perturbed Biogas Yield		Spearman's Correlation		
Sample	Resil. Coef.	Rank (a)	PBY (mL/mL)	Rank (b)	d_i	d_i^2	Rank Corr. Coef. (r_s)
1	3.70	5	0.991	7	-2	4	
1+0%	4.09	1	1.013	5	-4	16	
1+1.3%	3.97	2	1.024	4	-2	4	
1+6.7%	3.84	4	1.031	2	2	4	
1+12.5%	3.89	3	1.026	3	0	0	
2	3.31	10	0.937	19	-9	81	
2+0%	3.56	7	0.925	23	-16	256	
2+1.3%	3.65	6	0.941	16	-10	100	
2+6.7%	3.47	8	0.928	22	-14	196	
2+12.5%	3.34	9	0.918	25	-16	256	
3	0.44	49	0.743	48	1	1	
3+0%	1.55	35	0.878	39	-4	16	
3+1.3%	1.96	26	0.916	27	-1	1	
3+6.7%	2.54	12	0.990	8	4	16	
3+12.5%	2.63	11	1.003	6	5	25	
4	2.31	17	0.914	28	-11	121	
4+0%	2.49	13	0.944	15	-2	4	
4+1.3%	2.26	18	0.903	32	-14	196	
4+6.7%	2.23	19	0.937	18	1	1	
4+12.5%	2.19	20	0.913	29	-9	81	
5	0.70	47	0.804	47	0	0	
5+0%	0.63	48	0.734	49	-1	1	0.816
5+1.3%	1.24	42	0.863	42	0	0	
5+6.7%	1.20	45	0.874	41	4	16	
5+12.5%	1.21	44	0.881	38	6	36	
6	1.38	40	0.895	33	7	49	
6+0%	1.64	32	0.903	31	1	1	
6+1.3%	1.60	34	0.907	30	4	16	
6+6.7%	1.48	38	0.917	26	12	144	
6+12.5%	0.99	46	0.931	21	25	625	
7	2.38	15	1.036	1	14	196	
7+0%	1.99	25	0.933	20	5	25	
7+1.3%	1.94	27	0.920	24	3	9	
7+6.7%	1.93	28	0.940	17	11	121	
7+12.5%	2.04	24	0.973	10	14	196	
8	2.11	23	0.952	14	9	81	
8+0%	2.41	14	0.959	13	1	1	
8+1.3%	2.34	16	0.980	9	7	49	

8+6.7%	2.13	22	0.969	12	10	100	
8+12.5%	2.13	21	0.973	11	10	100	
9	1.76	30	0.882	37	-7	49	
9+0%	1.63	33	0.890	34	-1	1	
9+1.3%	1.68	31	0.884	35	-4	16	
9+6.7%	1.55	36	0.883	36	0	0	
9+12.5%	1.22	43	0.877	40	3	9	
0.0%	1.83	29	0.806	46	-17	289	
1.3%	1.42	39	0.813	45	-6	36	
6.7%	1.54	37	0.819	44	-7	49	
12.5%	1.25	41	0.831	43	-2	4	
				Sum	0	3598	

f)

Biomass	Perturbed Biogas Yield		Capacity		Spearman's Correlation		
Sample	PBY (mL/mL)	Rank (a)	Cap (mL)	Rank (b)	d_i	d_i^2	Rank Corr. Coef. (r_s)
1	0.991	7	117	7	0	0	
1+0%	1.013	5	120	5	0	0	
1+1.3%	1.024	4	121	4	0	0	
1+6.7%	1.031	2	122	2	0	0	
1+12.5%	1.026	3	122	3	0	0	
2	0.937	19	111	18	1	1	
2+0%	0.925	23	110	23	0	0	
2+1.3%	0.941	16	111	16	0	0	
2+6.7%	0.928	22	110	22	0	0	
2+12.5%	0.918	25	109	25	0	0	
3	0.743	48	88	48	0	0	
3+0%	0.878	39	104	38	1	1	
3+1.3%	0.916	27	108	27	0	0	
3+6.7%	0.990	8	117	8	0	0	
3+12.5%	1.003	6	119	6	0	0	
4	0.914	28	108	28	0	0	
4+0%	0.944	15	112	15	0	0	
4+1.3%	0.903	32	107	32	0	0	
4+6.7%	0.937	18	111	19	-1	1	
4+12.5%	0.913	29	108	29	0	0	
5	0.804	47	94	47	0	0	
5+0%	0.734	49	86	49	0	0	0.9995
5+1.3%	0.863	42	101	42	0	0	
5+6.7%	0.874	41	103	41	0	0	

5+12.5%	0.881	38	103	40	-2	4
6	0.895	33	106	33	0	0
6+0%	0.903	31	107	31	0	0
6+1.3%	0.907	30	107	30	0	0
6+6.7%	0.917	26	109	26	0	0
6+12.5%	0.931	21	110	21	0	0
7	1.036	1	123	1	0	0
7+0%	0.933	20	110	20	0	0
7+1.3%	0.920	24	109	24	0	0
7+6.7%	0.940	17	111	17	0	0
7+12.5%	0.973	10	115	11	-1	1
8	0.952	14	113	14	0	0
8+0%	0.959	13	114	13	0	0
8+1.3%	0.980	9	116	9	0	0
8+6.7%	0.969	12	115	12	0	0
8+12.5%	0.973	11	115	10	1	1
9	0.882	37	104	37	0	0
9+0%	0.890	34	105	34	0	0
9+1.3%	0.884	35	105	35	0	0
9+6.7%	0.883	36	105	36	0	0
9+12.5%	0.877	40	104	39	1	1
0.0%	0.806	46	96	46	0	0
1.3%	0.813	45	96	45	0	0
6.7%	0.819	44	97	44	0	0
12.5%	0.831	43	99	43	0	0
				Sum	0	10

5.5.4 Appendix D: Correlation between SMA and Overload Response

Since 49 samples were analyzed using Spearman's Correlation Coefficient, the critical values provided in Table 5D-1 apply to the tabulated data used to determine Spearman's Rank Correlation Coefficients for SMA and OOPA parameters (Tables 5D-2 through 5D-6).

Table 5D-1. Critical Values of the Spearman's Rank Correlation Coefficients for Two-Tailed Probabilities at n = 49 (Zar, 1972)

Probability	**0.50**	**0.20**	**0.10**	**0.05**	**0.02**	**0.01**	**0.005**	**0.002**	**0.001**
r_s	0.098	0.186	0.238	0.282	0.333	0.366	0.397	0.434	0.460

Table 5D-2. SMA Correlation with Methanogenesis Rate in OOPA Tests Using Spearman's Rank Correlation Coefficient was 0.561

Biomass Sample	SMA ($mL\ CH_4$/ mg iATP-h)	SMA Rank	OOPA Meth. Rate (mL/h)	Meth. Rate Rank	d_i	d_i^2	Spearman's Correlation Rank Corr. Coef. (r_s)
1	77	5	1.45	9	-4	16	
1+0%	87	3	1.56	3	0	0	
1+1.3%	91	1	1.33	15	-14	196	
1+6.7%	88	2	1.40	10	-8	64	
1+12.5%	83	4	1.54	5	-1	1	
2	62	7	1.63	1	6	36	
2+0%	64	6	1.49	8	-2	4	
2+1.3%	56	9	1.49	7	2	4	
2+6.7%	55	10	1.57	2	8	64	
2+12.5%	61	8	1.56	4	4	16	
3	46	17	0.44	49	-32	1024	
3+0%	52	11	1.00	23	-12	144	
3+1.3%	45	18	1.06	20	-2	4	
3+6.7%	41	23	1.36	12	11	121	
3+12.5%	50	12	1.31	17	-5	25	
4	39	27	1.38	11	16	256	
4+0%	43	21	1.50	6	15	225	
4+1.3%	37	31	1.31	16	15	225	
4+6.7%	40	26	1.36	13	13	169	
4+12.5%	37	30	1.34	14	16	256	
5	35	35	0.50	47	-12	144	
5+0%	44	19	0.48	48	-29	841	0.561
5+1.3%	49	15	0.62	39	-24	576	
5+6.7%	41	22	0.59	40	-18	324	
5+12.5%	47	16	0.59	41	-25	625	
6	35	36	0.57	42	-6	36	
6+0%	40	24	0.65	37	-13	169	
6+1.3%	37	33	0.62	38	-5	25	
6+6.7%	40	25	0.57	44	-19	361	
6+12.5%	35	37	0.55	46	-9	81	
7	30	41	1.03	21	20	400	
7+0%	38	29	0.97	24	5	25	
7+1.3%	39	28	1.08	18	10	100	
7+6.7%	37	32	1.08	19	13	169	
7+12.5%	50	14	1.02	22	-8	64	
8	26	44	0.66	35	9	81	
8+0%	36	34	0.83	26	8	64	

8+1.3%	33	39	0.82	27	12	144
8+6.7%	30	40	0.73	31	9	81
8+12.5%	30	42	0.66	36	6	36
9	15	48	0.75	30	18	324
9+0%	24	45	0.68	34	11	121
9+1.3%	16	47	0.73	32	15	225
9+6.7%	14	49	0.68	33	16	256
9+12.5%	17	46	0.56	45	1	1
0.0%	50	13	0.94	25	-12	144
1.3%	44	20	0.78	29	-9	81
6.7%	29	43	0.81	28	15	225
12.5%	35	38	0.57	43	-5	25
					0	8598

Table 5D-3. SMA Correlation with M/F Ratio Using Spearman's Rank Correlation Coefficient was 0.628

Biomass	SMA		M/F Ratio		Spearman's Correlation		
Sample	(mL CH_4/ mg iATP-h)	SMA Rank	M/F Ratio	Rank	d_i	d_i^2	Rank Corr. Coef. (r_s)
1	77	5	0.29	11	-6	36	
1+0%	87	3	0.30	9	-6	36	
1+1.3%	91	1	0.25	19	-18	324	
1+6.7%	88	2	0.27	17	-15	225	
1+12.5%	83	4	0.31	7	-3	9	
2	62	7	0.33	3	4	16	
2+0%	64	6	0.29	10	-4	16	
2+1.3%	56	9	0.29	12	-3	9	
2+6.7%	55	10	0.31	5	5	25	
2+12.5%	61	8	0.31	4	4	16	
3	46	17	0.12	43	-26	676	
3+0%	52	11	0.26	18	-7	49	
3+1.3%	45	18	0.27	16	2	4	
3+6.7%	41	23	0.35	1	22	484	
3+12.5%	50	12	0.33	2	10	100	
4	39	27	0.23	21	6	36	
4+0%	43	21	0.24	20	1	1	
4+1.3%	37	31	0.22	24	7	49	
4+6.7%	40	26	0.23	22	4	16	
4+12.5%	37	30	0.22	23	7	49	
5	35	35	0.15	36	-1	1	
5+0%	44	19	0.14	38	-19	361	0.628
5+1.3%	49	15	0.18	32	-17	289	

5+6.7%	41	22	0.16	35	-13	169
5+12.5%	47	16	0.19	30	-14	196
6	35	36	0.09	49	-13	169
6+0%	40	24	0.11	44	-20	400
6+1.3%	37	33	0.11	48	-15	225
6+6.7%	40	25	0.13	41	-16	256
6+12.5%	35	37	0.12	42	-5	25
7	30	41	0.28	14	27	729
7+0%	38	29	0.27	15	14	196
7+1.3%	39	28	0.31	6	22	484
7+6.7%	37	32	0.30	8	24	576
7+12.5%	50	14	0.29	13	1	1
8	26	44	0.18	33	11	121
8+0%	36	34	0.20	29	5	25
8+1.3%	33	39	0.20	28	11	121
8+6.7%	30	40	0.18	31	9	81
8+12.5%	30	42	0.17	34	8	64
9	15	48	0.13	40	8	64
9+0%	24	45	0.11	45	0	0
9+1.3%	16	47	0.13	39	8	64
9+6.7%	14	49	0.11	46	3	9
9+12.5%	17	46	0.11	47	-1	1
0.0%	50	13	0.22	25	-12	144
1.3%	44	20	0.20	27	-7	49
6.7%	29	43	0.21	26	17	289
12.5%	35	38	0.14	37	1	1
					0	7286

Table 5D-4. SMA Correlation with Resilience Coefficient Using Spearman's Rank Correlation Coefficient was 0.481

Biomass Sample	SMA (mL CH_4/ mg iATP-h)	SMA Rank	Resil. Coef. RC	RC Rank	Spearman's Correlation d_i	d_i^2	Rank Corr. Coef. (r_s)
1	77	5	3.70	5	0	0	
1+0%	87	3	4.09	1	2	4	
1+1.3%	91	1	3.97	2	-1	1	
1+6.7%	88	2	3.84	4	-2	4	
1+12.5%	83	4	3.89	3	1	1	
2	62	7	3.31	10	-3	9	
2+0%	64	6	3.56	7	-1	1	
2+1.3%	56	9	3.65	6	3	9	
2+6.7%	55	10	3.47	8	2	4	

2+12.5%	61	8	3.34	9	-1	1	
3	46	17	0.44	49	-32	1024	
3+0%	52	11	1.55	35	-24	576	
3+1.3%	45	18	1.96	26	-8	64	
3+6.7%	41	23	2.54	12	11	121	
3+12.5%	50	12	2.63	11	1	1	
4	39	27	2.31	17	10	100	
4+0%	43	21	2.49	13	8	64	
4+1.3%	37	31	2.26	18	13	169	
4+6.7%	40	26	2.23	19	7	49	
4+12.5%	37	30	2.19	20	10	100	
5	35	35	0.70	47	-12	144	
5+0%	44	19	0.63	48	-29	841	0.481
5+1.3%	49	15	1.24	42	-27	729	
5+6.7%	41	22	1.20	45	-23	529	
5+12.5%	47	16	1.21	44	-28	784	
6	35	36	1.38	40	-4	16	
6+0%	40	24	1.64	32	-8	64	
6+1.3%	37	33	1.60	34	-1	1	
6+6.7%	40	25	1.48	38	-13	169	
6+12.5%	35	37	0.99	46	-9	81	
7	30	41	2.38	15	26	676	
7+0%	38	29	1.99	25	4	16	
7+1.3%	39	28	1.94	27	1	1	
7+6.7%	37	32	1.93	28	4	16	
7+12.5%	50	14	2.04	24	-10	100	
8	26	44	2.11	23	21	441	
8+0%	36	34	2.41	14	20	400	
8+1.3%	33	39	2.34	16	23	529	
8+6.7%	30	40	2.13	22	18	324	
8+12.5%	30	42	2.13	21	21	441	
9	15	48	1.76	30	18	324	
9+0%	24	45	1.63	33	12	144	
9+1.3%	16	47	1.68	31	16	256	
9+6.7%	14	49	1.55	36	13	169	
9+12.5%	17	46	1.22	43	3	9	
0.0%	50	13	1.83	29	-16	256	
1.3%	44	20	1.42	39	-19	361	
6.7%	29	43	1.54	37	6	36	
12.5%	35	38	1.25	41	-3	9	
					0	10168	

Table 5D-5 SMA Correlation with Capacity Using Spearman's Rank Correlation Coefficient was 0.266

Biomass Sample	SMA (mL CH_4/ mg iATP-h)	SMA Rank	Capacity (mL)	Capacity Rank	Spearman's Correlation d_i	d_i^2	Rank Corr. Coef. (r_s)
1	77	5	117	7	-2	4	
1+0%	87	3	120	5	-2	4	
1+1.3%	91	1	121	4	-3	9	
1+6.7%	88	2	122	2	0	0	
1+12.5%	83	4	122	3	1	1	
2	62	7	111	18	-11	121	
2+0%	64	6	110	23	-17	289	
2+1.3%	56	9	111	16	-7	49	
2+6.7%	55	10	110	22	-12	144	
2+12.5%	61	8	109	25	-17	289	
3	46	17	88	48	-31	961	
3+0%	52	11	104	38	-27	729	
3+1.3%	45	18	108	27	-9	81	
3+6.7%	41	23	117	8	15	225	
3+12.5%	50	12	119	6	6	36	
4	39	27	108	28	-1	1	
4+0%	43	21	112	15	6	36	
4+1.3%	37	31	107	32	-1	1	
4+6.7%	40	26	111	19	7	49	
4+12.5%	37	30	108	29	1	1	
5	35	35	94	47	-12	144	
5+0%	44	19	86	49	-30	900	0.266
5+1.3%	49	15	101	42	-27	729	
5+6.7%	41	22	103	41	-19	361	
5+12.5%	47	16	103	40	-24	576	
6	35	36	106	33	3	9	
6+0%	40	24	107	31	-7	49	
6+1.3%	37	33	107	30	3	9	
6+6.7%	40	25	109	26	-1	1	
6+12.5%	35	37	110	21	16	256	
7	30	41	123	1	40	1600	
7+0%	38	29	110	20	9	81	
7+1.3%	39	28	109	24	4	16	
7+6.7%	37	32	111	17	15	225	
7+12.5%	50	14	115	11	3	9	
8	26	44	113	14	30	900	
8+0%	36	34	114	13	21	441	
8+1.3%	33	39	116	9	30	900	

8+6.7%	30	40	115	12	28	784	
8+12.5%	30	42	115	10	32	1024	
9	15	48	104	37	11	121	
9+0%	24	45	105	34	11	121	
9+1.3%	16	47	105	35	12	144	
9+6.7%	14	49	105	36	13	169	
9+12.5%	17	46	104	39	7	49	
0.0%	50	13	96	46	-33	1089	
1.3%	44	20	96	45	-25	625	
6.7%	29	43	97	44	-1	1	
12.5%	35	38	99	43	-5	25	
					0	14388	

Table 5D-6. SMA Correlation with Perturbed Biogas (PBY) Yield Using Spearman's Rank Correlation Coefficient

Biomass Sample	SMA (mL CH_4/ mg iATP-h)	SMA Rank	PBY	Rank	d_i	d_i^2	Spearman's Correlation Rank Corr. Coef. (r_s)
1	77	5	0.991	7	-2	4	
1+0%	87	3	1.013	5	-2	4	
1+1.3%	91	1	1.024	4	-3	9	
1+6.7%	88	2	1.031	2	0	0	
1+12.5%	83	4	1.026	3	1	1	
2	62	7	0.937	19	-12	144	
2+0%	64	6	0.925	23	-17	289	
2+1.3%	56	9	0.941	16	-7	49	
2+6.7%	55	10	0.928	22	-12	144	
2+12.5%	61	8	0.918	25	-17	289	
3	46	17	0.743	48	-31	961	
3+0%	52	11	0.878	39	-28	784	
3+1.3%	45	18	0.916	27	-9	81	
3+6.7%	41	23	0.990	8	15	225	
3+12.5%	50	12	1.003	6	6	36	
4	39	27	0.914	28	-1	1	
4+0%	43	21	0.944	15	6	36	
4+1.3%	37	31	0.903	32	-1	1	
4+6.7%	40	26	0.937	18	8	64	
4+12.5%	37	30	0.913	29	1	1	
5	35	35	0.804	47	-12	144	
5+0%	44	19	0.734	49	-30	900	0.269
5+1.3%	49	15	0.863	42	-27	729	
5+6.7%	41	22	0.874	41	-19	361	
5+12.5%	47	16	0.881	38	-22	484	

6	35	36	0.895	33	3	9
6+0%	40	24	0.903	31	-7	49
6+1.3%	37	33	0.907	30	3	9
6+6.7%	40	25	0.917	26	-1	1
6+12.5%	35	37	0.931	21	16	256
7	30	41	1.036	1	40	1600
7+0%	38	29	0.933	20	9	81
7+1.3%	39	28	0.920	24	4	16
7+6.7%	37	32	0.940	17	15	225
7+12.5%	50	14	0.973	10	4	16
8	26	44	0.952	14	30	900
8+0%	36	34	0.959	13	21	441
8+1.3%	33	39	0.980	9	30	900
8+6.7%	30	40	0.969	12	28	784
8+12.5%	30	42	0.973	11	31	961
9	15	48	0.882	37	11	121
9+0%	24	45	0.890	34	11	121
9+1.3%	16	47	0.884	35	12	144
9+6.7%	14	49	0.883	36	13	169
9+12.5%	17	46	0.877	40	6	36
0.0%	50	13	0.806	46	-33	1089
1.3%	44	20	0.813	45	-25	625
6.7%	29	43	0.819	44	-1	1
12.5%	35	38	0.831	43	-5	25
					0	14320

5.5.5 Appendix E: Correlation between Structure and Function Using Spearman's Rank Correlation Coefficient

Spearman's Rank Correlation Coefficients and corresponding criteria levels are presented in Table 5E-1. SMA and densitometric data correlated above the 99.9% level (r_s = 0.486) (Table 5E-2), the secondary slope in the OOPA test and densitometric data correlated above the 90% level (r_s = 0.254) (Table 5E-3), and M/F ratio and densitometric data correlated above the 80% level (r_s = 0.223) (Table 5E-4) for two-tailed tests (Zar, 1972).

Table 5E-1. Critical Values of the Spearman's Rank Correlation Coefficients for Two-Tailed Probabilities at n = 49 (Zar, 1972)

Probability	**0.50**	**0.20**	**0.10**	**0.05**	**0.02**	**0.01**	**0.005**	**0.002**	**0.001**
r_s	0.098	0.186	0.238	0.282	0.333	0.366	0.397	0.434	0.460

Table 5E-2. Correlation Between SMA with propionate and Densitometric Data From DGGE Banding Patterns

Biomass Sample	SMA ($mL\ CH_4$/ mg iATP-h)	SMA Rank	Densitometric Data Distance from: 1+1.3%	DD Rank	d_i	d_i^2	Spearman's Correlation Rank Corr. Coef. (r_s)
1	76.95	5	0.031	4	1	1	
1+0%	87.30	3	0.309	24	-21	441	
1+1.3%	90.53	1	0.000	1	0	0	
1+6.7%	88.26	2	0.012	2	0	0	
1+12.5%	83.15	4	0.021	3	1	1	
2	62.09	7	0.296	23	-16	256	
2+0%	63.56	6	0.191	18	-12	144	
2+1.3%	56.08	9	0.110	12	-3	9	
2+6.7%	55.24	10	0.182	17	-7	49	
2+12.5%	61.23	8	0.461	31	-23	529	
3	46.11	17	0.400	28	-11	121	
3+0%	52.08	11	0.198	20	-9	81	
3+1.3%	45.29	18	0.690	41	-23	529	
3+6.7%	40.83	23	0.631	37	-14	196	
3+12.5%	50.42	12	0.368	25	-13	169	
4	39.03	27	0.074	7	20	400	
4+0%	42.95	21	0.117	13	8	64	
4+1.3%	37.08	31	0.059	5	26	676	
4+6.7%	39.80	26	0.196	19	7	49	
4+12.5%	37.36	30	0.085	10	20	400	
5	35.39	35	0.634	38	-3	9	
5+0%	44.22	19	0.693	42	-23	529	
5+1.3%	48.88	15	0.260	21	-6	36	
5+6.7%	40.94	22	0.374	26	-4	16	
5+12.5%	46.57	16	0.573	35	-19	361	0.486
6	35.28	36	0.560	34	2	4	
6+0%	40.16	24	0.643	39	-15	225	
6+1.3%	36.90	33	0.153	15	18	324	
6+6.7%	39.85	25	0.383	27	-2	4	
6+12.5%	34.89	37	0.163	16	21	441	
7	29.98	41	0.122	14	27	729	
7+0%	37.69	29	0.093	11	18	324	
7+1.3%	38.81	28	0.073	6	22	484	
7+6.7%	36.99	32	0.074	8	24	576	
7+12.5%	50.05	14	0.075	9	5	25	

8	25.84	44	0.557	33	11	121
8+0%	36.00	34	0.719	43	-9	81
8+1.3%	32.78	39	1.162	49	-10	100
8+6.7%	30.32	40	0.445	29	11	121
8+12.5%	29.63	42	0.624	36	6	36
9	15.39	48	1.107	48	0	0
9+0%	24.22	45	0.978	47	-2	4
9+1.3%	16.31	47	0.969	46	1	1
9+6.7%	13.74	49	0.914	44	5	25
9+12.5%	16.88	46	0.921	45	1	1
0%	50.29	13	0.648	40	-27	729
1.3%	44.01	20	0.467	32	-12	144
6.7%	29.33	43	0.292	22	21	441
12.5%	34.54	38	0.460	30	8	64
					0	10070

Table 5E-3. Correlation Between Secondary Slope of OOPA Test (i.e., M, methanogenesis rate) and Densitometric Data Using Spearman's Rank Correlation Coefficient

Biomass Sample	Initial Slope OOPA (Meth. Rate)	Rank	Densitometric Data Distance from: 2	Rank	d_i	d_i^2	Spearman's Correlation Rank Corr. Coef. (r_s)
1	1.45	9	0.2754	28	-19	361	
1+0%	1.56	3	0.0087	2	1	1	
1+1.3%	1.33	15	0.2956	30	-15	225	
1+6.7%	1.40	10	0.2074	20	-10	100	
1+12.5%	1.54	5	0.1885	18	-13	169	
2	1.63	1	0.0000	1	0	0	
2+0%	1.49	8	0.0567	7	1	1	
2+1.3%	1.49	7	0.1046	12	-5	25	
2+6.7%	1.57	2	0.0194	4	-2	4	
2+12.5%	1.56	4	0.0364	5	-1	1	
3	0.44	49	0.6980	42	7	49	
3+0%	1.00	23	0.5657	40	-17	289	
3+1.3%	1.06	20	1.0584	49	-29	841	
3+6.7%	1.36	12	1.0425	48	-36	1296	
3+12.5%	1.31	17	0.5283	39	-22	484	
4	1.38	11	0.1889	19	-8	64	
4+0%	1.50	6	0.3254	32	-26	676	
4+1.3%	1.31	16	0.3829	34	-18	324	
4+6.7%	1.36	13	0.4221	36	-23	529	0.254
4+12.5%	1.34	14	0.3159	31	-17	289	

5	0.50	47	0.9402	46	1	1
5+0%	0.48	48	0.9880	47	1	1
5+1.3%	0.62	39	0.6370	41	-2	4
5+6.7%	0.59	40	0.7185	43	-3	9
5+12.5%	0.59	41	0.9208	45	-4	16
6	0.57	42	0.0583	8	34	1156
6+0%	0.65	37	0.0918	10	27	729
6+1.3%	0.62	38	0.0470	6	32	1024
6+6.7%	0.57	44	0.0111	3	41	1681
6+12.5%	0.55	46	0.1155	14	32	1024
7	1.03	21	0.2387	22	-1	1
7+0%	0.97	24	0.1755	17	7	49
7+1.3%	1.08	18	0.2597	26	-8	64
7+6.7%	1.08	19	0.2131	21	-2	4
7+12.5%	1.02	22	0.2518	25	-3	9
8	0.66	35	0.0920	11	24	576
8+0%	0.83	26	0.1632	16	10	100
8+1.3%	0.82	27	0.4398	37	-10	100
8+6.7%	0.73	31	0.0686	9	22	484
8+12.5%	0.66	36	0.1148	13	23	529
9	0.75	30	0.4109	35	-5	25
9+0%	0.68	34	0.2813	29	5	25
9+1.3%	0.73	32	0.2747	27	5	25
9+6.7%	0.68	33	0.2388	23	10	100
9+12.5%	0.56	45	0.2488	24	21	441
0%	0.94	25	0.7487	44	-19	361
1.3%	0.78	29	0.5041	38	-9	81
6.7%	0.81	28	0.1368	15	13	169
12.5%	0.57	43	0.3396	33	10	100
					0	14616

Table 5E-4. Correlation Between M/F Ratio and Densitometric Data Using Spearman's Rank Correlation Coefficient

Biomass	M/F		Densitometric Data		Spearman's Correlation		
Sample	Ratio	M/F Rank	Distance from: 3+6.7%	DD Rank	d_i	d_i^2	Rank Corr. Coef. (r_s)
1	0.287	11	0.829	21	-10	100	
1+0%	0.303	9	1.056	35	-26	676	
1+1.3%	0.252	19	0.631	16	3	9	
1+6.7%	0.272	17	0.751	19	-2	4	
1+12.5%	0.307	7	0.686	17	-10	100	

2	0.332	3	1.043	33	-30	900	
2+0%	0.289	10	1.135	37	-27	729	
2+1.3%	0.286	12	0.986	29	-17	289	
2+6.7%	0.312	5	1.006	31	-26	676	
2+12.5%	0.313	4	1.012	32	-28	784	
3	0.117	43	0.069	7	36	1296	
3+0%	0.258	18	0.156	9	9	81	
3+1.3%	0.273	16	0.008	2	14	196	
3+6.7%	0.347	1	0.000	1	0	0	
3+12.5%	0.334	2	0.163	10	-8	64	
4	0.232	21	0.879	22	-1	1	
4+0%	0.243	20	0.880	23	-3	9	
4+1.3%	0.218	24	0.740	18	6	36	
4+6.7%	0.225	22	0.898	25	-3	9	
4+12.5%	0.223	23	0.790	20	3	9	
5	0.145	36	0.016	4	32	1024	
5+0%	0.136	38	0.021	5	33	1089	
5+1.3%	0.182	32	0.108	8	24	576	
5+6.7%	0.165	35	0.057	6	29	841	
5+12.5%	0.187	30	0.015	3	27	729	0.223
6	0.094	49	1.185	41	8	64	
6+0%	0.111	44	1.189	42	2	4	
6+1.3%	0.107	48	0.985	28	20	400	
6+6.7%	0.129	41	1.054	34	7	49	
6+12.5%	0.118	42	0.595	15	27	729	
7	0.279	14	1.057	36	-22	484	
7+0%	0.275	15	0.998	30	-15	225	
7+1.3%	0.307	6	0.882	24	-18	324	
7+6.7%	0.304	8	0.931	26	-18	324	
7+12.5%	0.285	13	0.945	27	-14	196	
8	0.179	33	1.176	40	-7	49	
8+0%	0.201	29	1.314	48	-19	361	
8+1.3%	0.203	28	1.431	49	-21	441	
8+6.7%	0.182	31	1.161	38	-7	49	
8+12.5%	0.172	34	1.265	44	-10	100	
9	0.132	40	1.172	39	1	1	
9+0%	0.111	45	1.308	47	-2	4	
9+1.3%	0.133	39	1.305	46	-7	49	
9+6.7%	0.109	46	1.282	45	1	1	
9+12.5%	0.108	47	1.254	43	4	16	
0%	0.215	25	0.280	11	14	196	
1.3%	0.204	27	0.356	12	15	225	
6.7%	0.210	26	0.558	14	12	144	

12.5%	0.143	37	0.451	13	24	576
					0	15238

5.6 REFERENCES

Allison, S. D., & Martiny, J. B. H. (2008). Resistance , resilience , and redundancy in microbial communities. *Proceedings of the National Academy of Sciences of the United States of America*, *105*, 11415-11519.

Angenent, L. T., Karim, K., Al-Dahhan, M. H., Wrenn, B. A., & Domíguez-Espinosa, R. (2004). Production of bioenergy and biochemicals from industrial and agricultural wastewater. *Trends in Biotechnology*, *22*(9), 477-85. doi:10.1016/j.tibtech.2004.07.001

Batstone, D. J., Keller, J., Angelidaki, I., Kalyuzhnyi, S. V., Pavlostathis, S. G., Rozzi, A, Sanders, W. T. M., et al. (2002). The IWA Anaerobic Digestion Model No. 1 (ADM1). *Water Science and Technology*, *45*(10), 65-73. Retrieved from http://www.ncbi.nlm.nih.gov/pubmed/12188579

Benigni, R., & Bossa, C. (2008). Predictivity of QSAR. *Journal of Chemical Information and Modeling*, *48*(5), 971-80. doi:10.1021/ci8000088

Curtis, T. P., Head, I. M., & Graham, D. W. (2003). Theoretical Ecology for Engineering Biology. *Environmental Science and Technology*, *37*(3), 64A-70A. doi:10.1021/es0323493

Dearman, B., Marschner, P., & Bentham, R. H. (2006). Methane production and microbial community structure in single-stage batch and sequential batch systems anaerobically co-digesting food waste and biosolids. *Applied Microbiology and Biotechnology*, *69*, 589-596. doi:10.1007/s00253-005-0076-9

Downing, A. L., Painter, H. A., & Knowles, G. (1964). Nitrification in the Activated-Sludge Process. *Journal of the Institute of Sewage Purification*, *2*, 130-158.

Eriksson, L., Jaworska, J., Worth, A. P., Cronin, M. T. D., McDowell, R. M., & Gramatica, P. (2003). Methods for Reliability and Uncertainty Assessment and for Applicability Evaluations of Classification- and Regression-Based QSARs. *Environmental Health Perspectives*, *111*(10), 1361-1375. doi:10.1289/ehp.5758

Fernandez, A. S., Hashsham, S. A., Dollhopf, S. L., Raskin, L., Glagoleva, O., Dazzo, F. B., Hickey, R. F., et al. (2000). Flexible Community Structure Correlates with Stable Community Function in Methanogenic Bioreactor Communities Perturbed by Glucose. *Applied and Environmental Microbiology*, *66*(9), 4058-4067. doi:10.1128/AEM.66.9.4058-4067.2000.Updated

Hashsham, S. A., Fernandez, A. S., Dollhopf, S. L., Dazzo, F. B., Hickey, R. F., Tiedje, J. M., & Criddle, C. S. (2000). Parallel processing of substrate correlates with greater functional stability in methanogenic bioreactor communities perturbed by glucose. *Applied and Environmental Microbiology*, *66*(9), 4050-7. Retrieved from http://www.pubmedcentral.nih.gov/articlerender.fcgi?artid=92258&tool=pmcentrez&rendertype=abstract

Holm-Nielsen, J. B., Al Seadi, T., & Oleskowicz-Popiel, P. (2009). The future of anaerobic digestion and biogas utilization. *Bioresource Technology*, *100*(22), 5478-84. Elsevier Ltd. doi:10.1016/j.biortech.2008.12.046

Karakashev, D., Batstone, D. J., & Angelidaki, I. (2005). Influence of Environmental Conditions on Methanogenic Compositions in Anaerobic Biogas Reactors. *Applied and Environmental Microbiology*, *71*(1), 331-338. doi:10.1128/AEM.71.1.331

Knowles, B. Y. G., Downing, A. L., & Barrett, M. J. (1965). Determination of Kinetic Constants for Nitrifying Bacteria in Mixed Culture, with the Aid of an Electronic Computer. *Journal of General Microbiology*, *38*, 263-278.

Konovalov, D. A., Llewellyn, L. E., Vander Heyden, Y., & Coomans, D. (2008). Robust cross-validation of linear regression QSAR models. *Journal of Chemical Information and Modeling*, *48*(10), 2081-94. doi:10.1021/ci800209k

Lawrence, A. W. and McCarty, P. L. (1970). Proceedings of the American Society of Civil Engineering: *Journal of Sanitation Engineering Division*, 96, 757.

Leitão, R. C., van Haandel, A. C., Zeeman, G., & Lettinga, G. (2006). The effects of operational and environmental variations on anaerobic wastewater treatment systems: a review. *Bioresource Technology*, *97*(9), 1105-18. doi:10.1016/j.biortech.2004.12.007

Luton, P. E., Wayne, J. M., Sharp, R. J., & Riley, P. W. (2002). The mcrA gene as an alternative to 16S rRNA in the phylogenetic analysis of methanogen populations in landfill. *Microbiology*, *148*, 3521-30. Retrieved from http://www.ncbi.nlm.nih.gov/pubmed/12427943

McCarty, P. L., Bae, J., & Kim, J. (2011). Domestic wastewater treatment as a net energy producer--can this be achieved? *Environmental Science and Technology*, *45*(17), 7100-6. doi:10.1021/es2014264

Mchugh, S., Carton, M., Mahony, T., & Flaherty, V. O. (2003). Methanogenic population structure in a variety of anaerobic bioreactors. *FEMS Microbiology Letters*, *219*, 297-304. doi:10.1016/S0378-1097(03)00055-7

Downing, A. L., Painter, H. A., & Knowles, G. (1964). Nitrification in the Activated-Sludge Process. *Journal of the Institute of Sewage Purification*, *2*, 130-158.

Keogh, E. Chu, S., Hart, D., and Pazzani, M. (2001) An online algorithm for segmenting time series. Data Mining, Proceeding IEEE International Conference on Data Mining. 289-296 _____

Morris, R. (2011). *Relating Methanogen Community Structure to Function in Anaerobic Wastewater Digesters*. Ph.D. Thesis. Biology: Marquette University, Milwaukee, WI, U.S.A.

Navaratnam, N. (2012). *Anaerobic co-digestion for enhanced renewable energy and green house gas emission reduction*, Ph.D. Thesis, Civil, Construction, and Environmental Engineering. Marquette University, Milwaukee, USA.

Novotny, V., Ahern, J., and Brown, P. (2010). *Water Centric Sustainable Communities*. John Wiley & Sons, Inc. Hoboken, NJ.

Nirmalakhandan, N. and Speece, R.E. (1988) Structure Activity relationships: Quantitative techniques for predicting the behavior of chemicals in the ecosystem. *Environmental Science and Technology*, 22(6) 606-615.

Nirmalakhandan, N.N. and Speece, R.E. (1988b). Prediction of Aqueous Solubility of Organic Chemicals Based on Molecular Structure. *Environmental Science and Technology*, 22(3) ,328-338.

Pimm, S. (1984). The complexity and stability of ecosystems. *Nature*, *307*, 321-326.

Quirk T. and Eckenfelder, W.W. (1986). Active biomass in activated sludge analysis and design. *Journal of Water Pollution Control Federation* 58 (9), 932.

Robinson, P. S., Lin, T. W., Jawad, A. F., Iozzo, R. V., & Soslowsky, L. J. (2004). Investigating tendon fascicle structure-function relationships in a transgenic-age mouse model using multiple regression models. *Annals of Biomedical Engineering*, *32*(7), 924-31. Retrieved from http://www.ncbi.nlm.nih.gov/pubmed/15298430

Röling, W. F. M., Ferrer, M., & Golyshin, P. N. (2010). Systems approaches to microbial communities and their functioning. *Current Opinion in Biotechnology*, *21*(4), 532-8. Elsevier Ltd. doi:10.1016/j.copbio.2010.06.007

Speece, R. (2008) *Anaerobic Biotechnology and Odor/Corrosion Control for Municipalities and Industries*. Nashville, TN: Archae Press.

Stephenson, R. J., Patoine, A., & Guiot, S. R. (1999). Effects of oxygenation and upflow liquid velocity on a coupled anaerobic/aerobic reactor system. *Water Research*, *33*(12), 2855-2863. doi:10.1016/S0043-1354(98)00505-3

Tale, V. P., Maki, J. S., Struble, C. A., & Zitomer, D. H. (2011). Methanogen community structure-activity relationship and bioaugmentation of overloaded anaerobic digesters. *Water Research*, *45*(16), 5249-5256. Elsevier Ltd. doi:10.1016/j.watres.2011.07.035

Topliss, J. G., & Costello, R. J. (1972). Chance Correlations in Structure-Activity Studies Using Multiple Regression Analysis. *Journal of Medical Chemistry*, *15*(10), 1066-1068.

Undas, A., Zawilska, K., Ciesla-Dul, M., Lehmann-Kopydłowska, A., Skubiszak, A., Ciepłuch, K., & Tracz, W. (2009). Altered fibrin clot structure/function in patients with idiopathic venous thromboembolism and in their relatives. *Blood*, *114*(19), 4272-8. doi:10.1182/blood-2009-05-222380

Watanabe, K., Futamata, H., & Harayama, S. (2002). Understanding the diversity in catabolic potential of microorganisms for the development of bioremediation strategies. *Antonie van Leeuwenhoek*, *81*, 655-663.

Wittebolle, L., Marzorati, M., Clement, L., Balloi, A., Daffonchio, D., Heylen, K., De Vos, P., et al. (2009). Initial community evenness favours functionality under selective stress. *Nature*, *458*(7238), 623-6. Nature Publishing Group. doi:10.1038/nature07840